Novel Best Management Practices for Improving Water Quality in Midwestern Agricultural Settings: Field and Lab Applications

SUBMITTED TO THE FACULTY OF THE
UNIVERSITY OF MINNESOTA
BY

Lori A. Krider

IN PARTIAL FULFILLMENT OF THE REQUIREMENTS
FOR THE DEGREE OF
DOCTOR OF PHILOSOPHY

Dr. Bruce Wilson, Advisor

February 2018

ACKNOWLEDMENTS

I would first like to thank Dr. Bruce Wilson for always believing in me and supporting me in so many ways over the past 8 years. I would also like to thank the current and former heads of the Department of Bioproducts and Biosystems Engineering (Dr. Shri Ramaswamy and Dr. Gary Sands) for the financial support so that I could pursue a PhD and conduct amazing research. I would also like to thank Dr. Fred Bergsrud and the late Dr. Bill Wilcke for their generous financial gifts. I would also like to thank the Mower County Soil and Water Conservation District and The Nature Conservancy for providing funding for the design and construction of the Mullenbach Two-Stage Ditch. I would also like to thank the University of Minnesota MnDrive Program for providing Undergraduate Research Scholar Funds to support an assistant on the bioreactor research project. I would also like to thank Dr. Joe Magner for his mentorship throughout the process, as well as the rest of my committee members (Dr. Jeff Strock and Dr. Gary Feyereisen), both whom taught me important concepts along the way. I would like to thank Nadine Hackshaw and Dr. Sebastian Behrens for their excellent collaboration. I am immensely appreciative of my fiancé, Eric Rieppel, who assisted in troubleshooting problems, meeting project deadlines, and editing various documents. I would also like to thank Sam Padelford, Sam Okkema, Dong Dong, John Mueller and Haley Bauer all very talented undergraduate students in BBE that assisted as employees or volunteers on the project. I would also like to thank Brad Hansen, Derrick Ferguson, Dr. John Nieber, Dr. Pete Marchetto, Dr. David Schmidt and Dr. Kevin Janni as well as graduate students Emily Deering, Keiran Cantillna, Hanna Lin and staff Carlos Zamalloa, Min Min, Lucas Stolp, Sue Olsen and Susan Seltz for their technical assistance when I had questions. Also, Curtis Borchert and Autumn Boos, industry partners whom were excellent to work with. Lastly, thanks to my wonderful friend Lu Zhang who loves and respects me for whom I am.

DEDICATION

This dissertation is dedicated to my fiancé, Eric Rieppel, who was the most patient, helpful, and understanding partner I could hope for through this process. On to the next chapter, my darling!

ABSTRACT

Water quality in agricultural watersheds is under greater scrutiny as the landscape and hydrologic pathways are altered to increase the production of affordable food. Agricultural best management practices (BMPs) are common tools to improve water quality on a local scale. This study examined the effectiveness of two-stage ditches using field data and the efficacy of bioreactors in a lab setting. In the field, the physical stability and nitrate removal of an alternatively designed drainage ditch in southern Minnesota (the Mullenbach Two-Stage Ditch) were assessed. Two-stage ditches are more stable than traditional, trapezoidal designs and may adjust slightly overtime to produce the most sustainable shape. This BMP is also effective at removing nitrate, although variably as it relates to temperature, hydraulic residence time, and influent nitrate loading. In the lab, a system to determine nitrate removal under reduced temperature conditions was used to evaluate novel media for bioreactors, including walnut shell biochar and Brotex™ material. A flow characterization and nitrate removal model was created in MS Excel™. Additionally, the model incorporated microbial processes found by a quantitative polymerase chain reaction (qPCR). This design is 2X more effective than traditional, woodchip only configurations. Multi-media bioreactors may have great potential for future applications by enhancing nitrate removal and microbial activity. Constant innovation is the key to sustainability, which can be achieved by creating optimized systems that highly effective under a range of environmental conditions and scenarios.

This dissertation is composed of individual, stand-alone chapters that have been or will be published in peer reviewed scientific journals. The first two chapters pertain to research performed on an alternatively designed drainage ditch in southern Minnesota (the Mullenbach Two-Stage Ditch). For chapter 1, the physical stability of the design was assessed through an evaluation of the fluvial geomorphology and sediment processes. This work was published with co-

authors Joseph Magner, Brad Hansen, Bruce Wilson, Geoffrie Kramer, Joel Peterson, and John Nieber in the August 2017 issue of the Journal of the American Water Resources Association. This includes an evaluation of the formation of pool-riffle sequences as well as changes in channel width and depth, channel stability using Rosgen (2008) field methods, and an estimate of the bankfull recurrence interval. For chapter 2, various methods for estimating nitrogen removal of this design were explored. Specifically, this included comparisons of a mass-balance approach using isotopic tracers, influent/effluent concentration differences, and the potential soil denitrification rate. The third chapter is a short ASABE conference transaction paper published in November of 2016 with co-authors Bruce Wilson and Joe Magner on the design and construction of the reduced temperature apparatus used in the novel media bioreactor experiment. This describes the specifications for all equipment used in the production. However, this paper was published before the inclusion of an additional, temporary, secondary tank (30 gal), water chiller (Blissfield Frigid BHL-1089-2, 25 amps, 1/12 HP), and pump (Sherwood Aqua-Tiger SS CMSV012D-XX, 12 V, 9.5 Amps, 20 GPM) to further cool the water. This additional component was added in the summer when influent water temperatures were near 30 ^{o}C but this component was only used for 2 weeks of the actual experiment. The fourth chapter pertains to the research conducted on the novel media bioreactor experiment. This work was done in collaboration with MS graduate student Nadine Hackshaw and Dr. Sebastian Behrens in Civil, Environmental and Geo-Engineering (CEGE) at the University of Minnesota. Media combinations include the innovative use of walnut shell biochar and Brotex material as well as the traditional woodchips housed in open topped containers (troughs) exposed to air and light and topped with wetland plants to create a biological system (a.k.a. biosystem). A flow characterization model was created using bromide tracer data in MS Excel^{TM}. This model was enhanced to predict nitrate removal capabilities using Excel Solver^{TM} to match a predicted curve to

minimal grab samples with a changing influent concentration. The design compares the treatments with and without Brotex under 12 and 4 hr HRTs. Additionally, microbial abundance data obtain by quantitative polymerase chain reaction (qPCR) assays and provided by the CEGE team was used to alter the existing model to reflect microbial processes. Important conclusions are drawn regarding bioreactor design and characterization, which a focus nitrogen removal. Secondarily, some conclusions are drawn regarding nitrous oxide emissions and modeling microbial processes, though they are not the focus of this dissertation. Multi-media bioreactors, with careful selection of biochar type, may have great potential for future applications, both in the field and laboratory, for enhancing nitrate removal and microbial activity.

TABLE OF CONTENTS

LIST OF TABLES

LIST OF FIGURES

LIST OF APPENDICES

INTRODUCTION

The introduction of nitrogen from agriculture into our natural waterways poses serious threats to biotic communities. Land use in southern Minnesota is largely agricultural with the dominant crops being corn and soybean. In 2016, 8.39 million acres of corn and 7.50 million acres of soybeans were harvested in Minnesota (USDA-NASS, 2017). Beginning around 1960, there was a drastic increase in the amount commercial fertilizer applied to these crops to increase yields (Fig. 1). Although application has remained fairly consistent over the past several decades, corn yields have continued to increase over time (Hicks, 2005). University extension entities have validated recommendations for nitrogen application to produce optimal yields without excess expenditures (EONR, economic optimal nitrogen range) under a range of soil and climate conditions and cropping scenarios (Randall *et al.,* ND). However, in some cases, the recommendation is more than needed and, in many other cases, more may be applied than is needed (Babcock, 1992). In many cases, this has created an issue of nitrogen over application, particularly to corn, which is creating concern due to the environmental consequences of excess nitrogen in natural waters (Schmidt *et al,*. 2002). Improved nutrient management can potentially reduce nitrate losses on drained lands by up to 30% (Randall and Mulla, 2001). While nitrogen fertilizer application rates and timing can help pre-empt nutrient loss (Lawlor *et al.,* 2008; Randall and Mulla, 2001), it will be necessary to combine it with other best management practices (BMPs) to achieve significant water quality improvements (Randall and Sawyer, 2008).

Portions of these nutrients are introduced into the soil profile through the process of leaching (Lamb *et al.,* 2014). There are several factors that influence leaching and nitrogen loss, including climate conditions and agricultural practices (Randall and Mulla, 2001; Lawlor *et al.,* 2008; Hernandez *et al.,* ND). However, nutrients that are in excess and not taken up by plants can move further into the soil profile by precipitation and can be transported off the field in sub-surface tile

drainage (Fig. 2). Tile drains transport these excess nutrients to nearby agricultural drainage ditches, streams, and rivers. Cropland sources account for as much as 95% of the nitrate loading in the Minnesota, Missouri, and Cedar Rivers and the Lower Mississippi River Basin (MPCA, 2013). In short, although drainage is beneficial for crop yield, agriculture is considered the primary driver behind rising nitrate levels in Minnesota's surface waters (Twin Cities Pioneer Press, 2013).

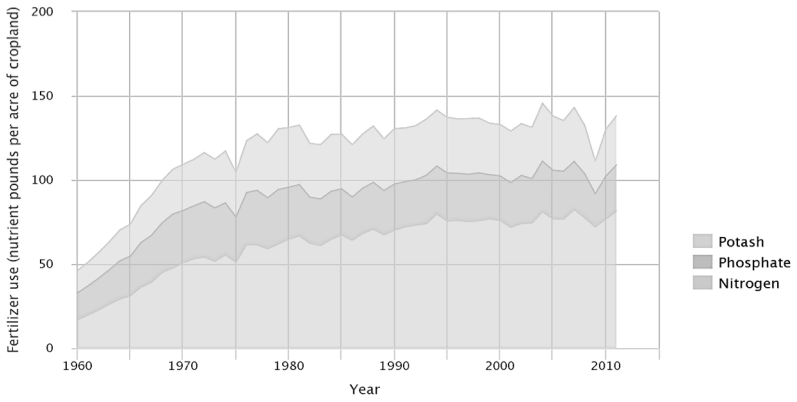

Figure 1. Commercial fertilizer use (lbs acre cropland^{-1}) in the US from 1960 to 2011 by major constituent (Source: USDA ERS. 2013, 2014. Report on the Environment: Agricultural Fertilizer. https://cfpub.epa.gov/roe/indicator_pdf.cfm?i=55). In order from the x-axis: nitrogen, phosphate, and potash.

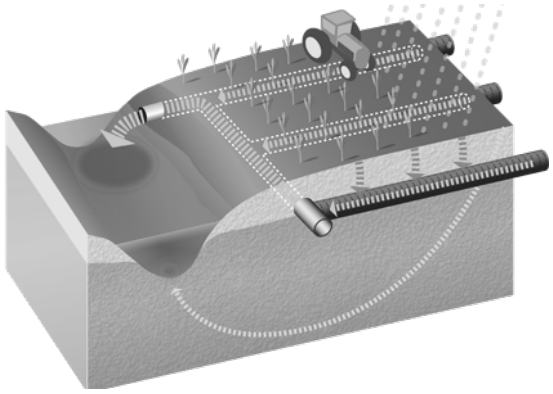

Figure 2. Pathway of nitrogen transport from an agricultural field to a drainage ditch through tile drains and groundwater transport (Source: MPCA. 2013. Water pollutants and sources: Nitrogen. https://www.pca.state.mn.us/water/nitrogen).

Climate and geology has made Minnesota a water rich state, capable of storing large quantities of water on the land in the form of wetlands and lakes. During the last glacial retreat, large ice boulders fell off the retreating edge to form a pocked landscape of shallow depressions that filled with water to form the "land of 10,000 lakes" (EPA, ND). However, water storage on the land is in direct contention with agricultural productivity. Upward of 90% of the wetlands in some areas of southern Minnesota have been drained and converted to agriculture (Anderson and Craig, 1984; Fig. 3). Additionally, excessive surface and sub-surface water can greatly reduce crop yields. Moreover, many water quality issues in agricultural landscapes are exacerbated by large storm events due to climate change; larger, higher intensity events occur more frequently (Dunbar and Kraker, 2015). To address this excess water, an extensive system of tile drains and drainage ditches has been, and continues to be, constructed throughout southern and western Minnesota (Lien and Orrick, 2016). Sub-surface tile drains clear fields of water quickly, prevent standing water, and reduce flooding in adjacent waterways (Lien and Orrick, 2016). In general, sub-surface drainage removes an additional 10% to 15% more water than just surface drainage only (UMN Extension, 2001). Drainage ditches transport this water away from the field to keep tile drains free-flowing. It has been estimated that there are approximately 33,800 km (21,000 mi) of drainage ditches in Minnesota (DNR, ND). Drain tiling has been largely undocumented and unregulated in most of Minnesota (Kotila, 2013). Extensive tiling increases flows to nearby ditches and streams (Robinson *et al.,* 1999), thus increasing erosion. A study done in a headwater agricultural watershed in Ohio showed that 21% of precipitation is transported through tile drainage annually and that tile drainage accounts for 47% of watershed discharge (King *et al.,* 2014). Drain tiles also provide a direct conduit for the transportation of nitrates downstream (Blann *et al.,* 2009).

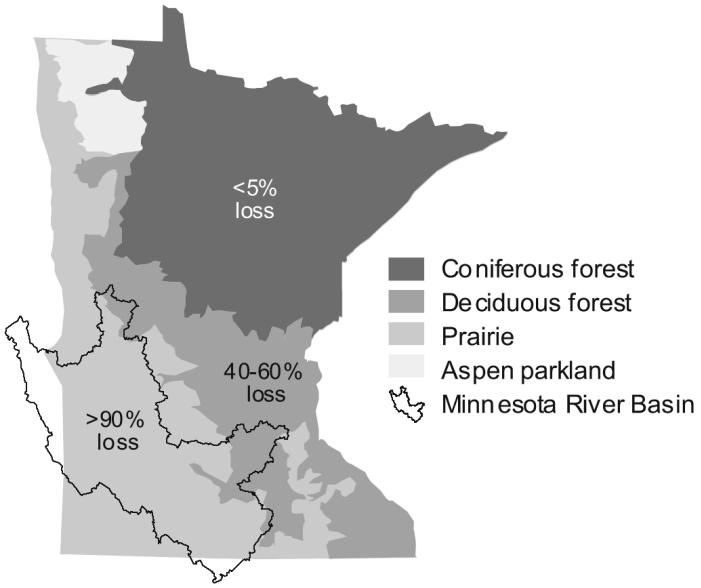

Figure 3. Wetland loss by Minnesota's major biomes and within the Minnesota River Basin, specifically. The Minnesota River Basin is highly agricultural, with corn and soybeans being the dominant crops (Source: Minnesota River Basin Data Center. 2011. Wetlands in the Minnesota River Basin. http://mrbdc.mnsu.edu/wetlands-minnesota-river-basin).

Row crop tile drainage contributes 37% of the nitrogen load to Minnesota's waters and approximately 67% of the nitrogen load to the Minnesota River Basin (MPCA, 2013). During a wet year, the fraction of nitrogen to waters from tile drainage increases to an estimated 43% of statewide nitrogen load and 72% of the Minnesota River nitrogen load (MPCA, 2013). Agricultural drainage ditches feed into major river systems in Minnesota (Fig. 4). "On average, [95 mil kg (211 mil lbs)] of TN [total nitrogen] leaves Minnesota each year in the Mississippi River at the Minnesota-Iowa border, with just over three-fourths of this load originating in Minnesota watersheds . . .," (MPCA, 2013). Minnesota is a major contributor (6^{th} as of 2008) of nitrogen to the Mississippi River, as well as several other midwestern states, including Iowa and Indiana (MPCA, 2013; Fig. 5). The Mississippi River then transports significant amounts of these nutrients to the Gulf of Mexico.

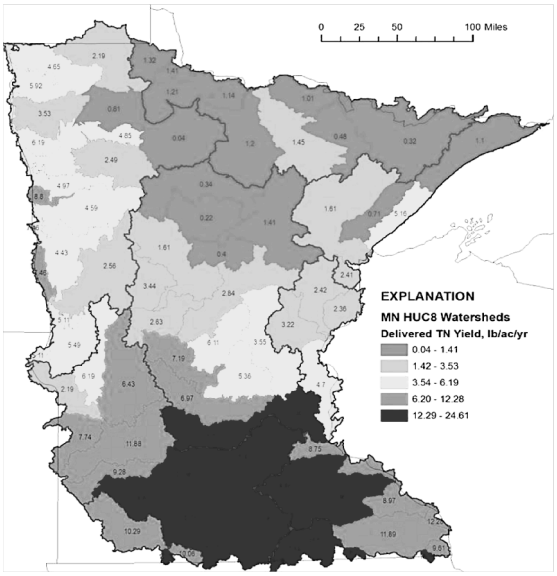

Figure 4. Total nitrogen delivered (lbs acre^{-1} yr^{-1}) to the outlet of each HUC 8 watershed in Minnesota in 2002 (Source: EPA SPARROW. Nitrogen Model. 2013. http://mrbdc.mnsu.edu/mnnutrients/sites/mrbdc.mnsu.edu.mnnutrients/files/public/watersheds/Le%20Sueur/modeling_n_yield.jpg).

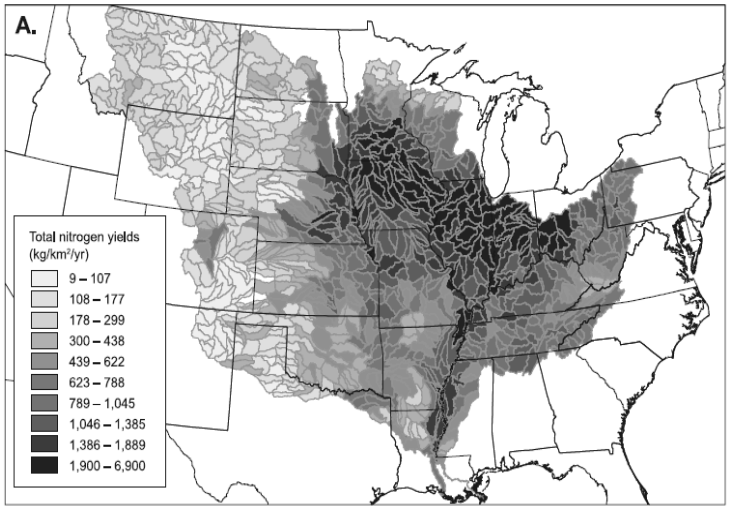

Figure 5. Total nitrogen yield by HUC 8 watershed within the Mississippi River Basin for Using the EPA SPARROW Model for conditions similar to 2002 (Source: USGS. SPARROW Nutrient Modeling: Mississippi/Atchafalaya River Basin. https://www.usgs.gov/centers/wisconsin-water-science-center/science/sparrow-watershed-modeling-mississippiatchafalaya?qt-science_center_objects=0#qt-science_center_objects).

As part of the Minnesota Nutrient Reduction Strategy, the MPCA defines agricultural tile drainage and other hydrologic pathways from cropland as the priority nitrogen sources to the Mississippi River (MPCA, 2014). In response to this issue, the State of Minnesota has created nitrogen reduction goals to the Mississippi River of 20% by 2025 and 45% by 2040 from average 1980 to 1996 conditions (MPCA, 2014). Current agricultural BMPs have only produced a 2% reduction in nitrogen pollution since 2000 (MPCA, 2014). This is partly due to a lack of vital research needed to improve some of these practices. The Minnesota Nutrient Reduction Strategy cites the need for further research and development of water quality BMPs, including bioreactors and two-stage ditches, for treating tile drainage water (MPCA, 2014).

The natural source pathway for surface waters to obtain nitrogen is through diffusion with the atmosphere. In general, and although it varies, this creates a baseline level of approximately 0.25 mg L^{-1} of dissolved inorganic nitrogen in streams and rivers (Lenntech, 2016). In agricultural settings, nitrogen can be artificially introduced into natural systems through the mineralization of organic matter or by humans when applied to agricultural fields as organic (manure) or inorganic (fertilizer) nitrogen. Excess nutrients introduced into aquatic systems can have major consequences for natural communities. Nitrate can directly affect the health of aquatic life in lakes and streams so the MPCA has created a draft standard for protecting cold (class 2A) uses and cool/warm (class 2B) surface water uses. The draft acute value (maximum standard) is 41 mg L^{-1} nitrate-N for a 1-day duration and the draft chronic value is 4.9 mg L^{-1} nitrate-N for 2B waters and 3.1 mg L^{-1} for 2A waters for a 4-day duration (MPCA, 2010). These toxicity levels are environmentally relevant to Minnesota's surface waters (Camargo and Alonso, 2006). It is common for agricultural drainage ditches in southern Minnesota, adjacent to farmlands with nitrogen applied, to have nitrate-N concentrations above the drinking water standard of 10 mg L^{-1}, especially in the spring and early summer months (Brouder *et al.,* 2005). Nitrate

concentrations above the toxicity standard can cause the delay of growth and development, nervous system damage and deterioration, and general overall stress for aquatic animals (Aquarium Forum, ND).

Excess growth of unwanted algae and duckweed *(Lemna spp.*) is often a consequence of having excess nutrients in natural systems where it is otherwise limited (King, 2011). This excess growth creates unstable oxygen conditions where there is an unusually high concentration during the day, which drops off dramatically over night (Wheatley River Improvement Group (WRIG)). This creates particularly stressful conditions for fish, which, over the short term, can affect behavior and reproduction, but in the long term, may cause the fish to leave the area or die (WRIG). Additionally, surface coverage of the water body reduces the amount of sunlight that is able to penetrate the water column (WRIG). The causes drastic changes in the habitat condition, which can affect an organism's ability to feed and reproduce (WRIG). The decomposition of this algae and duckweed consumes large amounts of dissolved oxygen (DO) in the water column, creating hypoxic conditions ($DO < 2$ mg L^{-1}) that are unsuitable for many plant and animal species, especially those that are particularly sensitive to low levels of dissolved oxygen (Fig. 6). The hypoxic zone in the Gulf of Mexico is an example of this decomposition on a large scale (NOAA, 2014).

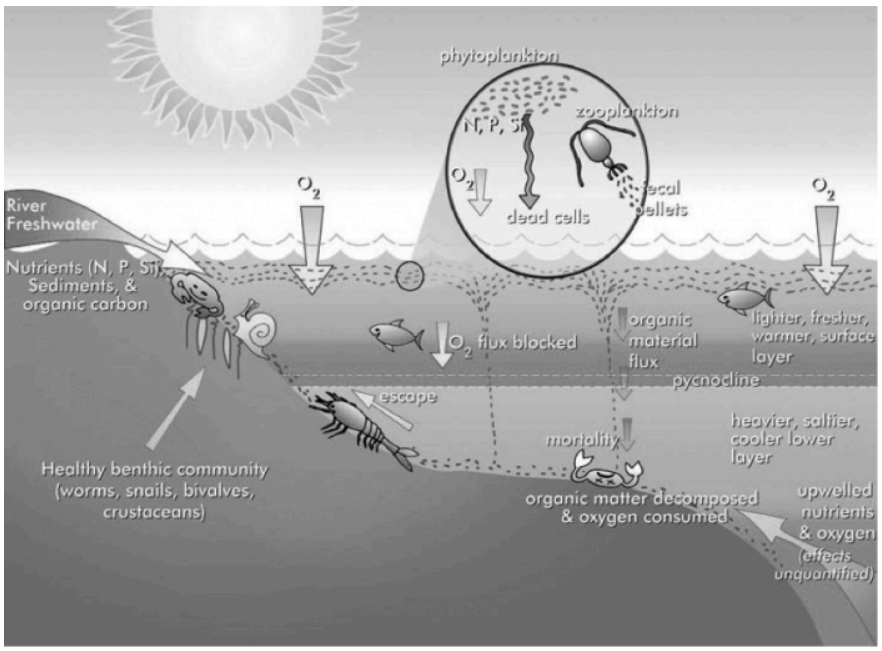

Figure 6. The eutrophication process of nutrients delivered to a water body, algal death and sinking, decomposition of organic material and subsequent oxygen consumption, and the resulting death or migration of organisms living in the oxygen depleted layer (Source: Penn State University. Mississippi River Case Study: Dead Zone in the Gulf of Mexico. https://www.e-education.psu.edu/earth131/node/1113).

Excess nutrients from the Mississippi River as well as seasonal stratification of the water column creates annual dead zones in the Gulf of Mexico in the late summer (EPA, 2017). In August of 2015, the Gulf of Mexico Dead Zone was measured at 16,768 km^2 (6,482 mi^2), approximately the size of the states of Rhode Island and Connecticut (NOAA, 2015). This is about 3,108 km^2 (1,200 mi^2) larger than the average size forecasted back in June of 2015 and about 3,885 km^2 (1,500 mi^2) larger than the size of the dead zone in 2014. However, in August of 2017, the dead zone was measured as the largest yet at 22,730 km^2 (8,776 mi^2), similar to the size of New Jersey (NOAA, 2017; Figs. 7 and 8). The Gulf of Mexico Dead Zone is the second largest human-caused hypoxic zone in the world (NOAA, 2015).

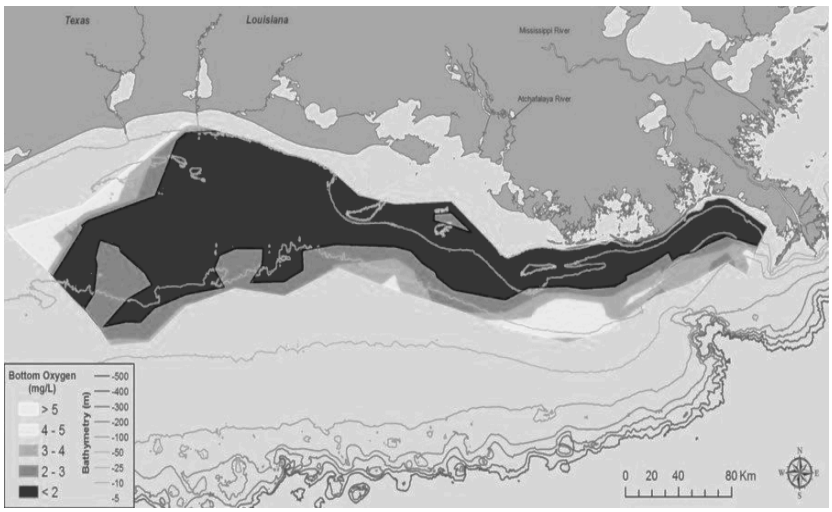

Figure 7. Distribution of bottom-water dissolved oxygen in August of 2017. Black line indicates dissolved oxygen level of 2 mg L^{-1}. Note the cut-off on both the west and east sides where monitoring vessels where not able to collect data (areal coverage is actually larger than what was measured) (Source: LUMCON, LSU. 2017. Press Release: Summary. https://gulfhypoxia.net/wp-content/uploads/2017/08/rev-PRESS-RELEASE-2017-LUMCON-LSU.pdf).

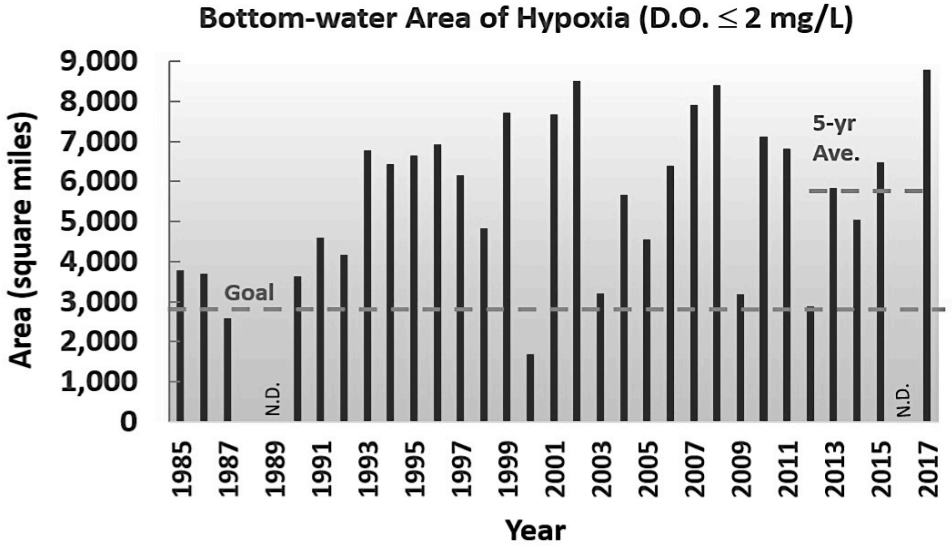

Figure 8. Graph showing the measured size of the hypoxia zone in the Louisiana Gulf of Mexico shelf, 1985–2017 (Source: LUMCON, LSU. 2017. Press Release: Summary. https://gulfhypoxia.net/wp-content/uploads/2017/08/rev-PRESS-RELEASE-2017-LUMCON-LSU.pdf).

Dead zones are widespread across the planet, with about 550 occurring annually (NOAA, 2015; Fig. 9). With the exception of Antarctica, there is no continent on earth without numerous dead zones along their coastlines (Palmer, 2014). The extent of dead zones is not currently fully known and it is estimated that the actual count is around 1,000, including ones currently unknown (Palmer, 2014). This translates to 1% of the continental shelf area (Palmer, 2014). Additionally, warmer water holds less oxygen so warmer oceans resulting from climate change will lead to further oxygen depletion.

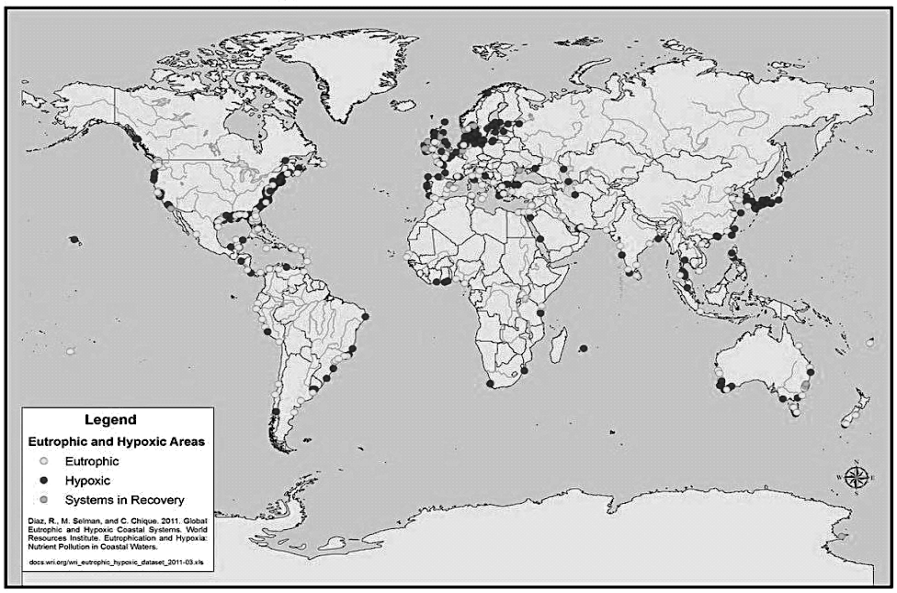

Figure 9. Hypoxic and eutrophic coastal areas around the world as of 2011 (LeBlanc, C. (Science News for Students). Suffocating Waters. 2012. https://www.sciencenewsforstudents.org/article/suffocating-waters).

LITERATURE REVIEW

Nitrate Attenuation

Denitrifying Bacteria

In agricultural settings, nitrogen is applied to agricultural fields as organic (manure) or inorganic (fertilizer) nitrogen. The process of ammonification

converts this organic or inorganic nitrogen to ammonia (NH_4^+ or NH_3), which is then converted to nitrite (NO_2^-) and then nitrate (NO_3^-) through the process of nitrification (Clanton, 2015). Nitrate attenuation is the removal of nitrate from a system by the process of denitrification. This process is performed by facultative heterotrophic bacteria including *Thiobacillus denitrificans, Micrococcus denitrificans*, and some species of *Serratia, Pseudomonas,* and *Achromobacter* (Encyclopaedia Britannica, ND). These bacteria form colonies of individuals known as a biofilm that attaches, colonizes, and grows on the surface of suitable material (Fig. 10). Under anoxic conditions, these bacteria use nitrate as an electron acceptor in their respiration electron transport chain to convert nitrate to ammonia for cell synthesis by assimilatory denitrification or nitrous oxide (N_2O) by dissimilatory denitrification (Christianson, 2011; NPTEL, ND). Due to the anoxic conditions in which the process takes place, very little assimilatory denitrification takes place and the majority is dissimilatory (NPTEL, ND). A carbon source serves as an electron donor and may come in the form of organic matter (i.e. mineralization of vegetation) or external sources such as acetate ($CH_3CO_2^-$) or ethanol ($C_2H_6O_2^-$) (NPTEL, ND). The denitrification process releases both inert nitrogen gas and oxygen back into the atmosphere during complete conversion or nitrous oxide during incomplete conversion (NPTEL, ND).

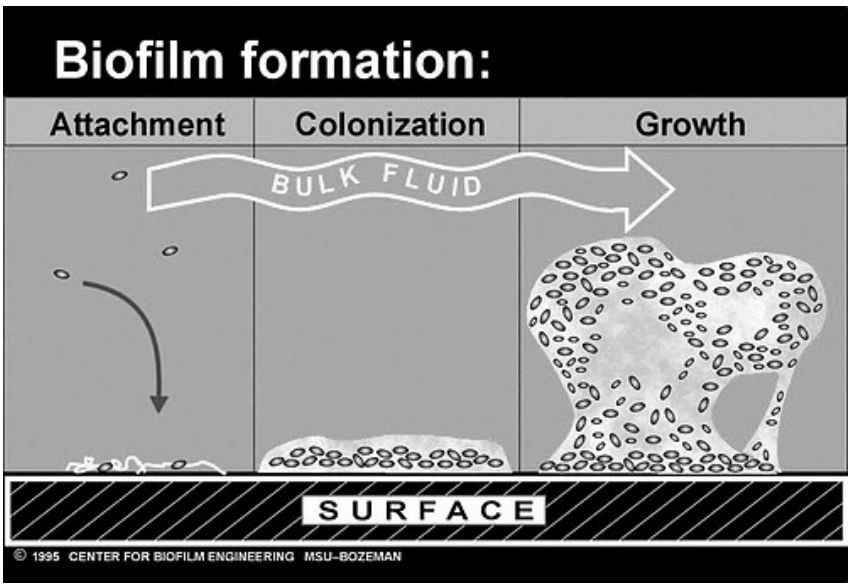

Figure 10. Diagram of biofilm growth stages on a surface (Source: Montana State University. 1995. https://www.uweb.engr.washington.edu/images/research/biofilmtutorial.JPG).

BMPs

Best management practices are common tools to improve water quality on smaller scales by increasing local rates of denitrification. BMPs placed on the land can either be in-field or edge-of-field. It is expensive and difficult to gain citizen buy-in for in-field BMPs because of the loss of agricultural land that results so much attention has been turned toward edge-of-field and in-stream practices (Lien and Magner, 2017). Many BMPs have the potential to produce large improvements in water quality, if they can be made less restrictive in how and where they can be applied (i.e. under a variety of environmental, climatological, and landscape variables). Experiments can be conducted in a laboratory setting prior to implementation in the field to test various environments and conditions. Constant innovation is the key to sustainability, which can be achieved by creating optimized systems that are economical and highly effective under a range of environmental conditions and scenarios.

Bioreactors

A common edge-of-field BMP is the bioreactor. Bioreactors consist of trenches intercepting sub-surface tile drainage water at the edge of an agricultural field and filled with a carbon source (Fig. 11). Traditional bioreactors use woodchips as a carbon source and can last 15 to 20 years in the field (Feyereisen, 2014; Moorman *et al.*, 2009). Bioreactor technology to treat agricultural drainage water has existed for just over 20 years, with the first published prototype consisting of barrels of organic matter being buried in a streambed (Blowes *et al.,* 1994). Bioreactors have moved beyond the proof of concept; field trials of woodchip bioreactors have been in place in the Midwest for over a decade. Research is moving in the direction of multi-media and novel design approaches (Christianson and Schipper, 2016). However, bioreactors are still thought of in terms of a "black box" in that we don't know exactly how and why they do what they do. Collaborations are needed to investigate the mechanisms for nitrate removal "through the use of more advanced monitoring techniques" (Christianson and Schipper, 2016).

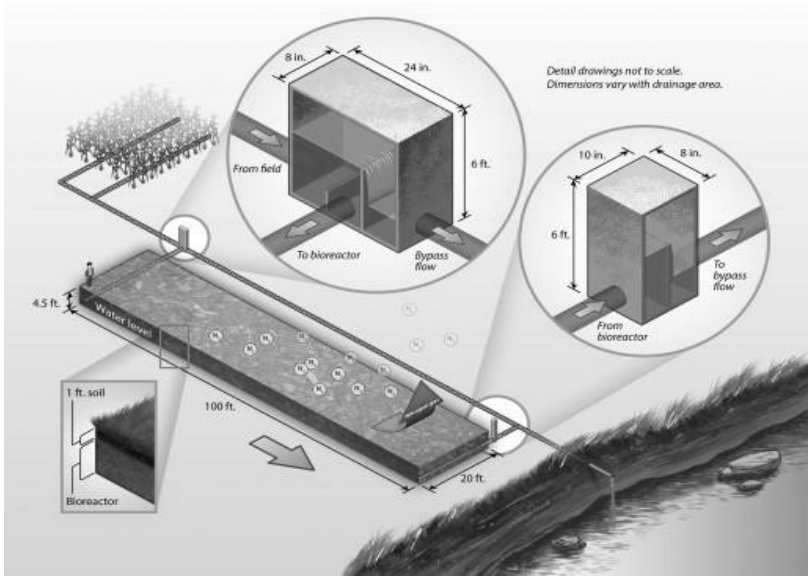

Figure 11. Diagram of a bioreactor field design, including piping, control structures, and media (Christianson, 2011).

Bioreactors are effective at removing nitrate from aquatic systems (Christianson *et al.,* 2012). However, there are several important and recurrent issues with traditional woodchip bioreactors. Current designs are less effective under reduced temperature conditions (Addy *et al.,* 2016). All existing designs require long hydraulic residence times (HRTs; the time it takes for the water to get from the inlet to outlet), such as 24 hours, to produce high rates of nitrate removal. Woodchip bioreactors that have shorter HRTs, such as 8 hours, can typically only remove around 50% of influent nitrates and treat only about 20% of peak flows (highest flow present throughout a year) (ISA, ND). A more effective bioreactor design will be able to produce high levels of nitrate attenuation within a shorter HRT under a variety of environmental conditions.

Two-Stage Ditches

Two-stage drainage ditches are designed to mimic the stable bank conditions found in natural low-order streams (Ward *et al.,* 2004; USDA-NRCS, 2007; Fig. 12). They are usually constructed to replace conventional ditches and are most beneficial at sites where present conventional drainage ditches are unstable and require frequent clean out. A low-flow channel is sized to replicate that of a natural channel in the surrounding region with a similar drainage area (Kramer, 2011). Two-stage channels are designed with small benches on both sides of the low-flow channel to serve as a floodplain. These floodplain benches allow for dissipation of the fluvial energy associated with high flow rates (Ward *et al.,* 2004) while allowing for taller and denser riparian plant growth to stabilize and shade the narrower low-flow channel (D'Ambrosio, 2013).

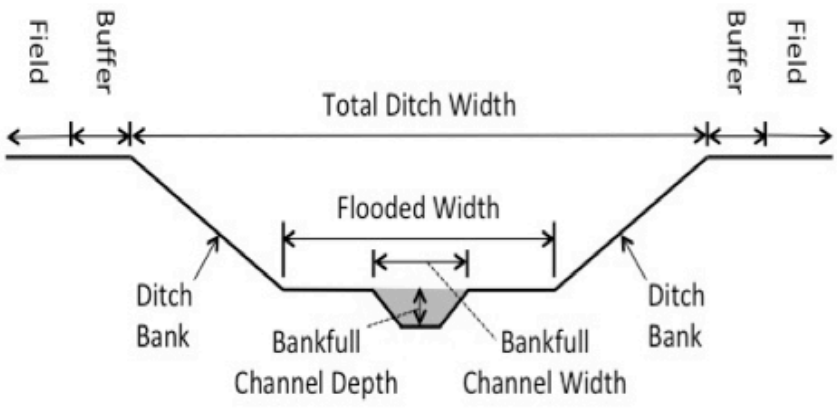

Figure 22. Two-stage drainage ditch cross - section (right) (Kramer, 2011).

Alternatively designed agricultural drainage ditches help facilitate higher levels of denitrification (Powell and Bouchard, 2010). As water level exceeds the bankfull depth during storm events, the flow spreads out across the floodplains. This has the effect of slowing water velocity, increasing water residence times, and reducing nitrogen transport during large flow events (Roley *et al.,* 2012a). Plant biomass serves as an important carbon source necessary to support denitrifying bacteria. Two-stage ditches have benches that support more than twice the amount of biomass compared to the slopes of the traditional drainage ditch (Powell and Bouchard 2010; Krider *et al.,* 2017). This vegetative cover increases nutrient uptake through the plant itself but also by providing roots that serve as microbial growth habitats and contributing carbon to the soil for use in the denitrification process.

The main value of a two-stage ditch is increased stability in the ditch system. This is mainly embodied in reduced ditch cleanout costs associated with sediment deposition (Ward *et al., 2*004; Powell *et al., 2*007; Peterson *et al., 2*010). Additionally, a reduction in erosive forces at the toe of the outer ditch bank is expected, as water will usually be confined to the low-flow channel (Ward *et al., 2*004). Increased stability at the toe of the ditch will also likely reduce the potential for sloughing and mass wasting on the outside ditch banks. This design

is also wider than the traditional design and can provide storage during storm events, depending on the downstream control (e.g. culvert size).

Drainage ditches are often regarded as different and separate from many natural systems although they function in a similar manner. Whether human-altered or natural, fluvial systems that are unbalanced with the amount of sediment eroded and the amount accumulated will work toward a dynamic equilibrium. Simon and Hupp's (1986) six-stage depiction of channel evolution is useful in understanding the response of drainage ditches. When a natural system is dredged and reconstructed to create an artificial channel with steep slopes and a wide low-flow channel, through a process of evolution, the system will create sides with reduced slopes to minimize erosion and a narrower low-flow channel to transport sediment. However, most farmers find that the sediment accumulation necessary to create the narrower low-flow channel is unacceptable and they will "clean-out" the ditch, preventing the channel from returning to a natural, effectively functioning system. This perpetual clean-out cycle prevents attaining the water quality, quantity, and habitat benefits of a more natural system.

Important Variables

HRT

Residence time is one of the most important features when considering a design for nitrate removal. In a bioreactor column (small containers, usually PVC pipe sections, filled with media) experiment by the University of Minnesota, woodchip bioreactor column nitrate reductions were approximately 85 and 25% at 24 and 8 hr HRTs, respectively (Feyereisen, Personal Communication). Too long of an HRT (> 25 hr) can result in nitrogen limitation and sulfate reducing conditions (Lepine *et al.,* 2015). Additionally, Cooke *et al.* (2001) predicted that increased retention times would be required at reduced temperatures. In general, nitrate removal in reactors with a HRT < 6 hr was significantly lower than in

reactors with a HRT from 6 to 20 hr and > 20 hr (Addy *et al.,* 2016). Also, there was minimal removal at a 1.5 hr HRT. However, a retention time that is too short could limit the ability of denitrifying microorganisms to utilize nitrate in respiration because dissolved oxygen levels in the water will be too high (Christianson *et al.,* 2011a). Spring tile flow rates can be quite high (5 to 10 L s^{-1}), so minimizing the HRT while still producing high rates of denitrification is essential (Krider, 2016b).

The HRT is also a key component within drainage ditch systems. Stream velocity (as discharge) is the key component dictating HRT and this is driven by precipitation and runoff as well as water storage on the landscape or within the soil profile. More specifically, the HRT determines the amount of contact time that the nutrient enriched surface water has with the soil surface and soil profile, influencing the microbial community encompassed in it. During conditions less than or equal to base flow, the slower moving channel water comes into direct contact with channel soils although there is likely a less apparent sub-surface and groundwater interaction. During times of greater discharge, stream velocities increase. Practices that increase stream discharge can have a negative impact on the denitrifying capabilities of the microbial communities (Hodaj *et al.,* 2017; Alexander *et al.,* 2009; Arango *et al.,* 2007). This includes practices such as drainage ditch channelization and dredging (Sharpley *et al.,* 2007). Best management practices that slow stream velocities and increase the contact time between the water and soil can significantly enhance denitrification rates.

Temperature

Temperature is a major factor influencing denitrification. There is a research need for more laboratory and field experiments testing BMPs under reduced temperature scenarios. As of 2015, all other published laboratory experiments have only gone down to 10 ^{o}C (Greenan *et al.,* 2016; Healy *et al.,* 2006). However, a column study conducted by Feyereisen at al. (2016) tested a variety of agricultural waste residues at warm (15.5 ^{o}C) and cold (1.5 ^{o}C)

temperatures. They found that corncobs had higher nitrate removal rates than all the other media (corn stover, barley straw, woodchips, and corn cobs followed by woodchips), significantly at 15.5 ^{o}C but not at 1.5 ^{o}C. Although agricultural residues exhibit more rapid decay, alternative, modular bioreactor designs may allow more efficient replacement of the media.

Much of the nitrate loading into ditches and streams occurs during the snowmelt period and high rainfall conditions of the springtime (Wasley, 2013). Most of the average annual tile flow (84%) occurs during the months from November to April (Fraser and Fleming, 2001). At a ditch in Indiana, the highest rates of in-stream sediment denitrification occurred in late winter/early spring with the least in late summer/early fall (Roley *et al.,* 2012a; Fig. 13). A similar statement was made by Powell and Bouchard (2010) when it was written that denitrification rates were greater in the spring, when nitrate concentrations in the ditches are elevated (Richards *et al.,* 2008). It has been found that there is a significant increase in denitrification rates between 5 and 10 ^{o}C (Powlson *et al.,* 1988; Stanford *et al.,* 1975), denitrification has been documented in agricultural fields at 2 ^{o}C (Robertson *et al.,* 2000; Firestone and Davidson, 1989) and extrapolation shows that denitrification would likely occur at or near 0 ^{o}C (Smid and Beauchamp, 1976). It has also been found that bacteria in temperate soils can denitrify at lower temperatures compared to bacteria in tropical soils (Powlson *et al.,* 1988). In this study, after 7 days at 10 ^{o}C, all the nitrate in the temperate soils had been reduced (92% denitrified and 8% immobilized). This supports the statement made by Christianson (2011) that the sensitivity to temperature may be reduced. This adaptation demonstrates that denitrification may be a major source of nitrate loss in temperate areas in the spring when much nitrate is mobilized from agricultural fields.

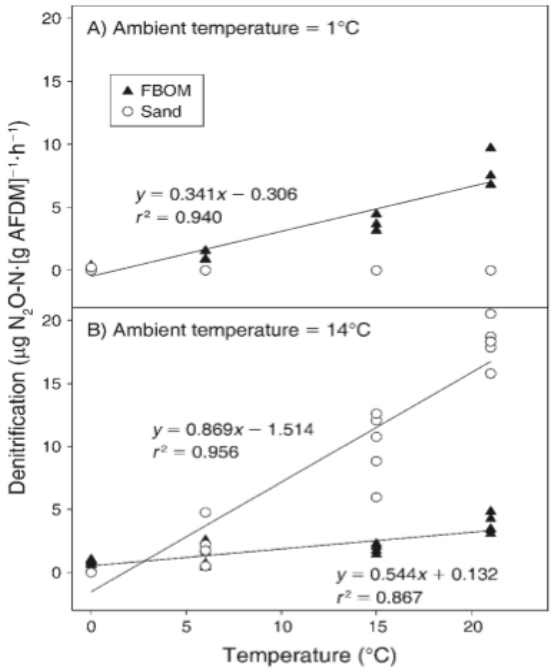

Figure 13. The effect of ambient air temperature on the denitrification rates within sand and fine benthic organic matter (FBOM) at various water temperatures (x-axis) (Roley *et al.,* 2012a). The acronym AFDM stands for ash free dry mass (y-axis).

For these reasons, it is important to test denitrification under a range of climatic conditions, including those found in the Midwest just after the spring snowmelt begins. A temperature of 6 ^{o}C reflects groundwater temperatures in winter and early spring whereas 17 ^{o}C reflects summer conditions in cold climate areas (Addy *et al.,* 2016). Soil in bare ground conditions, such as those found in agricultural fields in southern Minnesota, is typically frozen until early to mid-April (SWROC, ND). From mid-April to mid-May, sub-surface drainage water has been found to be in the 4.4 ^{o}C to 10 ^{o}C range (SWROC, ND). This corresponds to average air temperatures of 7.2 to 14.4 ^{o}C (US Climate Data, ND). By mid- to late-May, the average sub-surface drainage temperature is around 12.8 ^{o}C (SWROC, ND). However, tile drainage can increase soil temperatures by 4 ^{o}C, particularly between May and July (Jin *et al.,* 2008). These air and water temperatures are important to capture in denitrification experiments.

Traditional Bioreactors

Traditional bioreactors are woodchip only media configurations with limited lifespans that have been found to produce a range of nutrient attenuation rates and efficiencies (Blowes, 1994; Christianson *et al.,* 2012). Woodchip bioreactor systems in the Midwestern USA are reported to remove typically less than 10 g N m^{-3} d^{-1} with a range from 2 to 22 g N m^{-3} d^{-1} (Schipper *et al.,* 2010) and efficiencies ranging from 33% to 100% (Christianson *et al.,* 2012; Woli *et al.,* 2010). Woodchip media is expected to last several decades in the field, with half-lives up to 72 years (Blowes, 1994) but have only been found to maintain nitrogen removal for up to 15 years (Robertson *et al.,* 2008). Temperature, carbon source, and saturation all play an important role in woodchip bioreactor longevity. Under ideal conditions, carbon degradation occurs very slowly but unfavorable conditions, such as wet-dry cycles, can greatly increase the rate of degradation and shorten the half-life (Robertson *et al.,* 2008). Reactors that become degraded may then be limited in nitrate removal (Christianson, 2011). More stable, difficult to degrade material may allow bioreactors to last longer in the field under a wider range of environmental conditions.

Alternative Media Bioreactors

Wood-based biochar and corncobs are common alternative media in bioreactor systems. In a column lab study by Zhang (2015), hardwood biochar produced between 43 to 98% removal rates with a 24 hr HRT. In another column experiment, Christianson *et al.* (2011a) found that nitrate concentrations were reduced from 20 to between 9.5 and 11.8 mg L^{-1} (52.5 to 41%) with 14.4 and 13.4 hr HRTs, respectively, using pine biochar as the carbon source. A third column lab study testing the denitrification abilities of corncobs, woodchips, and a combination under 2 ^{o}C and a 12 hr HRT found a removal rate between 7.81 and 1.69 g m^{-3} d^{-1} (16.5 to 3.5%) (Slocum, 2013). Field experiments under a range of temperature conditions with HRTs less than 9 hrs produce 28 to 58% nitrate

removal (Jaynes *et al.,* 2016; Robertson, 2000; Chun *et al.,* 2010; van Driel *et al.,* 2006). In another pilot-scale field experiment, woodchip only reactors outperformed pine-based biochar reactors at low temperatures (average = 9.6 C) when NO_3-N was less than 5 mg L^{-1} (0.41 vs. 0.46 g N m^{-3} d^{-1}; Bock *et al.,* 2016). Wood-based biochar bioreactors have been found to have limited treatment abilities, especially with variation in air temperature (Zhang and Magner, 2014). If a system can be optimized, higher levels of nitrate removal may be possible during colder spring climate conditions when nitrate loading to Minnesota waters is highest.

Conventional Drainage Ditches

Conventional drainage ditches are typically constructed as a trapezoidal channel, with a flat bottom and outside banks with a side slope ratio generally from 1:1 to 2:1 (horizontal: vertical) (Fig. 14; Peterson *et al.,* 2010). The depth of a conventional drainage ditch is usually designed to carry a flow with a recurrence interval from 5 to 100 years (Ward and Trimble, 2004).

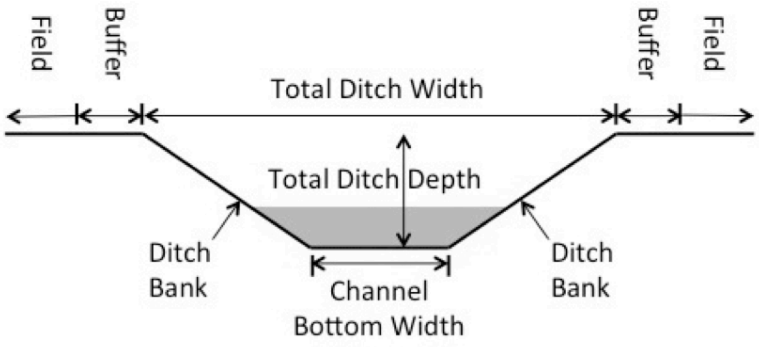

Figure 14. A typical conventional (trapezoidal) drainage ditch cross-section (Kramer, 2011).

The trapezoidal shape of conventional drainage ditches can result in an over-widened channel bottom (Christner *et al.,* 2004). A wide channel bottom greatly reduces flow velocity in the channel during low-flow conditions, which leads to sediment aggradation (Landwehr and Rhoads, 2003; Jayakaran and Ward, 2007). The sediment deposition can reduce the drainage capacity of ditches resulting in high maintenance (cleanout) costs (Christner *et al.,* 2004; Jayakaran and Ward 2007; Peterson *et al.,* 2010). Ditch cleanout disrupts the channel ecology (Kallio *et al.,* 2010) by removing some or all of the existing vegetation and exposing bare soil. After deposited sediment is removed and the channel shape is returned to trapezoidal, the ditch will again begin its movement toward dynamic equilibrium (Magner *et al.,* 2012). If the sediment supply is greater than the sediment transport capacity, sediment deposition will continue to occur, resulting in a cycle of high maintenance costs.

Traditional drainage ditch designs can lack consistent and sustainable amounts of plant biomass. However, the main problem that arises with the trapezoidal design, the toe slope of the ditch bank is continuously exposed to boundary shear forces (Ward *et al.,* 2004; Magner *et al.,* 2012). This continuous exposure leads to reduced soil strength along the toe of the ditch bank (bank/bed interface) and can cause mass wasting and bank sloughing (Ward *et al.,* 2004; Magner *et al.,* 2012). The cycle of stability degradation in traditional design does not provide adequate habitat for aquatic organisms. The dominance of finer bed material, lack of pool-riffle sequences, and shallow pool depth are common characteristics of the trapezoidal ditch that negatively affect biotic integrity.

Novel Multi-Media Bioreactor

Biochar is produced by the pyrolysis of organic material and typically lasts much longer in field applications. Biochar under temperate conditions has an estimated 4000 yr mean residence time in the field (Kuzyakov *et al.,* 2014) by the slow decomposition and leaching of sorbed organics. Walnut shell biochar has

very high carbon and nitrogen sorption, enhancing the retention of nitrate from aqueous solution and a high surface area in comparison to high and low temperature woodstock biochar (Figs. 15 and 16) (Ghazal, 2010; Yao *et al.,* 2012). Biochar polar sites may retain ions as well as enhance microbial colonization due to high surface areas (Kookana *et al.,* 2011; Laird *et al.,* 2010). Biochar may not only enhance the ion exchange capacity but also provide a refugia for microbes, who then further influence the binding of nutritive cations and anions (Liang *et al.,* 2006; Atkinson *et al.,* 2010). Other wood based biochars also show reduced N_2O emissions, a powerful greenhouse gas, particularly after long HRTs (+36 hours), compared to woodchip only reactors (Bock *et al.,* 2015). Walnut shell biochar has been found to increase soil labile nitrogen (Wang *et al.,* 2014), which stimulates the nitrogen cycle and produces higher rates of microbial activity (Spokas, Personal Communication).

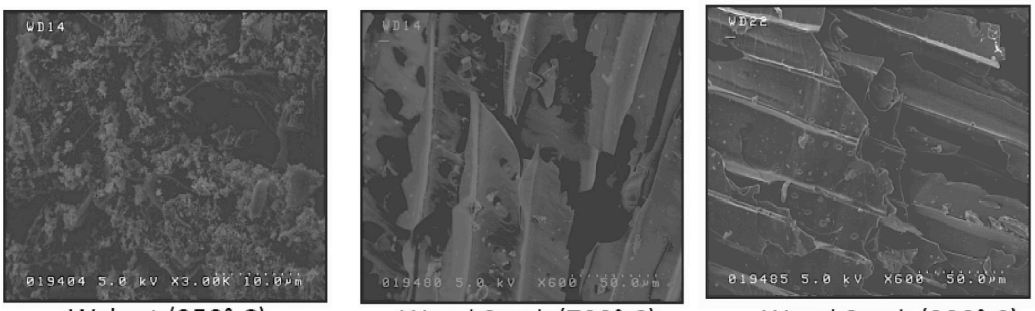

Figure 15. Surface area images of the walnut shell biochar in comparison to the 700 ^{O}C and 900 ^{O}C woodstock biochar (Ghazal, 2010).

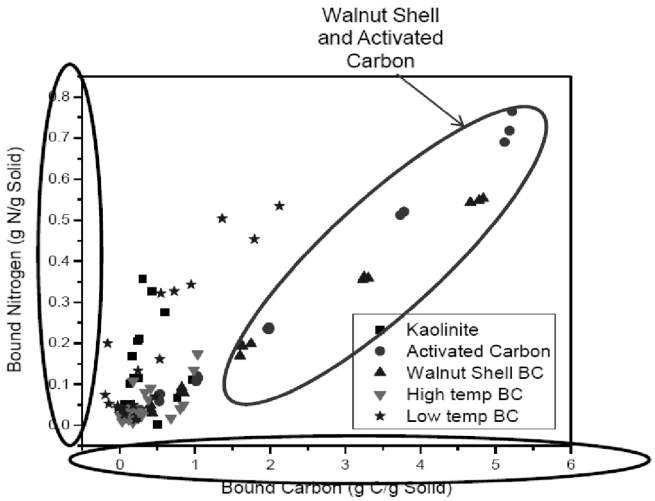

Figure 16. The mass of bound nitrogen and C per gram of soil for 5 tested organic carbons (Ghazal, 2010).

There are no studies that have looked directly at the nitrate removal capabilities of walnut shell biochar. However, some studies have found that it can greatly increase N_2O emissions when used as a soil amendment (Fig. 17; Mukome *et al.,* 2013b). Per the denitrification process, high levels of N_2O as the terminal product indicate that denitrification rates must be high as well. However, higher levels of N_2O may indicate more incomplete denitrification (Robertson *et al.,* 2008). Other studies state that denitrification may be altered by the introduction of biochar (Sanchez-garcia, 2014). However, this process is highly complex and likely soil type dependent (Suddick and Six, 2013; Sanchez-garcia, 2014). Nitrous oxide emissions from "biochar amended soils are still under investigation and can be influenced by the feedstock origin (e.g., animal litters and green wastes) and manufacturing process (e.g., temperature and pressure), as well as local soil conditions, agricultural management activities (e.g., nitrogen fertilizer amounts and timings), and climate," (Suddock and Six, 2013). Biochar is generally thought to retain nutrients (Beck *et al.,* 2011) where microbial communities may have a longer period of time to utilize them.

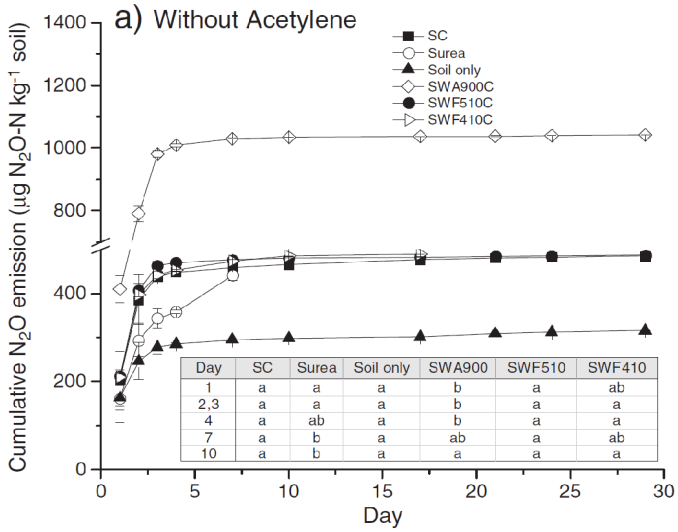

Figure 17. Cumulative N_2O emissions over time for various biochar treatments without acetylene (S=soil, C=compost, WA900=walnut shell biochar, WF410=low temperature wood biochar, and WF510=high temperature wood biochar) (Mukome *et al.,* 2013b).

A similar system was investigated as a green roof tray experiment, which tested nutrient levels in rainfall discharge on non-biochar and biochar amended (7% w/w) soils planted with ryegrass (Beck *et al.,* 2011). This study used a mixed biochar type; the blend was 70% agricultural char, derived from the processing of rice hulls, pecan shells, walnut shells, and coconut shells, and 30% manufactured waste char derived from pyrolysis of passenger car tires. This study was performed under two, 30-min rainfall simulations with 2 hrs of runoff collection after each event. They found this media and vegetation combination released 97% less nitrate in comparison to the no biochar control. When used as a soil amendment, experiments demonstrate that nutrients in the effluent can be greatly reduced by the use of biochar.

Another similar experiment tested the nitrate removal abilities of corncobs (CC) and corncobs followed by an additional chamber containing a plastic biofilm carrier (CC-PBC). This column laboratory experiment was conducted under two temperatures (1.5 ^{o}C and 15.5 ^{o}C) with a 12 hr HRT. Corncobs with a plastic

biofilm carrier significantly increased NO_3-N load removal by 9.2% (53.7 and 44.5% NO_3-N removal, CC vs. CC-PBC, respectively) when averaged across temperatures (P = 0.032) (Feyereisen *et al.,* 2017). However, the main effect of treatment was significant at 15 ^oC (P = 0.065) but not at 1.5 ^oC (P = 0.170), thus the combined effect of treatment and temperature was not significant (P = 0.21) (Feyereisen *et al.,* 2017). This study further demonstrates that low temperatures create challenges for nitrate removal in a variety of experimental situations.

Brotex is a fibrous PBC consisting of a matrix of recycled plastic fibers whose original use was in the creation of floating treatment wetlands (FTW) (Fig. 18). “The island bodies primarily comprise fine (0.007-inch diameter) polymer strands that are intertwined and bonded to provide a three-dimensional non-woven matrix that is highly porous, permeable, and resistant to environmental degradation,” (Stewart *et al.,* 2008). The material has a high surface area, serving as a microbial substrate to support larger microbial population densities (Fig. 19). “The floating island matrix, with its dense fibers and porous texture, is the perfect surface area for growing large amounts of microbes (in the form of biofilm) in a short time,” (Floating Island International). Floating treatment wetlands have produced 78 - 100% NO_3 removal as a floating treatment island with 100% coverage vs. 42 - 46% for a conventional treatment wetland (Van de Moortel *et al.,* 2010; Stewart *et al.,* 2008). Other studies have investigated the use of other similar PBCs in settings including wastewater (Andersson *et al.,* 2008), with other carbon sources (Saliling *et al.,* 2007), for removing other contaminates (Cantafio *et al.,* 1996), and suspended in stirred reactors (Welander and Mattiasson, 2003). However, there are no studies that have studied the effects of Brotex (or a similar) material in a bioreactor system.

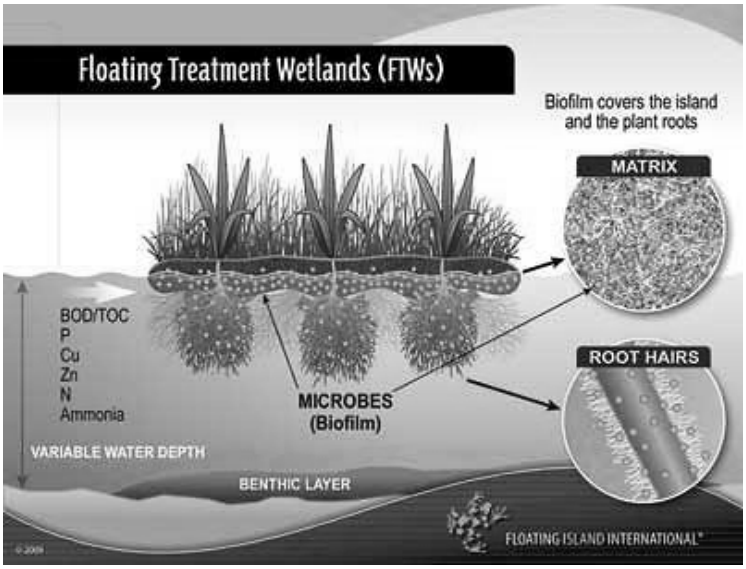

Figure 18. Floating Treatment Wetland diagram depicting the important characteristics and functions of the floating island system (Source: Reinsel, M. (WaterWorld). 2017. Floating Wetlands Help Boost Nitrogen Removal in Lagoons. http://www.waterworld.com/articles/print/volume-28/issue-6/editorial-features/floating-wetlands-help-boost--nitrogen-removal-in-lagoons.html).

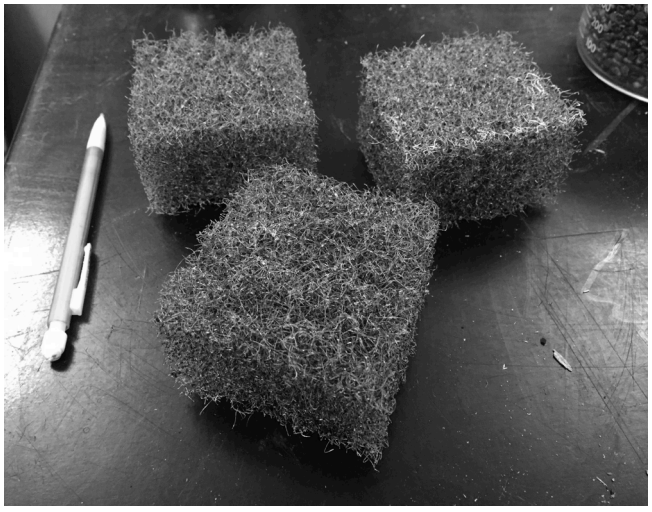

Figure 19. Brotex matrix (recycled PET material) cut into blocks for use in the bioreactor laboratory experiment. Notice the interwoven fibers that provide surface area for microbial growth.

Improvements in Fluvial Stability Associated with Two-stage Ditch Construction in Mower County, Minnesota

Lori Krider[1], Joseph Magner[1], Brad Hansen[1], Bruce Wilson[1], Geoffrie Kramer[2], Joel Peterson[3], and John Nieber[1]

[1]Department of Bioproducts and Biosystems Engineering, University of Minnesota

[2]RESPEC Consulting and Services, Roseville, Minnesota

[3]University of Wisconsin, Agricultural Engineering Technology, River Falls, Wisconsin

Abstract: Water quality and stream habitat in agricultural watersheds is under greater scrutiny as hydrologic pathways are altered to increase crop production. Agricultural drainage ditches function to remove water quickly from farmed landscapes. Conventional ditch designs lack the form and function of natural stream systems and tend to be unstable and provide inadequate habitat. In October of 2009, 1.89 km of a conventional drainage ditch in Mower County, Minnesota, was converted to an alternative system with a two-stage channel to investigate the improvements in water quality, stability, and habitat. Longitudinal surveys show a 12-fold increase in the pool-riffle formation. Cross-sectional surveys show an average increase in bankfull width of approximately 10% and may be associated to an increased frequency in large storm events. The average increase in bankfull depth was estimated as 18% but is largely influenced by pool formation. Rosgen Stability Analyses show the channel to be highly stable and the banks at a low risk of erosion. The average bankfull recurrence interval was estimated to be approximately 0.30 years. Overall, the two-stage ditch design demonstrates an increase in fluvial stability, creating a more consistent sediment budget, and increasing the frequency of important in-stream habitat features, making this best management practice a viable option for addressing issues of erosion, sediment imbalance, and poor habitat in agricultural drainage systems.

KEY WORDS: fluvial processes, best management practices (BMP's), physical stability, drainage ditches, erosion, in-stream habitat.

BACKGROUND

The southern Minnesota landscape is predominantly corn and soybean row crops. Tile drainage and ditching is a common practice to manage water conveyance. Drainage ditches are often undersized and trapezoidal shaped, causing them to be unstable. The trapezoidal shape of conventional drainage ditches can result in an over-widened channel bottom (Christner *et al.,* 2004). This over-widened channel bottom without adjacent floodplain benches causes continuous exposure of the outer ditch banks to water, leading to reduced soil strength along the toe of the ditch bank (bank/bed interface), which can cause mass wasting and bank sloughing (Fig. 1; Ward *et al.,* 2004). The wide channel bottom also greatly reduces flow velocity in the channel during low-flow conditions, which leads to sediment aggradation (Landwehr and Rhoads, 2003; Jayakaran and Ward, 2007). This sediment deposition can reduce the drainage capacity of ditches, resulting in high maintenance (cleanout) costs (Christner *et al.,* 2004; Jayakaran and Ward, 2007; Peterson *et al.,* 2010). If the sediment supply is greater than the sediment transport capacity, sediment deposition will continue to occur, resulting in a cycle of high maintenance costs.

After the ditch returns to its trapezoidal shape by the removal of deposited sediment, channel evolution models show that it moves toward dynamic equilibrium through a process of sediment aggradation, incision, and bank sloughing (Simon and Hupp, 1986). This is similar to the findings of Magner *et al.* (2012) in that some unmaintained drainage ditches in the Des Moines Lobe till area will naturally form floodplain benches within the channel to produce bankfull channel widths and cross-sectional areas, similar to natural streams with comparable hydrologic and watershed characteristics. Channels with floodplain benches have a more self-sustainable morphology and exhibit more stable sediment transport processes similar to those found in unchannelized streams (Davis *et al.,* 2015; Simon and Hupp, 1985; Rosgen, 1996).

Without maintenance, channelized ditches often naturally evolve to a two-stage channel type (D'Ambrosio *et al.,* 2015). Two-stage drainage ditches are designed to mimic the stable conditions found in natural low-order streams (Ward *et al.,* 2004; USDA-NRCS, 2007; Krider *et al.,* 2014; Fig. 20). They are usually constructed to replace conventional ditches and are most beneficial at sites where present conventional drainage ditches are unstable (Kramer, 2011). A low-flow channel is sized to replicate that of a natural channel (in the surrounding region) with a similar drainage area, soils, topography, and climate (Kramer, 2011; Krider *et al.,* 2016a). Two-stage channels are designed with small benches on both sides of the low-flow channel to serve as a floodplain and to create a bankfull channel, filling in some of the extra width produced during channelization. The benches allow for dissipation of the fluvial energy associated with high flow rates (Ward *et al.,* 2004). Dense plant growth on the benches also creates greater stability via the root system and reduces water velocities via the above ground mass of various grasses and forbs found to be present within two-stage ditches in the Midwest (Krider *et al.,* 2016c; Powell and Bouchard, 2010). The increased number of pool-riffle sequences allows more deep areas for fish refugia while the riffles provide habitat for macroinvertebrates, thus increasing fish biotic integrity (Krider *et al.,* 2016c; Lau *et al.,* 2006). These features have been found to increase fish habitat diversity and stream health as characterized by vegetation surveys and measured with a fish IBI (Krider *et al.,* 2016c).

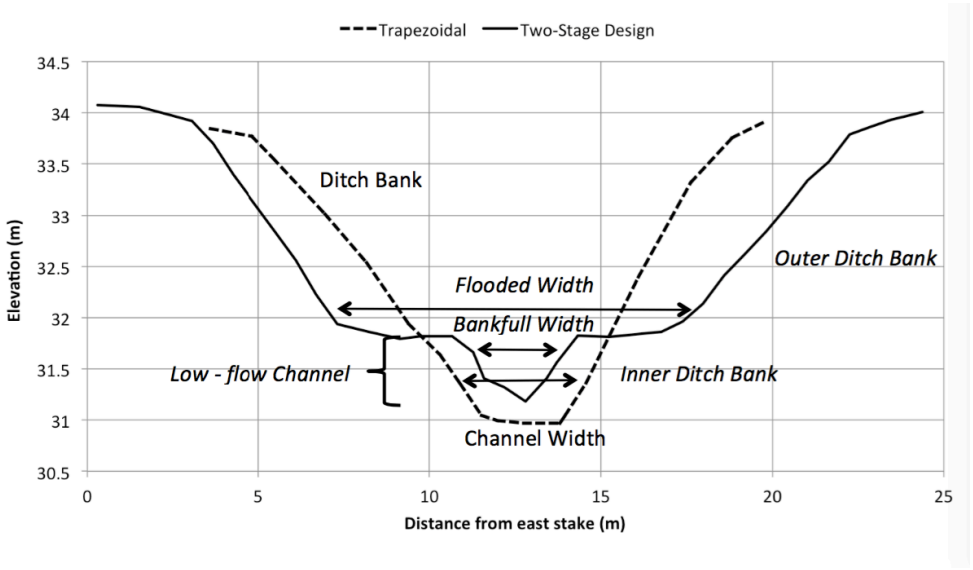

Figure 20. A typical conventional (dashed line) drainage ditch cross-section and a two-stage drainage ditch cross-section (solid line). Two-stage ditch features are written in italics.

The two-stage ditch design has several features that can increase fluvial stability. A reduction in erosive forces at the toe of the outer ditch bank is expected as the total shear forces are spread over a larger surface area (Ward *et al.,* 2004). Increased stability at the toe of the outer ditch banks reduces the potential for sloughing and mass wasting (Kramer, 2011). In addition, the design has outer banks with a more gradual sideslope (Fig. 20). This feature, combined with the bench construction, makes the two-stage ditch wider than the conventional design and can support larger flow capacities (Kramer *et al.,* 2016; Krider *et al.,* 2014). With less erosion and sediment deposition, this design reduces ditch cleanout costs associated sediment imbalance (Ward *et al.,* 2004; Powell *et al.,* 2007; Peterson *et al.,* 2010).

Experimental Site: Mullenbach Drainage Ditch

The Mullenbach Drainage Ditch is located in rural Mower County in southern Minnesota (MN), USA, approximately 30 km southeast of the city of

Austin, MN (Fig. 21). It is in the headwaters of the Little Cedar River within the Upper Cedar River Watershed (8-digit Hydrologic Unit Code (HUC): 07080201). The Mullenbach Two-Stage Ditch empties into the Little Cedar River approximately 4 km (2.48 mi) downstream of the constructed two-stage ditch reach, which then flows south into the state of Iowa. The watershed area is 12.6 km^2 (3,102 acres) and the land use is predominantly corn and soybean row crop agriculture.

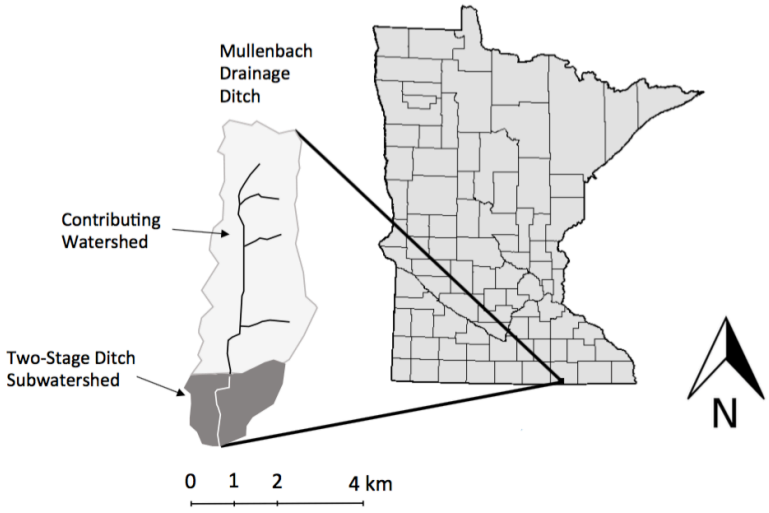

Figure 21. Location of the Upper Cedar River HUC 8 Watershed within the State of Minnesota (left) and the location of the Little Cedar River along with the DNR's 24K Streams to show important water bodies within the Upper Cedar River HUC 8 Watershed (right).

Unstable drainage ditches within the Upper Cedar River Watershed likely contribute to the turbidity impairments found in the watershed (Manger *et al.,* 2010). The Mullenbach Drainage Ditch, as conventionally (trapezoidal) designed, had numerous issues with stability and was scheduled for maintenance in 2009 or 2010. At this site, bank instability caused by seepage, planar failure, and toe erosion on ditch banks, as well as tile outlet failures where present (Kramer,

2011). Two-stage ditch conversion was supported by the landowners surrounding the ditch (Kramer, 2011; Krider *et al.,* 2016a). With funding and assistance from The Nature Conservancy and the Mower County Soil and Water Conservation District, 1.89 km (1.17 mi) of the Mullenbach Drainage Ditch was converted to the two-stage design in October of 2009.

METHODOLOGY

Design and Construction

At the Mullenbach Two-Stage Ditch site, longitudinal and cross-sectional surveys were conducted pre-two-stage ditch construction to set design and construction specifications as well as establish benchmarks for the ditch (Krider *et al.,* 2016b). A ratio of 3:1 flood width to low-flow channel width was used in order to reduce excavation costs and reduce the land loss of adjacent agricultural fields. This ratio falls within the recommended range of 3:1 to 5:1 provided by Ward *et al.* (2004) and Powell *et al.* (2007) (Krider *et al.,* 2016a). The outside ditch bank slope was designed at 2:1. Approximately 80% of the existing low-flow channel prior to construction was within the design specifications, thus, was left intact (Krider *et al.,* 2016a). If the low-flow channel width was greater than 3.35 m (10.99 ft), soil was added to one or both banks to narrow the channel to a width to 3.05 m (10.00 ft) (Kramer, 2011). Each bench width (toe of the outer bank to the top of the low-flow channel) was designed at 3.28 m (10.76 ft) and constructed between 2.74 and 3.35 m (8.99 and 10.99 ft) (Table 1; Krider *et al.,* 2016a). The cross-sectional flooded width (across the benches and low-flow channel) was designed at 9.83 m (32.24 ft) and constructed at 9.75 m (31.98 ft) (Table 1; Krider *et al.,* 2016a). The ditch top width varied along the profile to accommodate the channel and bench widths, to provide the 2:1 bank slope, and to match the existing top elevation of the ditch.

Table 1. Design and constructed channel dimensions for the Mullenbach Two-Stage Ditch.

Channel Feature	Designed (m)	Constructed (m)
Bankfull channel depth	0.57	~0.61 (varies)
Bankfull channel top width	3.28	2.74 to 3.35
Bench width	3.28	2.74 to 3.35
Flooded width	9.83	9.75

Longitudinal and Cross-Sectional Surveys

Longitudinal and cross-sectional surveys were also used to measure morphologic changes that took place over time. All channel geomorphic measurements were completed with a laser level or a total station and a stadia rod. The overall vertical change in the longitudinal profile was computed using the trapezoidal rule to calculate the area (along the channel profile) of the streambed thalweg relative to the project datum. The calculated area was divided by the length of the channel survey to determine average bed elevation. Measurements were taken at distinguishable changes in relief, and not at set intervals, to ensure the capture of key features. Longitudinal profiles were conducted in 2009, 2010, 2011, and 2013. Two surveys were conducted in 2009, one prior to construction (April) and one during construction (October). The 2009 pre-construction longitudinal profile was used as a baseline to compare to changes from post-construction surveys in 2010, 2011, and 2013. Longitudinal surveys were used to monitor changes in slope, pool-riffle formation, and channel depth. In this article, pools are described as localized maximum thalweg depth and riffles as localized minimum thalweg depth in a sequenced pattern with one feature following the other.

Seven cross-sectional surveys were conducted as part of the initial pre-construction site survey in April 2009 (Fig. 22). Cross-sectional surveys were conducted to monitor changes in inner and outer ditch bank slope as well as floodplain and channel widths. Four of the cross-sections were surveyed in October 2009 (pre-construction), all seven were surveyed in October 2010 and

April 2012, and six were surveyed in November of 2013 (all post-construction). The longitudinal and cross-sectional data were analyzed using RiverMorph Version 4.3 and the Reference Reach Spreadsheet (RiverMorph, LLC., 2010; Mecklenburg, 2006). These software packages were used to compute channel characteristics, such as low-flow width, cross-sectional area, bench elevation, as well as mean and maximum depth in the low-flow channel (Kramer, 2011; Krider *et al.,* 2016a). Profile data were also analyzed for pool-riffle sequences and low-flow channel slope.

Figure 22. Satellite Image of the Mullenbach Two-Stage Ditch Site showing the measured channel cross-sections and linear wetland locations (Base Map © Google EarthTM, 8/24/2013).

Stability and Bankfull Dimensions

The Modified Pfankuch Channel Stability Rating was calculated to determine the overall channel stability before and after two-stage construction (Rosgen, 2008). This stability rating can be used to indicate the relative sediment supply of a channel. It is largely qualitative with four condition categories of

excellent, good, fair, and poor. For indices that are quantitative, each condition is associated to a range of values (as percentages). A total of 15 indices are split into three location categories to evaluate the upper and lower banks as well as the channel bottom. For the purposes of evaluating the ditch, the components are described as the upper, outer banks and the lower, inner banks (Fig. 12). For indices in which the score didn't align very well with the two closest Pfankuch conditions, an average value was taken between the two for the numeric score and assigned as the lesser of the two conditions for tallying the number of indices for each condition. The Pfankuch calculates the stability rating based on the existing stream type. However, if the channel is highly modified from it's natural state then an existing stream type cannot be determined. The potential stream type for 2009 was chosen to match the actual stream type found in 2013.

Pre-construction bankfull conditions were estimated using two methods. One of the methods used data from observed channel cross-sections and the other method used characteristics obtained from regional curves. Observed channel features were taken from cross-sections that had distinct channel features and were relatively stable. The latter criterion required that features be consistent with data obtained from other ditches in the region. The selected observed cross-sections were used to determine the approximate width, depth, and cross-sectional area of the pre-construction low-flow channel. This information is then used to compute a discharge rate and estimate a stream classification. Regional curves for Southern Minnesota ditches were also used to determine the features of the pre-construction, low-flow channel (Magner and Brooks, 2007; Krider *et al.,* 2061a). Since both methods are partially dependent on stable ditch cross-sections in the region, similar pre-construction, bankfull conditions are obtained from our two methods.

The Bank Erosion Hazard Index (BEHI) was used to analyze bank stability for 2013. This index examines and quantifies stability based on numerous bank characteristics, including study bank height, bankfull height, root depth, root

density, surface protection, and bank angle (Rosgen, 2008). This index uses graphical conversions between measured field variables to produce a rating score for each category (Rosgen, 2008). The sum of the scores for each category produces an adjective score (very low to extreme bank erosion hazard) and a total numeric score (Rosgen, 2008). This index is typically calculated using measurements taken over a small section of the bank with the same characteristics. We applied this method to produce an overall summary of the two-stage ditch bank stability using generalizations of features over the entire length of the ditch. By nature of the low-flow channel, the bankfull height is equal to its study bank height. Left and right bank angles were calculated from the first two survey points at, or just below, the bankfull elevation and averaged across all cross-sections. Root density and surface protection percentages are subjective and based on visual estimation. Measurements were inferred from pictures and field notes, as well as from extensive knowledge of the site characteristics.

Channel Morphology

The Mecklenburg Reference Reach Spreadsheet was used to calculate various channel morphology characteristics based on the cross-sections from pre-and post-construction field surveys (Mecklenburg, 2006). Bankfull discharge is calculated as velocity multiplied by bankfull cross-sectional area. Mean channel velocity is estimated using Manning's equation based on hydraulic radius, energy slope approximated by the channel slope, and a Manning's n value. A Manning's n of 0.05 was chosen to represent the thick riparian Reed Canary Grass that bends over into the channel. The entrenchment ratio (flood prone width divided by bankfull width where the flood prone width is at the stage that is twice the maximum bankfull depth), width to depth ratio (mean values at bankfull), channel slope, and channel sediment type based on visual determination were used to characterize the stream type based on Rosgen's Classification of Natural Rivers (Rosgen, 2008).

Bankfull Flow and Recurrence Interval

Based on photographs of bankfull and greater than bankfull storm flow events, bankfull flow corresponds to full flow in the 0.9-m (2.95 ft) H-flumes (Brakensiek *et al.,* 1979) installed at the upstream and downstream ends of the ditch. Bankfull flow (after two-stage construction) was also calculated using the Mecklenburg Reference Reach Spreadsheet as an average for the 6 cross-section surveys from 2013. The recurrence interval of bankfull flow was obtained using the Storm Water Management Model (SWMM, Rossman, 2008). This model was used to create inflow and outflow hydrographs for the two-stage retrofit over a 29-year period (1971-1999) using precipitation for the Spring Valley Watershed located about 30 km (18.63 mi) east of our site (Peterson, 2010). Daily maximum and minimum flow rates were generated and the average of all average daily flow rates was used for comparison to bankfull discharge. Greater than bankfull discharge occurred when the SWMM model-generated a flow rate exceeding the flow rate determined by the maximum capacity in the flume and, separately, the average bankfull flow rate determined by the Reference Reach Spreadsheet. Our analysis uses an average flow rate between the 2013 Reference Reach Spreadsheet bankfull flow estimate and the flume calculated flow rate as well as an average of upstream and downstream SWMM generated flow rates. The number of days between the start of bankfull events is the bankfull recurrence interval and the sum of events based on the first day in a series in which the maximum daily flow rate exceeded the bankfull discharge. Events are considered independent if there are one or more days with less than bankfull flow between days with greater than bankfull flow. Since we are assessing both the recurrence interval and the number of events based on the start of an event, bankfull flow lasting more than a day were not considered independent events.

RESULTS AND DISCUSSION

Analysis of Physical Features

Longitudinal Profile.

Pool-riffle formation in streams and ditches provides variation in depth and velocity that is important for the ecological health of fish communities (Gorman and Karr, 1978). Prior to construction, the ditch profile had little channel relief and few pool-riffle formations (Figs. 23 and 24). The pool-riffle sequences are not distinct and are difficult to determine. Most of the pool-riffle formation occurs in the downstream 700 m of the channel. The elevation of pools and riffles is highly variable, particularly around 1500 m where the difference between pool and riffle elevations is 0.7 m (2.30 ft). There is a maximum of five pool-riffle sequences in the pre-construction longitudinal profile. Generally, the ideal stream type in this region given the watershed characteristics (E5 streams) is described as having numerous pool-riffle sequences in a highly meandering channel (Rosgen, 2008). Based on the Washington Qualitative Habitat Assessment Survey, the optimal pool to riffle ratio is five to seven (indicating a frequent sequence) (Plotnikoff and Polayes, 1999).

Figure 23. Photograph from within the Mullenbach Two-Stage Ditch showing bank failure (left), sediment aggradation (right), and few pool-riffle formations prior to two-stage construction

Figure 24. Mullenbach Two-Stage Ditch longitudinal channel thalweg elevations in profile from prior to (April 2009) and during (October 2009) two-stage construction.

The post-construction longitudinal survey completed in October 2010 has a higher pool-riffle sequence frequency (Fig. 25). This survey shows 24 pools and 25 riffles. There are few pool-riffle sequences between 600 and 1000 m (1968 and 3280 ft). The pool-riffle sequences are most evident between 200 and 400 m (656 and 1312 ft) as well as from 1100 to 1700 m (3608 to 5576 ft), where they were also most apparent prior to construction. Variability is likely due to pre-construction conditions setting a baseline for channel evolution. The pools and riffles have less distance between features in the 200 to 400 m section compared to the 1100 to 1700 m section. In the 200 to 400 m section, the average distance between pools and riffles in 18.2 m (59.70 ft). However, from 1100 to 1700 m, the pools and riffles are, on average, 29.0 m (95.12 ft) apart. There is also a dampening of the extreme high and low elevation values around 1500 m (4920 ft).

Figure 25. Mullenbach Two-Stage Ditch longitudinal channel thalweg elevations in profile from pre-(April 2009) and post-(October 2010) construction surveys.

There are reaches where the channel bed elevation has noticeably increased (notably upstream of 396 m (0.25 mi) and downstream of the field road crossing at 1081 m (0.67 mi). The survey also shows newly developed pool-riffle sequences in areas of channel aggradation from newly deposited bed sediments. A comparison shows an overall aggradation of 0.15 m (0.49 ft) from pre-construction to October 2010 (Table 2). The aggradation was likely the result of increased sediment from pre-construction instability and from ditch construction before the banks and floodplain could re-vegetate due to late fall flooding. This trend is consistent with the observations of recently constructed two-stage drainage ditches in Ohio, Michigan, and Indiana made by Kallio *et al.* (2010). This is also demonstrated by the fact that from 2010 to 2013, the channel aggraded slightly (another 0.02 m or 0.07 ft) for a total aggradation of 0.17 m (0.56 ft) from pre-construction to 2013. Since the benches became fully vegetated as of late 2010, there has been little additional sediment supply and the channel elevation has stabilized.

TABLE 2. Average elevation and average change in elevation (between successive years unless otherwise noted) of the Mullenbach Two-Stage Ditch channel from 0 to 1900 m for three longitudinal profiles. The section from 0 to station 8+00 was highly influenced by upstream inputs as well as the flume so it was removed from the analysis of this feature.

Measurement Date	Average Elevation (m)	Change in Elevation (m)
Prior to construction (April 2009)	29.28	
During construction (Oct.-Nov. 2009)	29.31	0.03
Oct. 2010	29.43	0.12
Nov. 2013	29.45	0.02
April 2009 to Nov. 2013		0.17

The post-construction longitudinal survey conducted in November of 2013 is quite different than the pre-construction survey (Fig. 26). These features are illustrated well with a close-up on the section from 200 m to 800 m (656 to 2624 ft) (Fig. 27). The first 100 m (328 ft) downstream of the north culvert is highly influenced by upstream conditions but is also affected by the flume put in at about 100 m in 2010. Here, the flume is forcing an artificial riffle to form. Upstream of the flume, coarse material from an unknown origin, likely washed out from the gravel road, collected within the channel while fine sediment was flushed out. The flume was removed from the channel in 2014 and it is expected that the low-flow channel will cut through the coarse sediment to form a new, lower elevation channel over time. Downstream of the flume, there is a gradual pool formation, likely due to the sediment deprivation caused by the sediment collection upstream of the flume. Conditions began to stabilize and pool-riffle sequences began to form about 80 m south of the flume where the influence of the flume likely had a small effect.

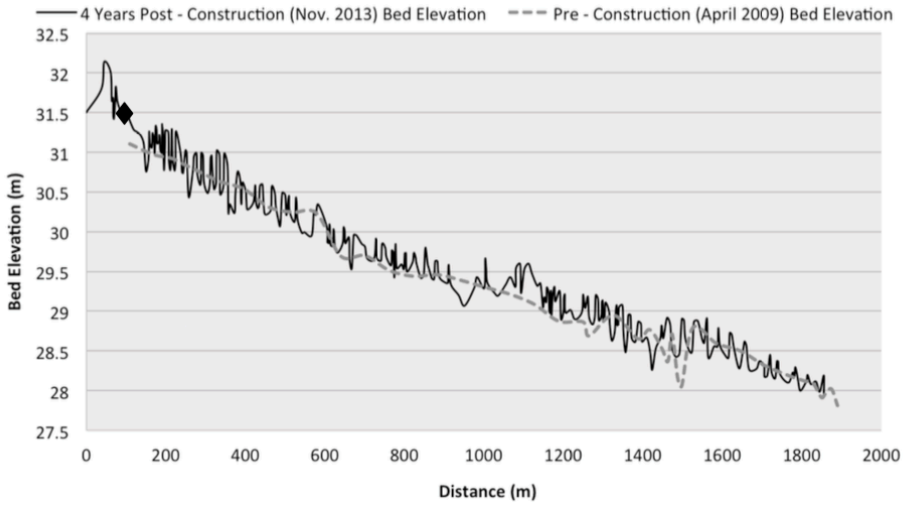

Figure 26. Mullenbach Two-Stage Ditch longitudinal channel thalweg elevations in profile from the pre-(April 2009) and four years post-construction (November 2013) surveys. The diamond indicates the location of the upstream flume

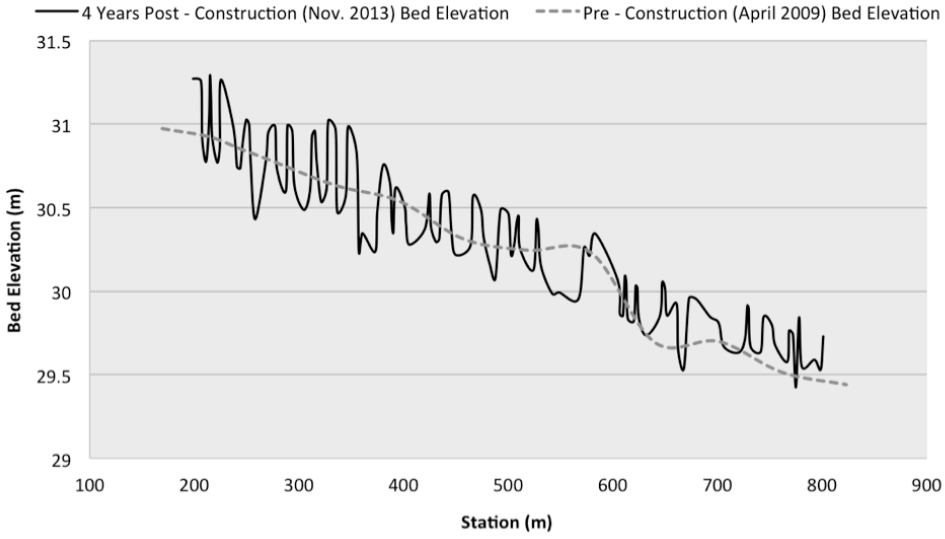

Figure 27. A close-up section (200 m to 800 m) of the Mullenbach Two-Stage Ditch longitudinal channel thalweg elevations in profile from the pre-(April 2009) and four years post-construction (November 2013) surveys

The 2013 profile survey found 68 pool-riffle sequences, which is a 12-fold increase in the number corresponding to pre-construction of the two-stage ditch.

In the upper 915 m of the ditch the aggraded sediment has been scoured out by a number of large runoff events. The distance between pools and riffles has decreased considerably to an average of 13.74 m (45.07 ft) with an average distance of 27.12 m (88.95 ft) between riffles and an average distance between pools of 27.54 m (09.33 ft). The average cross-section stream width based on 2013 data (6 points, top width of the bankfull channel) is 4.37 m (14.33 ft). This gives a pool to riffle ratio (as the distance between riffles divided by the stream width) of 6.21. This falls within the optimal pool to riffle ratio of five to seven (indicating a frequent sequence) (Plotnikoff and Polayes, 1999). There are clear transitions between pools and riffles (i.e. glides and runs), further indicating the formation of a natural sequence of stream features. The bottoms of the pools are scoured down to the clay till with the riffles being comprised of large sand and gravel. The downstream section has aggraded sediment that has yet to be moved downstream of the two-stage ditch. The pools and riffles formed in this section are comprised of redistributed sand with no clay till exposed.

Cross-Section Surveys.

Cross-sections at three different representative locations along the ditch length show changes over time (Figs. 9-11). The pre-construction cross-section is the most apparently different of all the dates. This depicts the wide low-flow channel, the steep banks, and the undersized ditch width. The low-flow channel depth appears to be returning to the pre-construction channel depth, possibly indicating the flushing of fine sediment due to the increased velocities in the low-flow channel (Fig. 28). There is also the formation of a pool between 2012 and 2013 (Fig. 29). Since the ditch was constructed at an average depth, pools are formed where depth has increased from the constructed depth; riffles are decreased where depth has decreased from the constructed depth. It also shows the linear wetland as a smooth, slight reduction in elevation below bankfull along the east bench near the ditch bank. There is the formation of a “false bench”

where the riparian vegetation has folded over into the channel, slowing velocity, and collecting loose sediment, which then builds up on the side of the low-flow channel (Figs. 28 and 30). The formation of a true, new bench within the low-flow channel would take considerably longer. If the new bench was formed only on one side of the channel it may be the start of a meander build. However, “false bench” sediments are likely flushed out regularly during high flow events. The three surveys post-construction are similar to one another with minor shifts, particularly in bankfull depth and width, over time. These minor shifts may be attributed to sediment flushing and redistribution as well as pool-riffle formation.

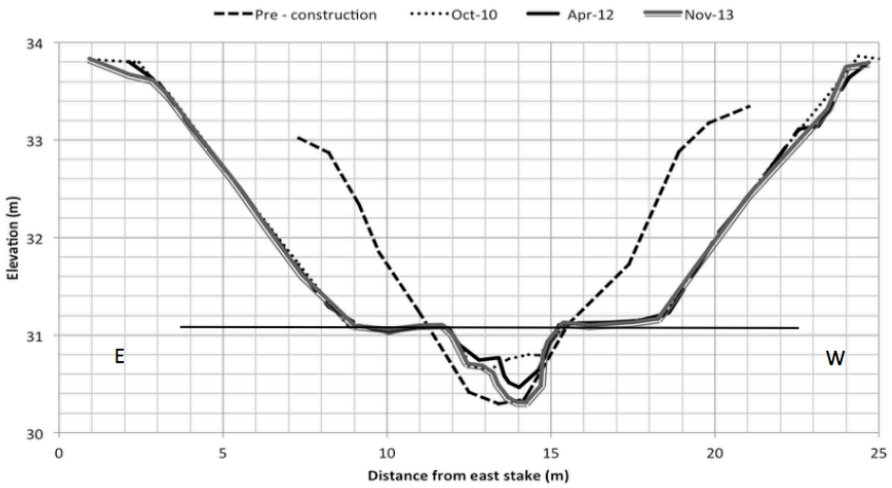

Figure 28. Mullenbach Two-Stage Ditch cross-section survey comparison between years at 447 m (bankfull indicated by the solid, black horizontal line; looking south downstream).

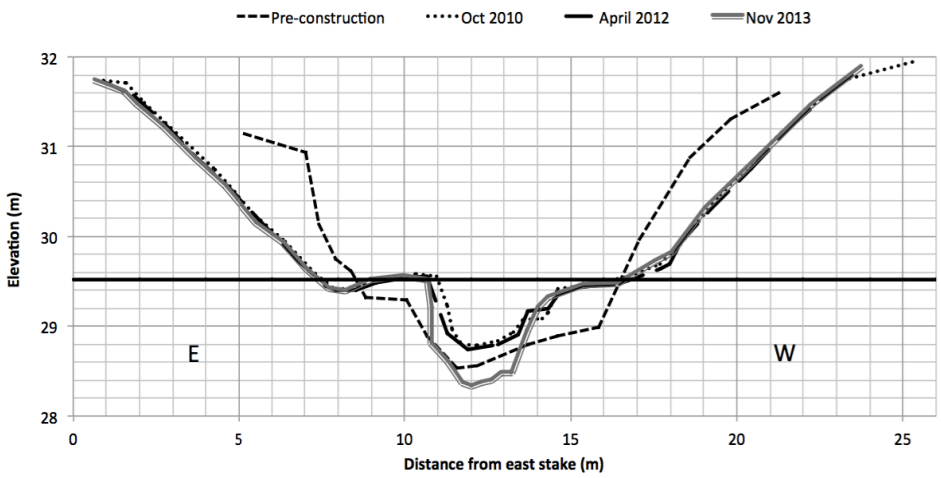

Figure 29. Mullenbach Two-Stage Ditch cross-section survey comparison between years at 1419 m (bankfull indicated by the solid, black horizontal line; looking south downstream)

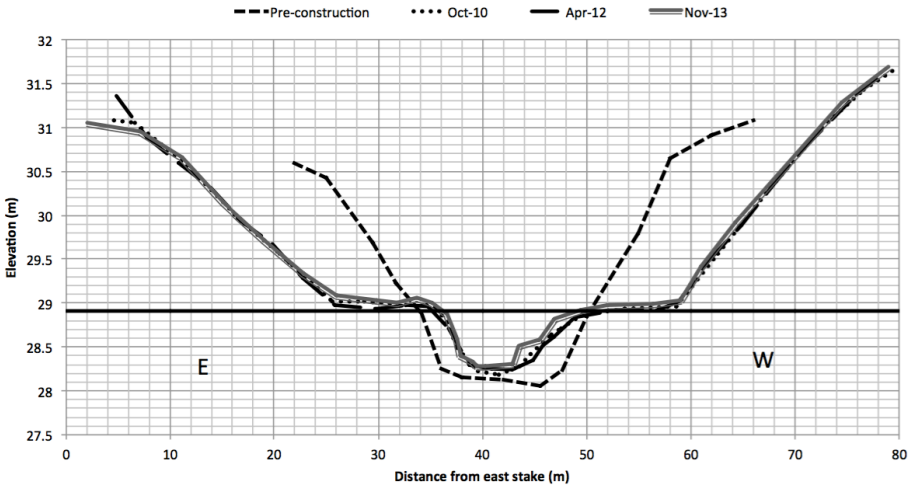

Figure 30. Mullenbach Two-Stage Ditch cross-section survey comparison between years at 1780 m (bankfull indicated by the solid, black horizontal line; looking south downstream)

Pre-construction channel widths were used as a guideline for bankfull channel widths during construction. During the pre-construction survey in 2009 the channel widths were recorded at 36 locations along the ditch. These pre-

construction channel widths were bank to bank and do not correspond to the full ditch width of the channel with benches after construction. The elevations of the benches during construction were designed as the bankfull elevation of the low-flow channel. There was no measured bankfull elevation prior to construction. The average of the 36 width measurements was 3.64 m (11.94 ft, SD = 1.37 m) (Table 3). However, this average includes measurements made on an approximately 245 m (803.60 ft) over-widened section of the ditch at a location of approximately 1600 m (5,248 ft, 7 measurements). This area is dominantly sand from the historic streambed, which is particularly erodible and not representative of the overall channel. During construction, spoil material from the excavation was added to this section to narrow the low-flow channel (Kramer, 2011; Krider *et al.,* 2016a). The average channel width over this section was 5.39 m (17.68 ft). By removing the data from this over-widened section to produce a more representative value for comparison between years, the average channel width was 2.90 m (8.53 ft) with a standard deviation of 0.67 m (2.20 ft, see Table 3). This matches well with the design bankfull width of 3.05 m and falls within the standard deviation range (Krider *et al.,* 2016a).

Investigation of the potential causes for this increase in bankfull width shows that it might be related to an increased frequency of large flow events, but probably not related to an increase in average annual precipitation. Annual precipitation in 2011 and 2012 was much lower (68.17 and 56.33 cm or 26.86 and 22.19 in, respectively) than the annual average from 1981 to 2010 (87.76 cm or 34.58 in), somewhat below average in 2009 (83.51 cm or 32.90 in), and considerably above average in 2010 and 2013 (97.99 and 100.36 cm or 38.61 and 39.54 in, respectively) (NOAA Weather Service, ND). Storm event data (flood, flash floods, and heavy rain) was obtained from October 1, 2009 through November 31, 2013 for Mower County, MN, from NOAA's National Weather Service Storm Events Database (NOAA, 2007). A total of 19 of the 40 flood and flash flood events as well as all of the heavy rain events (eight), all as defined by

NOAA (2007), since 1996 occurred between 2010 and 2013 (NOAA, 2007). These storm events could have played in role in the increase in bankfull width found to have occurred within the two-stage ditch between 2009 and 2013.

We can use the designed bankfull width of 3.05 m to compare the bankfull width of the low-flow channel obtained from post-construction surveys (see Table 3). In the 2013 survey, there is no longer an over-widened section near 1600 m. This table shows an average increase from the designed channel width of 3.05 m for each successive survey. The average bankfull width from all cross-sections from the November 2013 survey was 3.87 m (12.69 ft, see Table 3). This gives an estimated 27% increase in bankfull width from the designed channel width. To provide a systematic sample of all feature widths for comparison, a survey of bankfull widths from November 2013, which includes measurements taken approximately every 100 m (for a total of 24 data points), gives a value of 3.43 m(11.25 ft, SD = 0.45 m or 1.48 ft). This gives an estimated 12% increase in bankfull width compared to the designed width. The average percent increase in bankfull width over time across all cross-sections post-construction is 10% (see Table 3). This is within the range of findings of D'Ambrosio *et al.* (2015) of an average -9 to 30% change in bankfull width in seven, upper Midwest two-stage ditches surveyed two to eight years post-construction.

An increase in bankfull width with time could suggest an increase in flow velocity. The longitudinal profile data shows a substantial increase in pool -riffle formation with some of the pools now scoured down to till. This suggests that this increase in flow velocity does not have negative effect on the sediment sorting capability of the low-flow channel. Since the ditch banks are no longer actively eroding, the decrease in sediment supply to the channel is likely driving the pool-riffle formation. The ditch is, however, still receiving sediment from upstream of the two-stage retrofit. The increased velocity supplied by the narrower (compared to the wider channel of the conventional design) low-flow channel ensures that the retrofit actively flushes out this sediment to be able to form pool-riffle

sequences. Also, the channel is no longer confined within the banks of the conventional ditch and the benches are allowing the channel to adjust to the most sustainable geometry.

TABLE 3. Summary of bankfull width changes over time at the Mullenbach Two-Stage Ditch from seven channel surveys.

Bankfull Width (m)								
Distance (m)								
Date	**157**	**447**	**862**	**1220**	**1419**	**1671**	**1780**	**Average**
Oct. 2010	3.81	2.90	3.29	2.74	3.54	3.90	4.11	3.47
Aug. 2012	3.05	3.32	3.38	3.38	4.94	4.24	3.96	3.75
Nov. 2013		3.44	3.81	3.57	3.81	4.21	4.36	3.87
Average	3.44	3.23	3.51	3.23	4.08	4.11	4.15	
% Change	**na**	**19%**	**16%**	**30%**	**8%**	**8%**	**6%**	**10%**

There is an increase in average bankfull depth of 0.09 m or 0.30 ft (18%) across the 7 cross-sections measured in in November 2013 (Table 4). This is slightly larger than the mean depths presented by D'Ambrosio *et al.* (2015) showing a range of 0.04 m or 0.13 ft (13%) decrease to 0.05 m or 0.16 ft (17%) increase in channel elevation for seven, upper Midwest two-stage ditches surveyed 2 two to eight years post-construction. However, given the small difference as well as our small sample size, the average increase in bankfull depth is likely not significantly different than the results found by D'Ambrosio *et al.* (2015). Mean bankfull depth is properly obtained by taking measurements at a riffle section. Our benchmarked cross-sections didn't move with time but the formation of pools and riffles in the channel did change. However, all cross-sections were located in runs or riffles during the 2013 longitudinal survey. Thus, mean bankfull measurements may not be true indicators of bankfull depth changes. A better gage of depth changes in the channel is provided by the longitudinal profile, which shows the formation of a pool-riffle pattern not present prior to construction.

TABLE 4. Summary of bankfull depth changes over time at the Mullenbach Two-Stage Ditch from seven channel surveys.

Mean Bankfull Depth (m)								
	Distance (m)							
Date	**157**	**447**	**862**	**1220**	**1419**	**1671**	**1780**	**Average**
Oct 2010	0.34	0.30	0.55	0.37	0.43	0.49	0.40	0.40
Aug 2012	0.40	0.34	0.49	0.37	0.34	0.46	0.40	0.40
Nov 2013		0.43	0.55	0.37	0.67	0.49	0.43	0.49
Average	0.37	0.37	0.52	0.37	0.49	0.49	0.40	
% Change	**na**	**40%**	**0**	**0**	**57%**	**0**	**8%**	**18%**

Stability

The Modified Pfankuch Stability Rating worksheet produced an overall unstable score (114) for the ditch prior to two-stage retrofit in 2009 and an overall stable score (72.5) for the two-stage ditch on November 2013, based on an E5 stream type (Figs. 31 and 32). The majority of the indices prior to construction fell under either the fair (5) or poor (6) condition categories whereas the majority of the indices fell under either the good (5) or excellent (7) condition categories in November 2013. Indices that rate higher for having larger bed material intrinsically produced a lower score for the ditch, before and after the two-stage retrofit, because the sediment supply in this region is predominantly sand and gravel. Indices that rate higher for having less channel debris also intrinsically produced a higher score for the ditch, before and after construction, due to the lack of woody debris in the channel, its riparian area, and in the watershed overall. Characteristics that produced a higher score in the two-stage ditch and a lower score prior to construction mostly pertained to the angle of the bank slope (and the associated presence or absence of mass wasting), the presence or absence of a floodplain, aggradation and/or degradation of bed material, and the presence or absence of pool-riffle sequences. Although some indices are not considered very applicable to this region, the overall condition score aligns with

our perceived condition based on visual judgment. When the same indices are scored relatively between pre-and post-construction, then the difficulties associated with some indices are similar between surveys. Overall, the two-stage ditch showed a large improvement in stability compared to the pre-construction conventional ditch. This stability rating is a useful indicator of the overall stability of the ditch prior to and after two-stage construction.

Worksheet 3-10. Pfankuch (1975) channel stability rating procedure, as modified by Rosgen (1996, 2001c, 2006b).

Stream:			Location:				Valley Type:				Observers:				Date:	
Location	Key	Category	Excellent		Good		Fair		Poor							
			Description	Rating	Description	Rating	Description	Rating	Description	Rating						
Upper banks	1	Landform slope	Bank slope gradient <30%.	2	Bank slope gradient 30–40%.	4	Bank slope gradient 40–60%.	6	Bank slope gradient > 60%.	8						
	2	Mass erosion	No evidence of past or future mass erosion.	3	Infrequent. Mostly healed over. Low future potential.	6	Frequent or large, causing sediment nearly yearlong.	9	Frequent or large, causing sediment nearly yearlong OR imminent danger of same.	12						
	3	Debris jam potential	Essentially absent from immediate channel area.	2	Present, but mostly small twigs and limbs.	4	Moderate to heavy amounts, mostly larger sizes.	6	Moderate to heavy amounts, predominantly larger sizes.	8						
	4	Vegetative bank protection	> 90% plant density. Vigor and variety suggest a deep, dense soil-binding root mass.	3	70–90% density. Fewer species or less vigor suggest less dense or deep root mass.	6	50–70% density. Lower vigor and fewer species from a shallow, discontinuous root mass.	9	<50% density plus fewer species and less vigor indicating poor, discontinuous and shallow root mass.	12						
Lower banks	5	Channel capacity	Bank heights sufficient to contain the bankfull stage. Width/depth ratio departure from reference width/depth ratio = 1.0. Bank-Height Ratio (BHR) = 1.0.	1	Bankfull stage is contained within banks. Width/depth ratio departure from reference width/depth ratio = 1.0–1.2. Bank-Height Ratio (BHR) = 1.0–1.1.	2	Bankfull stage is not contained. Width/depth ratio departure from reference width/depth ratio = 1.2–1.4. Bank-Height Ratio (BHR) = 1.1–1.3.	3	Bankfull stage is not contained; over-bank flows are common with flows less than bankfull. Width/depth ratio departure from reference width/depth ratio > 1.4. Bank-Height Ratio (BHR) > 1.3.	4						
	6	Bank rock content	> 65% with large angular boulders. 12"+ common.	2	40–65%. Mostly boulders and small cobbles 6–12".	4	20–40%. Most in the 3–6" diameter class.	6	<20% rock fragments of gravel sizes, 1–3" or less.	8						
	7	Obstructions to flow	Rocks and logs firmly imbedded. Flow pattern w/o cutting or deposition. Stable bed.	2	Some present causing erosive cross currents and minor pool filling. Obstructions fewer and less firm.	4	Moderately frequent, unstable obstructions move with high flows causing bank cutting and pool filling.	6	Frequent obstructions and deflectors cause bank erosion yearlong. Sediment traps full, channel migration occurring.	8						
	8	Cutting	Little or none. Infrequent raw banks <6".	4	Some, intermittently at outcurves and constrictions. Raw banks may be up to 12".	6	Significant. Cuts 12–24" high. Root mat overhangs and sloughing evident.	12	Almost continuous cuts, some over 24" high. Failure of overhangs frequent.	16						
	9	Deposition	Little or no enlargement of channel or point bars.	4	Some new bar increase, mostly from coarse gravel.	8	Moderate depostion of new gravel and coarse sand on old and some new bars.	12	Extensive deposit of predominantly fine particles. Accelerated bar development.	16						
Bottom	10	Rock angularity	Sharp edges and corners. Plane surfaces rough.	1	Rounded corners and edges. Surfaces smooth and flat.	2	Corners and edges well rounded in 2 dimensions.	3	Well rounded in all dimensions, surfaces smooth.	4						
	11	Brightness	Surfaces dull, dark or stained. Generally not bright.	1	Mostly dull, but may have <35% bright surfaces.	2	Mixture dull and bright, i.e., 35–65% mixture range.	3	Predominantly bright, > 65%, exposed or scoured surfaces.	4						
	12	Consolidation of particles	Assorted sizes tightly packed or overlapping.	2	Moderately packed with some overlapping.	4	Mostly loose assortment with no apparent overlap.	6	No packing evident. Loose assortment, easily moved.	8						
	13	Bottom size distribution	No size change evident. Stable material 80–100%.	4	Distribution shift light. Stable material 50–80%.	8	Moderate change in sizes. Stable materials 20–50%.	12	Marked distribution change. Stable materials 0–20%.	16						
	14	Scouring and deposition	<5% of bottom affected by scour or deposition.	6	5–30% affected. Scour at constrictions and where grades steepen. Some deposition in pools.	12	30–50% affected. Deposits and scour at obstructions, constrictions and bends. Some filling of pools.	18	More than 50% of the bottom in a state of flux or change nearly yearlong.	24						
	15	Aquatic vegetation	Abundant growth moss-like, dark green perennial. In swift water too.	1	Common. Algae forms in low velocity and pool areas. Moss here too.	2	Present but spotty, mostly in backwater. Seasonal algae growth makes rocks slick.	3	Perennial types scarce or absent. Yellow-green, short-term bloom may be present.	4						
			Excellent total =	6	Good total =	0	Fair total =	63.8	Poor total =	43.75						

Stream type	A1	A2	A3	A4	A5	A6	B1	B2	B3	B4	B5	B6	C1	C2	C3	C4	C5	C6	D3	D4	D5	D6
Good (Stable)	38-43	38-43	54-90	60-95	60-95	50-80	38-45	38-45	40-60	40-64	48-68	40-60	38-50	38-50	60-85	70-90	70-90	60-85	85-107	85-107	85-107	67-98
Fair (Mod. unstable)	44-47	44-47	91-129	96-132	96-142	81-110	46-58	46-58	61-78	65-84	69-88	61-78	51-61	51-61	86-105	91-110	91-110	86-105	108-132	108-132	108-132	99-125
Poor (Unstable)	48+	48+	130+	133+	143+	111+	59+	59+	79+	85+	89+	79+	62+	62+	106+	111+	111+	106+	133+	133+	133+	126+

Stream type	DA3	DA4	DA5	DA6	E3	E4	E5	E6	F1	F2	F3	F4	F5	F6	G1	G2	G3	G4	G5	G6
Good (Stable)	40-63	40-63	40-63	40-63	40-63	50-75	50-75	40-63	60-85	60-85	85-110	85-110	90-115	80-95	40-60	40-60	85-107	85-107	90-112	85-107
Fair (Mod. unstable)	64-86	64-86	64-86	64-86	64-86	76-96	76-96	64-86	86-105	86-105	111-125	111-125	116-130	96-110	61-78	61-78	108-120	108-120	113-125	108-120
Poor (Unstable)	87+	87+	87+	87+	87+	97+	97+	87+	106+	106+	126+	126+	131+	111+	79+	79+	121+	121+	126+	121+

*Rating is adjusted to potential stream type, not existing.

Grand total =	113.5
Existing stream type =	
*Potential stream type =	E5
Modified channel stability rating =	Poor

Figure 31. The Modified Pfankuch Stability Rating Worksheet for the Mullenbach Two-Stage Ditch prior to two-stage construction. Medium gray cells indicate that one value was chosen for that index and a dark gray cell indicates that a value between the two scores was used and split equally among the categories.

Worksheet 3-10. Pfankuch (1975) channel stability rating procedure, as modified by Rosgen (1996, 2001c, 2006b).

Stream:			Location:		Valley Type:		Observers:		Date:	
Location	Key	Category	Excellent		Good		Fair		Poor	
			Description	Rating	Description	Rating	Description	Rating	Description	Rating
Upper banks	1	Landform slope	Bank slope gradient <30%.	2	Bank slope gradient 30–40%.	4	Bank slope gradient 40–60%.	6	Bank slope gradient > 60%.	8
	2	Mass erosion	No evidence of past or future mass erosion.	3	Infrequent. Mostly healed over. Low future potential.	6	Frequent or large, causing sediment nearly yearlong.	9	Frequent or large, causing sediment nearly yearlong OR imminent danger of same.	12
	3	Debris jam potential	Essentially absent from immediate channel area.	2	Present, but mostly small twigs and limbs.	4	Moderate to heavy amounts, mostly larger sizes.	6	Moderate to heavy amounts, predominantly larger sizes.	8
	4	Vegetative bank protection	> 90% plant density. Vigor and variety suggest a deep, dense soil-binding root mass.	3	70–90% density. Fewer species or less vigor suggest less dense or deep root mass.	6	50–70% density. Lower vigor and fewer species from a shallow, discontinuous root mass.	9	<50% density plus fewer species and less vigor indicating poor, discontinuous and shallow root mass.	12
Lower banks	5	Channel capacity	Bank heights sufficient to contain the bankfull stage. Width/depth ratio departure from reference width/depth ratio = 1.0. Bank-Height Ratio (BHR) = 1.0.	1	Bankfull stage is contained within banks. Width/depth ratio departure from reference width/depth ratio = 1.0–1.2. Bank-Height Ratio (BHR) = 1.0–1.1.	2	Bankfull stage is not contained. Width/depth ratio departure from reference width/depth ratio = 1.2–1.4. Bank-Height Ratio (BHR) = 1.1–1.3.	3	Bankfull stage is not contained; over-bank flows are common with flows less than bankfull. Width/depth ratio departure from reference width/depth ratio > 1.4. Bank-Height Ratio (BHR) > 1.3.	4
	6	Bank rock content	> 65% with large angular boulders. 12"+ common.	2	40–65%. Mostly boulders and small cobbles 6–12".	4	20–40%. Most in the 3–6" diameter class.	6	<20% rock fragments of gravel sizes, 1–3" or less.	8
	7	Obstructions to flow	Rocks and logs firmly imbedded. Flow pattern w/o cutting or deposition. Stable bed.	2	Some present causing erosive cross currents and minor pool filling. Obstructions fewer and less firm.	4	Moderately frequent, unstable obstructions move with high flows causing bank cutting and pool filling.	6	Frequent obstructions and deflectors cause bank erosion yearlong. Sediment traps full, channel migration occurring.	8
	8	Cutting	Little or none. Infrequent raw banks <6".	4	Some, intermittently at outcurves and constrictions. Raw banks may be up to 12".	6	Significant. Cuts 12–24" high. Root mat overhangs and sloughing evident.	12	Almost continuous cuts, some over 24" high. Failure of overhangs frequent.	16
	9	Deposition	Little or no enlargement of channel or point bars.	4	Some new bar increase, mostly from coarse gravel.	8	Moderate depostion of new gravel and coarse sand on old and some new bars.	12	Extensive deposit of predominantly fine particles. Accelerated bar development.	16
Bottom	10	Rock angularity	Sharp edges and corners. Plane surfaces rough.	1	Rounded corners and edges. Surfaces smooth and flat.	2	Corners and edges well rounded in 2 dimensions.	3	Well rounded in all dimensions, surfaces smooth.	4
	11	Brightness	Surfaces dull, dark or stained. Generally not bright.	1	Mostly dull, but may have <35% bright surfaces.	2	Mixture dull and bright, i.e., 35–65% mixture range.	3	Predominantly bright, > 65%, exposed or scoured surfaces.	4
	12	Consolidation of particles	Assorted sizes tightly packed or overlapping.	2	Moderately packed with some overlapping.	4	Mostly loose assortment with no apparent overlap.	6	No packing evident. Loose assortment, easily moved.	8
	13	Bottom size distribution	No size change evident. Stable material 80–100%.	4	Distribution shift light. Stable material 50–80%.	8	Moderate change in sizes. Stable materials 20–50%.	12	Marked distribution change. Stable materials 0–20%.	16
	14	Scouring and deposition	<5% of bottom affected by scour or deposition.	6	5–30% affected. Scour at constrictions and where grades steepen. Some deposition in pools.	12	30–50% affected. Deposits and scour at obstructions, constrictions and bends. Some filling of pools.	18	More than 50% of the bottom in a state of flux or change nearly yearlong.	24
	15	Aquatic vegetation	Abundant growth moss-like, dark green perennial. In swift water too.	1	Common. Algae forms in low velocity and pool areas. Moss here too.	2	Present but spotty, mostly in backwater. Seasonal algae growth makes rocks slick.	3	Perennial types scarce or absent. Yellow-green, short-term bloom may be present.	4
			Excellent total =	12.3	Good total =	33.3	Fair total =	21	Poor total =	8

Stream type	A1	A2	A3	A4	A5	A6	B1	B2	B3	B4	B5	B6	C1	C2	C3	C4	C5	C6	D3	D4	D5	D6
Good (Stable)	38-43	38-43	54-90	60-95	60-95	50-80	38-45	38-45	40-60	40-64	48-68	40-60	38-50	38-50	60-85	70-90	70-90	60-85	85-107	85-107	85-107	67-98
Fair (Mod. unstable)	44-47	44-47	91-129	96-132	96-142	81-110	46-58	46-58	61-78	65-84	69-88	61-78	51-61	51-61	86-105	91-110	91-110	86-105	108-132	108-132	108-132	99-125
Poor (Unstable)	48+	48+	130+	133+	143+	111+	59+	59+	79+	85+	89+	79+	62+	62+	106+	111+	111+	106+	133+	133+	133+	126+

Stream type	DA3	DA4	DA5	DA6	E3	E4	E5	E6	F1	F2	F3	F4	F5	F6	G1	G2	G3	G4	G5	G6
Good (Stable)	40-63	40-63	40-63	40-63	40-63	50-75	50-75	40-63	60-85	60-85	85-110	85-110	90-115	80-95	40-60	40-60	85-107	85-107	90-112	85-107
Fair (Mod. unstable)	64-86	64-86	64-86	64-86	64-86	76-96	76-96	64-86	86-105	86-105	111-125	111-125	116-130	96-110	61-78	61-78	108-120	108-120	113-125	108-120
Poor (Unstable)	87+	87+	87+	87+	87+	97+	97+	87+	106+	106+	126+	126+	131+	111+	79+	79+	121+	121+	126+	121+

Grand total =	74.5
Existing stream type =	E5
*Potential stream type =	E5
Modified channel stability rating =	Good

*Rating is adjusted to potential stream type, not existing.

River Stability Field Guide pages 3-46 to 3-47

Figure 32. The Modified Pfankuch Stability Rating Worksheet for the Mullenbach Two-Stage Ditch after two-stage construction. Medium gray cells indicate that one value was chosen for that index and a dark gray cell indicates that a value between the two scores was used and split equally among the categories.

The BEHI rating produced a low bank erosion hazard index score of 17 for the Mullenbach Two-Stage Ditch in 2013 (Fig. 33). Rooting depth is based upon the creeping rhizome root system of Reed Canary Grass (*Phalaris arundinacae*), the most common species found along the low-flow channel banks during post-construction vegetation surveys (Krider *et al.,* 2016c). For Reed Canary Grass the roots are typically very abundant to 38.1 cm (15 in) and most extend to 63.5 cm (25 in), so a value of 45.72 cm (18 in or 1.5 ft) was chosen (Weaver, 1926). A root density of 30% was chosen based on photographs in the River Stability Field Guide (2008) which show grasses similar to Reed Canary Grass in above ground biomass density and rooting depth as having 30% root density. The average bank angle across all cross-sections was 32.17^{o}. Due to the high density of above ground biomass for Reed Canary Grass at the site, a surface protection of 40% was chosen. The soils are silty clay loam without stratification, so no bank material or stratification adjustments were added. Overall, a score of 17 is in the low BEHI scoring range and can be considered very good for an agricultural drainage ditch.

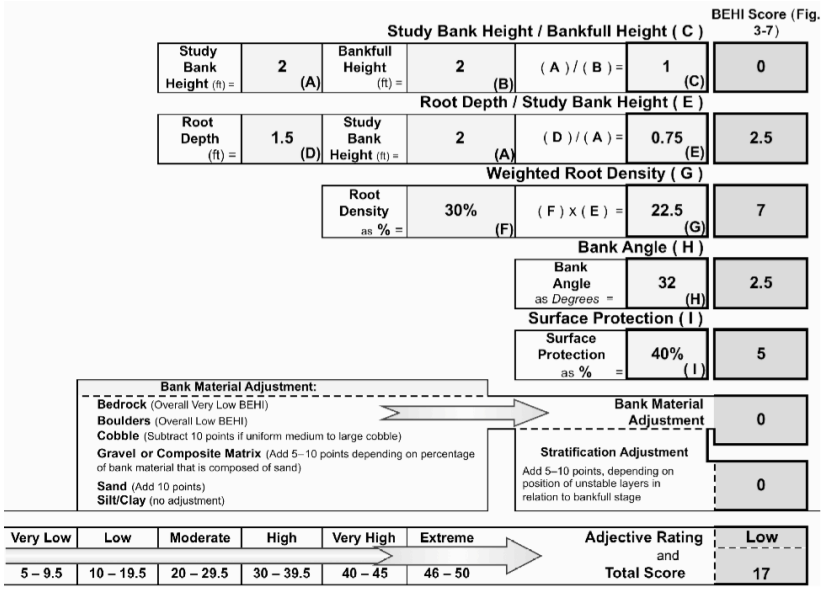

Figure 33. The Bank Erosion Hazard Index Worksheet for the Mullenbach Two-Stage Ditch for 2013.

Other studies have shown similar increases in stability associated with the two-stage design as evidenced by reduced sediment loading. Mahl *et al.* (2015) found that a two-stage ditch decreased turbidity, as compared to the conventional design, by 15% to 82%. They concluded that this decrease is likely due to less sediment transport during floodplain inundation. One aspect of channel stability not addressed in our study was bench aggradation and degradation. D'Ambrosio *et al.* (2015) investigated this characteristic for seven, two-stage ditches in Ohio, Michigan, and Indiana three to 10 years post-construction. They found that benches had both degraded and aggraded at a rate of -8.9 to 13 mm yr^{-1} (-0.35 to 0.51 in yr^{-1}). They also found that some of the systems were still in process toward quasi-equilibrium. However, these changes were not found to negatively impact tile drain outlets or require maintenance on the ditch system (D'amdrosio *et al.,* 2015).

Channel Morphology.

Prior to two-stage construction, the ditch was highly modified from a natural form and function through channelization and most of the channel no longer resembled a natural or stable system. The majority of the morphological characterizations presented in the Mecklenburg Reference Reach Spreadsheet are dependent on an accurate measurement of bankfull depth. Although bank sloughing formed one-sided benches at several cross-sections, the permanency of these features was unknown and could not be assumed to be part of the channel forming flow. In a drainage ditch, bankfull can be estimated as the second grade break or a distinct scour line along the side slopes of the ditch (Mecklenburg, 2000). No data for this feature were collected in 2009.

Channel forming flow at the two-stage ditch was approximated using the 862 m (0.54 mi) cross -section station (Fig. 34). This cross-section had distinct features expected for a stable ditch in the region. Bankfull for the pre-construction condition corresponds to the constructed bankfull elevation relative to the survey

datum. Based on this cross-section, the cross-sectional area of the pre-construction low-flow channel is 1.56 m^2 (16.97 ft^2), the width is 3.31 m (10.86 ft), and the average depth is 0.48 m (1.57 ft). This produces a discharge rate of 0.75 $m^3\ s^{-1}$ (26.4 $ft^3\ s^{-1}$). The entrenchment ratio is 2.1 and the average width to depth ratio is 6.9. The Rosgen Classification of Natural Rivers (Rosgen, 2008) does not have a stream type description fitting this entrenchment ratio for stream types C through G. Therefore, stream type classification could not be accurately determined for the original Mullenbach Two-Stage Ditch. However, Rosgen (1996) found that drainage ditches were often of the Gc or F stream type due to the lack of sinuosity and floodplain area. Characteristics of our pre-constructed ditch are consistent with his results.

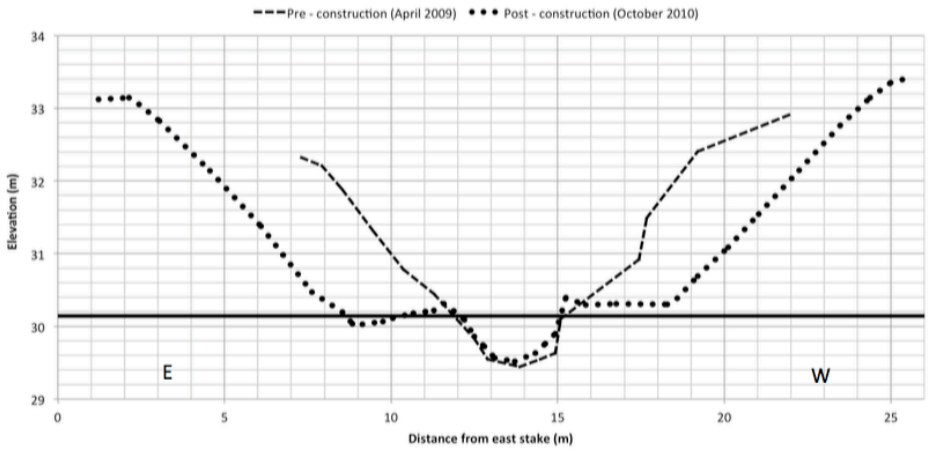

Figure 34. Mullenbach Two-Stage Ditch cross-section survey comparison between pre- and post-construction at 862 m (bankfull indicated by the solid, black horizontal line; looking south downstream)

The pre-construction channel morphology was also estimated using regional curves. By using this method, the original cross-sectional area of the low-flow channel is 1.83 m^2 (19.70 ft^2), the width is 3.24 m (10.73 ft), and the depth is 0.58 m (1.90 ft). These values are in good agreement with those obtained using the features obtained from the 862 m (0.54 mi) cross-section. The

0.95 m^3 s^{-1} (33.5 ft^3 s^{-1}) bankfull discharge from the Reference Reach Spreadsheet is slightly larger than that obtained from the 862 m (0.54 mi) cross – section.

Based on the Reference Reach Spreadsheet, the channel geomorphology was characterized after two-stage ditch construction. In 2013, the channel slope was 0.19% with an average flood prone width of 13.35 m (43.79 ft). This gave an average bankfull discharge of 0.91 m^3 s^{-1} (32.2 ft^3 s^{-1}). The 0.9-m H-flume full flow is 0.87 m^3 s^{-1} (30.7 ft^3 s^{-1}). The average entrenchment ratio is 3.5 and the average width to depth ratio is 9.07. There is only one sinuosity option associated to this entrenchment and width to depth ratio, which is high sinuosity (>1.5), which is not true for the two-stage ditch. However, if the ditch were not confined within its banks, it would likely meander more than it currently does. For a slope < 0.02 and a sand channel sediment, the resulting stream type is E5. The Rosgen Classification of Natural Rivers (2008) appears to be applicable in determining stream type of the ditch after two-stage construction because the channel morphology is more similar to a natural stream than a channelized ditch.

The Mullenbach Drainage Ditch has been shown to be stable, based on the Pfankuch and BEHI analyses for both the inner and outer banks as well as the low-flow channel, since two-stage construction in 2009, and will likely continue to remain stable over time and in the near future. Since construction, bank instability caused by seepage, planar failure and toe erosion on ditch banks, as well as tile outlet failures were no longer present. The ditch transitioned from an unstable stream type (G of F) given the features of the region and watershed size to an appropriately classified stream type (E5). Since the ditch is located within a small watershed with a lower stream power as well as having protected banks, the ditch will likely gain some meander but not nearly as much as a natural E5 stream without confining bank walls. This is expected and acceptable given the function of the waterway as a ditch. In general, there will be less bank

and bed erosion in the system thus the channel is expected to adjust at a very slow pace.

Bankfull Flow and Recurrence Interval

Jayakaran *et al.* (2005) have found that the bankfull recurrence interval for ditches in Ohio is less than the expected 1.5 years for natural streams and, instead, is more along the lines of six months. They determined bankfull flow by using power law functions relating channel characteristics to bankfull discharge and compared to published regional curves (Jayakaran *et al.,* 2005). By using Manning's equation and a daily runoff model, they found the bankfull recurrence interval between 0.25 and 0.5 years for 18 sites at 10 drainage ditches in Ohio (Jayakaran *et al.,* 2005). Similar results were obtained by Jayakaran and Ward (2007) for thirteen other sites in Ohio.

The recurrence interval at the Mullenbach Two-Stage Ditch site was computed using an average bankfull discharge value of 0.89 $m^3 s^{-1}$ (31.45 $ft^3 s^{-1}$). The average recurrence interval was 0.30 years (3.6 months) between station locations (upstream and downstream) and discharge rates (0.87 $m^3 s^{-1}$ from the flume specifications or 0.91 $m^3 s^{-1}$ from the Reference Reach Spreadsheet for the 2013 data) (Mecklenburg, 2006). Most of the longer recurrence intervals occur in early spring (March or April), presumably due to a snow melt event following a dry year, or mid-summer (July), presumably due to a large rain event following a dry year with little snow pack. Using a slightly larger bankfull discharge value based on the cross-sections (as opposed to the flume) produced slightly fewer bankfull events. Our average recurrence interval is consistent with the low end of the results found by Jayakaran, Ward, and others (2005 and 2007) for conventional agricultural drainage ditches in Ohio.

CONCLUSION

As part of the two-stage ditch construction, the low-flow channel of the conventional ditch was narrowed and deepened, in part, to facilitate higher rates of sediment removal. This resulted in places where the channel was scoured down to clay material (pools) and other places where larger sand and gravel sized particles accumulated and were well sorted (riffles). Given its lack of need for maintenance since construction, the design is not likely to require maintenance and clean-out often associated with the conventional design, making it an economically viable option in many cases (Krider *et al.,* 2016a; Krider *et al.,* 2014). Increased stability can be attributed to the two-stage design with a narrow, low-flow channel and floodplain benches that support a larger amount of plant biomass (Krider *et al.,* 2016c; Powell and Bouchard, 2010).

Overall, the Mullenbach Two-Stage Ditch shows an improvement to the conventional ditch design. This is based on physical attributes that improve function and increase benefits similar to natural streams in this region of Minnesota given the current land use and hydrology. Two-stage designs create a geomorphically stable condition with little degradation and aggradation through the natural process of sediment flushing and sorting. This design also helps to create stable fluvial conditions through the use of an appropriately sized low-flow channel and floodplain benches. This type of best management practice is an important tool for the water resource manager that can be utilized on larger scales within the appropriate hydrologic setting.

Nitrogen Processes Within a Two-Stage Agricultural Drainage Ditch in Mower County, MN: Methods for Estimating Nitrogen Removal

Lori Krider[1], Bruce Wilson, Joseph Magner[1] Linse Lahti[2], Geoff Kramer[1], Brad Hansen[1], and John Nieber[1]

[1]Department of Bioproducts and Biosystems Engineering, University of Minnesota

[2]Minnesota Department of Natural Resources, St. Paul, MN

Abstract: Water quality in agricultural watersheds is under greater scrutiny as hydrologic pathways are altered to increase the production of affordable food. Agricultural drainage ditches often create an important pathway for the movement of water and the associated nutrients applied to fields to obtain optimal crop yields. There has been much focus on designing ditches based on the priority of water conveyance but little attention has been placed on alternative designs that are inherently more stable, assimilate nutrients, and provide healthy ecosystems. In 2009, 1.89 km of a conventional drainage ditch in Mower County, MN, was converted to an alternative drainage system with a two-stage channel. Using isotopic tracers within matrix formulations, the water balance, as well as nitrogen loading and removal efficiencies were calculated. Three different methods were used to calculate nitrogen removal: (1) comparison of the average influent and effluent concentrations (2) mass-balance relationships for in-channel denitrification, (2) potential soil denitrification using the acetylene inhibition assay in a controlled laboratory setting. Three different dates were used in the mass-balance approach: 2013 as a 84-m test section and 2011 and 2010 and as estimates for the entire ditch reach. Continuous data from 2010 was also used to produce average monthly removal efficiencies for the growing season by comparing average influent and effluent concentrations. The removal efficiency was estimated at 17% for the 2013 data, 32% for the 2011 data, and 20% for the

2010 data. Average monthly removal efficiencies ranged from 19.50% in May to 12.88% in September 2010. Nitrous oxide production estimated using the acetylene inhibition assay varied greatly amongst habitat zones, ranging from 0.08 to 1.85 μg N_2O-N g DW^{-1} h^{-1}. The largest areal denitrification rate was obtained in the riparian zone of the channel and the lowest rates were obtained for the channel itself. Potential habitat-weighted soil denitrification ranged from 18.89% to 41.96% compared to 1.24% to 3.09% estimated for a conventional drainage ditch. The estimated habitat-weighted denitrification rate for the entire ditch is similar to the result obtained using the mass-balance approach for the September 2011 in-stream data. Although denitrification rates and removal efficiencies are difficult to quantify, all removal methods produced results that were similar to one another as well as similar to results found in the literature for other two-stage ditches.

KEY WORDS: agricultural landscapes, best management practice, nutrient management, agricultural drainage ditch.

INTRODUCTION

Water quality in agricultural watersheds is under greater scrutiny as the landscape and hydrologic pathways are altered to increase the production of affordable food. Land use in southern Minnesota is largely agricultural with the dominant crops being corn and soybean. In 2016, 8.39 million acres of corn and 7.50 million acres of soybeans were harvested in Minnesota (USDA-NASS, 2017). Each year, large quantities of nitrogen are applied to these crops to increase yields. However, portions of this nutrient are lost from these fields and are ultimately transferred to major river systems in Minnesota and beyond. “On average, 211 million pounds of TN [total nitrogen] leaves Minnesota each year in the Mississippi River at the Minnesota-Iowa border, with just over three-fourths of

this load originating in Minnesota watersheds …," (MPCA, 2013). The Mississippi River transports significant amounts of these nutrients to the Gulf of Mexico.

Excess nutrients introduced into natural systems can have major consequences for aquatic communities. Extensive surface and sub-surface drainage allows the useable forms of nitrogen meant for crop uptake to be transported to agricultural drainage ditches and natural channel systems. Excess growth of unwanted algae and duckweed *(Lemna spp.*) is often a consequence of having excess nutrients in natural systems. The decomposition of algae and duckweed consumes large amounts of dissolved oxygen in the water column, creating hypoxic conditions (dissolved oxygen < 2 mg L^{-1}) that are unsuitable for many plant and animal species, especially those that are particularly sensitive to low levels of dissolved oxygen (Louisiana Universities Marine Consortium). The hypoxic zone in the Gulf of Mexico is an example of this decomposition on a large scale (NOAA, 2014). Drainage ditches provide an opportunity to remove some of the nutrients before the water is discharged into natural channels.

Conventional ditches are designed to remove water, minimize construction costs and reduce the loss of farmland. They have relatively small surface areas available to remove nutrients. Two-stage drainage ditches are not only designed to convey water but also to mimic the geomorphologic character found in natural low-order streams (Ward *et al., 2*004; USDA-NRCS 2007). They have a low-flow channel sized to replicate that of a natural channel using regional hydraulic geometric curves (Krider *et al.,* 2017). When the flow depth exceeds the bankfull depth of this channel, flow spreads out across the designated benches. This has the effect of slowing water velocity, increasing water residence times, and reducing nitrogen transport during large flow events (Roley *et al.,* 2012a). Plant biomass on the benches serves as an important carbon source necessary to support denitrifying bacteria (Powell and Bouchard, 2010).

BACKGROUND

Nitrogen loading to surface waters in agricultural watersheds in Minnesota is an important and complex water quality issue. The main avenue by which nitrogen is transported from the field to a nearby body of water is through sub-surface drainage or within the base flow (Randall and Mulla, 2001). In fact, very little loading occurs due to surface runoff from these types of landscapes (Jackson *et al.,* 1973). Several factors contribute to the amount and timing of nitrogen loading. Watersheds with predominantly agricultural land use have higher loading rates than those that are naturally vegetated (Randall and Mulla, 2001). Precipitation is directly tied to the volume of water passed by tile drains (Gentry *et al.,* 1998). Not only is precipitation a factor but timing is as well (Mitsch *et al., 2*001). Factors such as saturated soil conditions and evapotranspiration rates often create situations where loading is higher in the springtime and less in the summer (Randall and Mulla, 2001). Wet/dry cycles produce conditions where nitrogen is built up in the soil profile and released during wet conditions (Mitsch *et al., 2*001, Randall and Mulla, 2001). The use of nitrogen fertilizer has increased substantially over time, although there are now tools available through government or extension services to assist farmers in calculating the optimum applications rates (Mitsch *et al.,* 2001; Rajsic and Weersink, 2007). Often, a combination of several of these factors is responsible for the nutrient dynamics that occur on the small and large watershed scale.

In general, two key methods are typically employed to estimate nitrogen budgets: mass-balance calculations and potential soil denitrification estimates. Mass-balance approaches have been employed to estimate nitrogen reductions at macro and micro scales (Watson and Atkinson, 1999). Groundwater is often the most difficult variable to quantify. There are several methods that can be employed to quantify groundwater inputs in the mass-balance approach. One method used to identify a groundwater component involves heat or environmental chemical tracers (Kalbus *et al.,* 2006). Oxygen tracers are based

on the fractionation of rainwater, which creates the separation of light and heavy oxygen isotopes. The evaporation of the lighter oxygen isotope (^{16}O) and the condensation of the heavier oxygen isotope (^{18}O) produce rainwater enriched in ^{18}O. The ratio of these isotopes ($\delta^{18}O$) provides useful information on the age and source of the water in question. Several studies have used spatiotemporal variations in stable oxygen isotopic composition to characterize the interactions between ground and surface waters within mass-balance equations (Hameed *et al.,* 2015; Krabbenhoft *et al.,* 1990).

In-stream denitrification in drainage ditches is important to the nitrogen loading occurring downstream. Several researchers have estimated drainage ditches to be substantial nitrogen sinks (David and Gentry, 2000, Alexander *et al.,* 2000). Roley *et al.* (2012a) found the highest rates of in-stream sediment denitrification in mid-western drainage ditches to be in late winter/early spring and the least in late summer/early fall. It has also been found that in-stream nitrification is highest in the springtime due to the mineralization caused by decaying benthic organic matter that senesced the previous fall (Arango and Tank, 2007). Additionally, researchers have found that in-stream denitrification rates are correlated to NO_3^- in the stream and not adjacent landuse or the presence/absence of riparian buffers (Arango and Tank, 2007). Therefore, nitrogen removal equations within drainage ditches need to cover a range of flow and climatic conditions as well as take into account influent NO_3-N concentrations.

The surface area available for denitrification is an important factor in determining removal rates. Previous work has demonstrated that denitrification is substantial from both within the channel as well as on the benches in a two-stage ditch (Roley *et al.,* 2012a). To investigate potential denitrification via the acetylene inhibition assay, soil samples were taken from a two-stage ditch streambed in Illinois. They found that 44% of the total in-stream core denitrification occurred in the upper 2 cm (Roley *et al.,* 2012a). On the benches,

56% of the total core denitrification was found to occur in the top 5 cm of sediment (Roley *et al.,* 2012a). In many respects, the bottom of the channel substrate between a one-stage and two-stage ditch is very similar thus denitrification rates for these sediments does not differ significantly (Powell and Bouchard, 2010). However, the slopes of the one-stage ditch are limited in carbon and nitrate whereas the bench of the two-stage ditch is only limited by nitrate (Powell and Bouchard, 2010). However, bench soils near the water table may be less limited in nitrate if the sub-surface water is shown to be high in nitrogen.

Since bench soils may be limited in their ability to denitrify due to a lack of contact with high nitrogen surface water, two-stage ditch bench inundation has a positive effect on bench denitrification rates (Davis *et al., 2*015, Roley *et al., 2*012a). This is tied to the nutrient limitation in the soil surface until it is inundated with high nutrient surface waters. By utilizing the benches, nitrogen removal increased by ~500% as a result of two-stage construction at the Shatto Ditch in Illinois (Tank, ND). When the floodplain was inundated for 29 days of the year, the floodplains contributed 12% of total nitrogen removal (Roley *et al.,* 2012a). When the floodplain was inundated for 132 days, floodplains contributed 47% of total nitrogen removal (Roley *et al.,* 2012a). The number of days of bench inundation is inversely related to bench height (Mahl *et al.,* 2015). Roley *et al.* (2012a) also showed that the mean denitrification rate was 9.2 +/- 1.3 mg m^{-2} h^{-1} during a storm event and that inundation also greatly increases hyporheic (4 – 20 cm below channel) denitrification from 0.04 kg/d to 0.73 kg/d (Roley *et al.,* 2012b). However, inundation did not change the depth of the denitrification rates (Roley *et al., 2*012b).

Vegetation is particularly important in two-stage ditches because of the larger plant biomass (Powell and Bouchard, 2010). This factor can both increase denitrification by the additional carbon or by the uptake of nitrogen in the plants themselves. Roley *et al.* (2012b) found that, denitrification rates in the top 5 cm

(6.77 +/- 1.37 mg m^{-2} h^{-1}) and lower 5 to 10 cm (3.35 +/- 1.06 mg m^{-2} h^{-1}) of soil were highest in areas with wetland plants vs. all other habitat types (non-vegetated, de-vegetated, roots-only, reed canary grass, natives, wetland plants) with the addition of surface water. A study by Larson *et al.* (2001) measured the activity of a key enzyme, nitrate reductase, in several common mid-western US plant species. Larson *et al.* (2001) found that reed canarygrass has the highest initial (day 1) nitrate uptake rate (compared to borage, swiss chard, hornwort and switchgrass) at about 240 ppb nitrate g $plant^{-1}$. At the Big Ditch in east central Illinois, the maximum plant-associated denitrification rate was 0.29 mg N m^{-2} h^{-1} (Schaller *et al.,* 2004). Where species are mixed, soil sampling from habitat zones based on hydrology may be a useful way to distinguish between different types of plant associated potential denitrification.

Since nitrogen removal is often coupled to in-stream nitrogen concentration and available C, it is important to explore a variety of techniques to estimate nitrogen removal. Mass-balance approaches often introduce much error and uncertainty associated to variables that are difficult to quantify or define. Potential removal rates in the soil often ignore the influent NO_3-N concentration as an important contributing factor and can over estimate removal through the mixing with surface water. Removal efficiencies only give a comparison of the influent concentration against the effluent concentrations, regardless of the mechanism for removal. Nitrogen removal rates as well as removal efficiencies could provide validation to one another to create a more robust and reliable estimate of nitrogen removal.

Only a limited number of studies have examined the removal of nitrogen by processes within agricultural drainage ditches, regardless of the type of design (Powell and Bouchard, 2010; Schaller *et al.,* 2004; Inwood *et al.,* 2005; Arango and Tank, 2007). These studies focus on the potential denitrification rates found within the soil profile and do not employ mass or energy balance techniques needed to draw larger scale conclusions about the nitrogen process with the

ditch system as a whole. Since determining the removal rate of nitrogen is well known to be difficult (Groffman *et al.,* 2006), field and laboratory methods are used to produce a more robust study. The objectives are to collect and analyze (physical and chemical) water and soil data to determine the nitrogen removal by natural processes as calculated by a comparison of average influent and effluent concentrations, by mass-balance equations and by using potential soil denitrification estimates for a two-stage ditch located in Mower County, MN USA. When assessing the effectiveness of a two-stage ditch it is important to compare the results to a conventional drainage ditch to determine if this design has enhanced nitrate removal. However, no known studies have directly measured nitrogen removal within agricultural ditches under the climate and landscape conditions of Minnesota. We compare our nitrogen removal results from a hypothetical conventional drainage ditch to the current condition found in the two-stage ditch. This component is based on the potential soil denitrification rate found in various habitat zones within the two-stage ditch.

METHODS

Site Description and Instrumentation

The Mullenbach Drainage Ditch is located in rural Mower County in southern Minnesota, USA, approximately 8 km southwest of the town of Adams, MN (Fig. 35). It is in the headwaters of the Little Cedar River within the Upper Cedar River Watershed (8-digit HUC: 07080201). The Mullenbach Two-Stage Ditch empties into the Little Cedar River approximately 4 km downstream of the constructed two-stage ditch reach, which then flows south into the state of Iowa. The watershed area is 12.6 km^2 (3,102 acres) and the land use is predominantly row crop agriculture, with the main crops being corn and soybeans. The Mullenbach Drainage Ditch, as conventionally (trapezoidal) designed, had numerous issues with stability and was scheduled for maintenance in 2009 or 2010 (Krider *et al.,* 2017). With funding and assistance from The Nature

Conservancy and the Mower County SWCD, approximately 1.89 km of the Mullenbach Drainage Ditch was converted to the two-stage design in October of 2009 (Krider *et al.,* 2017). The existing channel was retrofitted to the two-stage channel type through the widening of the total drainage cross section and building floodplain benches while leaving the majority of the low-flow channel intact (Fig. 35, Krider *et al.,* 2017). The edges of the pre-existing channel can be used to define the sub-surface treatment area for the conventional drainage ditch while the edges of the benches can be used to define the sub-surface treatment area for the two-stage ditch (Fig. 36).

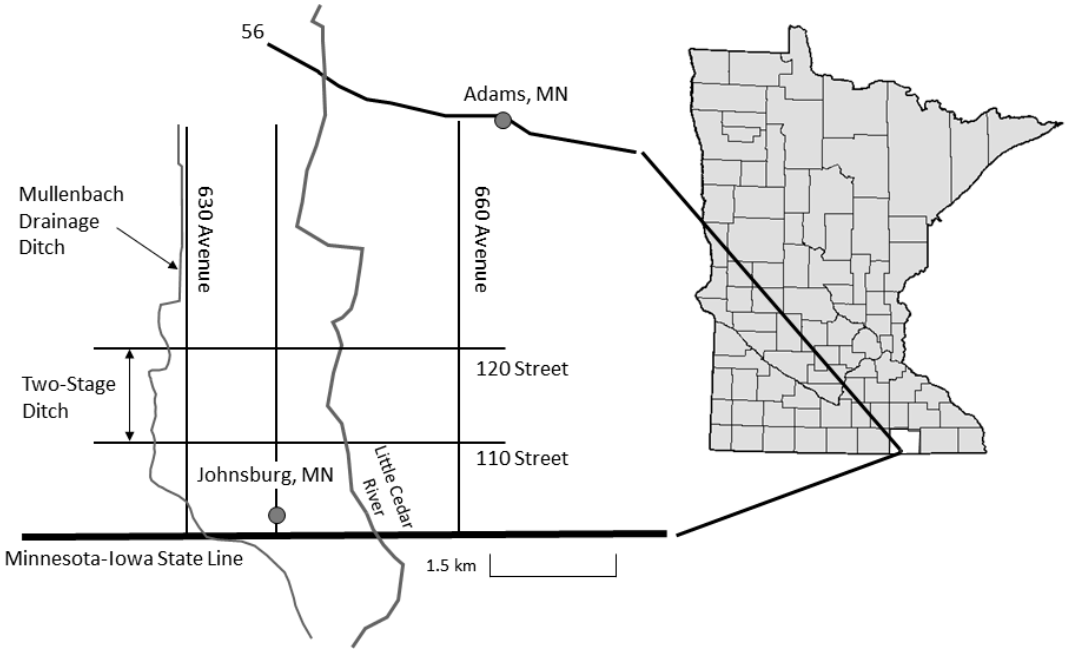

Figure 35. Location of the Mullenbach Drainage Ditch in relation to the state of Minnesota as well as the town of Adams, MN (subset).

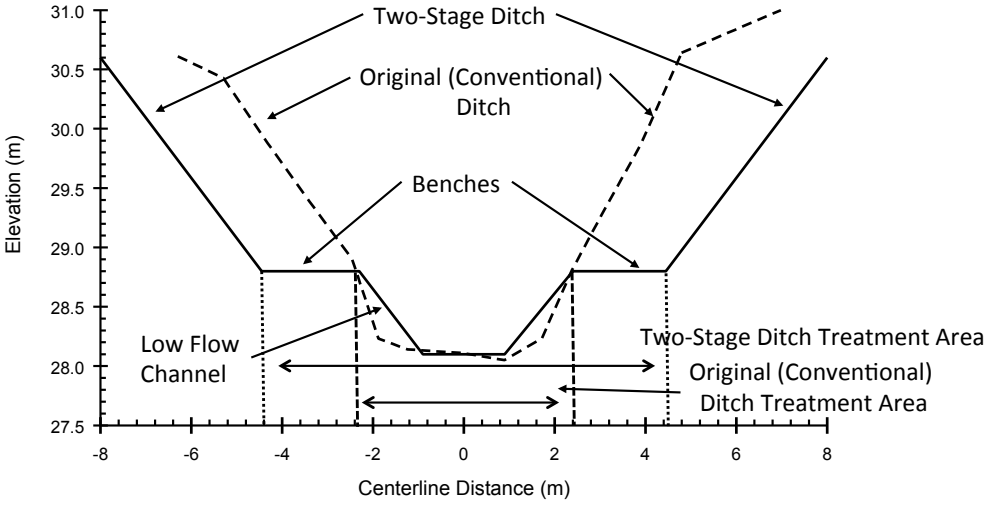

Figure 36. Original (trapezoidal) ditch and the Two-Stage Ditch design using an original Mullenbach cross-section against the proposed two-stage design showing the hypothetical nitrogen treatment areas for both types.

Semi-permanent, wooden H-flumes (0.9-m) were installed at the upstream and downstream locations (inlet and outlet of two-stage retrofit) to measure flow rates (Brakensiek *et al.,* 1979; Krider *et al.,* 2017). Flow rates were also measured at selected sub-surface tile outlets. A number of wells were placed near and within the ditch to better understand the groundwater flow and its contribution to the chemical composition of water within the ditch (Fig. 37). Starting at the north flume, groundwater wells were installed every 366 m. Most of the wells were installed within the bench at the toe of the ditch bank. A number of shallow and deeper wells were installed between 1524 m and 1658 m in an area of high groundwater contribution. The wells were used to determine the piezometric head and to collect grab samples for water quality analysis. All of the wells were sampled manually using an ISCO^{TM} pump.

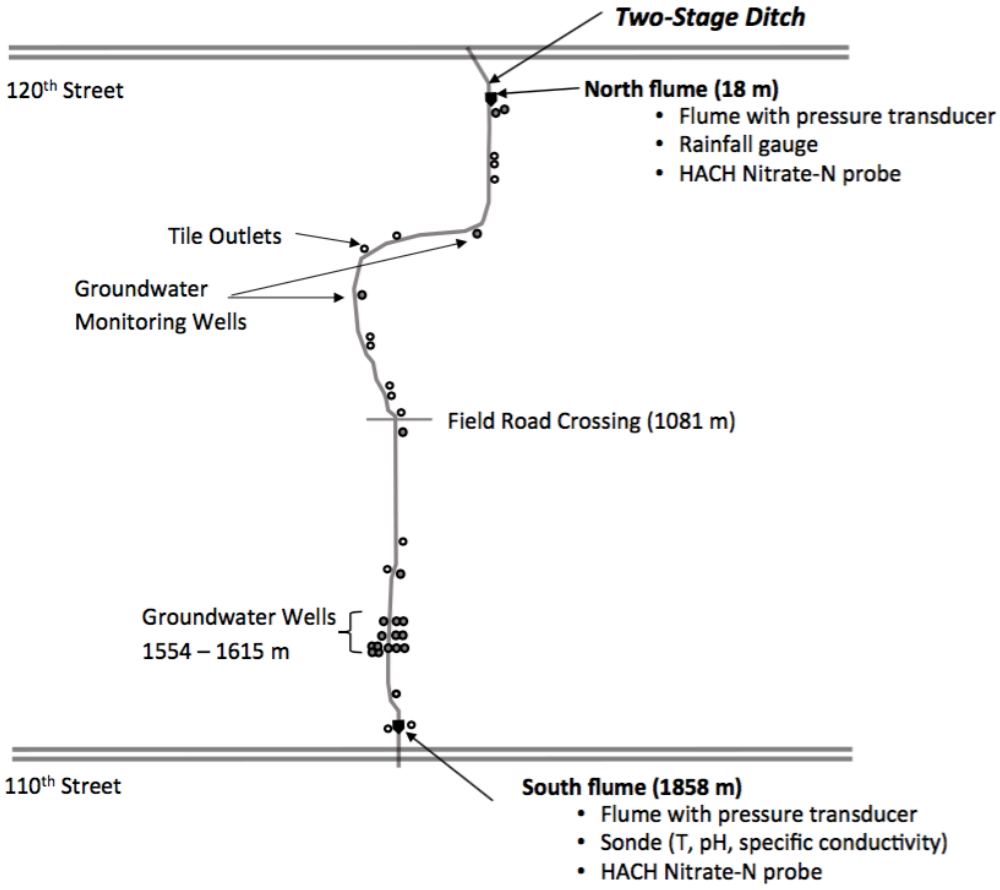

Figure 37. Locations of the surface water quality monitoring stations along the length of the Mullenbach Two-Stage Ditch.

Water quality was monitored to determine the contributions from various sources (tile, groundwater, channel) within the ditch system and to assess the performance of the ditch in improving water quality. Grab samples and water quality probes were used to collect data with some lab analyses for QA/QC. A total of 145 temperature, 17 dissolved oxygen, 38 pH, 65 specific conductance, 193 nitrate, 35 nitrite-nitrate, 31 total phosphorous, 9 metal suites, and 94 deuterium and ^{18}O values were obtained by grab samples. At different times during the study period, nearly continuous water quality data was also collected using a YSI 6800 Sonde™ and a Hach Nitratax Plus SC™ nitrate probe.

Approximately 8,000 continuous readings of pH and specific conductance and 2,500 temperature values were measured with the Sonde probe. Approximately 60,000 continuous readings of nitrate concentrations were obtained with the nitrate probe.

In-channel denitrification was determined using mass-balance relationships. Three different time periods were selected for a more intense analysis of data necessary to define the parameters for these relationships. The three time periods were (1) August 3, 2010, (2) September 21, 2011, and (3) September 18, 2013. The first two dates are used for estimates of the entire ditch reach and the third is for a 84 m test section near the outlet of the retrofit. In addition, an estimate of the removal efficiency was also obtained using the continuous nitrate data collected at the inlet and outlet of the two-stage retrofit for the growing season of 2010. Different mass and energy terms were explored based on the availability of data at the site during the selected time periods. However, mass was determined to provide the most reliable results. In determining significant differences between water quality variables, ANOVA was used to run the parametric tests of Fisher LSD in XLSTAT^{TM}.

For the first sample period of August 3, 2010, in-stream nitrate concentrations were measured in the field with the nitrate probe, tile discharge was measured using the stopwatch and bucket method, upstream flow was measured at the flume, and in-stream water samples were analyzed for deuterium and ^{18}O. However, data from the groundwater wells was not available, and therefore deuterium, ^{18}O, nitrate concentrations and discharge rates from the groundwater sources are unknown. Other problems include unreliable flow rates from the downstream flume and missing other potentially useful tracer information, such as temperature and specific conductance. The unknown parameters for the first time period are (1) the downstream flow rate, (2) the groundwater flow rate, (3) groundwater tracer such as deuterium or O^{18}, (4) the

ground water nitrate concentration, and (5) the removal rate of nitrogen by in-channel processes.

For the second sample period of September 21, 2011, nitrate concentrations were measured in the channel, wells, and from tile lines using the nitrate probe. In addition, samples from the groundwater wells and tile lines were evaluated at the University of Minnesota Research Analytical Lab for nitrate, orthophosphate, total dissolved phosphorus, soluble reactive phosphorus, fluorescence index, specific UV absorption, dissolved inorganic carbon, non-particulate organic carbon, total dissolved nitrogen, and ammonia. Specific conductance, temperature, and pH were measured using the Sonde probe for water in the channel, from the tile lines, and from selected groundwater wells. For this time period, flow rates at the downstream and upstream flumes were reliably measured. The key unknown parameters for the second time period are (1) the groundwater flow rate and (2) the removal rate of nitrogen by in-channel processes.

For the third sample period of September 18, 2013, the collection of data was focused on denitrification processes between locations 1554 m and 1638 m (Fig. 3). This period corresponds to late summer conditions of low rainfall. There was no discharge from the tile lines in our test section. Flow rates at the upstream and downstream ends of this test section were measured using 1-H fiberglass flumes. Water samples from the channel and groundwater wells were collected and analyzed for nitrate and nitrite concentrations using the nitrate probe as well as lab QA/QC performed using standard laboratory methods by Pace Analytical. Temperatures and specific conductance were determined for the 13 wells located in this section as well as within the channel. Deuterium and ^{18}O concentrations were also analyzed for these groundwater and surface water locations using data collected on September 5, 2013. For this sample period, the nitrate concentration in the groundwater wells varied substantially, suggesting two different sources for the groundwater input. The groundwater contributions

were, therefore, divided into two different zones. For the two-zone representation, the important unknown parameters for the third time period are (1) the groundwater rate for Zone 1, (2) the groundwater flow rate for Zone 2, and (3) the removal rate of nitrogen by in-channel processes.

An estimate of the average monthly removal efficiency was also obtained using the continuous nitrate data collected at the inlet and outlet of the two-stage retrofit for the growing season of 2010. Data collected at 15-minute increments were used to produce daily and monthly average concentrations. Removal efficiencies using continuous data could only be applied to days in which both effluent and influent nitrate concentrations were gathered (i.e. days in common). Gaps in the data are caused by equipment problems with the nitrate probes, such as the lack of daily effluent NO_3-N in the month of July and the lack of daily influent NO_3-N concentrations for the first 2 weeks in August. Since April had 3 days in common, July had 1 day, and October had zero, removal efficiencies were only calculated for May, June, August, and September of 2010.

In addition to the analysis of channel processes, soil samples were taken to estimate the potential of the various habitat zones to remove nitrogen via soil denitrification. Soil samples collected from the ditch profile on July 1, 2013, were analyzed in a controlled laboratory environment (Fig. 38). The upper (surface) 4 cm from 7 cores along a 9.75 m transect were homogenized for 4 habitat zones (east and west riparian, channel and non-riparian bench treatment system) at a north site (863 m) and a south site (1394 m). The riparian zone occurred at the soil-water interface, the channel was inundated, and the non-riparian bench area was moist. These sites were chosen because they were not understood to be areas of particularly high groundwater influence and included the bench treatment systems (a linear depressional area along the bench to intercept tile water before entering the stream) and are approximately 9.1 m south of the bench treatment tile inlets (to avoid localized influence). In-stream and tile water

samples were also collected at each location and stored in a cooler at ~2 ^{o}C until analysis the following day.

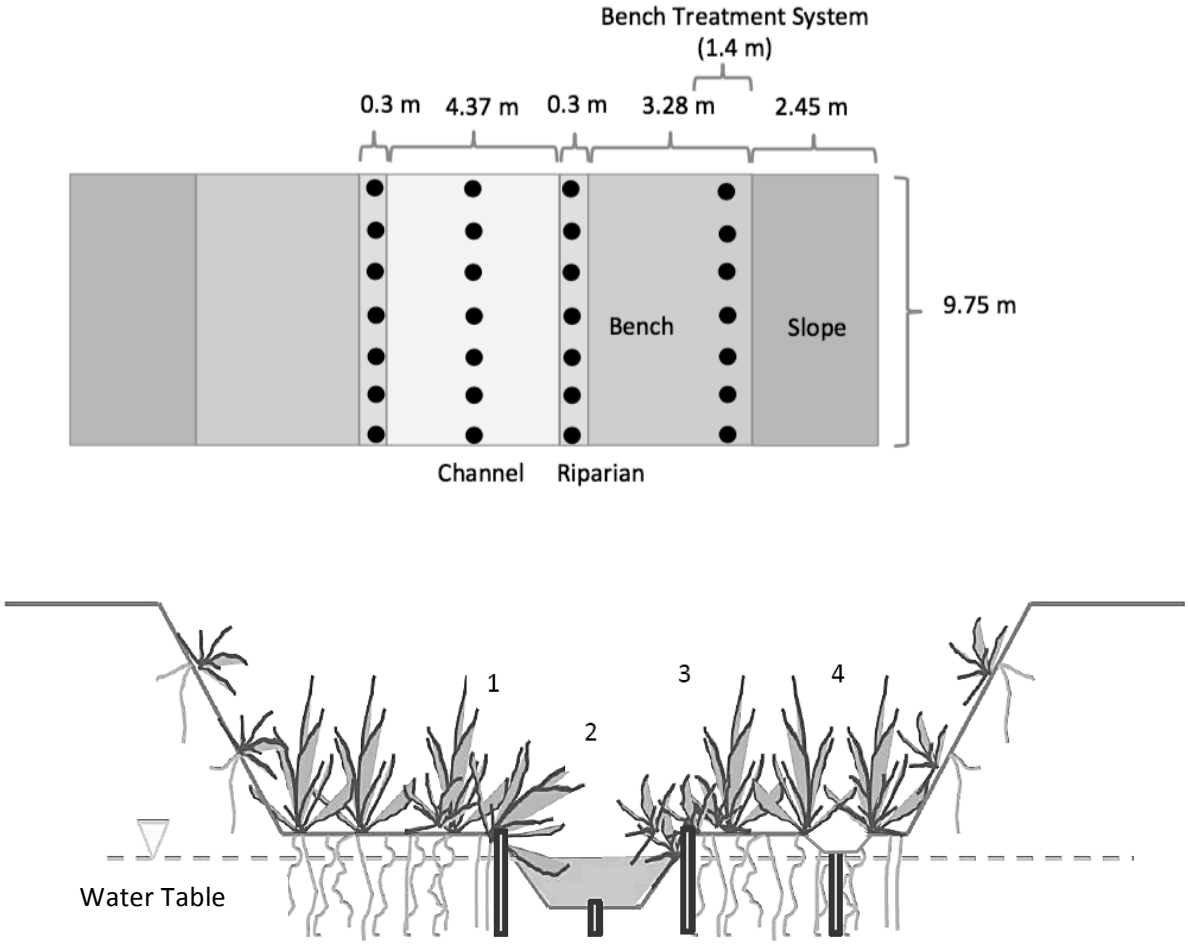

Figure 38. Soil sampling locations along a cross-section of the Mullenbach Two-Stage Ditch, shown in plan (upper) and cross-sectional views (lower).

Analysis Framework for Field Data

Conceptually, the nitrate removal rate can be obtained from measured flow rates and nitrate concentrations for the upstream, downstream, and tile locations as well as measured nitrate concentration from groundwater sources. However, because of instrumentation problems, not all of the flow rates were measured. In addition, the variability of nitrate concentrations in the wells

suggests that a framework of more than one source for groundwater is more appropriate for representing the response of the two-stage ditch. To account for these issues, a general framework is developed to estimate the nitrogen removal rate.

There are several key variables used to thoroughly represent the framework (Fig. 39). The subscripts of "us", "t","gw1","gw2", "ch", and "ds" are used to represent upstream, tile, groundwater source 1 (say, shallower aquifer), groundwater source 2 (say, deeper aquifer), channel, and downstream components of mass balances, respectively. The balances can be represented by the following generic representation:

$$\chi_{US}\, Q_{US} dt + \int_{t}^{t+\Delta t} \chi_T\, Q_T dt + \int_{t}^{t+\Delta t} \chi_{GW1}\, Q_{GW1} dt + \int_{t}^{t+\Delta t} \chi_{GW2}\, Q_{GW2}\, dt - \int_{t}^{t+\Delta t} r_\chi dt = \int_{V(t)}^{V(t+\Delta t)} \chi_{CH}\, \mathrm{dV_{CH}} \quad (1)$$

where χ is the chemical concentration in units of mass per volume, Q is the volumetric flow rate (volume per time), r_χ is a removal or source rate of physical and bio-chemical processes and V is the volume in the channel. We are particularly interested in determining r_x for nitrogen. The groundwater component can be positive for flow into the system or it can be negative for flow out of the system. If groundwater flow is negative, then $\chi_{gw} = \chi_{ch}$. For our analysis, we assume steady-state flow conditions such that $dV_{ch} = 0$. Under these conditions, Eq. 1 can be rewritten as

$$\chi_{us}\, Q_{us} + \chi_t\, Q_t + \chi_{gw1}\, Q_{gw1} + \chi_{gw2}\, Q_{gw2} - \chi_{ds} Q_{ds} - r_\chi = 0 \quad (2)$$

where, formally, each of the above terms represents an average value over a time step of Δt.

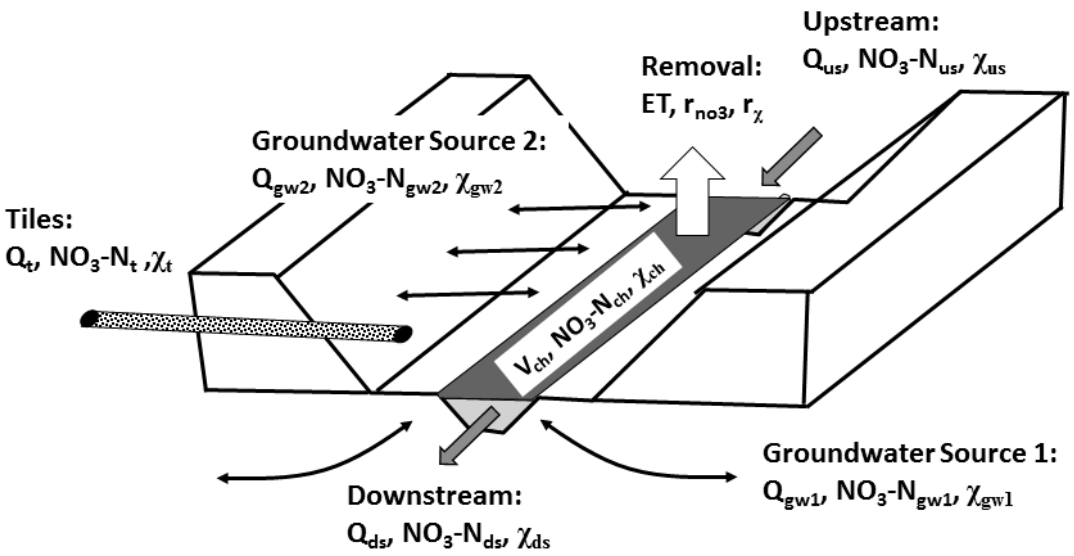

Figure 39. Definition of terms for the mass balance equations within the two-stage ditch.

The two constituents of greatest interest are liquid water and nitrate-nitrogen. Mass-balances for these constituents can be written in the form of Eq. 2 for $\chi = \rho$ and $\chi = NO_3$-N, respectively, where ρ is the density of liquid water and NO_3-N is the nitrate-nitrogen concentration (mg L^{-1}). For constant ρ and negligible evaporation/condensation ($r_\rho \approx 0$), Eq. 2 can be evaluated for each of these two constituents as

$$Q_{us} + Q_t + Q_{gw1} + Q_{gw2} - Q_{ds} = 0 \tag{3}$$

$$NO_3\text{-}N_{us}\, Q_{us} + NO_3\text{-}N_t\, Q_t + NO_3\text{-}N_{gw1}\, Q_{gw1} + NO_3\text{-}N_{gw2}\, Q_{gw2} - NO_3\text{-}N_{ds} Q_{ds} - r_{NO3} = 0 \tag{4}$$

For the special case where all of the influent concentrations are equal (NO_3-N_{in} = NO_3-N_{us} = NO_3-N_t = NO3-N_{gw1} = NO3-N_{gw2}) and groundwater flow is always positive, we can rearrange Eqs. 3 and 4 to solve for the removal mass rate of nitrate-nitrogen as

$$r_{NO3-N} = \left(Q_{us} + Q_t + Q_{gw}\right)(NO_3\text{-}N_{in} - NO_3\text{-}N_{ds}) \quad (5)$$

where the flow rate from the groundwater component has been combined into a single term, that is, $Q_{gw} = Q_{gw1}+Q_{gw2} = Q_{ds}-Q_{us}-Q_t$. The removal efficiency is defined as the removal rate relative to the inflow mass rate. For the special condition of constant NO_3-N for all inflow sources, the removal efficiency (R_{NO3-N}) is defined as

$$R_{NO3-N} = \frac{r_{no3}}{Q_{us}NO_3\text{-}N_{in} + Q_tNO_3\text{-}N_{in} + Q_{gw}NO_3\text{-}N_{in}} = \frac{NO_3\text{-}N_{in} - NO_3\text{-}N_{ds}}{NO_3\text{-}N_{in}} \quad (6)$$

which is evaluated as the difference between influent and effluent concentrations divided by influent concentration.

If the influent concentrations are not equal, then separate estimates are needed for flow rates and the NO_3-N concentrations for the different sources. If reliable flow rate measurements are available, then groundwater flow can, again, be obtained as the difference between downstream flow rate and the combined flow rates of upstream and tile sources. By using measured NO_3-N concentrations for the upstream, downstream, and tile sources, an arithmetic average of well data for the groundwater source, and by having groundwater flow into the ditch, the removal rate (from Eq. 4) and the removal efficiency is defined as

$$r_{NO3-N} = Q_{us}NO_3\text{-}N_{us} + Q_tNO_3\text{-}N_t + (Q_{ds} - Q_{us} - Q_t)NO_3\text{-}N_{gw} - Q_{ds}NO_3\text{-}N_{ds} \quad (7)$$

$$R_{NO3-N} = \frac{r_{no3}}{Q_{us}NO_3\text{-}N_{us} + Q_tNO_3\text{-}N_t + Q_{gw}NO_3\text{-}N_{gw}} \quad (8)$$

As discussed later, the nitrate-nitrogen concentrations of the groundwater varied substantially among the wells. Due to of the uncertainty in this source, the removal efficiency is preferred as a measure of the response of the drainage

ditch. Potential errors in computing the removal rates from groundwater uncertainty tend to be balanced by similar errors in computing the total influent mass rate.

Solutions for removal rate are straightforward if the only other unknown variable is groundwater flow rate. However, for data collected in 2010, the downstream flume was unable to reliably measure downstream flow rates, resulting in another unknown variable for this data set. Furthermore, the division of groundwater into two zones also introduces another unknown variable. The removal rate can still be estimated with these additional unknowns as long as suitable tracer constituents are used. Stable isotopes are often used as tracers to better understand hydrologic systems (Simpkins, 1995; Clark and Fritz, 1997). The mass-balance equation for the oxygen isotope is defined by Eq. 2 for $\chi=^{18}O$ and for a conservative tracer where $r_{O18} \approx 0$. Isotopic composition is defined by its degree of fractionation and is obtained using the ratio of $^{18}O/^{16}O$ or $\delta^{18}O$. It is most useful as a comparison against the global mean weighted meteoric water line defined as

$$\delta^{18}O = 1000\left(\frac{(^{18}O/^{16}O) - R_s}{R_s}\right) \quad (9)$$

where R_s is the standard ratio for oceanic water, ^{18}O and ^{16}O are the concentrations of oxygen isotope and oxygen, respectively. A similar δ value is used for deuterium (δ^2H). Water stable isotopes are normally reported using their δ values ($^{o}/_{oo}$). By rearranging terms in Eq. 9, the mass-balance for $\delta^{18}O$ can be written as a function of $\delta^{18}O$, R_s, and ^{16}O. Since R_s and ^{16}O are constant for all components in Figure 5, the mass-balance relationship can be evaluated using isotopic composition as

$$\delta^{18}O_{us}Q_{us} + \delta^{18}O_tQ_t + \delta^{18}O_{gw1}Q_{gw1} + \delta^{18}O_{gw2}Q_{gw2} - \delta^{18}O_{ds}Q_{ds} = 0 \quad (10)$$

A general matrix representation of the equations used for three or more unknowns can be written as

$$\boldsymbol{A}\,\boldsymbol{x} = \boldsymbol{b} \tag{11}$$

where **A** is a matrix of known quantities, **x** is a vector containing unknown variables. and **b** is a vector with known variables. For unknowns of Q_{gw1}, $Q_{gw2,}$ Q_{ds} and $r_{NO3\text{-}N}$, the matrix and vectors are defined

$$\boldsymbol{A} = \begin{bmatrix} 1 & 1 & -1 & 0 \\ NO_3\text{-}N_{gw1} & NO_3\text{-}N_{gw2} & -NO_3\text{-}N_{ds} & -1 \\ \chi_{1gw1} & \chi_{1gw2} & -\chi_{1ds} & 0 \\ \chi_{2gw1} & \chi_{2gw2} & -\chi_{2ds} & 0 \end{bmatrix} \quad , \quad \boldsymbol{x} = \begin{bmatrix} Q_{gw1} \\ Q_{gw2} \\ Q_{ds} \\ r_{NO3-N} \end{bmatrix}, \boldsymbol{b} = \begin{bmatrix} -Q_{us} - Q_t \\ -Q_{us}NO_3\text{-}N_{us} - Q_tNO_3\text{-}N_t \\ -\chi_{1us}Q_{us} - \chi_{1t}Q_t \\ -\chi_{2us}Q_{us} - \chi_{2t}Q_t \end{bmatrix} \tag{12}$$

where χ_1 and χ_2 can be measured or estimated for $\delta^{18}O$ or other tracers. If groundwater flows are negative, then water is leaving the ditch. Under these conditions, the NO_3-N, χ_1, and χ_2 are defined by the concentrations in the ditch (Eq. 14). In this study, these concentrations are defined as

$$NO_3\text{-}N_{gw1} = NO_3\text{-}N_{gw2} = NO_3\text{-}N_{ch} = \frac{NO_3\text{-}N_{us}\,Q_{us} + NO_3\text{-}N_t\,Q_t}{Q_{us} + Q_t} \tag{13}$$

$$\chi_{gw1} = \chi_{gw2} = \chi_{ch} = \frac{\chi_{us}\,Q_{us} + \chi_t\,Q_t}{Q_{us} + Q_t} \tag{14}$$

If the downstream flow rate is known, then the matrix and vectors of Eq. 12 are defined as

$$\boldsymbol{A} = \begin{bmatrix} 1 & 1 & 0 \\ NO_3\text{-}N_{gw1} & NO_3\text{-}N_{gw2} & -1 \\ \chi_{gw1} & \chi_{gw2} & 0 \end{bmatrix}, \boldsymbol{x} = \begin{bmatrix} Q_{gw1} \\ Q_{gw2} \\ r_{NO3-N} \end{bmatrix}, \boldsymbol{b} = \begin{bmatrix} -Q_{us} - Q_t + Q_{ds} \\ -Q_{us}\, NO_3\text{-}N_{us} - Q_t\, NO_3\text{-}N_t + Q_{ds}\, NO_3\text{-}N_{ds} \\ -\chi_{us}Q_{us} - \chi_t Q_t + \chi_{ds}Q_{ds} \end{bmatrix} \quad (15)$$

If the groundwater flow is negative, then Eqs. 13 and 14 are modified to include the flow rate and NO_3-N concentrations at the downstream location. If the groundwater flow is combined into a single matrix, Eq. 12 can be simplified to a system of three unknowns of Q_{gw}, Q_{ds} and $r_{NO3\text{-}N}$. The matrices of Eq. 15 are then defined and solved using values corresponding to subscripts of "gw" instead of "gw1", and "ds" instead of "gw2".

Problems arise in the solution of Eq. 11 if **A** is an ill-conditioned matrix. The condition numbers often provide useful information on ill-conditioning. For ill-conditioned matrices, a relatively small change in the values of vector **b** results in large changes to the solution vector **x** (Atkinson, 1978). To reduce the condition numbers, each row of **A** is divided by its largest element. Corresponding adjustments are also made to the elements of **x** and **b**. Matrix manipulation and computations for the observed data sets were done using the R statistical package (R Core Team, 2015).

Potential Soil Denitrification Rate

The soil potential denitrification rate is obtained using the acetylene inhibition method (Groffman *et al.,* 2006). This method uses an acetylene inhibition assay to block the conversion of nitrous oxide (N_2O) to nitrogen gas (N_2). Nitrous oxide then becomes the terminal product of denitrification. Nitrous oxide is a more convenient to measure than the ubiquitous N_2 gas. However, this method has been found to possibly underestimate the denitrification rate because it inhibits the production of nitrate by nitrification (Groffman *et al.,* 2006). This method does not take into account nitrogen uptake by plants. The alternative

method (water chemistry analyses) requires well sampling and can be used to determine if denitrification is likely occurring in soils - the extent or the potential of which is unknown and cannot be quantified. The benefit to the acetylene method is that well installation is not required and denitrification potential of dry and aerated soils can be assessed.

On July 2, 2013, homogenized soil samples were thoroughly mixed and about 15 g were removed and dried for 4 hours at 288 ^{o}C to measure organic matter content. Generally, for gas analysis, 3 replicates of 40 g of the samples where slurried with 40 mL of channel water, amended with 4,000 mg/L of chloramphenicol to measure the denitrification enzyme activity (DEA). For the soils collected from the southern bench treatment site, enough soil volume was collected for only 2 replicates. The sample bottles were placed on a bottle-rolling machine for mixing. The start (T_i) and ending (T_f, 2.5 hours after T_i) N_2O concentration was determined on a gas chromatograph and is a measure of the denitrification potential.

The Bunsen corrected production of N_2O-N is computed as

$$N_2O - N = \frac{M_f - M_I}{m_s \left(T_f - T_i\right)} \tag{16}$$

where m_s is the mass of the soil (dry weight, g), M_I and M_F are the initial and final masses of N_2O in the liquid water and gas phases (μg N_2O-N L^{-1}), respectively, T_f - T_i is the total incubation time (hr), and N_2O-N is the mass of nitrous oxide produced as nitrogen per soil mass per time with typical units of μg N_2O-N g DM^{-1} h^{-1}. The Bunsen solubility coefficient at room temperature was used to determine the mass of N_2O-N in the liquid water. The areal denitrification rate is obtained from the measured bulk density of the soil and known depth of the soil core as

$$r_{N2O-N} = N_2O\rho_b D_c \quad (17)$$

where ρ_b is the bulk density of the soil (g DM cm^{-3}), D_C is the depth of the core (cm) and $r_{N2O\text{-}N}$ is the denitrification rate per surface area of soil with typical units of mg N_2O-N m^{-2} h^{-1}. For application to agricultural drainage ditches, a habitat-weighted areal denitrification rate is used. It is defined as

$$\bar{r}_{N2O-N} = r^b_{N2O-N}\left(\frac{A_b}{A}\right) + r^r_{N2O-N}\left(\frac{A_r}{A}\right) + r^c_{N2O-N}\left(\frac{A_c}{A}\right) = r^b_{N2O-N}\,F_{Ab} + r^r_{N2O-N}\,F_{Ar} + r^c_{N2O-N}F_{Ac} \quad (18)$$

where $\bar{r}_{N2O-N}$ is the habitat-weighted areal denitrification rate with typical units of mg N_2O-N m^{-2} h^{-1} (often also converted to kg km^{-1} d^{-1} and kg d^{-1} for comparisons to the literature), the subscripts and superscripts of “c”, “r”, and “b” are used to represent the habitat zones corresponding to the channel, riparian and non-riparian bench components of the ditch system, respectively (Fig. 4), A is the surface area of each habitat zone, and F_x is the fraction of the area for each of the habitat zones.

For our two-stage ditch, the surface area of the channel is estimated using a length of 1890 m and an average channel width measured from 7 cross-sections in 2013 as 4.37 m (Krider *et al.,* 2017). An important source of NO_3-N for the riparian zone is groundwater flow. The surface area of this zone is estimated using east and west side lengths of 1890 m and widths of 0.3 m to capture the soil-water interface. This includes soil that is saturated above the water line at any given time and will move with the water level. In general, the non-riparian bench zone has a length of 1890 m and a designed width of 3.28 m for each side of the ditch (Krider *et al.,* 2017). For this zone, nitrate removal is likely just below the soil surface where soil is moist from interaction with the water table. This is best represented by samples taken from the non-riparian bench treatment system. We then obtain F_{Ac} = 0.379, F_{Ar} = 0. 0.026 for each side of the ditch and F_{Ab} = 0.569. Hypothetical denitrification of a conventional ditch is estimated by

removing the effect of the bench treatment system. This assumes that the side slopes of the conventional ditch above bankfull do not provide area for denitrification, similar to the two-stage ditch side slopes.

We also estimated potential N-removal at the reach scale (kg N_2O-N km^{-1} d^{-1}) and for the entire ditch length (kg d^{-1}) both under conventional and current conditions by multiplying site areal denitrification rates (mg N_2O-N m^{-2} d^{-1}) for the main channel and floodplain benches by their respective total areas (m^2 per 1 km reach and the entire ditch length; Roley *et al.,* 2012b). Percent nitrogen removal is calculated using the inflow nitrogen load from September 2011 (24.69 kg d^{-1}) from the mass-balance approach.

Analysis of Water Quality Data

Stable Isotope Comparison

Concentrations of $\delta^{18}O$ have been shown to generally vary with evaporative processes (Clark and Fritz, 1997). Each source of flow might then have a different representative concentration, an especially desirable feature of a tracer. This possibility was explored by plotting measured $\delta^{2}H$ values for groundwater, tile, and channel flows as a function of their corresponding $\delta^{18}O$ values against the global mean weighted meteoric water line (Fig. 6). Among other factors, deviations from this line are expected for water sources with different residence times and evaporation rates (Simpkins, 1995; Clark and Fritz, 1997; Magner and Alexander, 2008). Meteoric waters that have undergone evaporation define the evaporation line, which are typically comprised of surface waters and closely follow a linear regression line with a (relatively) reduced slope (Gibson *et al.,* 1993; Nyende *et al.,* 2013). Groundwater evaporation occurs through soil capillaries and is generally less than surface water, especially if the soil above the groundwater is saturated, hence producing a steeper slope to the isotopic signature (USGS, 1999). These differences allow the ability to distinguish

between different sources of water, which is crucial when using isotopes as a tracer.

Trends are apparent in the observed data as the difference between intercept and slope for the regression line for all two-stage ditch channel, tile, and groundwater isotope samples and the global mean weighted meteoric water line (all two-stage ditch samples: $y = 6.56x - 0.68$, $R^2 = 0.86$; GMWL: $y = 8.17x + 10.56$; Fig. 40). Specifically, the slope of the channel is less than the slope of the tile, which is less than the slope of the groundwater, which follows the expected pattern based on evaporation. A coincidence of regression was performed to decipher if the slopes and intercepts are significantly different for each source. There was no statistically significant difference among the slope and intercept terms, independently of one another. There was no significant difference between the combination of the slope and intercept terms between the channel and well or between the channel and tile. This is likely due to the higher amount of scatter in the channel data (adjusted $R^2 = 0.84$). However, the combination of the slope and intercept terms between the tiles and wells were significantly different than one another ($P = 0.009$). Additionally, the mean δ^2H and $\delta^{18}O$ values show a similar significant difference. The mean δ^2H and $\delta^{18}O$ values are significantly different between the tiles and wells (δ^2H $P = 0.007$ and $\delta^{18}O$ $P = 0.003$) but the channel is not significantly different than the tiles (δ^2H $P = 0.053$ and $\delta^{18}O$ $P = 0.07$) or the wells (δ^2H $P = 0.93$ and $\delta^{18}O$ $P = 0.68$). As evidenced by the high tile line input and consistent baseflow conditions, the channel flow is largely composed of tile drainage and upstream groundwater contributions, which could lessen the isotopic difference between the channel and the other sources.

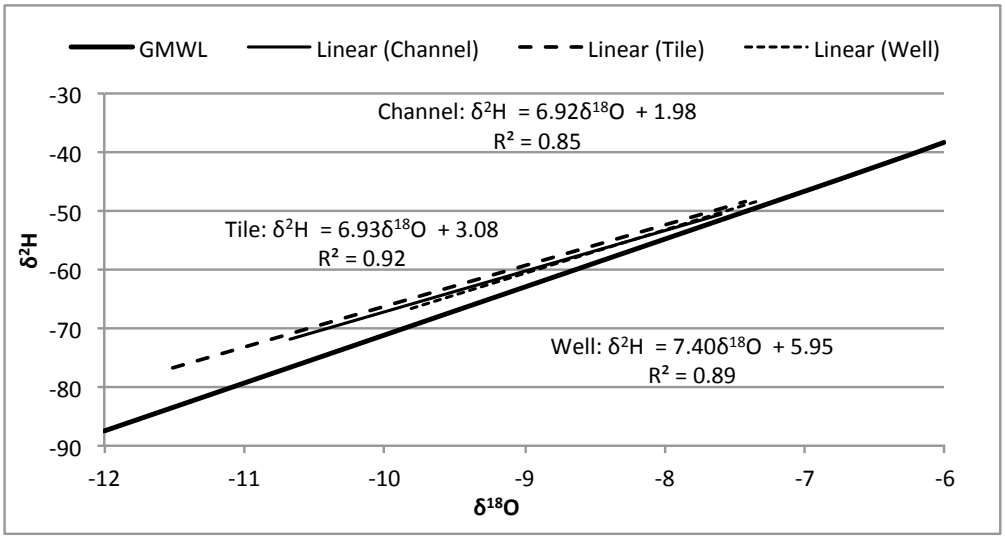

Figure 40. $\delta^{18}O$ vs. $\delta^{2}H$ for samples taken from the wells, tiles, and within the channel (R^2 = 0.89) against the global mean weighted meteoric water line $\delta^{2}H = 8.17\delta^{18}O + 10.56$ (Gat, 1981).

Values of $\delta^{18}O$ vary throughout the longitudinal transect of the ditch for both the tile lines and channel with some clear patterns. This is demonstrated by using a particular sampling date (Aug. 3, 2010) as an example (Figs. 41 and 42). Although the two sources have very similar $\delta^{18}O$ minimum values, the maximum is slightly more negative for the channel than for the tile (-7.68 vs. -7.48). However, a student's two-tailed t-test shows that the means for these sources are not significantly different than one another (P = 0.253). The tile lines with the most negative $\delta^{18}O$ (179 and 631 m) correspond well to those with typically (and relatively) very low-flow rates (0.42 and 0.04 L s^{-1}) (Fig. 8). The $\delta^{18}O$ of the channel is generally more negative between 600 and 1100 m and 1500 to 1800 m from the north culvert. The average $\delta^{18}O$ between 600 and 1100 m and 1500 to 1800 m is significantly different than the average $\delta^{18}O$ from 0 to 600 m and 1100 to 1500 m, -8.53 vs. -7.92, respectively (P <0.0001) (Fig. 7). More negative values of $\delta^{18}O$ could indicate a higher input of groundwater or a lower input of tile line flow. This aligns with the area of high groundwater flow, particularly between 1500 and 1800 m, where the average channel temperature for August 4, 2010, is 0.32 ^{o}C less than the average channel temperature between 0 and 1500 m (Fig. 41).

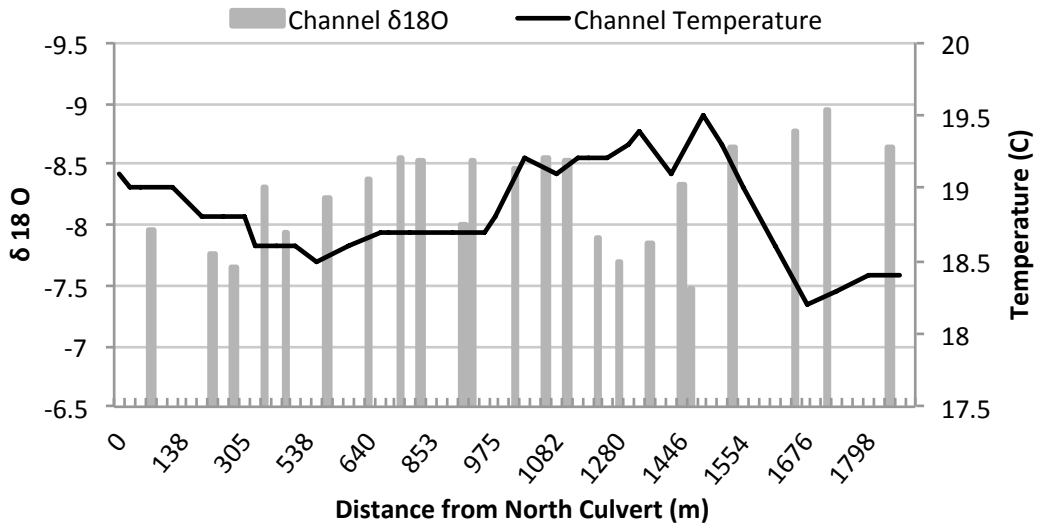

Figure 41. $\delta^{18}O$ on August 3, 2010, and temperature (C) on August 4, 2010, for the channel throughout the two-stage ditch reach length.

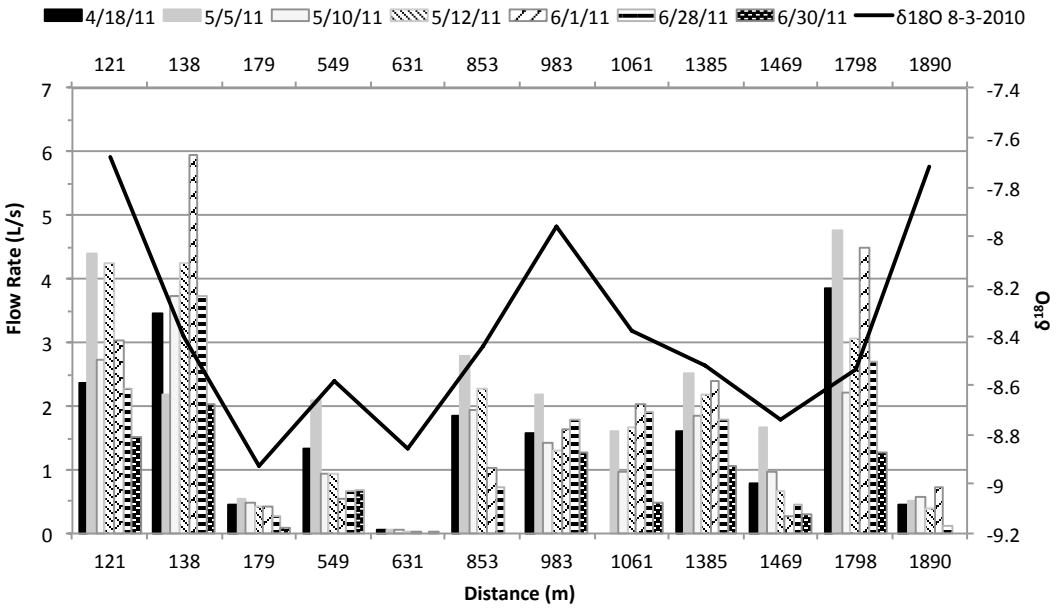

Figure 42. Tile flow rates (L s^{-1}) along the Mullenbach Two-Stage Ditch reach (m) for 7 representative dates in April, May, and June of 2011.

Overall, the isotopes levels were relatively stable over time for each well location and exhibited a similar pattern between $\delta^{18}O$ and $\delta^{2}H$, with some exceptions (Figs. 43 and 44). Considerably more negative values of both $\delta^{18}O$ and $\delta^{2}H$ occur on two of the four dates for some of the wells. However, no dates were found to be significantly different from another. The wells had statistically significant difference values for both $\delta^{18}O$ and $\delta^{2}H$ with location across dates. The Fisher LSD post hoc test shows that 8 wells were significantly different from another well(s) in $\delta^{2}H$ based on location (<0.043) and 6 wells were statistically different from another well in $\delta^{18}O$ (P <0.045) based on location. Additionally, $\delta^{18}O$ and $\delta^{2}H$ values varied with well depths. This could be attributed to the location within the ditch (side or distance). The well depth of 61 cm (24") is significantly different from 99 and 122 cm (39 and 48") in $\delta^{2}H$ (P <0.01); while the well depth of 61 cm is only significantly different from the depth of 99 cm in $\delta^{18}O$ (P <0.001). However, the shallowest well depth of 61 cm has the most negative average value for both $\delta^{2}H$ and $\delta^{18}O$, which could indicate an area where there is a more direct conduit to deeper groundwater.

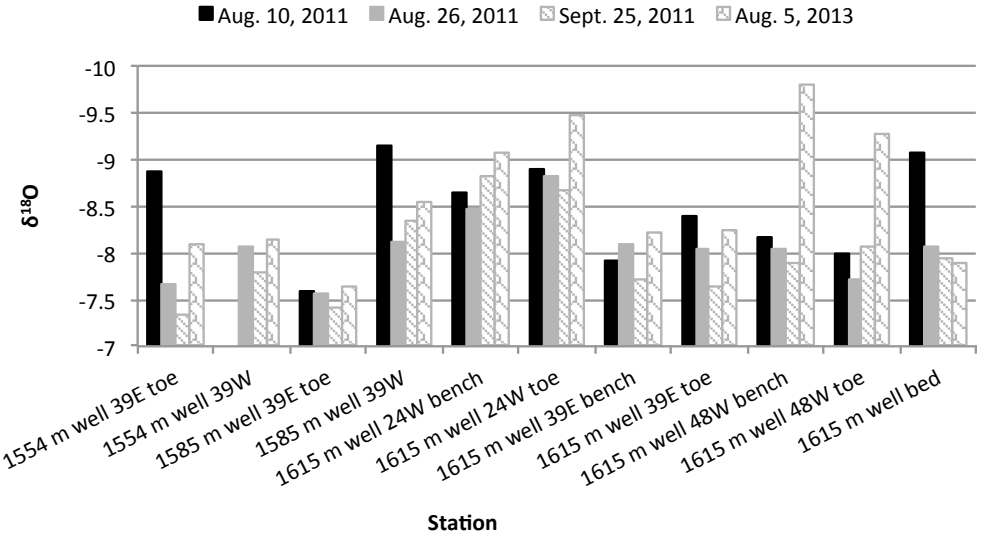

Figure 43. $\delta^{18}O$ for wells in the test section (1554 m to 1615 m) of the Mullenbach Two-Stage Ditch for 4 dates from 2011 to 2013.

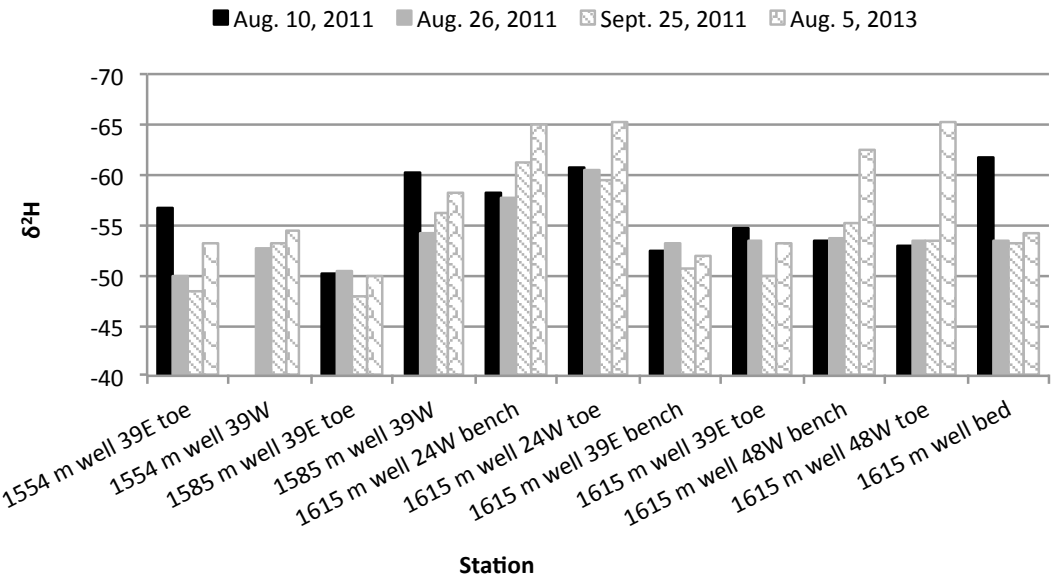

Figure 44. δ^2H for wells in the test section (1554 - 1615 m) of the Mullenbach Two-Stage Ditch for 4 dates from 2011 to 2013.

General Trends in Nitrate-Nitrogen Concentrations

Nitrate-nitrogen concentrations vary both spatially and temporally (Figs. 45 and 46). Spatial variability from the upstream to downstream locations and is represented by a springtime nitrogen profile taken on April 11, 2012 (Fig. 45). Nitrate-N levels on this date spiked at 2.62 mg L^{-1} at 366 m. At around 1463 m, the nitrate-N levels dropped from 2.19 to 1.76 mg L^{-1} and remained less than 1.84 mg L^{-1} for the remaining ditch length. There is a significant difference between the average NO_3-N upstream (0 to 1402 m) and the average downstream (1463 to 1892 m) concentration at 2.44 vs. 1.88 mg L^{-1}, respectively ($P < 0.001$). This reduction in NO_3-N over the longitudinal profile of the ditch could indicate dilution by a lower concentration source water such as the groundwater. The distance, in this case at about 1500 m, corresponds to a large groundwater contribution area caused by sandy soils of the historic streambed. Additionally, an early spring date such as April 11 could have occurred prior to spring rains or

snowmelt which can contribute high concentration surface runoff and that deeper groundwater above less permeable soils such as loess typically has nitrate-N concentrations below 2 mg L^{-1} (Mueller *et al.,* 1995).

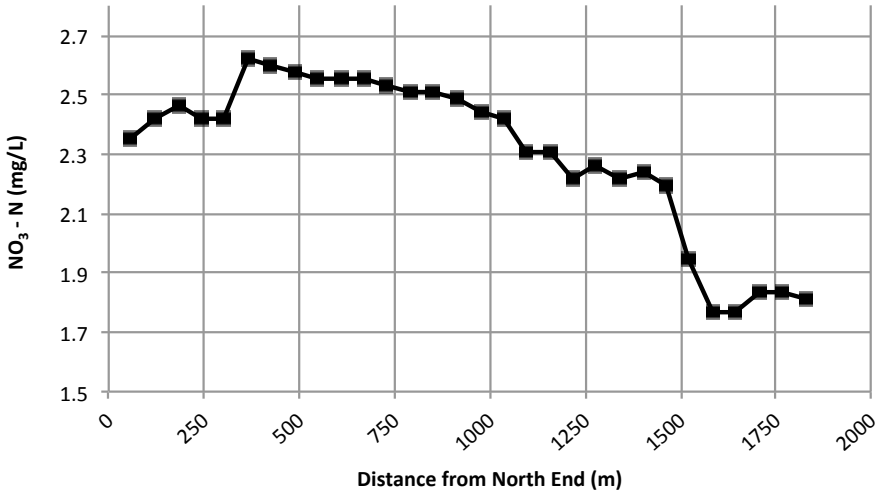

Figure 45. NO_3-N concentration (mg L^{-1}) profile within the channel of the Mullenbach Two-Stage Ditch from north to south on April 11, 2012.

The total tile flow rate and nitrogen loading as well as the average tile line NO_3-N concentrations vary through time from spring to early summer. This is demonstrated using tile line data from spring and summer of 2011. Average NO_3-N concentrations in the tile line discharge are fairly consistent between 4.1 and 5.6 mg L^{-1} (Fig. 46). Flow rates are largest for between mid-April to mid-May with a maximum of 108.25 L s^{-1} on April 28, 2011. These large total flow rates and loadings are likely related to spring snowmelt and spring rainfall. Moderate flows between about 18 and 44 L s^{-1} occur throughout the rest of the season and are likely related to rainfall events (Fig. 57). These results are consistent with those reported by Randall (2004) who found that 50% of the total annual tile drainage typically occurs in a 7 to 14 day time period. Due to the nearly constant concentration and the larger flow rates during the early spring, the largest nitrate-

nitrogen loads occur during this time period with a maximum of 45.2 kg d^{-1} on April 28, 2011.

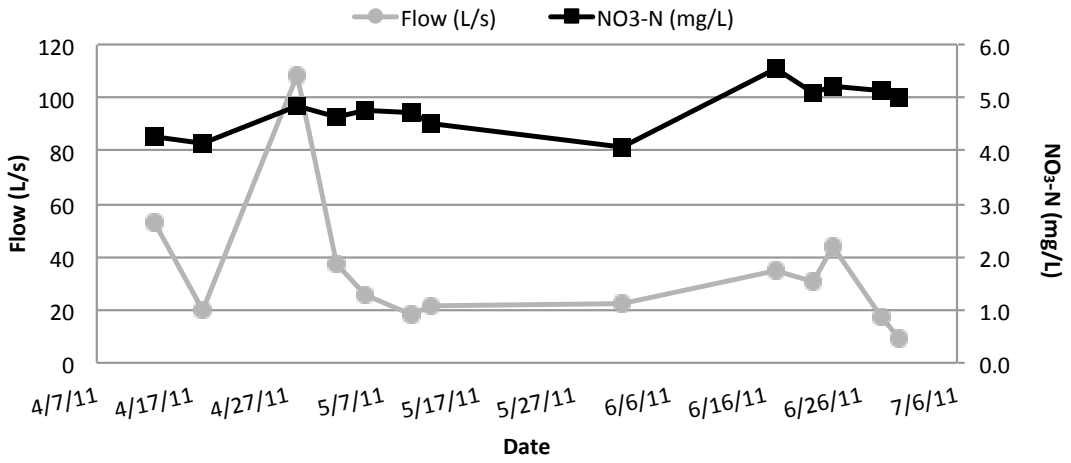

Figure 46. Total tile flow rate (L s^{-1}) and average tile NO_3-N (mg L^{-1}) concentration by date from the Mullenbach Two-Stage Ditch in 2011.

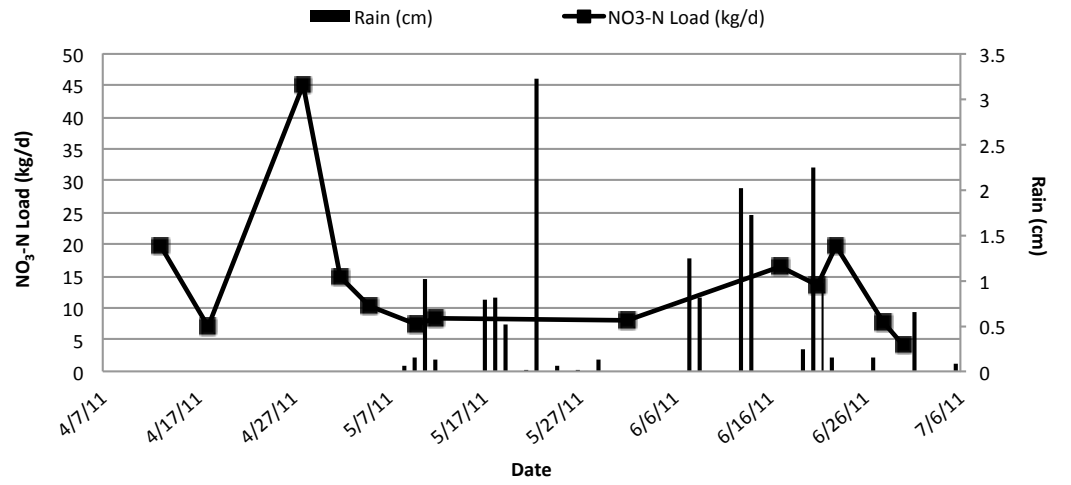

Figure 47. Total NO_3-N load (kg d^{-1}) from tile flow and rainfall events (cm) by date for the Mullenbach Two-Stage Ditch in 2011. Missing rainfall data from before 5/12/11.

Nitrate-N concentrations also varied throughout time and location amongst the tile lines. This is demonstrated using 7 dates of tile line data from the spring and summer

of 2010 (Fig. 48). Although no dates are significantly different from one another, June 16, 2010, occurred 1 day after a 3.51 cm rainfall event, which could explain the larger difference in concentration from several of the tile lines on this date (138, 853, and 1061 m). The tile line at 179 m is significantly different in NO_3-N concentration from most of the other tile lines, except those at 121 m (P = 0.079), 983 m (P = 0.514), and 1061 m (P = 0.221). Also, the tile line at 631 is significantly different in NO_3-N concentration from the tiles at 121, 549, 853, and 1385 m (P <0.041). Some tiles (179 and 631 m) have consistently low nitrate-N concentrations throughout time. It is unclear what may be causing the difference in tile line NO_3-N concentration across space and time but it may be associated to soil type or groundwater input.

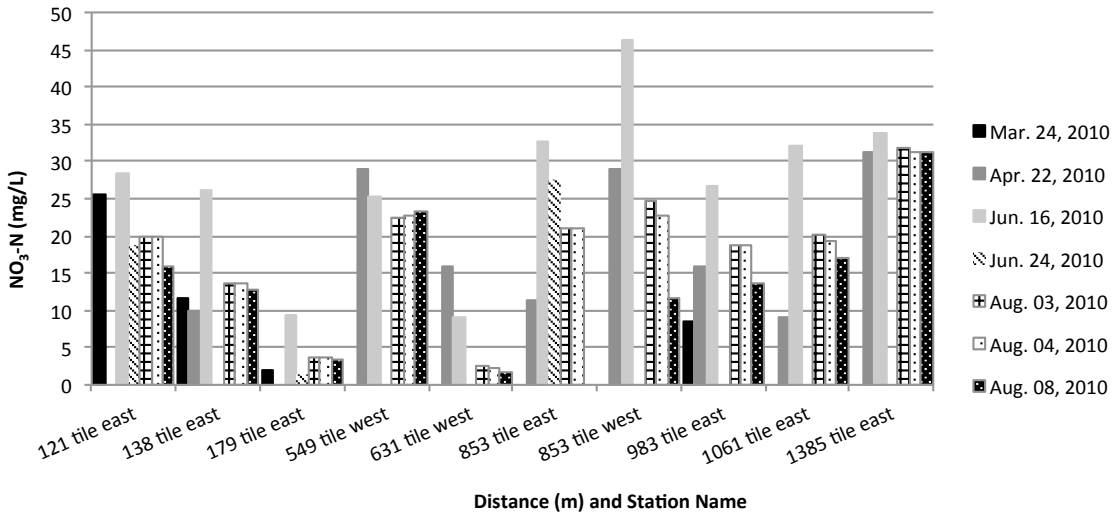

Figure 48. Nitrate-N (mg L^{-1}) across 10 tile lines along the Mullenbach Two-Stage Ditch reach for 7 dates in the spring and summer of 2010.

Nitrate-N levels in grab samples collected from shallow wells varied considerably throughout the ditch profile. The lowest detected NO_3-N concentration occurred on August 26, 2011, and was reported as 0.2 mg L^{-1} for the 1615 m well sampled just below the channel bed and the highest level as 46 mg L^{-1} in the 1615 m well 48W bench (Fig. 49). Extreme variability was also

detected over wells located at station 1615 m (1615 m well 48W bench and 1615 m well 24W bench). Nitrate-N levels from these two wells differed by 40 mg L^{-1} NO_3-N but they were located approximately 0.9 m apart from each other and only varied in depth by 0.3 m. The reason for these large NO_3-N concentrations and rapid changes are unclear but it may be associated to different sources of water or preferential flow pathways. It may be speculated that the high concentration water is sub-surface flow from the adjacent farm field and the lower concentration water is from either the channel or a deeper source aquifer.

Nitrate-N levels in the well grab samples also varied over time. For the samples collected on September 18 and 20, 2013, water entering the test section had a nitrate concentration at 11.3 and 12.4 mg L^{-1} NO_3-N, respectively (Fig. 49). In general, the concentrations from the tile lines and groundwater wells were larger than this upstream concentration. Exceptions to this trend are the 1615 m east and bed wells and the 1585 m well E bench 24 on Sept 18, which have the lowest nitrate concentrations of the sample set at less than 15 mg L^{-1} NO_3-N. Extreme variability in the nitrate concentration was, again, found among the wells clustered at 1615 m. They range in concentration from 10.1 mg L^{-1} to 130 mg L^{-1} NO_3-N. In general, the concentrations are larger for the wells located on the west side of the ditch. On September 18, the average NO_3-N concentration at 1615 m on the east side of the ditch was 13 mg L^{-1} but 88 mg L^{-1} on the west side of the ditch. Concentrations are also generally greater for shallow wells. A total of 10 of the 13 wells in the test section have NO_3-N concentrations that are greater on September 20 than on September 18, most slightly to moderately higher, with the exception of the 1585 well E bench 24, 1615 m well W bench 24, and 1615 m well W toe 48, which is considerably higher on September 20 (53.1, 28.0, and 26.4 mg L^{-1} NO_3-N higher, respectively). The 1615 m west wells have the highest concentrations within the entire test section. Again, the reason for these patterns is unclear.

A comparison of all three dates shows similar trends for each individual well over time with more variability occurring in the 1615 m wells W and the 1585 m well E bench 24 (var.> 500 mg L^{-1}). The least variability occurs in the 1615 m well bed (var.< 0.5 mg L^{-1}). The Fisher LSD test shows the 1615 well W toe at both depths are significantly different than the rest of the wells ($P < 0.049$). Furthermore, the results on Sept. 20, 2013 are significantly different from Aug. 26, 2011 ($P = 0.01$). The general difference between August and the latter September date could be due to nitrate accumulation in the soil, a lack of precipitation, or based on yearly fluctuations.

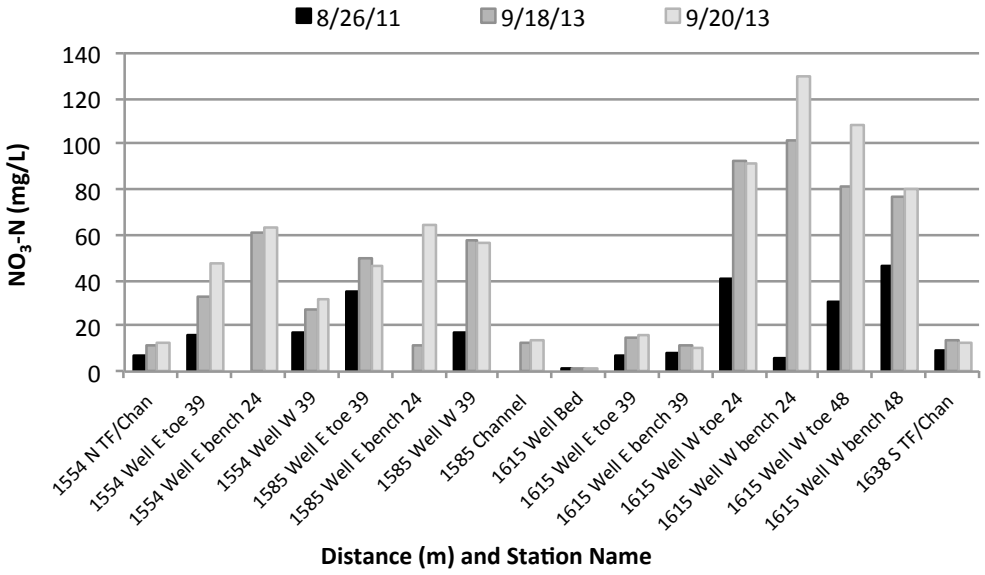

Figure 49. Nitrate-N (mg L^{-1}) for the well sample sites within the test section (1554 to 1615 m) as well as at the north (1554 m) and south temporary flumes (1638 m) for the Mullenbach Two-Stage Ditch over three sampling dates. Data is missing for the 1554 m well E and W bench 24 and the channel at 1585 m for 8/26/11.

In-Channel Denitrification

Nitrogen removal is computed using data collected in the selected time periods of 2010, 2011, and 2013. The least amount of information for these computations is available in 2010, with the most in 2013. In 2010, the downstream flume did not accurately measure the flow rate and delays in the installation of wells prevented the collection of reliable NO_3-N concentrations, $\delta^{18}O$, and other possible tracer data from potential groundwater flow. Our mass-balance methods did not account of evapotranspiration by plants within the ditch. These values were calculated as 1.59 and 2.46 mm d^{-1} on September 18, 2013, and September 21, 2011, respectively, which falls within the estimated values of 1.1 to 3.6 mm d^{-1} presented by Lahti (2012) but was considered negligible in the overall water balance for the ditch, similar to Gentry *et al.* (2009), as given by Eq. 3.

Approximate estimates of removal efficiency can be obtained without groundwater information. These estimates require that the inflow concentrations of NO_3-N from different sources within the study reach are approximately equal. Nitrogen removal can be estimated using the trend lines for the upstream and downstream concentration for 2010 (Fig. 50). The highest average monthly influent and effluent NO_3-N concentrations occurred in June at 5.05 and 4.13 mg L^{-1}, respectively. The highest average daily influent NO_3-N concentration occurred on June 17th at 6.31 mg L^{-1} and the highest average daily effluent concentration occurred 2 days prior (June 15th) at 5.65 mg L^{-1}. This corresponds to the 3.51 cm rainfall event that occurred on June 15. Monthly percent removals decreased slightly from the spring through the summer with May having the highest percent removal at 19.50% and September having the lowest percent removal at 12.88% (Table 5). The Fisher LSD test showed that May was significantly different than September in percent removal ($P = 0.027$). This difference may be explained by high influent nitrate loading occurring earlier in the year, likely in the springtime. Daily percent removal varied between -11.64

and 45.36% with a mean of 16.46% (SD = 9.17). The intercept for the trend line of the effluent concentration is considerably less than the intercept for the influent concentration (2.36 vs. 3.61 mg L^{-1} NO_3-N), which further supports that the influent concentration is typically higher than the effluent.

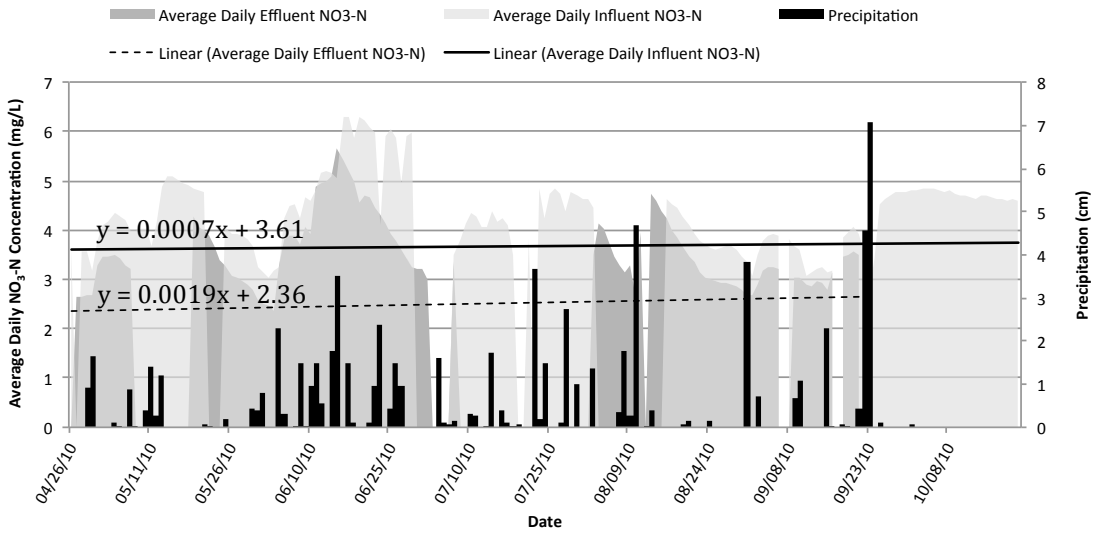

Figure 50. Daily average upstream (north flume influent) and downstream (south flume effluent) concentrations of NO_3-N (mg L^{-1}) and total daily precipitation (cm) for April 26 – Oct 21, 2010 at the Mullenbach Two-Stage Ditch. Linear regression lines show the slope and intercept for the influent and effluent concentrations (placed above the corresponding regression line). Downstream effluent NO_3-N data ends on September 21, 2010.

Table 5. Average monthly influent and effluent NO_3-N concentrations (mg L^{-1}) for 2010 at the Mullenbach Two-Stage Ditch as well as the difference between the two (mg L^{-1}) and the NO_3-N removal efficiency.

Time Period	Influent (mg L^{-1})	Effluent (mg L^{-1})	Difference (mg L^{-1})	Removal (%)
May	4.09	3.30	0.80	19.50
June	5.05	4.13	0.92	18.16
Aug	3.88	3.23	0.65	16.65
Sept	3.58	3.11	0.46	12.88

The first week in August 2010 was selected for a more detailed analysis of the ditch nutrient response. Flow rates as well as NO_3-N and $\delta^{18}O$ concentrations were measured in the tile discharge. Upstream and downstream NO_3-N concentrations and numerous $\delta^{18}O$ samples were taken in the channel (Figs. 43 and 48). The flow rate was measured at the upstream flume but a reliable flow rate could not be obtained at the downstream outlet. Concentrations of NO_3-N and $\delta^{18}O$ were unavailable for groundwater sources. Estimates of the removal efficiency were obtained using the matrix formulations for the elements of vector **x** as Q_{gw}, Q_{ds} and $r_{NO3\text{-}N}$ (Eq. 15). Unknown groundwater NO_3-N and $\delta^{18}O$ data were considered by using a range of possible values for the less fractionated or more pure groundwater found at the more negative end of the $\delta^{18}O$ spectrum. These values are likely less than -11 and approximately -10 to -8.5 based on previous estimations of the water balance within the Mullenbach Two-Stage Ditch (Kramer, 2011) and data from north-central Minnesota (Reddy *et al.,* 2006). Groundwater values of $\delta^{18}O$ of -9, -9.5, and -10 were selected. For $\delta^{18}O$ = -9, the groundwater contribution to the downstream flow (obtained by Eq. 15) is approximately two times larger than the upstream flow rate; whereas for $\delta^{18}O$ = -10 the groundwater contribution is roughly one-half of the upstream inflow rate. Groundwater NO_3-N concentrations were varied between 18 mg L^{-1} to 36 mg L^{-1} to represent an average range in well concentrations. The removal efficiencies under different possible values of $\delta^{18}O$ and groundwater NO_3-N concentrations range from approximately 10% to 40% (Fig. 51). For a large groundwater contribution and groundwater concentrations of NO_3-N of 25 mg L^{-1}, the percent removal of NO_3-N is approximately equal to 20%. Assuming that this section corresponds to a typical removal rate for the entire ditch, these values are similar to the September 2013 value found using Eq. 6.

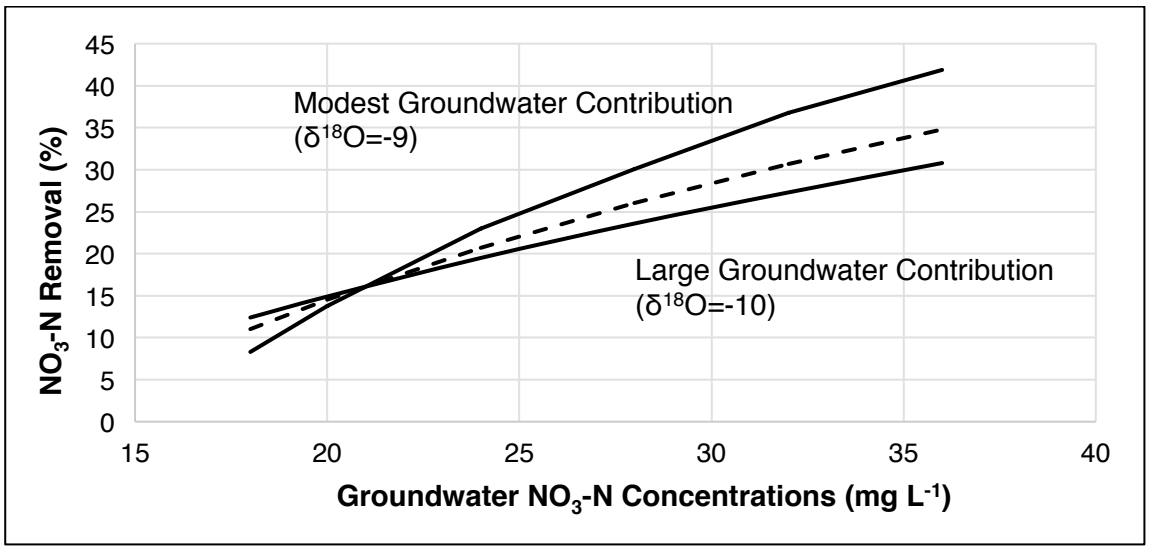

Figure 51. Removal efficiencies of NO_3-N (%) based on a range of $\delta^{18}O$ and NO_3-N concentrations for the Mullenbach Two-Stage Ditch for the time period of August 3, 2010.

Detailed measurements were also collected on September 21, 2011. The flow rates for the entire ditch reach were reliably measured as 4.3 L s^{-1}, 0.3 L s^{-1} and 19.0 L s^{-1} for the upstream, tile, and downstream components, respectively. The groundwater flow rate was, therefore, estimated as 14.4 L s^{-1}. The groundwater component was evaluated as a single source using the groundwater concentration of NO_3-N obtained by the average value measured in the wells. Only one of the tile lines had flow for this period with a NO_3-N concentration of 22.2 mg L^{-1}. The removal rate is determined as 7.9 kg NO_3-N d^{-1} with a removal efficiency of 32% (Eqs. 7 and 8).

The time period with the greatest amount of information for determining removal efficiency corresponds to data collected in September 2013. This analysis focused on the section of the ditch between locations 1554 m and 1638 m. The removal efficiency was estimated using the upstream and downstream flow rates and nitrate concentration measured on September 18th, 2013. There were no contributions from tile lines within this section. The flow rates at the upstream (1554 m) and downstream (1638 m) sites were 28.5 L s^{-1} and 32.2 L s^{-}

^{1}. The net groundwater contribution into the study section is, therefore, 3.7 L s^{-1}. The $\delta^{18}O$, $\delta^{2}H$, and NO_3-N data were used in this analysis (Figs. 43, 44, and 48, respectively). Due to the large variation in NO_3-N in the wells, the contributions of groundwater were divided into two zones. Initial attempts to define the zones based on depth and other factors were unsuccessful. Zones were eventually defined based on NO_3-N concentration. Zone 1 was defined by contributions from wells with concentrations less than or equal to 50 mg L^{-1}. The other wells were used to define the characteristics for Zone 2 (>50 mg L^{-1}). Average values for these variables were obtained from measured well data by zones. Inconsistent results were obtained using specific conductance. The most robust solution (lowest condition number) was obtained using $\delta^{2}H$. For $\chi = \delta^{2}H$, the groundwater flow rate from the Zone 1 was 18.1 L s^{-1} and -14.4 L s^{-1} from Zone 2. This produces a removal efficiency of 17% with a removal rate of 7.7 kg NO_3-N d^{-1}. An alternative approach is to evaluate removal using a single groundwater source. By using the average nitrate concentrations of all of the wells, the removal efficiency is computed as 12.1% and the removal rate is 5.2 kg NO_3-N d^{-1}.

Soil Denitrification Using Laboratory Data

The rates of nitrous oxide production found in our study are similar to those reported for other two-stage ditches (Table 6). Mahl *et al.* (2015) found rates of in-stream N_2O production up to 1.7 µg N_2O-N g DM^{-1} h^{-1} and up to 3.7 µg N_2O-N g DM^{-1} h^{-1} on the floodplain benches for 6 two-stage ditches in Indiana and Ohio, respectively. They found that the least production occurred in the summer and fall and the highest rates occurred in the spring when NO_3-N loading was highest. Powell and Bouchard (2010) investigated 10 naturally formed (not constructed) two-stage agricultural ditches in Ohio and found N_2O production between 0.1 and 3.4 µg N_2O-N g DM^{-1} h^{-1} for the channel sediments and between 0.1 and 9.2 µg N_2O-N g DM^{-1} h^{-1} for the bench and slope sediments. For samples taken in headwater agricultural streams, N_2O production between 0.1

and 4.3 µg N_2O-N g DM^{-1} h^{-1} was found in east-central Illinois (Schaller *et al.,* 2004), 0.03 to 0.69 µg N_2O-N g DM^{-1} h^{-1} in southern Michigan (Inwood *et al.,* 2005), and 0.34 to 1.88 µg N_2O-N g DM^{-1} h^{-1} in southern Michigan (Arango and Tank, 2008). Our range of 0.08 to 1.85 µg N_2O-N g DM^{-1} h^{-1} falls within the range expected for a two-stage ditch in the upper Midwest.

Soil denitrification rates for the same habitat zones differed between the north and south sites (Eq. 17, Table 6). The denitrification rate was higher for all habitat zones at the north site. Although the rates differ between the sites, similar patterns are obtained at both sites. The smallest areal denitrification rates were for the channel zones and the largest rates were for the riparian zones. Although the rate of nitrous oxide production was higher, the north non-riparian site had a smaller areal denitrification rate than the north riparian areas due to a lower, overall bulk density of the soil. The channel zones had less organic matter than the other zones. The non-riparian bench zone had more organic matter but smaller areal denitrification rates than the riparian zones. However, a linear regression analysis shows that there is no significant difference in the areal denitrification rate due to percent organic matter at the 5% level but there is at the 10% level ($P = 0.09$).

Table 6. Summary of soil denitrification results via the acetylene inhibition assay from July 1, 2013, at the Mullenbach Two-Stage Ditch. The habitat-weighted denitrification rates are for the entire ditch length.

Site	Habitat Zone	Organic Matter (%)	Bunsen Corrected N_2O Production ($\mu g\ N_2O\text{-}N\ g\ DW^{-1}\ h^{-1}$)	Areal Denitrification Rate ($mg\ N_2O\text{-}N\ m^{-2}\ h^{-1}$)	Denitirifcation Rate ($mg\ N_2O\text{-}N\ m^{-2}\ h^{-1}$)	
					Conventional	Two-Stage Ditch
South	Non-Riparian	8.39	0.75	25.74	0.00	14.64
	East Riparian	7.94	1.50	48.78	1.29	1.29
	West Riparian	6.47	1.62	59.01	1.56	1.56
	Channel	1.2	0.08	3.57	1.35	1.35
North	Non-Riparian	7.21	1.85	56.72	0.00	32.25
	East Riparian	5.32	1.79	69.19	1.83	1.83
	West Riparian	6.65	1.73	61.14	1.62	1.62
	Channel	4.22	0.29	9.53	3.61	3.61
Habitat-weighted Denitrification Rate			Total Using South Rates		4.20	18.84
			Total Using North Rates		7.05	39.30

The habitat-weighted denitrification rates for the two sites are also similar to those reported by others. Roley *et al.* (2012a) found a range of habitat-weighted denitrification rates, from 0.02 to 6.7 mg N_2O-N m^{-2} h^{-1} for the benches of a two-stage ditch in Illinois. They found habitat-weighted denitrification between 3.2 and 20.3 mg N_2O-N m^{-2} h^{-1} for in-stream data. Schaller *et al.* (2004) obtained similar results for headwater agricultural ditches in Illinois with benthic sediment supporting denitrification rates upwards of 15.8 mg N m^{-2} h^{-1}. Royer *et al.* (2004) found denitrification rates upwards of 15 mg N m^{-2} h^{-1} during times of high in-stream NO_3-N in five agricultural headwater streams in east-central Illinois. The range of denitrification rates found at 7 of the 8 total habitat zones (1.29 to 14.64 mg N_2O-N m^{-2} h^{-1}) is similar to the values found in the literature, besides the highest value of 32.25 mg N_2O-N m^{-2} h^{-1} found in the non-riparian bench treatment section on the north site. This produces a total habitat-weighted denitrification rate in the range of 18.84 to 39.30 mg N_2O-N m^{-2} h^{-1} and includes all of the cumulative treatment areas for the two-stage ditch.

The hypothetical conventional drainage ditch removes 0.16 to 0.40 kg N_2O-N km^{-1} d^{-1} at the reach scale and 0.31 to 0.76 kg NO_3-N d^{-1} for the entire ditch, removing 1.24% to 3.09% of the inflow load using the 2011 mass-balance approach. By using the total surface area of all three zones (21,806 m^2) and applying the non-riparian denitrification rate to the benches, the removal rates using the south and north site rates, respectively, are 2.47 and 5.48 kg N_2O-N km^{-1} d^{-1} on a reach scale and 4.66 and 10.36 kg N_2O-N d^{-1} for the entire ditch. The estimates of removal efficiencies are limited by a lack of data necessary to produce a full water and nitrate balance for this date. Instead, comparing the values to the in-stream mass-balance removal rate found in 2011 shows the numbers to be very similar (5.2 to 7.9 kg NO_3-N d^{-1}). Additionally, using the NO_3-N_{in} for 2011 (24.69 kg NO_3-N d^{-1}), the removal efficiencies are estimated as 18.89% and 41.96%, usin the north and south rates, respectively. The average of these values is similar to the removal efficiencies found using the 2011 mass-balance approaches for in-stream data (32%).

DISCUSSION

Groundwater is an important source of flow and nitrogen for the two-stage ditch in this study. Difficulties in determining the removal rate of NO_3-N are largely tied to obtaining reliable measurements of these contributions. For no equipment malfunctions, total groundwater flow rate was reliably obtained from the difference between measured upstream, tile, and downstream flow rates. Numerous wells were installed to estimate the NO_3-N concentration the of groundwater. The spatial and temporal variability in these concentrations was greater than expected. The NO_3-N contributions vary substantially depending what portion of the total groundwater flow was entering from the east versus the west side of the ditch. Measured piezometric heads were not useful in partitioning flows among the different wells. Isotopic tracers were significantly different in the combined slope and intercept terms between the tiles and wells but not between

the channel and the other sources. This provided a physical difference in the means that could be used as the best estimate to calculate nitrogen removal.

Mass-balance approaches were used to determine in-channel removal rate of nitrates. Removal efficiencies are the preferred measure of this process because the impacts of uncertainty in the groundwater contribution are reflected in both effluent and influent loads. However, this method does not account for decreases in the water balance due to evaporation. Depending on the reliability of data, the removal efficiency was computed by assuming the groundwater concentration equals the upstream concentration, by using the arithmetic average of groundwater wells, by assuming 1 or 2 groundwater sources and by using isotope tracers. The removal efficiency from the different methods at different times is fairly consistent, varying between 12% and 32% (Table 7). These efficiencies account for tile, upstream, and groundwater flows and are able to capture some of the sub-surface processes that influence nitrogen removal.

Table 7. Summary of removal efficiencies and removal rates across all dates and methods at the Mullenbach Two-Stage Ditch, organized by date.

Time Frame	Location	Method	Section	Groundwater Sources	Nitrogen Removal (%)	Nitrogen Removal Rate (kg NO_3-N d^{-1})
May-10	In-channel	Influent vs. effluent concentrations	Entire ditch	NA	20	NA
Jun-10	In-channel	Influent vs. effluent concentrations	Entire ditch	NA	18	NA
Aug-10	In-channel	Influent vs. effluent concentrations	Entire ditch	NA	17	NA
Aug-10	In-channel	Mass balance	Entire ditch	1	10 - 40 (20 est.)	NA
Sep-10	In-channel	Influent vs. effluent concentrations	Entire ditch	NA	13	NA
Sep-11	In-channel	Mass balance	Entire ditch	1	32	7.9
Jul-13	Channel and benches	Potential soil denitrification	N and S sites	NA	19 - 42	4.7 - 10.4
Sep-13	In-channel	Mass balance	Test Section	1	17	7.7
Sep-13	In-channel	Mass balance	Test Section	2	12	5.2

A comparison of the average influent and effluent concentrations display variations throughout the growing season. Percent nitrate removal was highest in early in the season, likely because the influent concentrations were higher and the decay coefficient generally assumes a linear relationship between the reaction rate and the concentration (Chun *et al.,* 2009; Christianson *et al.,* 2011; Pluer *et al.,* 2016). However, removal rates could not be calculated without a full knowledge of the entire water balance within the ditch. Additionally, this method

is not process based. Removal efficiencies are similar to the values found by both the mass balance approach and the potential soil denitrification and vary between 13% and 20% (Table 5). The congruency between the numbers indicates that this more simple approach may be similarly accurate in comparison to the more rigorous approaches. A comparison of corresponding time frames for several instances will be needed to verify this possible conclusion.

Potential denitrification rates of the soil were also examined in the laboratory using the acetylene inhibition method. These rates are not dependent on accurately determining groundwater contributions. There may be some inherent issues with calculating removal efficiencies based on removal rates from 2013 and influent nitrate loading from 2011. This is due to the plethora of variables that can change on a daily, weekly, monthly, and yearly time scale. However, the typical loading through the late summer and fall months is likely to vary minimally. By using the inflow load for the 2011 data, the removal efficiencies were estimated between 19% and 42%. This range could be attributed to the difference in the N_2O production between the north and south non-riparian bench areas.

The riparian zones generally displayed higher N_2O production and areal denitrification rates in comparison to the non-riparian bench zones. Non-riparian bench zones are typically not saturated for much of the year, which may negatively impact the population of denitrifying bacterial communities. Vegetation on benches may also decrease soil NO_3 availability, thus decreasing rates of microbial denitrification (Roley *et al.,* 2012a). In contrast, the riparian zone is closer in elevation to the water table than the bench, which may have created the anaerobic conditions necessary for microbial denitrification. Also, the riparian samples were taken at water-air interface, meaning the soils were in close proximity to large amounts of carbon in the soil profile.

The difference in areal denitrification rates by habitat zone does not appear to be connected to either organic matter or bulk density (soil type) but

instead may be attributed to the differences in microhabitat (i.e. vegetation/carbon and/or saturation). Vegetation type can be a very important factor in the removal of nitrogen. The laboratory denitrification rate does not consider the removal of nitrates by plants or evaporation. Several additional sites are needed to improve the estimate of the average potential denitrification rates for the entire two-stage ditch.

Nitrate removal within the hypothetical conventional ditch was quite low (1.24% to 3.09%). This is likely due to carbon and nitrogen limitation (Powell and Bouchard, 2010). A two-stage retrofit is likely to increase this removal efficiency upwards of 4X. The estimate created using hypothetical conventional ditch conditions are likely fairly accurate. Denitrification rates in the low-flow channel of both the conventional and two-stage ditch have been found to be similar (Powell and Bouchard, 2010). It was unknown how much denitrification was occurring on both the conventional and two-stage ditch side slopes but it was assumed to be negligible for both. This additional information would be helpful in producing a full nitrogen budget for the entire profile.

Flooded conditions are likely to greatly improve the nitrogen removal capacity. The interaction of ponded water with the plants and soil surface as well as the flow rate, nitrate concentration, and days of inundation will likely greatly affect the nitrate removal rate and efficiency. Design considerations, including a lower bench elevation, may encourage more frequent inundation of the benches. Other possible designs could use gates or other flow constrictions to increase the floodplain flow depth to cover the benches more often. The removal rates of NO_3-N are likely to more than double. It is recommended that additional research be done to evaluate these types of designs and their impact on vegetation, stability, and other factors important in drainage ditch operations. Specific measurements of the denitrification rate of the benches under flooded conditions will lend merit to this condition.

CONCLUSION

Nitrate loading to agricultural headwater ditches can be substantially high, especially in the spring during snowmelt runoff and rain events. Some of this nitrate is stored and possibly accumulated, within the soil profile as well in the shallow sub-surface groundwater. In-stream BMP's are needed to help prevent the transportation of these excess nutrients to downstream locations. The two-stage ditch design facilitates higher levels of biomass along the floodplain benches, which provides a necessary source of carbon for elevated rates of denitrification by soil microbes. This design may increase denitrification by 4X compared to a conventional drainage ditch. Further in-stream or edge of field practices could provide a treatment train approach by reducing the initial loading. Modifying the design to artificially inundate benches for prolonged periods of time could greatly improve the design and increase the rates of denitrification within the two-stage ditch.

Design and Construction of a Reduced Temperature Testing Apparatus for Denitrification

[1]Lori Krider, [1]Bruce Wilson, and [1]Joe Magner

[1]Bioproducts and Biosystems Engineering, University of Minnesota

Abstract: Excess nitrogen in aquatic systems contributes to significant water quality degradation. Agricultural runoff during springtime snowmelt and rainfall events transports large quantities of nitrogen from agricultural fields into aquatic systems. Previous laboratory experiments to evaluate denitrification under reduced temperature scenarios are often limited to enclosed columns in small freezer spaces. This large-scale laboratory experiment uses individual housing units (chambers) to contain surface exposed bins (troughs), which house media, soil, and plants. This apparatus is designed for indoor application to test for denitrification under reduced temperature scenarios. Each chamber is equipped to simulate tile drainage flow under springtime air and water temperatures found in the Upper Midwest, USA.

KEY WORDS: bioreactors, denitrification, controlled environment.

INTRODUCTION

Water quality in agricultural watersheds is under greater scrutiny as the landscape and hydrologic pathways are altered to increase the production of affordable food. Land use in southern Minnesota is largely agricultural with the dominant crops being corn and soybean. Each year, large quantities of nitrogen and phosphorous are applied to these crops to increase yields. However, portions of these nutrients are lost from these fields and are ultimately transferred to major river systems in Minnesota and beyond. Extensive drainage allows the useable forms of nitrogen and phosphorus for crop uptake to be transported to

agricultural drainage ditches and natural channel systems. Excess nutrients introduced into natural systems can have major consequences for natural communities. Extensive growth of unwanted algae and duckweed (Lemna spp.) is often a consequence of having excess nutrients in natural systems where is it otherwise limited (King, 2011). The decomposition of algae and duckweed consumes large amounts of dissolved oxygen in the water column, creating hypoxic conditions (DO < 2 mg L-1) that are unsuitable for many plant and animal species, especially those that are particularly sensitive to low levels of dissolved oxygen. The hypoxic zone in the Gulf of Mexico is an example of this decomposition on a large scale (NOAA, 2014).

Currently, agricultural and urban land use practices are the driving forces behind most of the water quality issues faced in the state of Minnesota. Climate and geology have created a water-rich state capable of storing large quantities of water on the land in the form of wetlands and lakes. However, water storage on the land is in direct contention with agricultural productivity. Upward of 90% of the wetlands in some areas of southern Minnesota have been drained, mostly in the past 100 years, and converted to agriculture (BWSR). Rainfall, snowmelt and high water tables can greatly reduce crop yields. In order to clear fields of water quickly, prevent standing water and reduce flooding in adjacent waterways, an extensive system of tile drains and drainage ditches have been, and continue to be, constructed throughout southern and western Minnesota. It has been estimated that there is approximately 33,800 km of drainage ditches in Minnesota (Minnesota Department of Natural Resources). Extensive tiling not only increases flows to nearby ditches, but also provides a direct conduit for the transportation of nitrates downstream.

Nitrate attenuation is the removal of nitrate from a system by the process of denitrification. This process is performed by facultative heterotrophic bacteria including *Thiobacillus denitrificans, Micrococcus denitrificans*, and some species of *Serratia, Pseudomonas, and Achromobacter* (Encyclopaedia Brittanica).

Under anoxic conditions, these bacteria convert nitrate to ammonia for cell synthesis by assimilatory denitrification or nitrous oxide (N_2O) by dissimilatory denitrification (NPTEL). Due to the anoxic conditions under which the process takes place, very little assimilatory denitrification occurs and the majority is dissimilatory (NPTEL). A carbon source is a necessary component of the process and provides energy to the bacteria for the conversion. Carbon sources serve as electron donors and may come in the form of organic matter (i.e. mineralization of vegetation) or external sources such as acetate ($CH_3CO_2^-$) or ethanol ($C_2H_6O_2^-$) (NPTEL). Bioreactors are optimized denitrifying microbial habitats in which ideal conditions are artificially created by putting carbon sources under anoxic conditions. Bioreactor experiments can be conducted in a laboratory setting prior to future implementation in the field.

Temperature is a major component influencing denitrification. It has been found that there is a significant increase in denitrification rates between 5 and 10 ^oC (Powlson *et al.,* 1988; Stanford *et al.,* 1975) and extrapolation shows that denitrification would likely occur at or near 0 ^oC (Smid and Beauchamp, 1976). Denitrification has been documented in agricultural fields at 2 ^oC (Robertson *et al.,* 2000). It has also been found that bacteria in temperate soils can denitrify at lower temperatures compared to bacteria in tropical soils (Powlson *et al.,* 1988). This adaptation demonstrates that denitrification may be a major source of nitrate loss in temperate areas in the spring when much nitrate is mobilized from agricultural fields.

For these reasons, it is important to test denitrification under reduced temperature scenarios, for both the air and water, similar to those found in the mid-west just after the spring snowmelt begins. Typically, in southern Minnesota, soil is unfrozen under sod by mid to late-March (unpublished data, SWROC). Similar trends are likely for vegetated riparian areas along ditches. However, for bare ground conditions, such as those found in agricultural fields, soil is typically frozen until early to mid-April (SWROC). However, tile drainage can increase soil

temperatures by 4 ^{o}C, particularly between May and July (Jin *et al.,* 2008). From mid-April to mid-May, sub-surface drainage water has been found to be in the 4.4 - 10 ^{o}C range (unpublished data, SWROC, 2011). This corresponds to average air temperatures of 7.2 to 14.4 ^{o}C (US Climate Data). By mid- to late-May, the average sub-surface drainage temperature is around 12.8 ^{o}C (unpublished data, SWROC, 2011). These air and water temperature ranges are important to capture in laboratory denitrification experiments.

In 2015 and 2016, a large-scale indoor testing apparatus was built on the University of Minnesota St. Paul Campus. This testing apparatus consists of temperature control chambers and a water chiller to simulate springtime air and water temperatures in southern Minnesota. Chambers were designed and constructed to be modular (individually contained) and hold surface exposed (open topped), horizontal bioreactors receiving water at the inlet from above surface tubing to mimic tile drainage input. Chamber conditions can be easily adjusted and water samples can be collected externally, creating a self-contained biosystem for experimentation. Chambers are to be used in a future laboratory experiment to test for denitrification of a novel, multi-media biosystem under reduced temperature scenarios. The objective is to mimic springtime air and water temperature conditions to test for the benefits of using multiple types of media in combination to create an optimized microbial habitat for denitrification.

METHODS

Four insulated chambers house the media troughs in sets of three with the same treatment (replicates). Each chamber is equipped with a 6,050 BTU GE Electronic Display window air conditioning unit through the front wall of the chamber. Each air conditioner is installed with a Coolbot^{TM} walk-in cooler controller unit (Part # SY-WKB5-LGZD-CA) as an alternative sensor to override the air conditioner's pre-programmed minimum temperature of 15.6 ^{o}C. The air conditioning units where sized to easily sustain 10 ^{o}C within the chambers. The

walls are made of 12.7-mm (0.5-in) wafer board sheets lined with R13 batt insulation between 38-mm x 89-mm (nominal 2-in x 4-in) studs and covered in 3-mm thick polyclear plastic sheeting to prevent mold and mildew growth on the insulation. A level surface for the chambers was verified or produced using a Stanley Laser Level. The chambers are covered by a clear, twin wall, insulated, polycarbonate greenhouse panel (1.22-m x 2.33-m) to allow natural and artificial light into the chambers. Each chamber has an individual light source provided by one, Sun Blaze T5 High Output 48-in, 8-bulb light. Lights are placed on top of the chambers over two wooden planks placed perpendicularly to the lights. These wooden planks placed under the lights (wall to wall) help support the weight of the light and prevent the light bulbs from coming in direct contact with the greenhouse panels. The rear wall of the chamber has three, 3.18-cm (1.25-in) openings to equalize pressure within the chambers. These openings can be plugged with rubber gaskets to control airflow and air temperature more precisely.

A solenoid valve controls the spigot discharging tap water through an inline water filter into a 264.98-L (70-gal) mixing tank. The water filter is a two-stage, Home Master Whole Home System designed to treat particulates with a 5-micron filter (stage 1) and chlorine/chloramine/heavy metals with a catalytic carbon filter (stage 2). Chlorine compounds act as disinfectants and may harm the denitrifying bacteria growing in the bioreactors so removal is necessary. The particulate filter is used to prolong the life of the carbon filter. A data logger (Campbell Scientific CR10X) is programed to control a relay switch (Crydom D1D07L DC Solid State Relay) that supplies power to the solenoid valve. Water level readings are taken with a pressure transducer every 10 seconds. When the water level drops below 96.52-cm (38-in), the switch closes and the solenoid valve opens to refill the tank. When the water level reaches 104.14-cm (41-in), the relay opens and closes the solenoid to shut off the flow from the spigot. The flow from the spigot is set to 7.57 L min-1 (2 GPM) and refills the lost volume in

approximately 3 minutes. Since the flow to the trough dispersal line is 2.69 L min-1 (0.71 GPM), the tank is drawn down 7.62 cm (3 in) in 8 minutes.

The mixing tank receives concentrated nutrient water to allow inflow to be similar to tile drainage. A pond pump (Little Giant PE-2F-PW 566611 300 GPH Premium Pond Pump) supplies constant flow from a secondary, 757.08-L (200-gal) nutrient feed tank and is controlled by a flow meter (Gilmont Flow Meter 150-mm, stainless steel float, 6 - 217 mL min-1). The continuous feed from this tank is set to match the volume of additional water supplied from the spigot to the mixing tank as controlled by the solenoid valve. It is covered (externally) with black plastic sheeting to prevent algal and bacterial growth within the tank. The water is not chilled, and the volume is too small to noticeably impact the temperature of the water in the continuously cooled mixing tank. When the water level reaches near the unusable volume (about 6 inches from the bottom, at the level of the pump inlet, which is 723.01-L (191-gal) at about 9 days), the tank is refilled from a secondary hose off the spigot and a previously prepared concentrated nutrient water mixture is added to create the tile drainage water recipe.

Water is continuously cycled to and from the mixing tank through an aquarium chiller (Tradewinds ¾ HP inline) that can maintain a specific temperature, depending on tank size. The chiller is sized to be able to cool the entire volume (70-gal) of the mixing tank to 7.2 ^{o}C in about 1 hour based on an influent water temperature from the spigot of 15.5 ^{o}C. The water is pumped out of the tank near the bottom through a secondary, ad-hoc bulkhead fitting using an aquarium pump (Little Giant 1,325 GPH Mag Drive Aquarium Pump), as specified by the chiller requirements. A hand held remote device is used to set the desired temperature of the water in the mixing tank. After cycling through the chiller, the water is discharged back into the mixing tank through the main, top opening. Pumping from the bottom to the top provides more even mixing and temperature distribution. This tank and the hose to and from the chiller are covered in

reflective, insulating wrap (Reflectix™) to reduce the temperature impact of the external environment (non-air conditioned, indoor building space).

Flow to each individual chamber is controlled using Dwyer Variable Area Glass Flow Meters (150 mm, stainless steel float, 40.00 mL min-1 to 396.06 mL min-1). Each flow meter is placed off the main line from the pump. Flexible tubing (Tygon™) connects the main flow line to each flow meter and from the flow meter through a small, circular hole in the front wall, to each trough. Flow rates can be verified externally (outside of the chamber) before entering the chamber via a clamped, secondary tube at the outlet of the flow meter. Calibration curves are used to accurately set the flow meters to the desired flow rate.

Bioreactor material is housed in troughs within the chambers (Fig. 54). These troughs are plastic welded from polypropylene sheets. Troughs are constructed to allow for three of the same treatments per chamber. They are at approximately 0.31-m wide, 0.61-m deep, and 1.83-m long. A perforated pipe placed vertically near the end of the trough and connected with an elbow tee through a hole in the rear wall near the top of the trough is installed to help create a flow pattern more similar to plug flow, thereby minimizing the amount of unusable or stagnant areas.

Water at the outlet is directed by 2.54-cm (1-in) PVC pipe through the rear chamber wall and samples can be collected externally by an inline ball valve. When the valve is closed, water flows to a main 2.54-cm (1-in) PVC collection line which outlets into a collection basin (0.31-m x 0.61-m x 0.61-m). When the water level in the basin reaches 20.32-cm (8-in), a sump pump (Hydromatic HP33 1/3 HP Submersible Sump Pump) sends the water vertically up the outlet, which sits overhead (to avoid a tripping hazard) and runs along the wall to outlet in the nearest sink. This sink is able to handle up to 15.14 L min-1 (4 GPM), ultimately creating a flow rate maximum discharging from the experiment.

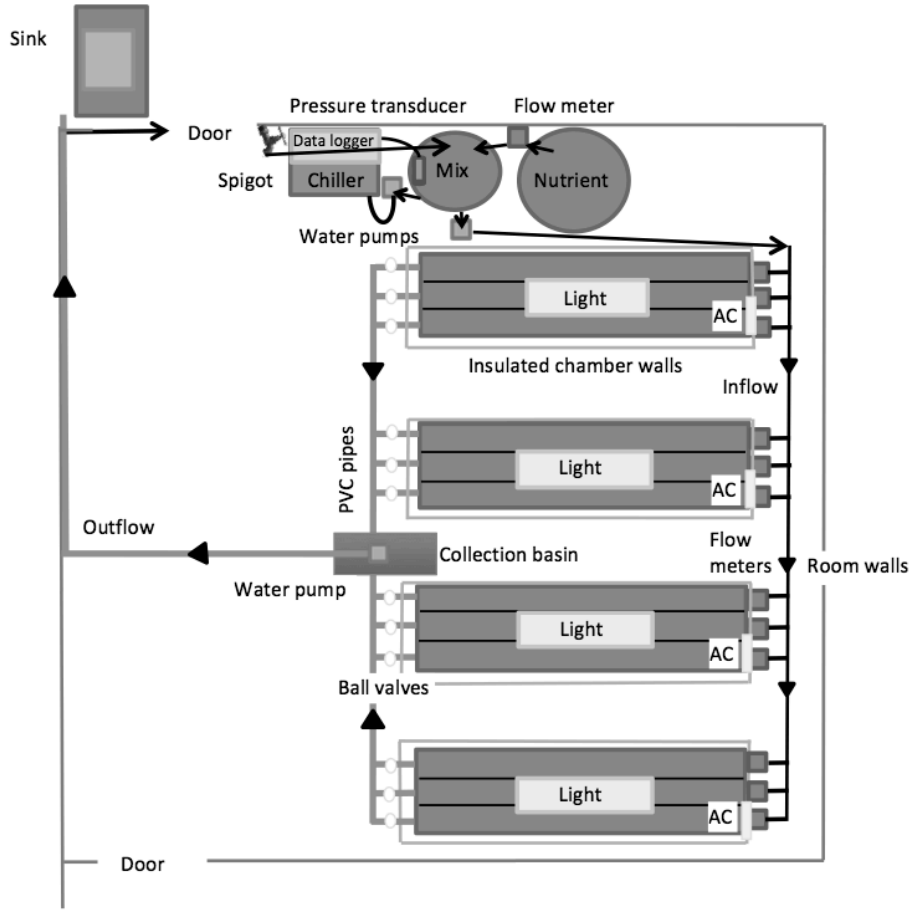

Figure 52. Diagram of the testing apparatus layout, including all major components, inside of the experimental space.

DISCUSSION

Our reduced temperature indoor testing apparatus is an alterative to using a walk-in cooler or building a cold room. Walk-in coolers may be too small or simply not available. Construction of a cold room can be subject to the codes and permits necessary for an inhabited space. Our apparatus was sized to be as large as possible while minimizing labor and material costs. This corresponds to the dimensions of the wafer board, greenhouse panels, and polypropylene sheets. The components can be sized alternatively, if so desired. In a larger space, more chambers could be added as long as the total flow rate in and out of the experiment does not exceed the faucet and drain capacity. Larger air

conditioning units, along with Coolbots, would be able to cool the chambers even further, down to 1.67 ^{o}C at the minimum. Temperatures within the chambers can be adjusted between the minimum and room temperature, which could give the researcher a large temperature range for testing of 10 to 20 ^{o}C.

CONCLUSION

Testing for denitrification under reduced temperature scenarios is necessary to determine if there is a specific media combination or microbial community composition that can function at a higher capacity under these conditions. A large-scale testing apparatus will provide the ability to test entire systems under conditions more similar to the field. If an ideal system were determined, field trials would be able to treat agricultural nutrient pollution more effectively during the springtime, when snowmelt and consistent rainfall typically occurs.

Mass Balance and Process-based Nitrate Removal Models for a Novel Multi-Media Denitrifying Bioreactor

Lori Krider[1], Bruce Wilson[1], and Joe Magner[1]

[1]Department of Bioproducts and Biosystems Engineering, University of Minnesota

Abstract: Numeric, mass-balance and microbial, process-based models were created to characterize the flow pattern and calculate nitrogen removal for combined plug and CSTRs in a series bioreactors with changing influent loads. The mass-balance model was used to match a conservative tracer (bromide) outflow curve to existing data by optimizing flow parameters. These parameters include dead space fraction, short-circuiting fraction, and the number of tanks in a series. For a laboratory experiment utilizing novel media (walnut shell biochar, Brotex, and woodchips) the model characterized the bioreactors as having 1.1% plug flow and 4 CSTRs with 3.7% short-circuiting and 1.1% dead space. Hydraulic residence times (HRTs) were reasonably close to those used in the original experimental designs. This model was then altered to include microbial processes and used to compute percent nitrate removal and nitrogen removal efficiency. Two treatments, with and without Brotex, where tested under 4 hr and 12 hr HRTs and temperatures ranging from 6 ^{o}C to 14.5 ^{o}C. Nitrate removal for the 4 hr Brotex varied from 7.66% to 51.56% (1.07 to 7.50 g N m^{-3} d^{-1}), 4 hr non-Brotex from 11.27% to 63.32% (2.07 to 9.66 g N m^{-3} d^{-1}), 12 hr Brotex from 29.99% to 80.17% (2.22 to 6.12 g N m^{-3} d^{-1}) and 12 hr non-Brotex from 44.70% to 84.06% (3.26 to 6.22 g N m^{-3} d^{-1}), under low and high temperatures, respectively. Based on influent loading, the 4 hr HRT had a higher average removal rate than the 12 hr HRT. These values are approximately 2X those found for traditional woodchip bioreactor column experiments at warmer temperatures. The microbial, process-based model infers that there may be an upper limit to the population of microbes that can be supported within a

bioreactor that is not reached at low temperatures. The media configuration produces slightly more nitrous oxide than traditional woodchip bioreactors. Average nitrous oxide emissions as a percent of the influent nitrate loading was 1.18%, compared to < 1% for other lab studies. These types of smaller laboratory scale models can help better inform the processes that occur in the "black-box" for which many bioreactors are considered. These models can be used to predict the behavior of larger, field scale bioreactors, which can be used to optimize engineering design.

KEY WORDS: bioreactor, flow characterization model, nitrogen removal.

BACKGROUND

Bioreactors are media filled trenches placed at the edge of an agricultural field to remove nitrogen by creating a microbial habitat for denitrifying bacteria. Traditional bioreactors use woodchip media as a carbon source and operate by intercepting a tile line before the sub-surface drainage water enters a nearby ditch or stream. Under saturated, anoxic conditions, denitrifying bacteria housed in the media convert nitrate to nitrous oxide (N_2O) or nitrogen gas (N_2). The most efficient use of this media is needed for optimal water quality treatment. Bioreactor design affects the hydraulic and biotic efficiency, particularly the flow pattern and ability to remove nitrogen. Accurate characterization of these parameters is necessary to understand the processes that occur within bioreactors.

Bioreactors are typically designed using Darcy's equation for porous media flow (Van Driel *et al.*, 2006; Robertson et al., 2000). However, this approach requires knowledge of the hydraulic conductivity of a media and the head differential from inlet to outlet. Each specific media or media combination has a unique hydraulic conductivity (Christianson *et al.,* 2011a; Feyereisen and Christianson, 2015). Determining hydraulic conductivity is difficult, especially for

bioreactors with multiple media where the hydraulic conductivity is inconsistent and varies substantially. Because of these issues, flow characteristics have been determined alternatively by coupling retention time with Darcy's equation to treat a portion of peak flow, typically 20% (Christianson *et al.,* 2011a; USDA-NRCS, 2009). Without extensive field data, this peak flow rate needs to be estimated using Manning's equation for gravity-driven flow velocity through a structure (Christianson *et al.,* 2011a). For this equation, the grade of the tile line needs to be known to obtain accurate results (Christianson *et al.,* 2011a). However, others have found that woodchip column reactors exhibit dominantly non-Darcian flow (Ghane *et al.,* 2014). These factors can create difficulties when designing and characterizing bioreactors, whether in the field or lab.

There are several other key characteristics that need to be considered in the design. In the field, the below-surface depth is dictated by the intercepting tile line (usually 1.2 to 1.5 m). The length of the reactor is determined by the HRT while the width is estimated based on the peak flow rate (Christianson, 2011). To achieve a HRT of 4 hours, bioreactors in Iowa were designed using a combined Darcy's equation and a fraction of the peak flow rate to produce a length:width ratio of at least 5:1 (Christianson *et al.,* 2011a). Generally, the scale effect (Gelhar *et al.,* 1992) between the lab and field scale is typically negligible if the two are similar in proportion (Chun *et al.,* 2010). Others have investigated the hydraulic response based on overall shape, with narrow rectangular shaped bioreactors showing the most efficient flow patterns per the Morrill Dispersion Index (MDI; described in detail later) (Christianson, 2011).

Bioreactor flow pattern is affected by the design. This includes inlet and outlet placement and configuration as well as media types (porosity, in particular) and methods of media combination (mixing, layering, etc.). Bioreactors tend not to fully follow idealized, theoretical plug flow patterns so typical modeling focuses on continuously stirred reactors (CSTRs) in a series (Christianson *et al*., 2011; Kandlec and Wallace, 2009). However, varying the kinds and structure of the

media may produce a reactor this is partial plug flow and partial CSTRs. Additionally, bioreactors tend to display hydraulic insufficiencies not easily captured by some models. There will likely be preferential flow pathways due to the media type(s). There will also, likely be, flow variability throughout the vertical profile due to friction against the sides and bottom as well as along objects such as plant roots. Short-circuiting via preferential flow through macropores may cause some volume to bypass the mixing process. Dead space (areas of little to no water flow or mixing) may cause water to become stagnant and further reduce the HRT. Knowledge of the amount of these parameters can assist in accurate design and characterization of bioreactors.

Conservative (non-degradable) tracers can be used to characterize flow within a bioreactor. In denitrifying bioreactors, bromide or chloride is typically used as tracers to investigate internal hydraulics (Schipper *et al.,* 2004; Schipper *et al.,* 2005; Van Driel *et al.,* 2006a; Cameron and Schipper, 2011; Christianson *et al.,* 2011a; Christianson *et al.,* 2011b). This data can be used in a model to determine the specific hydraulic dynamics and make broader assumptions about other processes, including nitrate removal.

There is the need for a model that can be used to inform design and predict removal under a variety of environmental conditions (Pluer *et al.,* 2016). There are several ways to model flow character through bioreactors. Some studies use RTD (residence time distributions) (Martinez and Wise, 2003), DTD (detention time distributions), or gamma distributions to model CSTRs in a series (Kandlec and Wallace, 2009). Chun *et al.* (2009) used a transport model based on convection-dispersion through a uniform media. Other models use dual-porosity to describe mobile (pore water flow by advection-dispersion) and immobile (water inside the media that moves by dispersion), a.k.a. MIM, transport (Jaynes *et al.,* 2016) but these require a large set of estimated parameters and numerous experiments to estimate each (Chun *et al.,* 2010). Solute transport software packages such as HYDRUS are often restricted in their

abilities due to limitations and errors (Chun *et al.,* 2010). One-dimensional transport models only account for the longitudinal direction (Chun *et al.,* 2009). Particle tracking models for 2-dimensional flow in reactors using dispersion via the Random Walk Method, which computes fluctuating concentrations with each run as a result of a random process, can result in poor estimation, sensitivity, and representation of the process (Chun *et al.,* 2010). All models operate under the premise that bromide is a non-absorbing, non-degrading, conservative tracer. None are known to include both plug and CSTRs components and incorporate short-circuiting or dead space. These parameters directly affect the ability to understand which variables impact the effectiveness of each design.

There is contention in the literature as to whether the first or zero order models more accurately represent denitrification reaction rates in bioreactors. It has been shown that both methods estimate removal rates well (Jaynes *et al.,* 2016). A first-order removal rate assumes a linear relationship between influent concentration and nitrate removed. This relationship is ideal for conditions when nutrient supply is unlimited and microbial growth is nearly optimal (Wan *et al.,* 2017). The first order rate reaction is common in wetland treatment studies (Kandlec and Wallace, 2009). In both pilot scale and laboratory experiments, it has been found that first order kinetics best represents removal parameters for NO_3-N concentrations similar to that of agricultural drainage (Chun *et al.,* 2009; Leverenz *et al.,* 2010). It has also been found that first order removal may provide a better fit for experiments conducted at reduced temperatures (Christianson, 2011). Additionally, lab experiments show a linear increase in nitrogen species removed with both increased inflow concentrations and increased residence time (Pluer *et al.,* 2016).

Methods for calculating nitrogen removal are more challenging for unsteady conditions. Accurate determination of influent and effluent loads requires reliable estimates of possibly varying concentrations and flow rates. Laboratory bioreactor experiments can become clogged with algal growth inside

the water conveyance structures, including pipes, tanks and flow meters, which can change the flow rate and/or concentration of the influent water. Additionally, frequent or nearly continuous sampling of both the influent and effluent may be necessary to gain a full picture of how the dynamics change over time. All bioreactor researchers need to determine influent loads that occurred one HRT back in time because this when the water entered the bioreactor. However, if the influent conditions change over time, then the previous condition may be difficult to determine. In any of these cases, calculations of nitrogen removal can become complicated and difficult to determine. A model is likely needed to capture these complexities.

A numeric, mass-balance model was created to characterize the flow pattern for combined plug and CSTRs in a series bioreactors. It was compared to an analytical approach (Personal Communication, Wilson, 2017), which uses a solution by convolution based on single pulse input. A model was developed based on the numeric solution in which outflow concentration can be estimated based on either a pulse or continuous input system. This model was used to match a conservative tracer (bromide) outflow curve to existing data by optimizing parameters that describe flow. These parameters include an approximation of dead space, short-circuiting, and the number of tanks in a series. Other parameters were calculated from the fitted curve, including hydraulic efficiency, volumetric efficiency, tracer detention time, HRT and MDI. An additional 1st order nutrient removal parameter (decay coefficient (κ_d)) was added to calculate nitrate removal. The model is used to calculate nitrogen removal in g m^{-3} d^{-1} and nitrate removal in percent by adjusting a predicted effluent nitrate curve to match that of actual grab sample data by optimizing the decay coefficient using Excel Solver™ to produce a minimal sums of squares error (chi^2). This model automatically accounts for the time lag due to HRT and calculates removal by time step for up to five consecutive days based on a changing influent concentration.

METHODS

Experimental Set-up

Troughs were designed at a 6:1 scale following guidelines presented by Christianson *et al.* (2011a). The average drainable porosities of the treatments with and without Brotex were 55.4% and 53.6%, respectively. It was anticipated, based on porosity, that the addition of biochar would reduce the hydraulic conductivity of the material from a woodchip baseline (4.5 cm s^{-1}) and that the addition of Brotex would increase it. Bioreactors were designed to have 4 and 12 hr HRT based on porous volume and flow rate. Darcy's equation is based on a head drop produced by slope (Ghane *et al.,* 2014) and was used to estimate the hydraulic gradient with a hydraulic conductivity of 4.95 cm s^{-1} for the woodchip, Brotex, biochar treatment and 4.05 cm s^{-1} for the woodchip and biochar treatment. However, for this experiment, chambers were made level because the calculated slope as well as the slope in the field is very minimal (< 0.2%) and likely to produce little influence on the system. Also, a slope will increase the hydraulic gradient and the unused portion of woodchips near the outlet and will increase the flow rate within the system, making the flow rate measured prior to entering the system not as accurate.

It has been expressed in peer-reviewed literature that there is a research need for laboratory experiments testing bioreactors under reduced temperature scenarios. As of 2016, only one other published laboratory experiment went below 10 ^{o}C (Addy *et al.,* 2016; Feyereisen *et al*., 2016). In 2015 and 2016, a large-scale indoor testing apparatus was built on the University of Minnesota St. Paul Campus (Krider *et al.,* 2016a; Figure 52). This testing apparatus uses temperature control chambers to simulate springtime air and water temperatures in southern Minnesota. This system consisted of a series of water chillers, pumps, tanks, valves, flow meters, and piping to provide continuous, regulated flow of nutrient-enriched water to individual bioreactors.

Chambers were designed and constructed to be modular (individually contained) and hold surface-exposed (open-topped), horizontal bioreactors receiving water at the inlet from above-surface tube to mimic tile drainage input (Fig. 53). The walls where insulated and the chambers artificially lighted during daytime hours to support plant growth. Each chamber contained an air-conditioning unit to create reduced air temperatures. Conditions can be easily adjusted and water samples can be collected externally, creating a self-contained biosystem for experimentation. These chambers were used in a laboratory experiment to test for denitrification with a novel, multi-media bioreactor under reduced temperature scenarios.

Figure 53. Picture of experimental bioreactors inside a temperature control chamber (2.44 m L x 1.22 m W x 1.83 m H) as part of the testing apparatus.

A laboratory experiment was conducted in the winter of 2016/2017 to test two different bioreactor media combinations under 4 and 12 hr HRTs (4 treatments, 3 replicates per treatment for a total of 12 troughs (containers housing the media)) under a range of temperature conditions from 6 to 14.5 ^{o}C.

Chambers were kept at 6 ^{o}C for four weeks and 14.5 ^{o}C for four weeks with a warming period of four weeks in between where the air and water temperatures where increased by 2.1 ^{o}C per week. Half of the troughs (6) contained one media combination while the other half contained another. One media combination consisted of 10% Brotex material, 10% walnut shell biochar, and 80% hardwood woodchips by volume by volume (1:1:8) while the other combination was 10% walnut shell biochar and 90% hardwood woodchips (1:9).

Coarse grit black walnut shells (size 4/6, ~4.76 mm) were purchased from Hammon's Products Company in Missouri and charred by slow pyrolysis in a mobile downdraft gasifier (patent 5555574) at 600 ^{o}C for 3 hours (1 hr of heating and 2 hours of cooling) by Char Energy, LLC. in Ada, MN. Non-wood biochars produced at lower temperatures may have more aliphatic functional groups (i.e. microbially-available carbon) (Christianson *et al.,* 2011a; Mukome *et al.,* 2013a). The walnut shell biochar was chemically characterized by Eurofins Scientific Product Testing Lab in Hamburg, Germany, using thermogravimetry. The resulting size of the 50% passing particles in a sieve analysis was approximately 1.9 mm (approximately 60% volume loss after charring). Brotex material was purchased from Floating Island International (St. Paul, MN).

Troughs where filled with 0.016 m^3 of pea gravel below the inlet through the vertical profile to dissipate the kinetic energy of inflow and to assist in creating plug flow conditions (Fig. 54). Media were arranged in a layered fashion with 3 layers of woodchips containing 1 layer of staggered Brotex blocks (~4" by 4") within it. A layer of walnut shell biochar separated each woodchip/Brotex layer and all layers were inoculated with 80 mLs of soil (based on soil to media ratios by volume presented in Schipper *et al.,* 2012a) collected from an agricultural drainage ditch in southern Minnesota (Clyde silty clay loam/clay loam: average of 2 samples = 35% sand, 31.5% silt, 34.5% clay; BD = 1.79 g cm^{-3}). Soil was air dried for 7 days at 22.2 ^{o}C, mixed in a stainless steel double ribbon soil mixer (15 minutes per batch of 5 gallons), sieved through a 1" wire mesh tray to remove

hard clay clumps and rocks to create a uniform texture common amongst the troughs, and stored in a cooler at -12 ^{o}C until use. Troughs were topped with 0.025 m^3 of the same agricultural drainage ditch soil and further topped with another 0.008 m^3 of landscaping topsoil (Kern Landscaping) to complete the system and help mitigate N_2O surface emissions (Christianson *et al.,* 2013a). A small opening, biodegradable plastic mesh (Industrial Netting Co. XN2950: 5 mm x 3 mm) was used to separate the soil from the media with minimal soil fall through (11.08%) while allowing plant roots to grow through the media without changing the water chemistry.

Troughs were planted with wetland plant plugs (2 of each Fox Sedge, Dark-green Bulrush and Rice Cutgrass) purchased from Cardno Native Plant Nursery in Indiana. These plants were chosen because they represent common native, wetland, obligate plants in southern Minnesota as well as the Midwest, USA. Plant roots did not extend into the media due to a high water table and were, therefore, not considered as a significant part of the nitrate removal process. If the plants did contribute to nitrate removal it was likely less than the maximum of 10% reported elsewhere in the literature (Vymazal, 2006; Hammer, 1992; Kantawanichkul, 2009). Instead, they may have provided stable, structural support and habitat diversity for the denitrifying bacteria (Zhao, 2010). Additionally, vegetation has been shown to increase the amount of ammonia-oxidizing bacteria as well as provide organic carbon to the soil (Kantawanichkul, 2009; Triska, 2007). Previous woodchip-only bioreactor experiments conducted by other researchers (Christianson, 2011; Chun *et al.,* 2009; Zhang, 2015) served as the control for comparison.

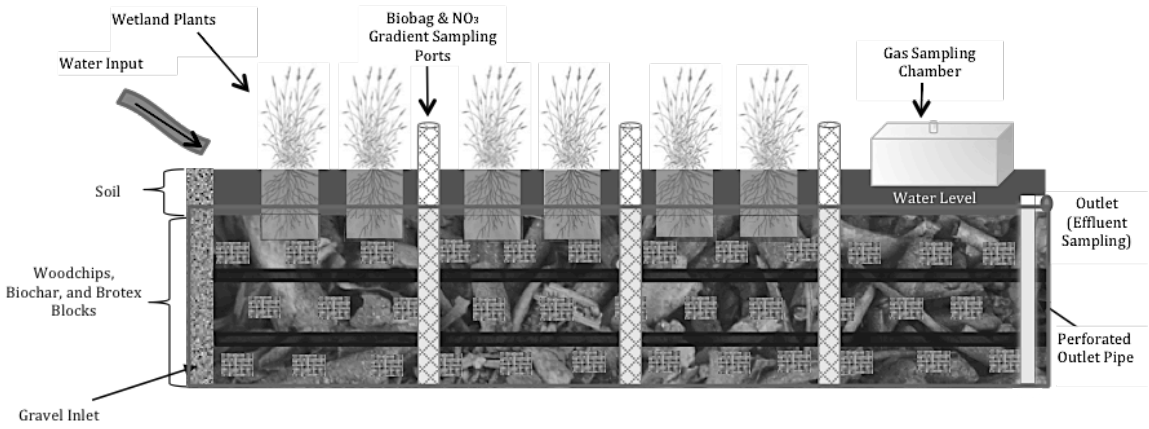

Figure 54. Side view of trough components (media, plants, sampling locations, inflow, and outflow).

Throughout the course of the experiment, troughs received a water recipe designed to mimic the major chemical constituents and concentrations of agricultural drainage water in southern Minnesota. This recipe was determined based on water quality data collected at the Mullenbach Two-Stage Ditch in Mower County, Minnesota (chapter 2) as well as information provided by Zhang (2015). This recipe contained nitrate (30 mg L-1), phosphate (0.5 mg L-1), calcium (55 mg L-1), chloride (150 mg L-1), magnesium (20 mg L-1) and potassium (5 mg L-1). Micronutrients were not added due to a lack of evidence that they produce a significant effect on nitrate removal as well as the tedious nature of measuring them in the influent and effluent (Personal Communication, Feyereisen, 2016). This nutrient laden water was continuously added to a mixing tank that was combined with filtered tap water before delivery to the media troughs (Krider *et al.,* 2017). The system utilized a catalytic carbon and particulate filter to remove chlorine and chloramine from the tap water, which can harm denitrifying bacteria, which was then by mixed with nutrients to produce a final water recipe. A consistent and appropriate water recipe is necessary to maintain conditions within a suitable range for denitrifying microbes. Environmental conditions such as low pH, low temperature, high solution DO and

low carbon to nitrogen ratio (C:N) may result in incomplete denitrification and higher N_2O emissions (Christianson, 2011).

The experiment was conducted in the temperature-controlled chambers with air, water, light, soil, plants, gravel, and media, all interacting as a system, to serve as an intermediary between the traditional column experiment and the field setting. Setting up adequately reduced conditions took place over a span of 4 weeks prior to running the tracer test. The temperature in the chambers was slowly reduced over the period from 30 ^oC to 7 ^oC. Troughs were saturated in filtered tap water for the first week. The second week employed a 24 hr HRT of the drainage water nutrient recipe and 100 mg L^{-1} sodium acetate. The drainage water recipe (no acetate) with a 24 hr HRT was used for the following 2 weeks while reducing the temperature by 2.8 ^oC every other day. The HRTs were reduced to 4 and 12 hours for the corresponding treatments and the temperature reduced another 2.8 ^oC two days prior to the tracer test. The experiment began 4 days later on December 5th, 2016.

Data Collection

Influent and effluent samples were collected twice daily for each trough for 6 days per week and analyzed for nitrate and nitrite (separately) using a Hach Nitratax Plus^{TM} nitrate probe, flow rate by timing a volume collected, and DO, conductivity, pH and ORP (oxidation reduction potential) using a YSI 6-Series Sonde^{TM}. Further information on the calibration of these probes is given in Appendix A. Continuous influent nitrate measurements were collected every 15 minutes overnight from 5 pm to 9 am with the nitrate probe as well. Air, water, and media temperatures where collected once daily for each trough for 6 days per week using Type K (chromel-alumel) thermocouples connected to a Campbell Scientific CR10X data logger. Water samples were analyzed periodically at the University of Minnesota Research and Analytical Lab for QA/QC of nitrate and nitrite concentrations.

Gas samples were collected weekly from insulated metal chambers (7201.60 cm^3 inner volume, each half) made from 2 metal buffet pans secured using folder clips in a clam-shell fashion with the lower part of the bottom pan cut off, acting as a press-punch mechanism, inserted 3.8 cm into the soil to define an area for soil sampling (Fig. 55). General methodical guidelines follow USDA-ARS GRACEnet Project Protocols Chapter 3: Chamber-Based Trace Gas Flux Measurements (Parkin and Venterea, 2010). The upper pan contained a top valve with a rubber septum (replaced every two weeks) for collecting gas samples and a small outlet port (~5 mm ID) on the side to equalize pressure and cycle gas emitted from the soil. Each week, 5 mL of gas were collected from each trough using a 10 mL BD Luer-Lok syringe inserted through the rubber septa port and injected into helium flushed, aluminum-capped 5 mL gas vials with rubber septa. For each sampling period, four samples were collected from each trough at 15-minute intervals. Samples were analyzed for N_2O in a gas chromatographer (HP 5890 GC/FID/TCD/ECD) within 48 hours of sample collection.

Figure 55. Picture of the gas collection chambers showing the punch-press bottom, insulated top, and gas collection valve on top.

Troughs 2, 4, 7 and 10 were used in conducting the bromide tracer test (1 trough per treatment). These troughs were chosen due to ease of access and

overall consistent and accurate flow measurements. The bromide tracer plug concentration was based on a peak concentration of 50 mg L^{-1}, which is 4 to 5 times the peak to mean concentration for HSSF wetlands over 3 detention times (Kandlec and Wallace, 2009). Due to slight differences in the constructed size of trough 10 vs. troughs 2, 4, and 7, trough 10 received a slightly higher plug concentration: 4400 mg L^{-1} (troughs 2, 4 and 7) and 4600 mg L^{-1} (trough 10). This gives a benchmark concentration of 10.57 mg L^{-1} and 10.49 mg L^{-1}, a lower end of the peak as 15.09 mg L^{-1} and 14.99 mg L^{-1}, and an upper end of the peak of 35.22 mg L^{-1} and 34.98 mg L^{-1}, for troughs 2, 4 and 7 and 10, respectively.

The first set of tracer tests (4 hour HRT, troughs 7 and 10) were conducted 4 days before running the experiment for nitrate removal. At T = 0, the plug was poured into the gravel inlet slowly over 1 minute. A total of 27 samples were collected manually at the outlet over 12 hours, 3 (11% of total) before the bromide slug was poured in (background) and 24 samples after (89% of total). This included 9 samples between 10% and 90% of the HRT (33%), 9 samples between 100% and 150% (33%), and 6 samples between 150% and 300% of the HRT (22%). This is a slightly modified version of methods suggested by Kandlec and Wallace (2009) to collect just over the minimum recommended samples with even time intervals between the samples.

The second set of tracer tests (12 hr HRT, troughs 2 and 4) was conducted 2 weeks after nutrient removal portion of the experiment was complete. Background samples (3) were taken at 10 minute increments pre-bromide pouring. Again, the plug was poured into the gravel inlet slowly over 1 minute. An ISCO automated sampler (ISCO 3700, 12V DC) was used to collect hourly samples from the outlet for each of 36 hours thereafter.

All samples were stored at 2 ^{o}C until analysis. A Thermo Scientific Orion Star A324 pH/ISE Meter (accuracy = ± 0.2 mV or ± 0.05% of reading, whichever is greater) and Thermo Scientific IonPlus Bromide Electrode were used to measure the bromide concentrations in the samples within 48 hours of collection.

Some samples were also measured for QA/QC using ion chromatography at UMNRAL (low standard (1.0 ppm) accuracy = ± 3% (0.97 - 1.03 ppm)).

Data Analysis: Bromide

The probe presents results in both mg L^{-1} and mV but gives coarse readings for mV (zero decimal points above 10 mV and one decimal point below 10 mV). Since the water recipe included KBr, background bromide concentrations were analyzed at UMNRAL and subtracted from the lab and probe results (1.80 mg L^{-1} for trough 7 and 3.10 mg L^{-1} for trough 10). There are 6 data points in common between the lab and probe (i.e. duplicate samples taken at the same time, one for measurement with the probe and one to be sent to the lab). For trough 7, the probe was stable throughout the tracer test (followed the expected bell shaped curve with the peak near what was expected based on calculations) so a power regression was created between mV from the probe and mg L^{-1} from the lab for the common data points ($y = 1E\text{-}09x^{5.03}$, $R^2 = 0.98$; Figure 5). This equation was used to convert mV from the probe into more accurate mg L-1 readings. Only the probe values were used for trough 7 to create a full and complete bromide tracer test curve because the corresponding lab data fell within 3 mg L^{-1} for all data points.

For trough 10, the probe had difficulties capturing the peak of the tracer curve (the probe values were about 10 mg L^{-1} less than the lab values during the ascension and near the peak) but restabilized around 254 minutes, causing about ¾ of the tail to fall back in line with the results from the lab (Fig. 56). However, since the probe was unstable during first part of tracer test, a power regression between mV from the probe and mg L^{-1} from the lab, similar to trough 7, could not be accurately created. Instead, a power regression was created using values obtained during calibration to translate mV from the probe into mg L^{-1} from the probe. However, using the lab data points up until 254 minutes and then the probe data points for the tail produced a lower percent recovery of

bromide than just using the lab data points for the entire test. For trough 10, only the lab results (6) were used to create the best fitting bromide tracer curve.

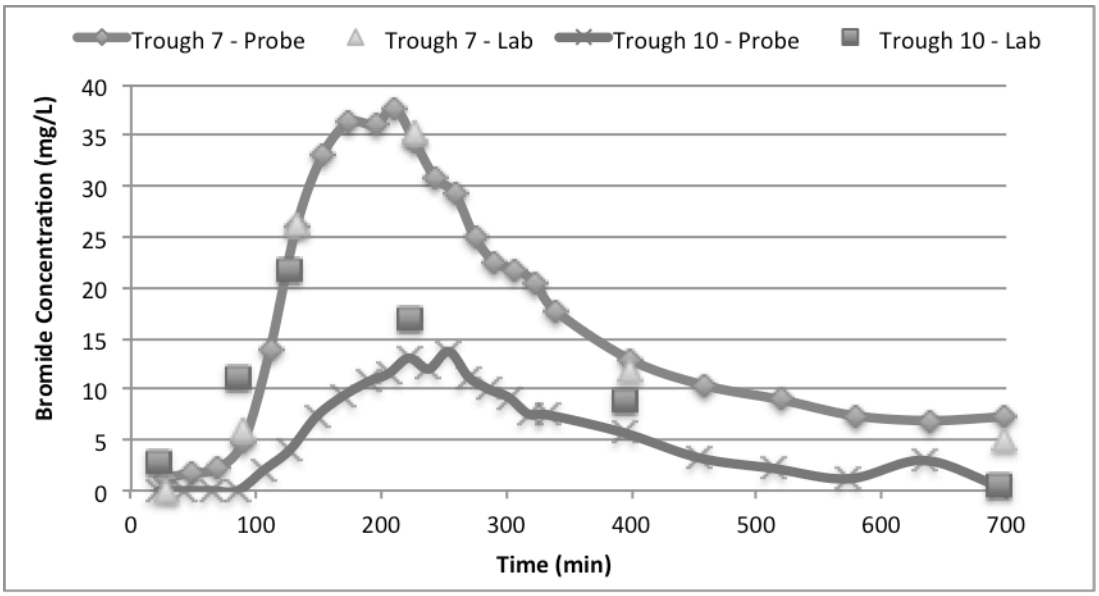

Figure 56. Bromide concentration (mg L^{-1}) in the effluent as a function of time in the bioreactor for troughs 7 and 10. Notice the pattern between the lab and probe data for the same troughs.

For troughs 2 and 4, there were no duplicate samples taken so there are no probe and lab samples corresponding to the exact same times. Three pre-bromide slug samples were taken as well as at every hour during the test for 36 hours. However, due to equipment user error, the last 6 hours of sample collection for trough 2 did not take place (Fig. 57). A total of 8 samples where measured with the probe that corresponded best to the time divisions set forth by Kandlec and Wallace (2009). In addition to the eight samples measured with the probe, 3 samples were sent to the lab, 1 each representing the ascension, near the peak, and the descention. Since this bromide test took place about 1 month after the experiment ended and the chemical water recipe was no longer being added, the background concentration is considered negligible because there was < 0.2 mg L^{-1} in the tap water (St. Paul (MN) City Water Report; June 2015). A

power regression was done using the values obtained during calibration between the mV of from the probe and mg L^{-1} from the probe ($y = 0.0006x^{2.27}$, $R^2 = 0.85$). This tranformation adjusted the probe curve so that the shape was more suitable but the curve needed further adjustment downwards by subtracting the same value from all data points in order to produce a better match to the lab data (3.00 mg L^{-1} for trough 2 and 2.70 mg L^{-1} for trough 4). Even still, probe samples 7 (1080 mins) and 8 (1800 mins) did not fall in line with lab sample 3 (1620 mins). In order to determine which probe values to use and to include all of the lab results, a 5% confidence interval (CI) was created around the predicted curve. Probe values that fell outside of this 5% CI were not used in the curve analysis. For this reason, the last 2 probe samples were removed from the analysis.

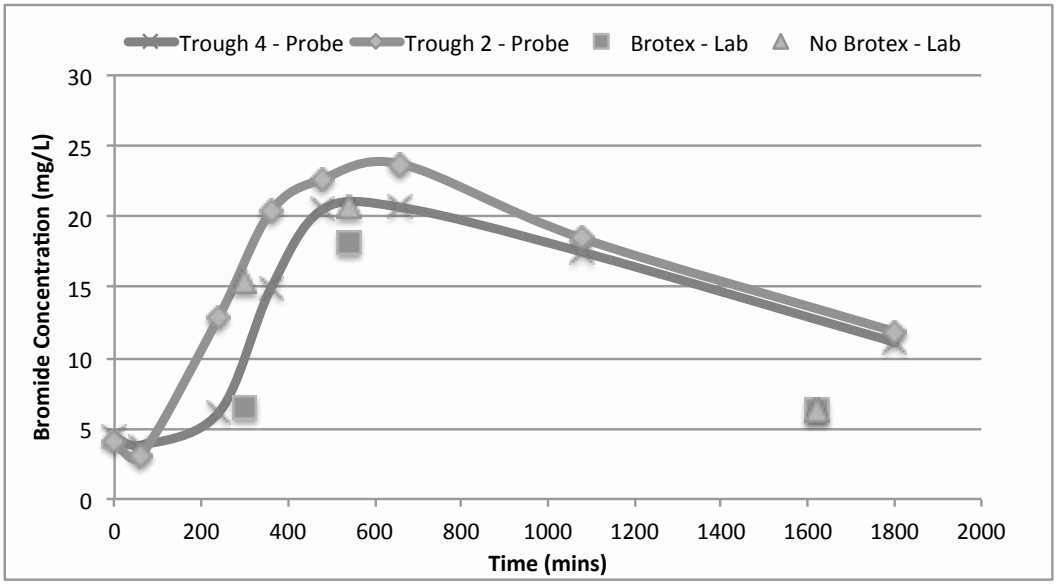

Figure 57. Bromide concentration (mg L^{-1}) in the effluent as a function of time in the bioreactor for troughs 2 and 4. Notice the pattern between the lab and probe data for the same troughs.

Universal curve

Percent recovery of bromide was adjusted up to 100% to produce an accurate flow characterization model based on a conservative tracer (Eq. 21). A universal curve was created by combining and plotting the bromide tracer test results normalized by detention time for two of the four troughs tested. Brotex and non-Brotex treatments were combined to create the universal curve because there was not a significant difference in flow pattern due to presence of Brotex (individual optimization results where less than 3% different from the universal curve). Additionally, the maximum concentration was removed, as recommended by the Grubb's Test for Outliers in XLSTAT^{TM}. Parameters were optimized using Excel Solver GRG Nonlinear Method to produce one universal curve. The model was validated by comparing the optimization results at half dt. Solver was unable to properly optimize troughs 7 and 4. At all tank configurations, Solver would choose an f_{s2} value greater than 1 to produce the lowest chi^2 value. Constraining f_{s2} to be less than 1 did not allow for the other parameters to adjust properly. For these reasons, troughs 7 and 4 were not included in the final, universal curve optimization. The lowest chi^2 value was created through optimization of a universal curve by combining trough 10 (minus the outlier) with trough 2. This result was then applied to all 4 test troughs to determine HRT. HRTs for each treatment were applied to all 3 replicates for each treatment.

Other Defining Parameters

In addition to the parameters determined using the bromide tracer test, secondary parameters were calculated for comparisons to other literature values.

The mass out (M_0) or mass of tracer in outflow (mg) is defined as

$$M_0 = \sum_{i=1}^{n} QC\Delta t \quad (19)$$

Where Q is the flow rate in L hr^{-1}, C is the concentration of bromide in the sample in mg L^{-1} (minus the background concentration), and Δt is the time interval between samples in hours (Martinez and Wise, 2003). Percent recovery (R_p) is

$$R_p = \left({}^{M_0}/_{M_T}\right) * 100 \quad (20)$$

Where M_T is the mass of the tracer added in mg. For purposes of model creation, percent recovery was adjusted to 100% (C') by normalizing each concentration by the fraction recovered

$$C' = C\left(\frac{M_T}{M_o}\right) \quad (21)$$

Theoretical (nominal) detention time (τ_n) (days) is

$$\tau_n = {}^{V\,n}/_{Q_{ave}} \quad (22)$$

where V is the reactor volume (L), n is the porosity of the media (fraction), and Q_{ave} is the average inflow rate (L hr^{-1}) to the reactors (Ghane, unpublished; Christianson *et al.,* 2011a). It does not take into account short-circuiting, dead space, or mixing. If the flow rate is constant, Q_{ave} can be substituted for Q.

Tracer detention time (τ) (days), the mass-weighted average time it takes for the tracer to reach the outlet, is

$$\tau = {}^{1}/_{M_0} \sum_{i=1}^{n} tQC\Delta t \quad (23)$$

where M_0 is in grams, t and Δt are in days, Q is in $m^3\ d^{-1}$, and C is in mg L^{-1} (Kadlec and Wallace, 2009).The volumetric efficiency (e_v) is

$$e_v = {}^{\tau}/_{\tau_n} \quad (24)$$

There is no unit on this term and the ideal is unity (Kadlec and Wallace, 2009).

The effective volume (V_e) is

$$V_e = \bar{\tau}\,\bar{Q} \quad (25)$$

where V_e is in m^3 (Martinez and Wise, 2003).The hydraulic efficiency, which incorporates some degree of short-circuiting, (n_i) is

$$n_i = \frac{V_e}{V} \quad (26)$$

where V is the total reactor volume (media and water; Martinez and Wise, 2003).

The Morrill Dispersion Index (MDI) is a measure of dispersion within the reactors and is calculated by

$$MDI = \frac{t_{90}}{t_{10}} \quad (27)$$

where t is the time when 90% and 10% of the bromide is exuded, respectively (Christianson, 2011). The US Environmental Protection Agency considers

reactors with MDIs less than 2.0 to have “effective” plug flow (Metcalf and Eddy, 2003).

The hydraulic residence time (HRT) or actual, in-situ retention time ($\bar{t}_{\Delta c}$), can be calculated as

$$HRT = \frac{\sum_{i=1}^{n} t\ C}{\sum_{i=1}^{n} C} \quad (28)$$

For each time increment i for all n samples (adapted from Metcalf and Eddy, 2003). Equation 28 equals Eq. 23 for constant Δt and steady flow rates.

Gas

N_2O concentrations were compared to influent NO_3^- concentrations (as a percentage). Linear regressions from the numeric model were used to define the overnight influent concentrations. Median effluent sampling times were used to back-calculate influent concentrations for 1 HRT prior to sampling (i.e. the median effluent sampling time for the 12 hr HRT was 10 am minus 1 HRT is 10 pm). Weeks 2 and 3 did not have the appropriate influent nitrate data for the 12 hr HRT and week 11 did not have any influent nitrate data. Additionally, the two highest N_2O results were removed from analysis because they were nearly twice the expected concentration and likely double injected or not flushed properly.

Data Transformation

Nitrate data were not normally distributed with unequal variances between treatments. Box-cox transformations were performed by hand using the preferred form presented by Draper and Smith (1998) in an attempt to improve the results. Box-cox transformations allow the data to determine the appropriate form of the equation since lambda (L) can be varied. The selection of lambda is based on the

minimum SSE. When L = 0, y' = $\tilde{y}$ * ln(y) where $\tilde{y}$ is the geometric mean of all samples results ($\tilde{y} = (y_1 * y_2 * y_3 \ldots . y_n)^{1/n}$). When L ≠ 0, y' = $\frac{\left((y^L)-1\right)}{L*\tilde{y}^{L-1}}$. The minimum SSE = $(y' - \bar{y})^2$ where $\bar{y}$ is the arithmetic mean. For percent removal, the minimum SSE was produced with a L of 1 so the data were not transformed prior to analysis (Fig. 60). For removal rate, the minimum SSE was produced by values with an L of 0.4 so the data were transformed prior to analysis (Fig. 61).

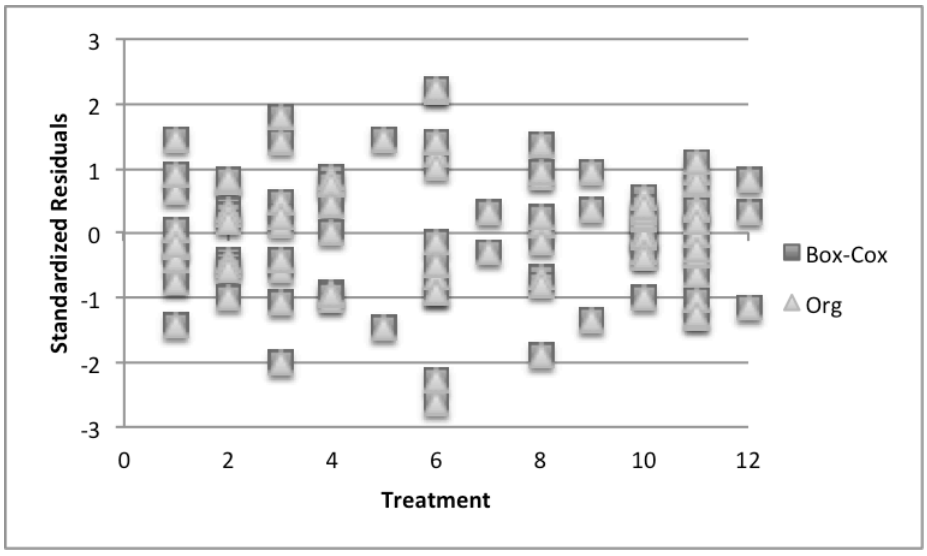

Figure 58. Percent nitrate removal standardized residuals. X axis shows treatment (temperature regime, material, HRT) by number: 1 = low, non-Brotex, 12 hr; 2 = low, non-Brotex, 4 hr; 3 = low, Brotex, 12 hr; 4 = low, Brotex, 4 hr; 5 = mid, non-Brotex, 4 hr; 6 = high, non-Brotex, 4 hr; 7 = mid, Brotex, 4 hr; 8 = high, Brotex, 4 hr; 9 = mid, Brotex, 12 hr; 10 = high, Brotex, 12 hr; 11 = high, non-Brotex, 12 hr; 12 = mid, non-Brotex, 12 hr.

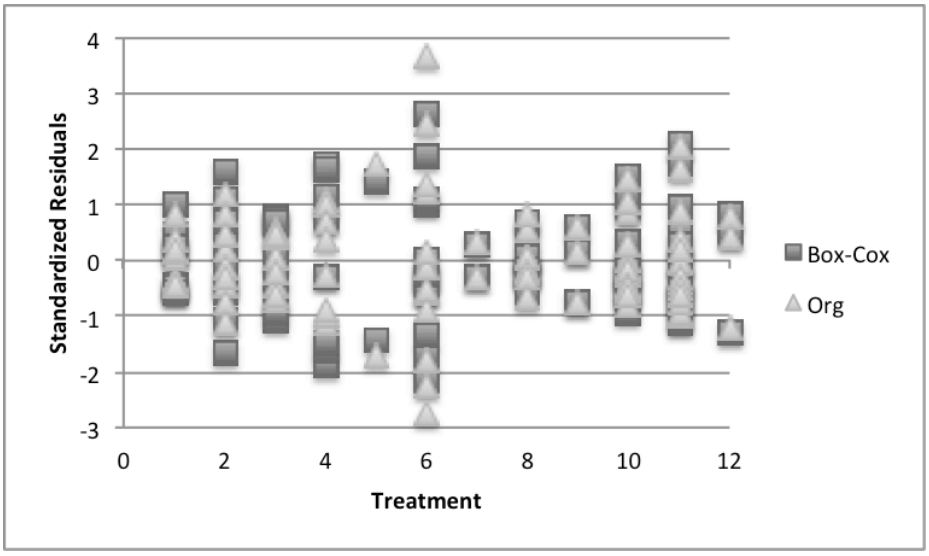

Figure 59. Nitrogen removal rate standardized residuals. X axis shows treatment (temperature regime, material, HRT) by number: 1 = low, non-Brotex, 12 hr; 2 = low, non-Brotex, 4 hr; 3 = low, Brotex, 12 hr; 4 = low, Brotex, 4 hr; 5 = mid, non-Brotex, 4 hr; 6 = high, non-Brotex, 4 hr; 7 = mid, Brotex, 4 hr; 8 = high, Brotex, 4 hr; 9 = mid, Brotex, 12 hr; 10 = high, Brotex, 12 hr; 11 = high, non-Brotex, 12 hr; 12 = mid, non-Brotex, 12 hr.

N_2O gas data were found to not be normally distributed ($P < 0.0001$ for Shapiro-Wilk, Anderson-Darling, Lilliefors and Jaque-Bera tests) so data were adjusted using a natural log transformation ($P > 0.08$ for all tests after transformation).

Data were analyzed in SPSS using a 3-way mixed model ANOVA with the subjects of trough*replicate, the repeated measure of temperature regime, and the fixed factors of temperature regime, material, and HRT. This analysis is based on a restricted maximum likelihood estimation, a type III sums of squares, and a diagonal repeated covariance type.

PLUG/CSTRS IN A SERIES MODEL

Theoretical Framework

The model was created in Microsoft Excel™ using a series of mass-balance equations. The general framework is given first. Key features of this framework

are given in Figure 60. The numerical approximation is presented in the next subsection.

As shown in Fig. 60, the total reactor volume (V_T) is divided into a plug-flow reactor and series of CSTR, that is,

$$V_T = V_p + V_c \tag{29}$$

where V_p is the plug reactor volume and V_c is the CSTR volume. In this section, volume refers to the void volume. The volume of all CSTRs (V_c) is then the total volume minus the plug volume

$$V_c = V_T - V_p = V_T(1 - f_p) \tag{30}$$

where f_p is the fraction of the total volume corresponding to the plug flow. The active volume of each CSTR is the total volume of reactors divided by the number of reactors (n) multiplied by the fraction that is active (minus the dead space (f_{dc})).

$$V_{cc} = \frac{V_c}{n}(1 - f_{dc}) \tag{31}$$

By substituting V_T (1 - f_p) for V_c in Eq. 31, one obtains

$$V_{cc} = \frac{V_T\,(1 - f_p)(1 - f_{dc})}{n} = K_c V_T \tag{32}$$

where

$$K_c = \frac{(1 - f_p)(1 - f_{dc})}{n} \tag{33}$$

By using retention time (T_d) defined for a given flow rate (Q)

$$T_d = \frac{V_T}{Q} \tag{34}$$

The active volume for each reactor is also defined as

$$V_{cc} = K_c T_d Q \tag{35}$$

Mass (M) is

$$M = CV \tag{36}$$

The mass balance for each reactor shown in Figure 60 is defined as

$$\frac{dM}{dt} = \dot{M}_{in} - \dot{M}_{out} - \dot{R} \tag{37}$$

where $\dot{R}$ is the removal rate (mass/time), $\dot{M}_{in} and\ \dot{M}_{out}$ are rates of mass flow into and out of the reactors, respectively, and dM/dt is the rate of change in mass in the reactor. The mass in the reactor is defined as

$$M = C\ V = C_{out} V_{cc} \tag{38}$$

where, for a perfectly mixed reactor, the concentration is equal to the effluent concentration (C_{out}) and the volume is the active volume of the reactor. The mass flow rate is defined, in general, as

$$\dot{M} = QC \tag{39}$$

First-order nitrate removal, $\dot{R}$, is defined as

$$\dot{R} = \kappa_d C V_{cc} \tag{40}$$

where κ_d is first-order decay coefficient (time^{-1}).

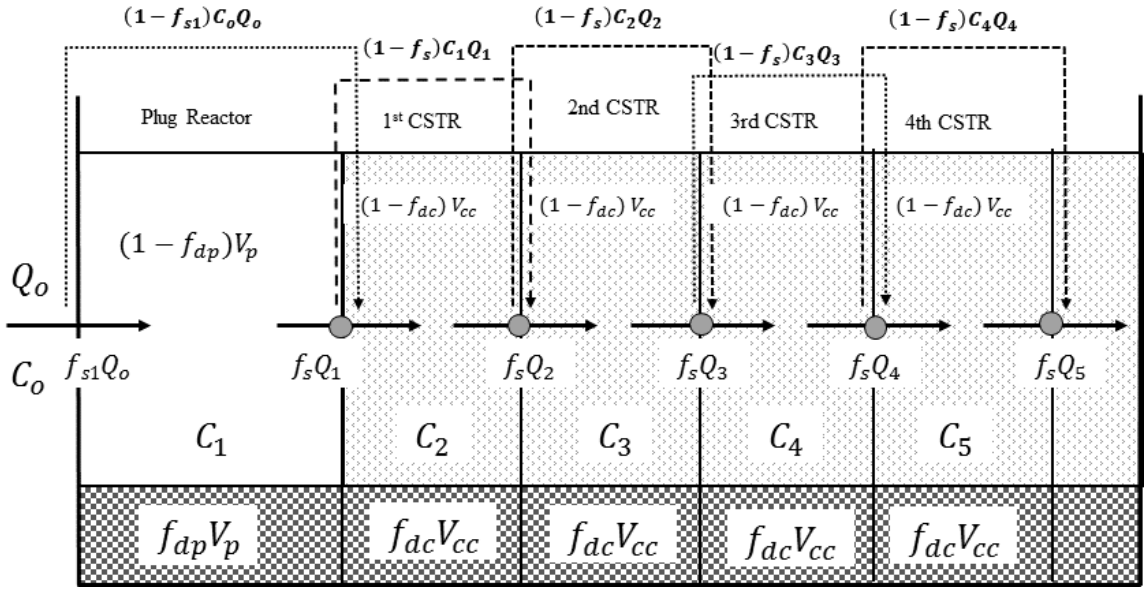

Figure 60. Diagram of model concepts and terms, where 1 - f_s = short-circuiting (fraction), κ_d = decay coefficient (1 T^{-1}) and f_{dc} = CSTR dead space (fraction), V_{cc} is the volume of each CSTR, and V_p is the volume of the plug (m^3) (Bruce Wilson, unpublished).

For the system in Fig. 60, the mass rate into the reactor is defined as

$$QC_{in} = Qf_sC_{in} + Q(1-f_s)C'_{in} \tag{41}$$

where f_s can refer to either f_{s1} (plug) or f_{s2} (CSTR), C_{in} is the effluent from the the previous reactor (whether plug reactor or any of the CSTRs), and C' refers to the 2nd previous reactor (for CSTR 1 this is C_p, for CSTR 2 this is C_0). For simplification, f_{s1} is set at 0 (no short-circuiting for the plug flow reactor).

By assuming that the concentration in the reactor equals the effluent concentration ($C=C_{out}$), the mass balance of Eq. 41 can be greatly simplified. By multiplying both sides by dt/Q and by evaluating V_{cc} by Eq. 35 and $\dot{R}$ by $\kappa_d C_{out} K_c T_d Q$, we obtain

$$f_s C_{in} dt + (1 - f_s) C'_{in} dt - C_{out} dt - \kappa_d K_c T_d C_{out}\, dt = K_c T_d\, dC_{out} \tag{42}$$

Numerical Approximation

Equation 42 is solved numerically by integrating over a time interval of Δt, that is,

$$\int_t^{t+\Delta t} f_s C_{in} dt + \int_t^{t+\Delta t} (1 - f_s) C'_{in} dt - \int_t^{t+\Delta t} C_{out} dt - \kappa_d K_c T_d \int_t^{t+\Delta t} C_{out}\, dt = K_c T_d \left(C_{out,2} - C_{out,1}\right) \tag{43}$$

By using average concentrations and removal rates over this time step (1 = previous time step, 2 = current time step), the integration terms are equal to the height of a rectangle multiplied by the width of Δt.

$$\left(\frac{C_{in,2} + C_{in,1}}{2}\right) f_s \Delta t + \left(\frac{C'_{in,2} + C'_{in,1}}{2}\right)(1 - f_s)\Delta t - \left(\frac{C_{out,2} + C_{out,1}}{2}\right)\Delta t - \kappa_d K_c T_d \left(\frac{C_{out,2} + C_{out,1}}{2}\right)\Delta t = K_c T_d \left(C_{out,2} - C_{out,1}\right) \tag{44}$$

By rearranging and simplifying, the unknown concentration at the end of the time step can be obtained as

$$C_{out,2} = \frac{\left(C_{in,2} + C_{in,1}\right)\frac{f_s \Delta t}{2}}{\left(K_c T_d \ + \ (1 \ + \kappa_d \ K_c T_d)\frac{\Delta t}{2}\right)} + \frac{\left(C'_{in,2} + C'_{in,1}\right)\frac{(1 - f_s)\Delta t}{2}}{\left(K_c T_d \ + \ (1 \ + \kappa_d \ K_c T_d)\frac{\Delta t}{2}\right)} + \frac{\left(K_c T_d \ - (1 \ + \kappa_d K_c T_d \ )\ \frac{\Delta t}{2}\right) C_{out,1}}{\left(K_c T_d \ + \ (1 \ + \kappa_d \ K_c T_d)\frac{\Delta t}{2}\right)} \quad (45)$$

The concentration out of each CSTR (mg L^{-1}) for any given time step is

$$C_{out,2} = \ W_0\left(C_{in,2} + C_{in,1}\right) + \ W_1\left(C'_{in,2} + C'_{in,1}\right) + W_2\left(C_{out,1}\right) \quad (46)$$

where the W coefficients are dimensionless and are defined as

$$W_0 = \frac{f_s\left(\frac{\Delta t}{2}\right)}{\left(K_c T_d \ + \ (1 \ + \kappa_d K_c T_d)\frac{\Delta t}{2}\right)} \quad (47)$$

$$W_1 = \frac{(1 - f_s)\left(\frac{\Delta t}{2}\right)}{\left(K_c T_d \ + \ (1 \ + \kappa_d K_c T_d)\frac{\Delta t}{2}\right)} \quad (48)$$

$$W_2 = \frac{\left(K_c T_d \ - (1 \ + \kappa_d K_c T_d)\ \frac{\Delta t}{2}\right)}{\left(K_c T_d \ + \ (1 \ + \kappa_d K_c T_d)\frac{\Delta t}{2}\right)} \quad (49)$$

For the first CTSR, $f_s = 1$ (no short-circuiting from the plug) so the W_1 is zero.

In order to accurately capture the plug, it is important not to average the concentration at the beginning and end of the pulse. In order to capture the plug over these time increments, this requires replacing $\frac{\Delta t}{2}$ with Δt in the numerator of the W_0 and W_1 terms (W_1 is still 0). Since we are not averaging over the first time

step after t_{dp} (the beginning of the pulse input into the 1st CSTR), the C_{in} terms can be split. Since $W_1 = 0$, the C' terms can be removed.

$$C_{out,2} = W_0 C_{in,2} + W_1 C_{in,1} + W_2(C_{out,1}) \quad (50)$$

For the first CTSR, we need to take the concentration at the end of the time step before the pulse input ($C_{in,1}$), which is the first time step after t_{dp}. The previous time step of the plug reactor ($C_{in,2}$) can be neglected by creating a $W_0' = 0$ term when using the time step Δt.

Now

$$C_{out,2} = W_0 C_{in,2} + W_0' C_{in,1} + W_2(C_{out,1}) \quad (51)$$

It is important to also not average the concentration at the end of the pulse input. For this we need to use Δt as the time step and take the concentration at the beginning of the time step after the pulse input. This is accomplished by switching the W_0 and W_0' values. For the remaining time steps, in the middle of the pulse and beyond one time step after the pulse, $W_0' = W_0$ (when the time parameter in the numerator is $\frac{\Delta t}{2}$).

For the second CSTR, C' now refers back to the plug reactor. An additional term, W_1', is used to account for the jump in concentration from the plug reactor for the first time step after t_{dp} and for the first time step after the pulse input comes through where W' and W^{1}' = 0.

$$C_{out,2} = W_0 C_{in,2} + W_0' C_{in,1} + W_1 C'_{in,2} + W_1' C'_{in,1} + W_2(C_{out,1}) \quad (52)$$

For the time step after t_{dp}, the W terms (regular form and prime form) are switched to account for only the beginning of that time step for the plug reactor. The remaining time steps follow the original form of the equation (Eq. 52) with $W_0' = W_0$ and $W'_1 = W_1$.

For CTSRs 3, 4, 5 and 6, the first time step after t_{dp} follows the form in Eq. 51 but without the need for the W'_1 term since there is no longer any direct reference back to the plug reactor. The remaining time steps refer back to the form of Eq. 52, without the need for W'_0 or W'_1.

Nitrate Removal

For nitrate removal from a continuous input, there is no need to capture the beginning or end of the plug so there is no need for the alternative forms of the previous equations (dt in the numerator or the switched W terms). All equations follow the same, original form found in Eqs. 47, 48, and 49.

Going back to Eq. 40, the nitrate removal rate (mass/time) for each time step is

$$\dot{R} = \kappa_d C V_{cc} \tag{53}$$

For each time step i, the mass of nitrate removed is

$$R_i = \kappa_d C V_{cc} dt \tag{54}$$

Therefore, the total mass of nitrate removed (R_R) for all n tanks at each time step is

$$R_R = \sum_{i=1}^{n} R_i \tag{55}$$

The total mass of nitrate removed for all n tanks over a time interval (t_i to t_f) (R_T) is

$$R_T = \sum_{t_i}^{t_f} R_R \tag{56}$$

Removal efficiency (R_e) (fraction) as the mass of nitrate removed per inflow nitrate mass (M_{in}) over the time interval is now

$$R_e = \frac{R_T}{M_{in}} \tag{57}$$

The nitrate removal rate (R_L) is found by

$$R_L = {}^{(R_T)}\Big/_{V}\Big/_{(T_f - T_s)} \tag{58}$$

where the difference in mass removed (R_T) is in grams, total reactor volume (water and media, V) is in m^3, and the difference in time (T) is in days. To calculate the nitrogen removal rate, R_L is multiplied by 0.225 (the ratio of the mass of N in NO_3^-). Significant differences in percent nitrate removal and the nitrogen removal rate by temperature are presented as results from the Fisher LSD test in ANOVA using XLSTAT™. Additionally, the Q_{10} value was calculated as the proportional change in the nitrogen removal rate with a 10 ^oC temperature change based on a linear regression model.

Process-based Nitrate Removal Model

Nitrate removal is closely related to the microbial population. This population can vary among reactors and with time. To account for this variation, a simple microbial-based equation was incorporated into the numerical model. This equation requires observed data from a qPCR analysis. For this study, Nadine

Hackshaw (UMN CEGE MS Student) under the direction of Dr. Sebastian Behrens (UMN CEGE) collected data from the reactors using removable biobags and DNA analysis was performed to determine the relative abundance of functional denitrifying genes. The biobags were placed within tubes (3) along the horizontal profile and corresponded to the number of tanks (4) found for the reactors (Fig. 54). For our analysis, tube 1 corresponds to the end of tank 1, tube 2 to tank 2, tube 3 to tank 3, and tube 4 to the reactor outlet. Additionally, the total bacteria count (16S; rRNA) was used because it demonstrated the clearest trends in population by tube. Each value of 16S was normalized by the average value across all tubes for any given time using

$$R = \frac{16S_n}{\overline{16S_n}} \tag{59}$$

The "n" subscript refers to tubes/tanks 1, 2, 3, or 4.

This variable (16S) was chosen as an example but other possibilities that represent various steps in the nitrate reduction process, including nirK, napA/narG, norB and nosZ, could have been used. However, other studies have demonstrated difficulties with other variables. Feyereisen *et al*. (2016) found that the nosZ gene abundance was similar for woodchips at 1.5 and 15.5 ^{o}C. Since there are no tubes corresponding to the reactor outlet, an exponential regression equation was used to interpolate the value for the outlet using the R values for tubes 1 - 3 plotted against reactor volume. Linear and polynomial regression equations estimated some outlet values as < 0 so these options were not considered reasonable.

The decay coefficient was adjusted using a multiple (M) to reflect the ratio of the total number of bacteria by volume of pore space to the average. This assumes a power relationship, with the constant exponent (n) and scaling

coefficient (α), between decay coefficients in each tube (κ_{dj}) and bacteria count. The effect of the adjustments (Rj') for reactor j is

$$R_j' = \frac{\kappa_{dj}}{\kappa_d} = \frac{\alpha\left(16S_j\right)^n}{\alpha\left(\overline{16S}\right)^n} = \left(\frac{16S_j}{\overline{16S}}\right)^n = M_j^n \tag{60}$$

The adjusted first-order decay coefficient is now defined as

$$\kappa_{dj} = \kappa_d\, M_j^n \tag{61}$$

Now, all equations that include κ_d are altered to be in the form of Eq. 61, including the W terms as well as the mass removed. Significant differences in the exponent n by temperature are presented as results from the Fisher LSD test in ANOVA using XLSTAT™.

Nitrate Removal Model Set-up

The nitrate removal model was set-up to accommodate the method of data collection as well as changing influent concentrations. All flow meters were cleaned, if necessary, and reset at 5 pm each day. Polynomial regression equations were created for continuous, overnight influent concentration taken every 15 minutes from 5 pm to 9 am with the nitrate probe. Where needed, two separate polynomial regression equations were created for the rise in concentration immediately after reset and another for the decline in concentration that followed. The decline in concentration was a result of the nutrient flow meter becoming slowly clogged with algal growth overnight. Since continuous, overnight influent measurements didn't begin until 20 days after the experiment started, linear regression equations were made using between 2 and 4 influent grab samples collected during the following day. For the rest of the experiment with continuous overnight influent data, influent regression equations were used to estimate nitrate concentrations for each 24-hr period (5 pm to 5 pm), restarting each day with the reset at 5 pm. Between 2 and 3 days were evaluated for nitrate

removal (depending on available, consecutive data) with the first day providing starting conditions for influent flow and nitrate conditions. Removal was calculated after 6.75 hrs to allow dampening of the initial conditions. Removal was estimated by optimizing κ_d with Excel Solver to match the predicted effluent curve to the actual grab sample data (2 samples, typically) taken between 9 am and 5 pm the following day.

Nitrate removal was calculated for sequences of days in which the $\chi^2 = \sum(O_i - P_i)^2$ value was less than 30, where O_i and P_i are the observed and predicted values, respectively. This was chosen due to the natural split of the data (the χ^2 was either greater than 100 or less than 30 for most day sequences). This allowed some variation between the model data and the actual data, within reason. If the flow rate was greater than $0.25Q_L$ (where Q_L is the 12 hr HRT flow rate; 0.043 L min^{-1}) away from the set flow rate (for either 12 hr or 4 hr) then the trough was flagged for unusual flow. This indicates an unacceptable deviation from the flow meter reset value, which could produce inaccurate removal results. If more than 25% of the troughs had unusual flow for that same day, that day was removed from the sequence. This only applied to the first or last (or both) days in a sequence since removing mid-sequence days would remove the entire data set. The remaining troughs with unusual flow that were not remedied by removing a day(s) were removed from that day sequence. Longer sequences of days were split into 2 sequences so that all sequences were 2 or 3 days long to avoid introducing unknown variability. There were 9 day sequences ranging in temperatures from 6 ^oC to 14.5 ^oC. Also, since there was frequently small temperature variation introduced from the piping and within the troughs, the temperature was determined based on the chiller setting. Temperatures were then categorized as low (6 and 7.2 C), mid (10 C), or high (12.2 and 14.5 C) for statistical analysis. An example model simulation is given in Figure 59.

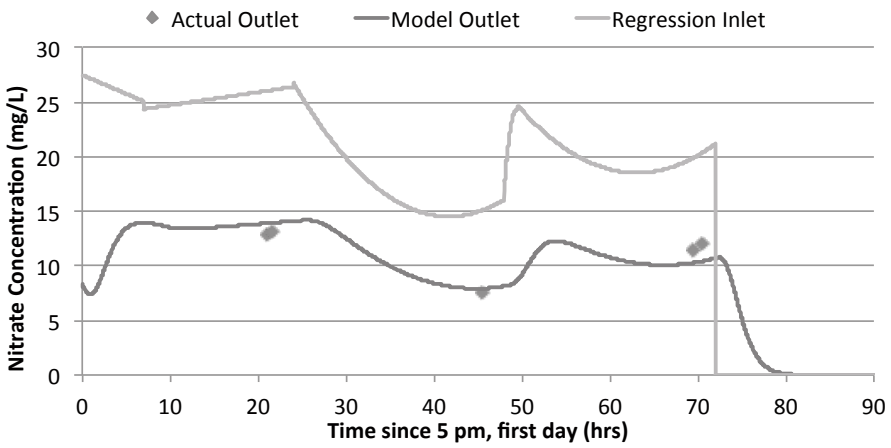

Figure 61. Graph of nitrate removal model results for February 12 – 15, 2017; 14.5 ^{O}C; 4 hr HRT: treatment with Brotex, biochar, and woodchips; 47.53% nitrate removal; chi^2 = 5.97.

RESULTS

Biochar Characterization

The biochar was 87.6% carbon and 0.44% nitrogen to yield a C:N ratio of 199. There were also several positively charged ions, including calcium (1400 mg kg^{-1}), iron (1700 mg kg^{-1}), and potassium (5,000 mg kg^{-1}). The surface area was 0.63 m^2 g^{-1} and the electrical conductivity was 116 μS cm^{-1}. There were also numerous trace metals present, including chromium (2 mg kg^{-1}), copper (11 mg kg^{-1}), and nickel (1 mg kg^{-1}). The full biochar chemical characterization is listed in Appendix C.

Bromide Tracer

The original percent recovery was high for trough 7 (106%) but low for troughs 10, 2, and 4 (48, 55, and 50%, respectively; Fig. 62). The universal curve optimization shows both minimal short-circuiting and dead space in both the plug tank and CSTRs (Table 8). The χ^2 value was 143 for a 4-tank CSTR configuration.

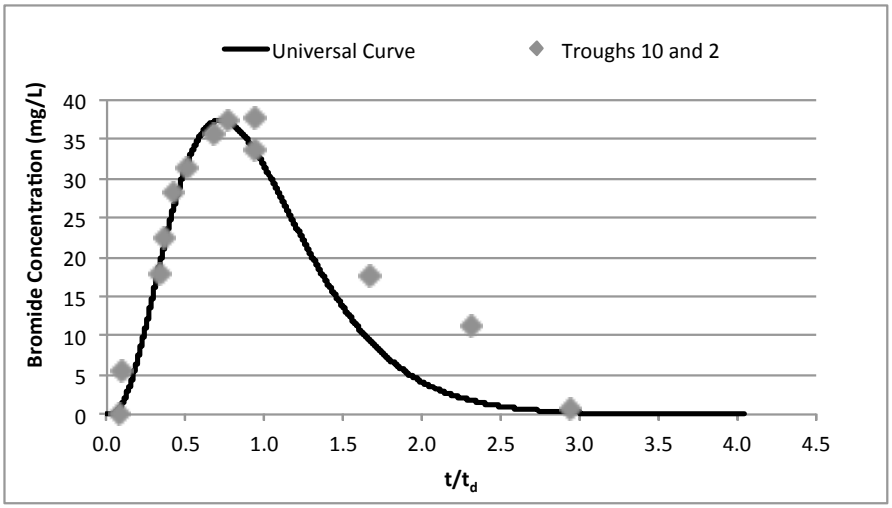

Figure 62. Bromide concentration (mg L^{-1}) as a function of normalized time for troughs 10 and 2 along with the universal bromide tracer curve created from the optimization of plug and CSTR parameters, as applied to trough 2.

Table 8. Parameter results of the universal curve created by minimizing the difference between the actual and predicted results (χ^2) for the bromide tracer curves of troughs 10 and 2.

Plug	f_{s1}	0	%
	f_{dp}	0	%
	f_p	1.1	%
CSTRs	f_{s2}	3.7	%
	f_{dc}	1.1	%
	n	4	tanks
Fit	χ^2	143	Σ(act. - model)^2

Several flow characterization parameters were similar to the expected results (Table 9). The theoretical retention time is slightly less than the designed HRT (4 hr and 12 hr), likely due to errors fluctuating flow rates. Tracer detention times are slightly less than the theoretical detention time, creating a volumetric

efficiency slightly less than 1, likely due to retardation of the tracer by the media. Total reactor volume was approximately 0.20 m^3 with an overall porosity of about 52%. Since the bromide recovery was adjusted upwards (to 100%), the hydraulic efficiency is approximately equal to the overall porosity (52%). The effective volume was approximately half of the total volume (0.10 m^3). The MDI values show that the reactors are not plug flow in nature (+> 2.0). The bromide based HRT (last row) was slightly less than the theoretical detention time by about 10 minutes for the 4 hr HRT and about 35 minutes for the 12 hr HRT, both of which are about 4.5% of their respective HRTs. This is likely due to the presence of 1.1% dead space and 3.7% short-circuiting in the CSTRs.

Table 9. Results of the secondary characterization parameters created by applying the results of the universal curve to all 4 test troughs.

Trough	2	4	7	10	Units	Descriptor
τ	11.68	11.08	3.94	3.93	hr	Theoretical Detention Time
t	11.21	10.71	3.78	3.79	hr	Tracer Detention Time
n_i	0.51	0.52	0.51	0.53	fraction	Hydraulic Efficiency
V_e	0.10	0.10	0.10	0.11	m^3	Effective Volume
e_v	0.92	0.94	0.96	0.97	fraction	Volumetric Efficiency
MDI	3.79	3.82	3.89	3.89	NA	Morrill Disperison Index
HRT	10.98	10.49	3.81	3.79	hr	Hydraulic Residence Time

Nitrogen Removal

The range and average percent nitrate removal as well as removal rate varied by treatment and across temperatures (Tables 10 and 11, Figures 63 and 64). The range of nitrate removal for the 4 hr Brotex varied from 7.66% to 51.56% (1.07 to 7.50 g N m^{-3} d^{-1}), 4 hr non-Brotex from 11.27% to 63.32% (2.07 to 9.66 g N m^{-3} d^{-1}), 12 hr Brotex from 29.99% to 80.17% (2.22 to 6.12 g N m^{-3} d^{-1}) and 12 hr non-Brotex from 44.70% to 84.06% (3.26 to 6.22 g N m^{-3} d^{-1}). Average nitrate removal for the 4 hr Brotex varied 11.90% to 46.02% (2.38 to 7.03 g N m^{-3} d^{-1}), 4

hr non-Brotex from 15.28% to 54.18% (3.21 to 7.86 g N m^{-3} d^{-1}), 12 hr Brotex from 38.24% to 77.92% (2.97 to 4.86 g N m^{-3} d^{-1}) and 12 hr non-Brotex from 50.49% to 79.67% (3.66 to 4.77 g N m^{-3} d^{-1}), under low and high temperatures, respectively. The Q_{10} value across all treatments was 1.79.

Table 10. Descriptive statistics from SPSS mixed model analysis in SPSS for percent nitrate removal under high, mid and low temperatures as well as across temperatures, including the mean, standard deviation, and number of samples for each treatment.

Descriptive Statistics					
Dependent Variable: Percent Nitrate Removal					
Regime	Material	HRT	Mean	Std. Deviation	N
High	12 hr	Brotex	77.92	1.66	14
		Non-Brotex	79.67	3.19	15
	4 hr	Brotex	46.02	4.15	9
		Non-Brotex	54.18	6.60	12
Mid	12 hr	Brotex	74.73	4.84	3
		Non-Brotex	79.58	4.26	3
	4 hr	Brotex	28.62	1.80	2
		Non-Brotex	39.41	8.42	2
Low	12 hr	Brotex	38.24	4.84	9
		Non-Brotex	50.49	3.58	9
	4 hr	Brotex	11.90	3.46	8
		Non-Brotex	15.28	2.59	9
Total	12 hr	Brotex	63.82	19.29	26
		Non-Brotex	69.94	14.39	27
	4 hr	Brotex	29.82	16.93	19
		Non-Brotex	37.67	19.53	23

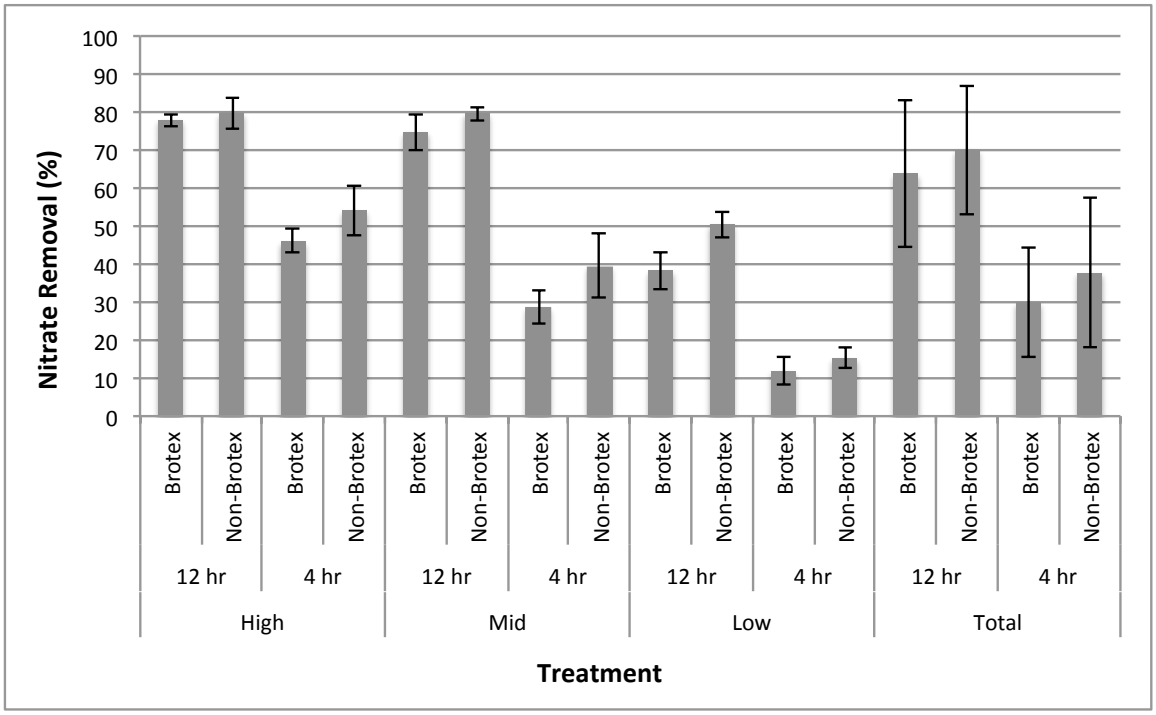

Figure 63. Percent nitrate removal as a function of bioreactor treatment with error bars of 1 SD around the mean. Graph includes a breakdown by temperature regime as well as a total across temperature regimes.

There was no significant difference between replicates (days with the same temperature and troughs of the same treatment; $P > 0.43$). All three dependent variables (regime, HRT, and material) had a significant effect on percent nitrate removal, both independently ($P < 0.001$) and combined ($P = 0.003$), as well as the combined effect of regime and HRT ($P = 0.006$). The combined effects of material with HRT and, separately, material with regime, did not have a significantly different effect on nitrate removal ($P = 0.651$ and 0.274, respectively). Upon graphing the linear regressions for each variable independently as well combined, results show that the regression trend lines intersect for variable combinations that are not significantly different than one another. This effect is more apparent at high temperatures for the 12 hr HRT but equally apparent for the 4 hr HRT at all temperatures. Within regime, all three

temperature categories were significantly different than one another ($P < 0.001$). The Brotex material had a significant (though slight) negative effect on percent nitrate removed. Both increasing temperature and a longer HRT had a significant positive effect on percent nitrate removal.

All three dependent variables (regime, HRT, and material) had a significant effect on the nitrogen removal rate, all independently ($P < 0.001$, < 0.001 and $= 0.023$ for each variable, respectively), but not the combined interaction ($P = 0.254$). Additionally, the combined effects of regime and HRT as well as material and HRT had a significant effect on the nitrogen removal rate ($P < 0.001$ and $= 0.032$, respectively). Within temperature, the low temperature regime was significantly different than the mid and high temperature regimes ($P < 0.001$) but the mid temperature was not significantly different than the high temperature ($P = 0.50$). The Brotex material had a slight positive impact at the high temperature regime for the 12 hr HRT. The nitrate removal rate is higher for the 4 hr HRT due to differences in loading associated to flow rate. The removal rate is also higher for the non-Brotex treatments, clearly for the 4 hr HRT but varying across temperatures, with the 12 hr HRT showing no clear trend.

Table 11. Descriptive statistics from SPSS mixed model analysis in SPSS for nitrogen removal rate (g N m^{-3} d^{-1}) under high, mid and low temperatures as well as across temperatures, including the mean, standard deviation, and number of samples for each treatment.

Descriptive Statistics					
Dependent Variable: Nitrogen Removal Rate					
Regime	Material	HRT	Mean	Std. Deviation	N
High	12 hr	Brotex	4.86	0.50	14
		Non-Brotex	4.77	0.67	9
	4 hr	Brotex	7.03	0.26	15
		Non-Brotex	7.86	0.99	12
Mid	12 hr	Brotex	5.72	0.47	3
		Non-Brotex	5.22	0.79	2
	4 hr	Brotex	5.90	0.30	3
		Non-Brotex	7.24	1.37	2
Low	12 hr	Brotex	2.97	0.52	9
		Non-Brotex	3.66	0.38	8
	4 hr	Brotex	2.38	1.04	9
		Non-Brotex	3.21	0.71	9
Total	12 hr	Brotex	4.30	1.14	26
		Non-Brotex	4.45	0.82	19
	4 hr	Brotex	4.95	2.38	27
		Non-Brotex	5.99	2.45	23

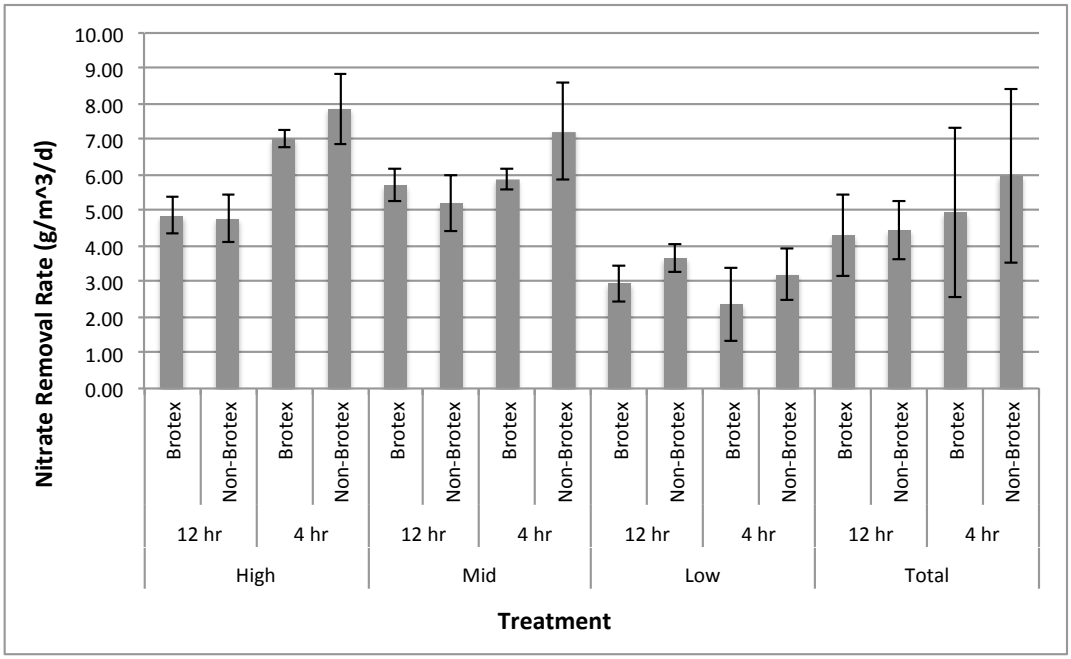

Figure 64. Nitrogen removal rate (g N m^{-3} d^{-1}) as a function of bioreactor treatment with error bars of 1 SD around the mean. Graph includes a breakdown by temperature regime as well as a total across temperature regimes.

Gas

The 12 hr HRTs produce higher N_2O emissions than the 4 hr HRT across temperatures (average of 314.60 vs. 256.74 ppm, respectively; Table 12, Fig. 65). Additionally, the Brotex treatments produced more N_2O emissions across temperatures (average of 324.70 vs 246.64 pmm, respectively) with the exception of the 4 hr HRT at the low temperature, which shows the opposite effect. All treatment variables and combinations thereof produce a significant difference in N_2O production ($P < 0.026$). Additionally, low and high temperatures are significantly different than one other ($P = 0.001$) but the mid temperature is not significantly different than the low or high temperatures ($P > 0.082$). The Brotex treatments produced slightly higher N_2O emissions at the low temperatures as well as for the 12 hr HRT. The maximum percent of N_2O gas to influent NO_3 concentration was 3.85%. However, this occurred in trough 9, with

high numbers for the first three weeks. Trough 9 had been leaking prior to the experiment and was drained and re-wetted 2 times before the leak was fully fixed. This wet-dry cycling may have contributed to these higher N_2O concentrations during the first 3 weeks of the experiment. Removal of these values yields a maximum of 2.90%, a minimum of 0.40%, and an average of 1.18%. This slightly higher than the numbers reported in the literate that lab scale is less than 1% and field-scale is less than 4.5% (Elgood *et al.,* 2010; Moorman *et al.,* 2010; Warneke *et al.,* 2011; Woli *et al.,* 2010). However, another study of agricultural residue showed 7.5% at 1.5 ^{o}C and 1.9% at 15.5 ^{o}C but was also media dependent with woodchip only treatments exhibiting 9.7% (Feyereisen et al., 2016)

Table 12. Descriptive statistics from SPSS mixed model analysis in SPSS for the natural log of N_2O production (ppb) under high, mid and low temperatures as well as across temperatures, including the mean, standard deviation, and number of samples for each treatment.

Descriptive Statistics					
Dependent Variable: Ln N_2O					
Regime	Material	HRT	Mean	Std. Deviation	N
High	12 hr	Brotex	5.84	0.19	14
		Non-Brotex	5.53	0.15	9
	4 hr	Brotex	5.57	0.26	15
		Non-Brotex	5.03	0.13	12
Mid	12 hr	Brotex	5.83	0.36	3
		Non-Brotex	5.37	0.39	2
	4 hr	Brotex	5.62	0.16	3
		Non-Brotex	5.44	0.39	2
Low	12 hr	Brotex	6.00	0.37	9
		Non-Brotex	5.52	0.15	8
	4 hr	Brotex	5.49	0.20	9
		Non-Brotex	5.71	0.39	9
Total	12 hr	Brotex	5.90	0.33	26
		Non-Brotex	5.47	0.27	19
	4 hr	Brotex	5.56	0.21	27
		Non-Brotex	5.42	0.43	23

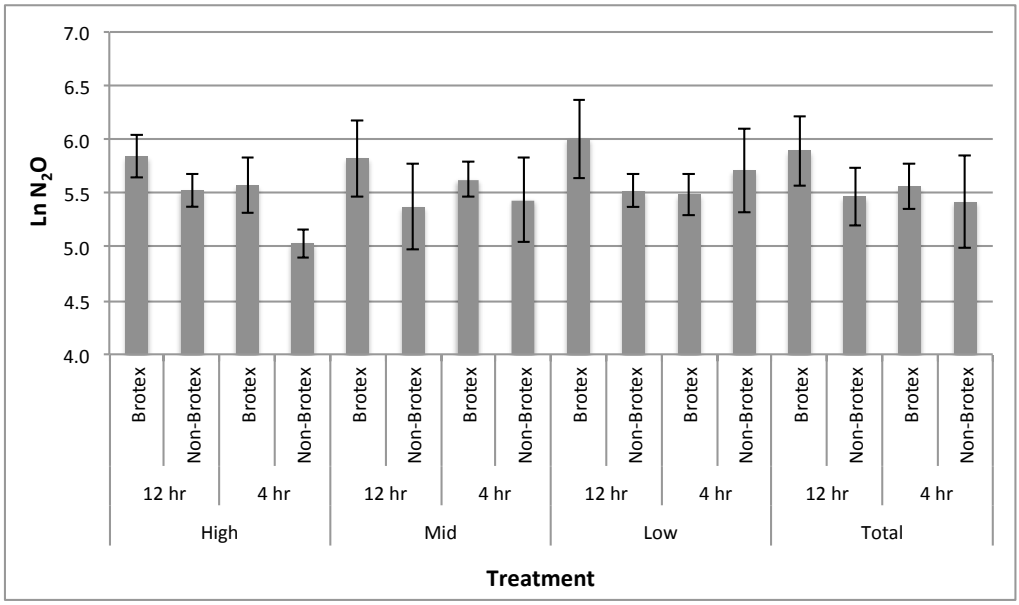

Figure 65. The natural log of N_2O production (ppb) as a function of bioreactor treatment with error bars of 1 SD around the mean. Graph includes a breakdown by temperature regime as well as a total across temperature regimes.

Microbial Model

Insight into the microbial model was explored by considering the exponent n for different conditions. This exponent is smaller for the high temperatures (0.039) than it is for the low temperatures (~0.052; Table 13). There is a significant difference ($P < 0.001$) in the values of the exponent at low temperatures and at high temperatures (mid temperature is neglected due to a lack of replicates). There is not a significance difference in the n value due to the HRT ($P = 0.182$) but there is for the combined effects of temperature and HRT ($P = 0.022$). The last biobag tubes had a lower average total bacterial counts under low temperatures with high n's and low κ_d values compared to high temperatures with low n's and high κ_d values (8.43% less for the 12 hr HRT and 53.89% less for the 4 hr HRT). This indicates that high n values occur in reactors that may have not met an upper threshold for the amount of bacteria that can be

supported. Under low temperatures more bacteria can be supported to obtain a higher nitrate removal. Under higher temperatures, nitrate removal is already very high, possibly meeting some upper threshold, that the addition of more bacteria would not produce a significant increase in nitrate removal.

Table 13. Descriptive statistics from SPSS mixed model analysis in SPSS for the exponent (n) value of the microbial model, including the mean, standard deviation, and number of samples for each treatment.

Descriptive Statistics				
Dependent Variable: Exponent (n)				
Regime	HRT	Mean	Std. Deviation	N
High	12 hr	0.039	1.7E-04	12
	4 hr	0.039	1.3E-04	10
Low	12 hr	0.051	3.0E-04	9
	4 hr	0.052	1.3E-03	9
Total	12 hr	0.044	5.9E-03	21
	4 hr	0.045	6.7E-03	19

DISCUSSION

Nitrogen Removal

Nitrate removal is much higher than the values shown in the literature for woodchip only bioreactors of a similar temperature and HRT. For a nearly direct comparison of percent nitrate removal to a traditional, woodchip-only bioreactor, Chun *et al.* (2009) conducted a column lab experiment that produced 30 to 40% nitrate removal under a 12 hr HRT at 16 to 17 ^{o}C and only 15% at 13 ^{o}C. With our novel media combination, we have attained similar removals under a lower temperature. At a temperature that is ~ 2 ^{o}C less than the Chun study (14.5 ^{o}C) we are able to produce removals nearly twice as large (75% vs. 40%) at the 12 hr HRT. Other values obtained in the literature were not directly comparable due to differences in temperature, HRT, or experimental set-up (i.e. was conducted in the field where there are more uncontrolled variables). Additionally, the range of

nitrogen removal rates is higher in comparison to other values in the literature as well. The mean nitrate removal (g N m^{-3} d^{-1}) across a range of HRTs from 1 to 10 hrs is 2.1 g N m^{-3} $d^{-}1$ at low (< 6 C) at low temperatures and 5.7 g N m^{-3} d^{-1} intermediate temperatures (6 to 16.9 C) (Addy *et al.,* 2016). For the novel media bioreactor experiment, the average removal rate across all temperatures (6 - 14.5 C) was in the range of 4 to 6 g N m^{-3} d^{-1} with an average in the range of 7 to 8 g N m^{-3} d^{-1} for the 4 hr HRT treatments at 14.5 ^{o}C. The Q_{10} value was similar to those found in the literature (1.0 to 3.4; Addy *et al.,* 2016; Feyereisen *et al.,* 2016; Cameron and Schipper, 2010). The novel media combination also removed a substantial amount of PO_4, however, it was not the focus of this study and the data were not thoroughly analyzed.

First order reaction rates (decay coefficient) are much higher than values found in the field and in the lab. For a field bioreactor in Iowa, the decay coefficients were found to be 0.99 and 1.02 d^{-1} (0.041 and 0.043 hr^{-1}) for 2013 and 2014, respectively (Jaynes *et al.,* 2016). Other experiments found 0.01 h^{-1} (field) (Chun *et al.,* 2010) and <0.001 to 0.13 h^{-1} (lab) (Chun *et al.,* 2009). Chun *et al.'s* (2009) lab experiment used creek water with NO_3-N ranging from 8 to 34 mg L^{-1} and temperatures ranging from 16 to 26 ^{o}C. The minimum decay coefficient for the novel media bioreactor experiment decay was 0.04 hr^{-1} (at low temperatures) with a maximum of 0.30 hr^{-1} (at high temperatures) and an average of 0.14 across all temperatures and treatments. It is intuitive to assume that the decay coefficients in the field should be quite less than the lab but it has been found that the first order decay coefficients are likely to be similar between the lab and the field, with the field possibly being slightly less, similar to Chun *et al.* (2009 and 2010). Our high decay coefficients reflect a similarly high percent nitrate removal and nitrogen removal rate.

Not only did the Brotex material not enhance nitrate removal, it, conversely, had a slight negative impact. Results in the literature are varied; some report enhanced removal with PBCs (Andersson *et al.,* 2008; Cantafio *et*

al., 1996; Welander and Mattiasson, 2003) and some report inconsistent results (Feyereisen *et al.,* 2017). The material and configuration could impact the colonization ability of the microbes. Some PBCs, including Brotex, may need more time to establish microbial communities. However, when mixed with the carbon source it may occupy space that would be more valuable as a carbon source (Feyeresien *et al.,* 2017). In general, any long lasting, not easily degradable carbon material with a high surface area and adequate porosity may function more efficiently than some PBCs.

The most important attributes of the biochar that likely contributed to nitrate removal were likely the high C:N ratio, the presence of positively charged ions, and the presence of trace metals. These trace metals are likely important in complex chemical reactions but the degree to which is unknown. The chemical characterization was performed on fresh (unused) biochar. The biochar is likely to change in its chemical characterization under the conditions present in a bioreactor system but the general behavior is not yet known. This may include C and N sorption, similar to Mukome *et al.* (2013a). The surface area was particularly small compared the European Biochar Certification (150 m^2 g^{-1}; Appendix C) so that was likely not a contributing factor.

Nitrate concentrations varied significantly over the course of the experiment. Nitrate removal rates may have been influenced by the influent concentration: beds with influent nitrogen concentrations > 30 mg N L-1 had higher nitrate removal rates than beds with intermediate (10 to 30 mg N L-1; P <0.1) or low (< 10 mg N L^{-1}; P <0.05) concentrations (Addy *et al.,* 2016). However, most of the time, the influent NO_3-N concentration in our experiment remained below 12 mg N L^{-1}. On the other extreme, nitrogen limitation was likely not an influencing factor, which is considered to occur when bed effluent is < 0.5 mg N L^{-1} (Addy *et al.,* 2016). Even though nitrate concentrations did vary, it was likely within a range that would not produce substantial changes in the denitrification abilities of the system.

The process of N_2O emissions is, perhaps, a complex situation with unknown mechanisms. In a meta-analysis of 30 field and lab studies, the addition of biochar as a soil amendment decreased N_2O emissions by 54% (Cayuela *et al.,* 2014). Our study showed slightly elevated N_2O emissions compared to the values found in the literature (1.18% ppb N_2O ppb influent $NO_3^{-\ -1}$ vs. <1% ppb N_2O ppb influent $NO_3^{-\ -1}$). There are several reasons why this may have occurred. First, the biochar feedstock, pyrolysis conditions as well as chemical character all influence N_2O emissions (Cayuela *et al.,* 2014). Another could be that the comparison of the application is not equivalent (bioreactor vs. fertilized soil). Lastly, our study showed elevated nitrate removal, which could translate to greater N_2O emissions, assuming the amount of N_2 gas to N_2O remains consistent. In the grand scheme of all possible sources of greenhouse gases, including N_2O, bioreactors should not be considered as a significant source of this pollutant.

Bromide Tracer

Dead (stagnant) areas are assumed to be in the corners of the reactors but it may also be in dead-end pores within the media (Jaynes *et al.,* 2016). Macro-pores for short-circuiting are possible along the sidewalls of the reactors and possibly within the reactor itself. Total recovery in other studies is also less than 100%. Jaynes *et al.* (2016) had 84% recovery. This could be due to leaching of bromide after sampling had stopped or permanent absorption of bromide into the media (Jaynes *et al.,* 2016). There is some evidence in the literature of bromide absorption to some soils but not to woodchips (Jaynes *et al., 2*016; Goldberg and Kabengi, 2010). The reduced peak and higher, longer tail of the actual data suggests there is an absorption/desorption process occurring, which retards the release of the bromide. This could be either physical or chemical in nature, the cause of which is unknown.

Overall, bromide is likely an imperfect tracer and not truly conservative in nature. This may be causing some early absorption and later desorption of bromide to the media and/or soil (Jaynes *et al.,* 2016; Goldberg and Kabengi, 2010). Mobile-immobile systems (MIM) can be helpful in explaining this observation; diffusion into and out of the woodchips can retard solute arrival at the outlet and result in a long tail of the bromide tracer curve (Jaynes *et al.,* 2016; Christianson *et al.,* 2013b). The presence of Brotex in some of the troughs may have affected the behavior of the tracer as well. Larger amounts of data points will likely produce a higher percent recovery, as was shown with trough 7.

There may have been an inherent issue with taking half of the tracer tests before the experiment and the other half afterwards. Some have found that biofilm formation can decrease hydraulic conductivity over time (Taylor *et al.,* 1990; Dennis and Turner, 1998; Daniels and Cherukuri, 2005). Our results for the 12 hr HRT were as expected (close but still less than 12 hours) so this may not have been a significant issue. It is speculated that over a long period of time the permeability will vary within a range due to the biological material sloughing from death or washing off during higher flow rates (Chun *et al.,* 2009). This process may make the timing for tracer tests moot as long as the bacterial community is well established.

CONCLUSION

Optimized bioreactor systems have the potential to work more efficiently at reduced temperatures typical of the spring thaw in southern Minnesota. In the case of the novel multi-media bioreactor containing woodchips, walnut shell biochar, and Brotex material, percent nitrate removal was doubled and the nitrogen removal rate was higher compared to other numbers found in the literature. However, the Brotex material produced a slight negative impact on the amount of denitrification as well as the degree to which complete denitrification took place (higher N_2O emissions). With its polar sites and presence of trace

metals, the walnut shell biochar was likely responsible for the majority of the increase in denitrification. Although the performance was improved, further work has the potential to improve this design to help meet the nutrient reduction goals set forth by the Minnesota Pollution Control Agency. These types of smaller laboratory scale models can help better inform the processes that occur in the "black-box" for which many bioreactors are considered. Models can be used to predict the behavior of larger, field scale bioreactors, which can be used to optimize engineering design.

This work paves the way for numerous possible future experiments with biochar and bioreactors in general. Further lab experiments can vary the media proportions, introduce wet-dry cycles, pulse the system with very high NO_3 concentrations, inoculate the system with different soils and bacteria, run under shorter (or longer) HRTs, and test different kinds of non-wood based biochar. Additional analysis could include testing for other nutrient or chemical removal, analyzing the media and/or water for degradation of the Brotex into plastic particulates, as well as gas and microbial sampling from suspected dead zones. Additionally, this model should be validated with the use of actual field data. Based on the nature of these preliminary results, the most ideal goal is to further expand this work to produce a more cost effective approach, possibly reducing the amount of biochar used.

Based on the microbial data, it is likely that more bacteria can be supported at lower temperatures. When habitat (surface area) and nutrients are mostly removed as limited factors then what remains is temperature. This could either be overcome by artificially heating the system, which may not be feasible or sustainable in the field. Another alternative is selectively breeding further cold-adapted denitrifying bacteria or transplanting them from more northerly climates, such as Northern Europe where intensive grain crops are grown at > 60^{o} latitude (Peltonen-Sainio *et al.,* 2009). However, climate change is expected to increase Minnesota's average winter temperatures by 3.3 to 5 ^{o}C by 2070 (University of

Massachusetts, ND). This may put Minnesota's winter temperature highs near the thawing mark. Denitrifying bacteria may not need to be as cold adapted and they may be active more of the time. Climate change is not easily predicted and research should focus on how to enhance the adaptability of these organisms to grow and function at lower temperatures for implementation under current or near future climate conditions.

BIBLIOGRAPHY

Addy, K., A.J. Gold, L. Christianson, M.B. David, L.A. Schipper, and N.A. Ratigan. 2016. Denitrifying Bioreactors for Nitrate Removal: A Meta-Analysis. Journal of Environmental Quality 45: 873 - 881.

Alexander, R.B., J.K. Böhlke, E.W. Boyer, M.B. David, J.W. Harvey, P.J. Mulholland, S.P. Seitzinger, C.R. Tobias, C. Tonitto, and W.M. Wollheim. 2009. Dynamic modeling of nitrogen losses in river networks unravels the coupled effects of hydrological and biogeochemical processes. Biogeochemistry 93: 91–116.

Alexander, R.B., R.A. Smith and G.E. Schwarz. 2000. Effect of stream channel size on the delivery of nitrogen to the Gulf of Mexico. Nature (London) 403: 758-761.

Anderson, J.P., and W.J. Craig. 1984. Growing Energy Crops on Minnesota's Wetlands: The Land Use Perspective. University of Minnesota, Minneapolis, MN. 95 pp.

Andersson, S., M. Nilsson, G. Dalhammar, and G.K. Rajarao. 2008. Assessment of carrier materials for biofilm formation and denitrification. Vatten 64: 201–207.

Aquarium Forum. Fish Poop and You: a Primer. Accessed 4 June 2017. http://www.aquariumforum.com/f66/fish-poop-you-primer-8310.html

Arango, C.P., and J.L. Tank. 2008. Land use influences the spatiotemporal controls on nitrification and denitrification in headwater streams. Journal of the North American Benthological Society 27(1): 90 - 107.

Arango, C.P., J.L. Tank, J.L. Schaller, T.V. Royer, M.J. Bernot, and M.B. David. 2007. Benthic organic carbon influences denitrification in streams with high nitrate concentration. Freshwater Biology 52: 1210-1222.

Atkinson, C.J., J.D. Fitzgerald, N.A. Hipps. 2010. Potential mechanisms for achieving agricultural benefits from biochar application to temperate soils: a review. Plant Soil 337: 1–18.

Atkinson, K.E. 1978. An Introduction to Numerical Analysis. John Wiley and Sons, Inc., New York, NY.

Babcock, B. 1992. The Effects of Uncertainty on Optimal Nitrogen Applications. Review of Agricultural Economics 14(2): 271-280.

Blann, K.L., J.L. Anderson, G.R. Sands, and B. Vondracek. 2009. Effects of Agricultural Drainage on Aquatic Ecosystems. A Review: Critical Reviews in Environmental Science and Technology, 39: 11, 909 — 1001.

Blowes, D.W., W.D. Robertson, C.J. Ptacek, and C. Merkley. 1994. Removal of agricultural nitrate from tile-drainage effluent water using in-line bioreactors. Journal of Contaminant Hydrology 15(3): 207-221.

Bock, E., B. Coleman and Z.M. Easton. 2016. Effect of Biochar on Nitrate Removal in a Pilot-Scale Denitrifying Bioreactor. Journal of Environmental Quality 45: 762-771.

Bock, E., N. Smith, M. Rogers, B. Coleman, M. Reiter, B. Benham, and Z. Easton. 2015. Enhanced Nitrate and Phosphate Removal in Denitrifying Bioreactor with Biochar. Journal of Environmental Quality 44: 605-613.

Brakensiek, D.L., H.B. Osborn, and W.J. Rawls. 1979. Field Manual for Research in Agricultural Hydrology. USDA, Agriculture Handbook 224, 550 pp.

Brouder, S., B. Hofmann, E. Kladivko, R. Turco, A. Bongen, and J. Frankenberger. 2005. Interpreting Nitrate Concentration in Tile Drainage Water. Agronomy Guide; Purdue Extension. https://www.extension.purdue.edu/extmedia/AY/AY-318-W.pdf.

Cameron, S.G., and L.A. Schipper. 2010. Nitrate removal and hydraulic performance of organic carbon for use in denitrification beds. Ecological Engineering 36(11): 1588-1595.

Cameron, S.G., and L.A. Schipper. 2011. Evaluation of passive solar heating and alternative flow regimes on nitrate removal in denitrification beds. Ecol. Eng. 37(8): 1195-1204.

Cantafio, A.W., K.D. Hagen, G.E. Lewis, T.L. Bledsoe, K.M. Nunan, and J.M. Macy. 1996. Pilot-scale selenium bioremediation of San Joaquin drainage water with Thauera selenatis. Appl. Environ. Microbiol. 62: 3298–3303.

Cayuela, M.L., L. van Zwieten, B.P. Singh, S. Jeffery, A. Roig, M.A. Sánchez-Monedero. 2013. Biochar's role in mitigating soil nitrous oxide emissions: A review and meta-analysis. Agriculture, Ecosystems and Environment 191: 5-16.

Christianson, L. 2011. Design and Performance of denitrification bioreactors for agricultural drainage. PhD Dissertation. Iowa State University; Ames, IA.

Christianson, L., A. Bhandari, M. Helmers, K. Kult, T. Sutphin and R. Wolf. 2012. Performance Evaluation of Four Field-Scale Agricultural Drainage Denitrification Bioreactors in Iowa. Transactions of the ASABE 55(6): 2163 – 2174.

Christianson, L., A. Bhandari, and M. Helmers. 2011a. Potential Design Methodology for Agricultural Drainage Denitrifying Bioreactors. World Environmental and Water Resources Congress: Bearing Knowledge for Sustainability: 2740-2748.

Christianson, L.E., J. Hanly, and M. Hedley. 2011b. Optimized denitrification bioreactor treatment through simulated drainage containment. Agric. Water Mgmt. 99(1): 85-92.

Christianson, L., J. Hanly, N. Jha, S. Saggar and M. Hedley. 2013a. Denitrification bioreactor nitrous oxide emissions under fluctuation flow conditions. ASABE Paper Number: 131597821. St. Joseph, MI: ASABE.

Christianson, L., M. Helmers, A. Bhandari, and T. Moorman. 2013b. Internal hydraulics of an agricultural drainage denitrification bioreactor. Ecol. Eng. 52: 298–307.

Christianson, L.A., and L.A. Schipper. 2016. Moving Denitrifying Bioreactors beyond Proof of Concept: Introduction to the Special Section. Journal of Environmental Quality 45:757-761.

Christner Jr. W.T., J.A. Magner, E.S. Verry, and K.N. Brooks. 2004. Natural channel design for agricultural ditches in south-western Minnesota. Proceedings of Self-sustaining Solutions for Streams, Wetlands, and Watersheds. St. Joseph, MI: ASAE.

Chun, J. A., R.A Cooke, J.W. Eheart, and M.S Kang. 2009. Estimation of flow and transport parameters for woodchip-based bioreactors: I. laboratory-scale bioreactor. Biosystems Engineering 10: 384-395.

Chun, J.A., R.A. Cooke, J.W. Eheart and J. Cho. 2010. Estimation of flow and transport parameters for woodchip-based bioreactors: II. Field-scale bioreactor. Biosystems Engineering 10: 95-102.

Clanton, C. 2015. “Chemical Characteristics: Part II”. Class Handout. BBE 4533: Sustainable Waste Management Engineering. Department of Bioproducts and Biosystems Engineering, University of Minnesota. St. Paul, MN.

Clark, I.D., and P. Fritz. 1997. Environmental Isotopes in Hydrogeology. Lewis Publishers: Boca Raton, New York.

D’Ambrosio J.L. 2013. Perspectives on the geomorphic evolution and ecology of modified channels and two-stage ditches in the agriculturally-dominated Midwestern United States. The Ohio State University, Columbus, OH.

D'Ambrosio, J.L., A.D. Ward, and J. D. Witter. 2015. Evaluating Geomorphic Change in Constructed Two-Stage Ditches. Journal of the American Water Resources Association 51(4): 910-922.

Daniels, J.L., and R. Cherukuri. 2005. Influence of biofilm on barrier material performance. Practice Periodical of Hazardous, Toxic, and Radioactive Waste Management 9(4): 245–252.

David, M.B., and L.E. Gentry. 2000. Nitrogen balance in and export form an agricultural watershed. Journal of Environmental Quality 26: 1038-1048.

Davis, R.T., J.L. Tank, U.H. Mahl, S.G. Winikoff, and S.S. Roley. 2015. The Influence of Two-Stage Ditches with Constructed Floodplains on Water

Column Nutrients and Sediments in Agricultural Streams. Journal of the American Water Resources Association 51(4): 941 – 955.

Dennis, M.L., and J.P. Turner. 1998. Hydraulic conductivity of compacted soil treated with biofilm. Journal of Geotechnical and Geoenvironmental Engineering 124(2): 120–127.

Draper, N.R., and H. Smith. 1998. Applied Regression Analysis: Third Edition. A Wiley-Interscience Publication; John Wiley and Sons, Inc., New York.

Elgood, Z., W.D. Robertson, S.L. Schiff, and R. Elgood. 2010. Nitrate removal and greenhouse gas production in a stream-bed denitrifying bioreactor. Ecological Engineering 36: 1575-1580.

Encyclopaedia Britannica. "Denitrifying bacteria". Assessed on 15 March 2015. Encyclopaedia Britannica, Inc., 2015. http://www.britannica.com/EBchecked/topic/157733/denitrifying-bacteria.

Environmental Protection Agency (EPA). 2017. Mississippi River/Gulf of Mexico Hypoxia Task Force. "Hypoxia 101: What is hypoxia and what causes it?" Accessed 2 Feb 2018. https://www.epa.gov/ms-htf/hypoxia-101.

Environmental Protection Agency (EPA). ND. Wetlands. "Prairie Potholes." Accessed 1 Jan. 2018. https://www.epa.gov/wetlands/prairie-potholes.

Feyereisen, G. Sept. 12, 2016; Personal (Email) Communication. Adjunct Assistant Professor, University of Minnesota, St. Paul MN. Regarding information obtained from Tom Moorman, USDA -ARS microbiologist and affiliate of Iowa State University, Ames, IA.

Feyereisen, G., A. Ranaivoson, J. Moncrief, C. Rosen, E. Dorsey and G. Nelson. "Bioreators for Nitrate Removal in Tile Drained Cropland." Minnesota Agricultural Resources Center, Wilmar, MN. April 3, 2014.

Feyereisen, G., and L.E. Christianson. 2015. Hydraulic Flow Characteristics of Agricultural Residues for Denitrifying Bioreactor Media. Applied Engineering in Agriculture 31(1): 89-96.

Feyereisen, G., L.E. Christianson, T.B. Moorman, R.T. Venterea, and J.A. Coulter. 2017. Plastic Biofilm Carrier after Corn Cobs Reduces Nitrate Loading in Laboratory Denitrifying Bioreactors. Journal of Environmental Quality 45: 915-920.

Feyereisen, G., T.B. Moorman. L.A. Christianson, R.T. Venterea, J.A. Coulter and U.W. Tschirner. 2016. Performance of Agricultural Residue Media in Laboratory Denitrifying Bioreactors at Low Temperatures. Journal of Environmental Quality 45: 779-787.

Firestone, M.K., and D.A. Davidson. 1989.Microbioloigcal Basis of NO and N2O Production and Consumption in Soil. Exchange of Trace Gases Between Terrestrial Ecosystems and the Atmosphere. John Wiley and Sons Ltd; pg 7 - 21.

Floating Island International. “Biohaven Technology.” 2015. Accessed 17 Dec. 2014. http://www.floatingislandinternational.com/products/biohaven-technology.

Fraser, H., and R. Fleming. 2001. Environmental Benefits of Tile Drainage – Literature Review. Ridgetown College, University of Guelph.

Gat, J.R. 1981. Stable isotope hydrology: deuterium and oxygen – 18 in the water cycle, Chapter 3, International Atomic Energy Agency, Vienna, 339p.

Gentry, L., M.B. David, K.M. Smith, and D.A. Kovacic. 1998. Nitrogen Cycling and tile drainage nitrate loss in a corn/soybean watershed. Agriculture, Ecosystems and Environment 68: 85 - 97.

Gentry, L.E., M.B. David, F.E. Below, T.V. Royer, and G.F. McIsaac. 2009. Nitrogen Mass Balance of a Tile-drained Agricultural Watershed in East-Central Illinois. Journal of Environmental Quality 39: 1841-1847.

Ghane, E., N.R. Fausey, and L.C. Brown. 2014. Non-Darcy flow of water through woodchip media. Journal of Hydrology 519: 3400-3409.

Ghazal, N. 2010. Investigating Dissolved Organic Carbon Uptake to Biochar. 2010 Kearney Fellowship Report. The University of California, Davis.

http://kearney.ucdavis.edu/Undergrad_Fellowship_Reports /GhazalPowerpoint.pdf.

Gibson, J.J., T.W.D. Edwards, and G.G. Bursey. 1993. Estimating Evaporation Using Stable Isotopes: Quantitative Results and Sensitivity Analysis for Two Catchments in Northern Canada. Paper presented at the 9th Northern Res. Basin Symposium/Workshop; Whitehorse/Dawson/Inuvik, Canada. Nordic Hydrology 24: 79-94.

Goldberg, S., and N.J. Kabengi. 2010 Bromide absorption by reference minerals and soils. Vadose Zone Journal 9: 780-786.

Greenan, C.M., T.B. Moorman, T.C. Kaspar, T.B. Parkin, and D.B. Jaynes. 2006. Comparing carbon substrates for denitrification of sub-surface drainage water. J. Environ. Qual. 35: 824–829.

Groffman, P.M., M.A. Altabet, J.K. Böhlke, K. Butterbach-Bahl, M.B. David, M.K. Firestone, A.E. Giblin, T. M. Kana, L.P. Nielsen, and M. A. Voytek. 2006. Methods for Measuring Denitrification: Diverse Approaches to a Difficult Problem. Ecological Applications 16(6): 2091 – 2122.

Hameed, A.S., T.R. Resmia, S. Suraja, C. Unnikrishnan Warriera, M. Sudheesha, and R.D. Deshpandeb. 2015. Isotopic characterization and mass-balance reveals groundwater recharge pattern in Chaliyar river basin, Kerala, India. Journal of Hydrology: Regional Studies 4(A): 48-58.

Hammer, DA. 1992. Designing constructed wetland systems to treat agricultural nonpoint sources pollution. Ecological Engineering 1: 49-82

Healy, M.G., M. Rodgers, and J. Mulqueen. 2006. Denitrification of a nitrate rich synthetic wastewater using various wood-based media materials. J. Environ. Sci. Health A Tox. Hazard. Subst. Environ. Eng. 41: 779–788.

Hicks, D.R. 2005. Minnesota Crop News. A Look and Minnesota Corn Yields over Time. Accessed 2 Feb 2018. http://blog-crop-news.extension.umn.edu/2005/11/a-look-at-minnesota-corn-yields-over.html.

Hodaj, A., L.C. Bowling, J.R. Frankenberger, and I. Chaubey. Impact of a two-stage ditch on channel water quality. Agricultural Water Management 192: 126-137.

Inwood, S.E., J. Tank, and M.J. Bernot. 2005. Patterns of denitrification associated with land use in 9 Midwestern headwater streams, J. N. Am. Benthol. Soc. 24: 227–245.

Iowa Soybean Association. ND. "Bioreactors." Environmental Programs. Accessed on 21 Oct. 2015. http://www.iasoybeans.com/environment/sites/default/files/bioreactors/Bioreactor%20Fact%20Sheet.pdf

Jackson, W.A., L.E. Asmussen, E.W. Hauser and A.W. White. 1973. Nitrate in Surface and Sub-surface Flow from a Small Agricultural Watershed. Journal of Environmental Quality 2(4): 480 - 482.

Jayakaran A.D., and A.D. Ward. 2007. Geometry of inset channels and the sediment composition of fluvial benches in agricultural drainage systems in Ohio. J. Soil and Water Cons. 62(4): 296-307.

Jayakaran, A., D. Mecklenburg, A. Ward, L. Brown and A. Weekes. 2005. Formation of Fluvial Benches in Headwater Channels in the Midwestern Region of the USA. International Agricultural Engineering Journal 12(4): 193-208.

Jaynes, D.B, T.B. Moorman, T.B. Parkin, and T.C. Kasper. 2016. Simulating Woodchip Bioreactor Performance Using a Dual-Porosity Model. Journal of Environmental Quality 45: 830-838.

Jin, C.X, G.R. Sands, H.J. Kandel, J.H. Wiersma, and B.J. Hansen. Influence of Sub-surface Drainage on Soil Temperature in a Cold Climate. Journal of Irrigation and Drainage Engineering 134(1): 83-88.

Kadlec, R.H., and S.D. Wallace 2009. Treatment Wetlands: Second Edition. Boca Raton: CRC Press. Assessed online 19 March 2015.

https://wiki.umn.edu/pub/Nieber/EcologicalEngineeringDesign/treatment_wetlands_-_kadlec_and_wallace_-_part_I.pdf.

Kalbus, E., F. Reinstorf and M. Schirmer. 2006. Measuring methods for groundwater - surface water interactions: a review. Hydrol. Earth. Syst. Sci. (10): 873-887.

Kallio, R., A. Ward, J. D'Ambrosio, and J.D. Witter. 2010. A Decade Later: The Establishment, Channel Evolution, and Stability of Innovative Two-Stage Agricultural Ditches in the Midwest Region of the United States. Presented at the 9th International Drainage Symposium. Paper #IDS-CSBE-100209. American Society of Agricultural and Biological Engineers. St. Joseph, Mich., USA.

Kantawanichkul S., S. Kladprasert, and H. Brix. 2009. Treatment of high-strength wastewater in tropical vertical flow constructed wetlands planted with Typha angustifolia and Cyperus involucratus. Ecological Engineering 35: 238-247.

King, W. 2011. “Life is Controlled by the Limiting Nutrient.” Colby at Sea. Accessed on 16 Mar. 2015. http://web.colby.edu/colbyatsea/2011/02/01/life-is-controlled-by-the-limiting-nutrient/.

King, K.W., N.R. Fausey, and M.R. Williams. 2014. Effect of subsurface drainage on streamflow in an agricultural watershed. Journal of hydrology 519: 483-445.

Kookana, R.S., A.K. Sarmah, L. Van Zwieten, E. Drull, and B. Singh. 2011. Chapter three: Biochar application to soil: Agronomic and environmental benefits and unintended consequences. Adv. Agron. 112: 103–143.

Kotila, J. “New study shows tiling causes increased flow in MN rivers.” Herald Journal: Farm Horizons. Accessed 9 Aug., 2017. http://www.herald-journal.com/farmhorizons/2013-farm/tiling.html.

Krabbenhoft, D.P., C.J. Bowser, M.P. Anderson, and J.W. Wiley. 1990. Estimating Groundwater Exchange With Lakes 1. The stable isotope mass-balance method. Water Resources Research 26(10): 2445-2453.

Kramer, G. 2011. Design, construction and assessment of a self-sustaining drainage ditch. Master's Thesis. University of Minnesota, St. Paul.

Krider, L., G. Kramer, B. Hansen, J. Magner, L. Lahti, B. DeZiel, L. Zhang, J. Peterson, B. Wilson, B. Lazarus, and J. Nieber. 2014. Cedar River Alternative Ditch Designs: the Assessment of a Self-Sustaining Ditch Design in Mower County, Minnesota. Prepared by the University of Minnesota, Department of Bioproducts and Biosystems Engineering for the Minnesota Pollution Control Agency. https://wiki.umn.edu/pub/Wilson/DownloadReports/AlternativeDitchDesign_EPA319_FinalReport.pdf.

Krider, L., B. Wilson, and J. Magner. 2016a. Design and Construction of a Reduced Temperature Testing Apparatus for Denitrification. 10th Int. Drainage Symp. St. Joseph, MI: ASABE. Paper number: 162493063.

Krider, L., B. Wilson, J. Magner, L. Lahti, G. Kramer, B. Hansen, and J. Nieber. 2016b. Nitrate removal at a two-stage ditch in Mower County, MN. Journal of Environmental Quality (Submitted for Publication).

Krider, L., B. (A) DeZiel, B. Hansen, G. Kramer, J. Magner, B. Wilson, J. Nieber. 2016c. Habitat improvements and fish community response associated with two-stage ditch construction in Mower County, MN. Journal of the American Water Resources Association (In-press).

Krider, L., J. Magner, B. Hansen, B. Wilson, G. Kramer, J. Peterson, and J. Nieber. 2017. Improvements in fluvial stability associated with two-stage ditch construction in Mower County, MN. Journal of the America Water Resources Association 53(4): 886-902.

Lahti, L. 2012. Investigating Evapotranspiration from a Two – Stage Ditch in Southern Minnesota. Plan B Master's Thesis. University of Minnesota, St. Paul.

Laird, D., P. Fleming, B. Wang, R. Horton, and D. Karlen. 2010. Biochar impact on nutrient leaching from a Midwestern agricultural soil. Geoderma 158: 436–442.

Lamb, J.A., F.G. Fernandez, and D.E. Kaiser. 2014. "Understanding Nitrogen in Soils." Nutrient Management. University of Minnesota Extension Publication # AG-FO-3770-B. Accessed on 20 Sept. 2017. https://www.extension.umn.edu/agriculture/nutrient-management/nitrogen/understanding-nitrogen-in-soils/docs/AG-FO-3770-B.pdf

Landwehr, K., and B.L. Rhoads, 2003. Depositional response of a headwater stream to channelization, East Central Illinois, USA. River Research and Applications 19: 77-100.

Larson, R.A., M. Montez-Ellis, K. Marley and G. K. Sims. 2001. Nitrate Uptake by Terrestrial and Aquatic Plants. Proceedings of the 2001 Illinois Groundwater Consortium. http://igc.siu.edu/proceedings /01/larson.pdf

Lau, J.K., T.E. Lauer, and M.Ll. Weinman, 2006. Impacts of channelization on stream habitats and associated fish assemblages in East Central Indiana. American Midland Naturalist 156: 319-330.

Lenntech. 1998 - 2016. "Nitrogen (N) and Water." Accessed on 5 April 2017. http://www.lenntech.com/periodic/water/nitrogen/nitrogen-and-water.htm

Leverenz, H.L., K. Haunschild, G.M. Hopes, G. Tchobanoglous, and J.L. Darby. 2010. Anoxic treatment wetlands for denitrification. Ecol. Eng. 36: 1544–1551.

Liang, B., J. Lehmann, D. Solomon, J. Kinyangi, J. Grossman, B. O'Neill, J.O. Skjemstad, J. Thies, F.J. Luizao, J. Petersen, and E.G. Neves. 2006.

Black Carbon increases cation exchange capacity in soils. Soil Sci. Soc. Am. J. 70: 1719–1730.

Lien, D., and D. Orrick. “Minnesota Farm Drain Tiling: Better crops, but at what cost?” Twin Cities Pioneer Press. Feb. 18, 2016. Accessed Aug. 9, 2017.

Lien, E., and J. Magner. 2017. Engineered biosystem treatment trains: A review of agricultural nutrient sequestration. Invention Journal of Research Technology in Engineering and Management 1(11): 1-8.

Louisiana Universities Marine Consortium. “What is hypoxia?” Hypoxia in the Northern Gulf of Mexico. Assessed on 12 September 2016. http://www.gulfhypoxia.net/overview/

Magner, J., B. Hansen, T. Sundby, G. Kramer, B. Wilson, and J. Nieber. 2012. Channel evolution of the Des Moines Lobe till drainage ditches in southern Minnesota (USA). Environmental Earth Sciences 67: 2359-2369.

Magner J.A., and K.N. Brooks. 2007 Stratified regional hydraulic geometry curves: a water quality management tool. Hydrologic Science and Technology 23: 159-172.

Magner, J., and S. Alexander. 2008. Drainage and nutrient attenuation in a riparian interception-wetland: southern Minnesota, USA. Environmental Geology 54(7): 1367-1376.

Magner, J., B. Hansen, C. Anderson, B. Wilson, and J. Nieber. 2010. Minnesota Agricultural Ditch Reach Assessment for Stability (MADRAS): A Decision Support Tool. Presented at ASABE’s 9th International Drainage Symposium. Congress of the International Commission of Agricultural and Biosystems Engineering, Québec City, Canada, June 13-17, 2010.

Mahl, U.H., J.L. Tank, S.S. Roley, and R.T. Davis. 2015. Two-Stage Ditch Floodplains Enhance N-Removal Capacity and Reduce Turbidity and Dissolved P in Agricultural Streams. Journal of the American Water Resources Association 51(4): 923-940.

Martinez, C.J. and W.R. Wise. 2003. Hydraulic Analysis of Orlando Easterly Wetland. Journal of Environmental Engineering 129: 553-560.

Mecklenburg, D. 2000. Statistical relationships of drainage ditch features to watershed characteristics, probable discharges, and maintenance practices. Paper 012211, Ohio Dept. of Natural Resources, Columbus, OH.

Mecklenburg, D. 2006. The Reference Reach Spreadsheet for Channel Survey and Data Management. A STREAM Module: Spreadsheet tools for river evaluation, assessment, and monitoring. Ohio Department of Natural Resources. http: www.dep.wv.gov.

Metcalf and Eddy, Inc. 2003. Wastewater Engineering Treatment and Reuse. 4th ed. ed. McGraw-Hill.

Minnesota Board of Water and Soil Resources (BWSR). Wetland Regulation in Minnesota. Accessed on 6 June 2016. http://www.bwsr.state.mn.us/wetlands/publications/wetlandregulation2.html.

Minnesota Department of Natural Resources (DNR) - MIS Bureau. DNR 24K Streams. Minnesota: Minnesota Department of Natural Resources - MIS Bureau, 2003.

Minnesota Pollution Control Agency (MPCA). 2010. Aquatic Life Water Quality Standards Technical Support Document for Nitrate. Triennial Water Quality Standard Amendments to Minn. R. chs. 7050 and 7052 DRAFT For External Review, November 12, 2010.

Minnesota Pollution Control Agency (MPCA). 2013. Nitrogen in Minnesota Surface Waters. Accessed on 22 Oct. 2014. http://www.pca.state.mn.us/index.php/viewdocument.html?gid=19623.

Minnesota Pollution Control Agency (MPCA). 2014. Minnesota Nutrient Reduction Strategy: Executive Summary. Accessed on 21 Oct. 2015. http://www.pca.state.mn.us/index.php/view-document.html?gid=20046.

Mitsch, W., J.W. Day, Jr., J.W. Gilliam, P.M. Groffman, D.L. Hey, G.W. Randall, and N. Wang. 2001. Reducing Nitrogen Loading to the Gulf of Mexico from the Mississippi River Basin: Strategies to Counter a Persistent Ecological Problem: Ecotechnology—the use of natural ecosystems to solve environmental problems—should be a part of efforts to shrink the zone of hypoxia in the Gulf of Mexico. Bioscience 51(5): 373 - 388.

Moorman, T.B., T.B. Parkin, T.C. Kaspar, and D.B. Jaynes. 2010. Denitrification activity, wood loss, and N_2O emissions over 9 years from a woodchip bioreactor. Ecological Engineering 36: 1567-1574.

Mueller, D.K., P.A. Hamilton, D.R., Helsel, K.J. Hitt and B.C. Ruddy. 1995. Nutrients in Ground Water and Surface Water of the United States - An Analysis of Data Through 1992. U.S. Geological Survey. Water0Resource Investigations Report 95-4031. Denver, CO. https://pubs.usgs.gov/wri/1995/4031/report.pdf

Mukome, F., X. Zhang, L. Silva, J. Six and S.J. Parikh. 2013a. Use of Chemical and Physical Characteristics To Investigate Trends in Biochar Feedstocks. Journal of Agricultural and Food Chemistry 61: 2196-2204.

Mukome, F.N.D., J. Six and S. Parikh. 2013b. The effects of walnut shell and wood feedstock biochar amendments on greenhouse gas emissions from a fertile soil. Geoderma 200-201: 90-98.

National Oceanic and Atmospheric Administration (NOAA) National Weather Service. Department of Commerce. National Weather Service Instruction 10-1065. August 17, 2007. Storm Data Preparation. http://www.ncdc.noaa.gov/stormevents/pd01016005curr.pdf

National Oceanic and Atmospheric Administration (NOAA). ND. U.S. Department of Commerce. National Environmental Satellite, Data, and Information Service. Climate Data Online Annual Climatological Summary (2009-2013). Data Download using the Data Search Tool. http://www.ncdc.noaa.gov/cdo-web/search?datasetid=ANNUAL

National Oceanic and Atmospheric Administration (NOAA). 2014. “What is a dead zone?” Ocean Facts. Accessed on 15 March 2015. http://oceanservice.noaa.gov/facts/deadzone.html

National Oceanic and Atmospheric Administration (NOAA). 2015. “2015 Gulf of Mexico dead zone “above average.”” Stories 2015. Accessed on 22 Oct. 2015. http://www.noaanews. http://noaa.gov/stories2015/080415-gulf-of-mexico-dead-zone-above-average.html.

National Oceanic and Atmospheric Administration (NOAA). 2017. “Gulf of Mexico “Dead Zone” Largest Ever Measured.” NCCOS news and features. Accessed 20 Sept. 2017. http://coastalscience.noaa.gov.

National Programme on Technology Enhanced Learning (NPTEL). ND. “Microbial Aspects of Denitrification.” Course 105104102: Waste and Wastewater Engineering. Free online course funded by the Ministry of HRD and the Government of India. Accessed on 15 March 2015. http://nptel.ac.in/courses/105104102/Lecture%2034.htm

Nyende, J., G. van Toder, and D. Vermeulen. 2013. Application of Isotopes and Recharge Analysis in Investigating Surface Water and Groundwater in Fractured Aquifer under Influence of Climate Variability. Journal of Earth Science and Climatic Change 4: 148.

Palmer, B. 2014. “Devil in the deep blue sea.” onEarth. Natural Resources Defense Council. Dec 2014. Accessed on 23 Oct. 2015. http://www.onearth.org/earthwire/devil-deep-blue-sea.

Parkin, T.B., and R.T. Venterea. 2010. USDA-ARS GRACEnet Project Protocols Chapter 3: Chamber-Based Trace Gas Flux Measurements. N Sampling Protocols. R.F. Follett, editor. p. 3-1 to 3-39. www.ars.usda.gov/research/GRACEnet.

Peltonen-Sainio, P., A. Rajala, H. Känkänen, K. Hakala. 2009. Improving farming systems in northern European conditions. In V.O. Sadras and D. Calderini, eds. Crop physiology: applications for genetic improvement and

agronomy, pp. 71–97. Amsterdam, Netherlands. Elsevier.

Peterson, J., B.N. Wilson, and G. Kramer. 2010 Two-stage ditch assessment using the CONCEPTS Model. Presented at the 2010 ASABE Annual International Meeting. ASABE Paper No. 1009158. American Soc. of Agric. and Biol. Eng. St. Joseph, Mich., USA.

Plotnikoff, R., and J. Polayes. 1999. The Relationship Between Stream Macroinvertebrates and Salmon in the Quilceda/Allen Drainage. Washington State Department of Ecology, Environmental Assessment Program. Publication No. 99-311.

Pluer, W.T, L.D. Geohring, T.S. Steenhuis, and M.T. Walter. 2016. Control Influencing the Treatment of Excess Agricultural Nitrate with Denitrifying Bioreactors. Journal of Environmental Quality 45: 772-778.

Powell, G.E., A.D. Ward, D.E. Mecklenburg, and A.D. Jayakaran, 2007. Two-Stage Channel Systems: Part 1, A Practical Approach for sizing Agricultural Ditches. Journal of Soil and Water Conservation 62(4): 277-286.

Powell, K.L., and V. Bouchard. 2010. Is denitrification enhanced by the development of natural fluvial morphology in agricultural headwater ditches? Journal of the North American Benthological Society 29(2): 761 – 772.

Powlson, D.S., P.G. Saffigna, and M. Kragt-Cottaar. 1988. Denitrification at sub-optimal temperatures in soils from different climatic zones. Soil Biology and Biochemistry 20(5): 719 – 723.

R Core Team. 2015. R: A language and environment for statistical computing. R Foundation for Statistical Computing, Vienna, Austria. ISBN 3-900051-07-0. http://www.R-project.org/

Rajsic, P., and A. Weersink. 2007. Do farmers waste fertilizer? A comparison of ex post optimal nitrogen rates and ex ante recommendations by model, site and year. Agricultural Systems 97(1-2): 56 -67.

Randall, G.W., and D.J. Mulla. 2001. Nitrate Nitrogen in Surface Waters as Influenced by Climatic Conditions. Journal of Environmental Quality 30: 337 - 344.

Randall, G.W. 2004. Sub-surface Drain Flow Characteristics During a 15-Year Period in Minnesota. In Drainage VIII Proceedings of the Eighth International Symposium. 21-24 March 2004. Pp. 17-24. ASABE publication #701P0304, ed. R. Cooke.

Randall, G.W., and J.E. Sawyer. 2008. Chapter 6: Nitrogen Application Timing, Forms, and Additives Final Report: Gulf Hypoxia and Local Water Quality Concerns Workshop. ed. ASABE, St. Joseph, MI.

Reddy, M.M., P. Schuster, C. Kendall, M.B. Reddy. 2006. Characterization of surface and ground water $\delta^{18}O$ seasonal variation and its use for estimating groundwater residence times. Hydrol. Process. 20: 1753-1772.

Richards, R.P., V. Bouchard, and R. McCall. 2008. Water quality in drainage ditches influenced by agricultural sub-surface drainage. WS-3857-08. Fact Sheet Extension, Agricultural and Natural Resources, Ohio State University, Columbus, Ohio. http://ohioline.osu.edu/ws-fact/pdf/WS_3857_08.pdf

RiverMorph, LLC. 2010. RIVERMorph: Stream Restoration Software v4.3. RiverMorph, LLC., Louisville, Kent., USA.

Robertson, W.D., D.W. Blowes, C.J. Ptacek and J.A. Cherry. 2000. Long-term performance of in situ reactive barriers for nitrate remediation. Ground Water 38: 689–695.

Robertson, W.D., J.L. Vogan, and P.S. Lombardo. 2008. Nitrate removal rates in a 15-year-old permeable reactive barrier treating septic system nitrate. Ground Water Monit. Rev. 28:65–72.

Robinson, M., and D.W. Rycroft. 1999. In R.W. Skaggs and J. van Schifgaarde (eds.) “Agricultural Drainage.” Agronomy Monograph number 38:767-800. ASA, CSSA, and SSSA, Madison, WI.

Roley, S.S., J.L. Tank, and M.A. Williams. 2012b. Hydrologic connectivity increases denitrification in the hyporheic zone and restored floodplains of an agricultural stream. Journal of Geophysical Research 117.

Roley, S.S., J.L. Tank, M.L. Stephen, L.T. Johnson, J.J Beaulieu, and J.D. Witter. 2012a. Floodplain Restoration Enhances Denitrification and Reach-Scale Nitrogen Removal in an Agricultural Stream. Ecol. Appl. 22(1): 281-297.

Rosgen, D. 1996. Applied River Morphology. Wildland Hydrology, Pagosa Springs, CO.

Rosgen, D. River Stability Field Guide. Wildland Hydrology, Colorado; 2008.

Rossman, L.A. 2008. Storm Water Management Model, User's Manual, Version 5.0 (EPA/600R-05/040), National Risk Management Research Laboratory, Office of Research and Development, US EPA, Cincinnati, Ohio, USA.

Royer, T., J.L. Tank, and M.B. David. 2004. Transport and Fate of Nitrate in Headwater Agricultural Stream in Illinois. Journal of Environmental Quality 33: 1296-1304.

Saliling, W.J.B., P.W. Westerman, and T.M. Losordo. 2007. Wood chips and wheat straw as alternative biofilter media for denitrification reactors treating aquaculture and other wastewaters with high nitrate concentrations. Aquacult. Eng. 37:222–233.

Schaller, J.L., T.V. Royer, M.B. David, and J.L. Tank. 2004.Denitrification associated with plants and sediments in an agricultural stream. Journal of the North American Benthological Society 23:667–676.

Schipper, L.A., G.F. Barkle, J.C. Hadfield, M. Vojvodic-Vukovic, and C.P. Burgess. 2004. Hydraulic constraints on the performance of a groundwater denitrification wall for nitrate removal from shallow groundwater. J. Contaminant Hydrol. 69(3-4): 263-279.

Schipper, L.A., G.F. Barkle, and M. Vojvodic-Vukovic. 2005. Maximum rates of nitrate removal in a denitrification wall. J. Environ. Qual. 34(4): 1270-1276.

Schipper, L.A., W.D. Robertson, A.J. Gold, D.B. Jaynes, and S.C. Stewart. 2010.

Denitrifying bioreactors: An approach for reducing nitrate loads to receiving waters. Ecol. Eng. 36:1532–1543.

Sharpley, A.N., T. Krogstad, P.J. Kleinman, and B. Haggard. 2007. Managing natural processes in drainage ditches for nonpoint source phosphorus control. J. Soil Water Conserv. 62: 197–206.

Smid, A.E., and E.G. Beauchamp. 1976. Effects of temperature and organic matter on denitrification in soil. Canadian Journal of Soil Science 56: 385-391.

Simon, A., and C. R. Hupp. 1986. Channel evolution in modified Tennessee channels. Pages 5-71 to 5-82. Proceedings, Fourth Federal Interagency Sedimentation Conference, Las Vegas, Nevada, March 24-27, 1986, Vol. 2.

Simpkins, W.W. 1995. Isotopic composition of precipitation in central Iowa. Journal of Hydrology 172(1-4): 185-207.

Slocum, N. 2013. Comparison of three agricultural residue-based filter media for use in a denitrifying bioreactor. Retrieved from the University of Minnesota Digital Conservancy. http://purl.umn.edu/148052.

Southwest Research and Outreach Center, Lamberton, MN; Frost Depth Readings for 2013 – 2015. http://swroc.cfans.umn.edu/WeatherInformation/FrostDepthReadings/index.htm.

Spokas, K. Personal communication. 7 Jan. 2015.

Stanford, G., S. Dzienia, and R. A. Vander Pol. 1975. Effect of Temperature on Denitrification Rate in Soils. Soil Sci. Soc. Amer. Proc. 39: 868 – 870.

Stewart, F. M., T. Mulholland, A.B. Cunningham, B.G. Kania, and M. T. Osterlund. 2008. Floating islands as an alternative to constructed wetlands for treatment of excess nutrients from agricultural and municipal wastes - results of laboratory scale tests. Land Contamination and Reclamation 16: 25–33.

Suddick, E.C., and J. Six. 2013. An estimation of annual nitrous oxide emissions and soil quality following the amendment of high temperature walnut shell and compost to a small scale vegetable crop rotation. Science of the Total Environment 465: 298-307.

Tank, J. ND. The Two-Stage Ditch and Nitrogen Dynamics. University of Notre Dame.

Taylor, S.W., P.C.D. Milly, and P.R. Jaffé. 1990. Biofilm growth and the related changes in the physical properties of a porous medium, 2.Permeability. Water Resources Research 26(9): 2161 -2169.

Triska, F.J., J.H. Duff, R.W. Sheibley, A.P. Jackma, and R.J. Avanzino. 2007. Din retention-transport through four hydrologically connected zones in a headwater catchment of the upper Mississippi River. Journal of the American Water Resources Association 43(1): 60-71.

Twin Cities Pioneer Press. 2013. “Minnesota report blames agriculture for rising nitrate levels in surface waters.” Accessed on 17 October 2016. http://www.twincities.com/2013/06/25/minnesota-report-blames-agriculture-for-rising-nitrate-levels-in-surface-waters/.

United States Climate Data. Weather Averages of Lamberton, MN. Accessed on 6 June 2016. http://www.usclimatedata.com/climate/lamberton/minnesota/united-states/usmn0430.

United States Department of Agriculture (USDA). National Agricultural Statistic Survey. 2017. Minnesota County Estimates: Corn for Grain (2015-2016), Corn for Silage (2015-2016), and Soybeans (2015-2016). https://www.nass.usda.gov/Statistics_by_State/Minnesota/Publications/County_Estimates/index.php.

United States Department of Agriculture Natural Resource Conservation Service (USDA-NRCS). 2007. Stream Restoration Design, Part 654, National Engineering Handbook. Washington, DC.

United States Department of Agriculture, Natural Resources Conservation Service (USDA-NRCS). 2009. "Natural Resources Conservation Service Conservation Practice Standard Denitrifying Bioreactor (Ac.) Interim Code 747."

United States Geological Survey (USGS). 1999. Sustainability of Ground-Water Resources: U.S. Geological Survey Circular 1186. Editors: W. A. Alley, T. E. Reilly, and O. L. Franke. ISBN 0–607–93040–3

University of Massachusetts, Climate System Research Center. ND. “How will global warming of 2^{o} C affect Minnesota? Observed and projected changes in climate and their impacts.” Accessed 4 January 2018. https://www.geo.umass.edu/climate/stateClimateReports/MN_ClimateReport_CSRC.pdf

University of Minnesota Extension: G. Sands. 2001. Agricultural Drainage. “Drainage Concepts: Soil water concepts.” Accessed on 5 May 2017. http://www.extension.umn.edu/agriculture/water/agricultural-drainage/soil-water-concepts/

University of Minnesota Extension: G. Randall, M. Schmitt, J. Strock and J. Lamb. ND. Nutrient Management. “Validating N rates for corn on farm fields in southern Minnesota: Recommendations to optimize profits and protect water quality.” http://www.extension.umn.edu/agriculture/nutrient-management/nitrogen/validating-n-rates-for-corn-on-farm-fields-in-southern-minnesota/

University of Minnesota Extension: M.A. Schmitt, G.W. Randall, and G.W. Rehm. 2002. Nutrient Management. “A soil nitrogen test option for N recommendations with corn.” http://www.extension.umn.edu/agriculture/nutrient-management/nitrogen/soil-nitrogen-test-option-for-n-recommendations/]

University of Minnesota Extension: J.A. Hernandez, J.A. Vetsch, and L.A. Everett. NA. Swine Manure Application Timing: Results of Experiments in

Southern Minnesota. http://www.extension.umn.edu/agriculture/manure-management-and-air-quality/manure-application/docs/manure-timing.pdf

United States Department of Agriculture (USDA). National Agricultural Statistic Survey. 2017. Minnesota County Estimates: Corn for Grain (2015-2016), Corn for Silage (2015-2016), and Soybeans (2015-2016). https://www.nass.usda.gov/Statistics_by_State/Minnesota/Publications/County_Estimates/index.php

Van de Moortel, A.M.K., E. Meers, N. Pauw, and F.M.G. Tack, 2010. Effects of Vegetation, Season and Temperature on the Removal of Pollutants in Experimental Floating Treatment Wetlands. Water, Air, and Soil Pollution 212: 281–297.

Van Driel, P.W., W.D. Robertson, and L.C. Merkley. 2006. Denitrification of agricultural drainage using wood-based reactors. Trans. ASABE 49(2): 565-573.

Vymazal J. 2006. Removal of nutrients in various types of constructed wetlands. Science of the Total Environment. 380: 48–65.

Wan, H., B.N. Wilson, and D.R. Schmidt. 2017. Biofilter Model Development for the Removal of Pollutants from Feedlot Runoff. Environment Protection Engineering 43(3): 61-80.

Wang. D., K.M. Scow, D.E. Griffin, S.J. Parikh, D. Yan, and H. Wang. 2014. The Impacts of Biochar on Soil Nutrient Leaching in the Context of Extreme Hydrological Processes. Russell Ranch Sustainable Agriculture Facility. University of California, Davis. https://www.soils.org/files/am/ecosystems/wang.pdf

Ward A., D. Mecklenburg, D.E. Powell, L.C. Brown, and A.C. Jayakaran. 2004. Designing Two- Stage Agricultural Drainage Ditches, Drainage VIII Proceedings of the Eighth International Drainage Symposium. P 386-397.

Ward A.D. and Trimble S.W. 2004. Environmental Hydrology, Second Edition. CRC Press, Boca Raton, FL.

Warneke, S., L.A. Schipper, D.A. Bruesewitz, I. McDonald, and S. Cameron. 2011a. Rates, controls and potential adverse effects of nitrate removal in a denitrification bed. Ecological Engineering 37: 511-522.

Wasley, D. 2013. Nitrogen in Minnesota Surface Waters. Minnesota Pollution Control Agency. https://www.pca.state.mn.us/sites/default/files/wq-s6-26b5.pdf.

Watson, C.A., and D. Atkinson. 1999. Using nitrogen budgets to indicate nitrogen use efficiency and losses from whole farm systems: A comparison of three methodological approaches. Nutr. Cycl. Agroecosyst. 53: 259–267.

Weaver, J.E. Root Development of Field Crops, First Edition. New York: McGraw-Hill Book Company, Inc., 1926.

Welander, U., and B. Mattiasson. 2003. Denitrification at low temperatures using a suspended carrier biofilm process. Water Res. 37: 2394–2398.

Wheatley River Improvement Group (WRIG). Nitrate and Their Effect on Water Quality - A Quick Study. http://www.wheatleyriver.ca/current-projects/wrig-pilot-nitrate-study/nitrates-and-their-effect-on-water-quality-a-quick-study/, Information provided by the Partnership For Environmental Education and Rural Health.

Wilson, B. July 2017. Personal Communication. Professor, University of Minnesota, St. Paul MN. Regarding the analytical approach to the combined plug and CSTRs in a series model.

Woli, K.P., M.B. David, R.A. Cooke, G.G. McIsaac, and C.A. Mitchell. 2010. Nitrogen balance in and export from agricultural fields associated with controlled drainage systems and denitrifying bioreactors. Ecol. Eng. 36: 1558–1566.

Zhang, L., and J. Magner. 2014. Midwestern Cornbelt Nutrient Sequestration: Fine Tuning Treatment Technology. Journal of Geology and Geosciences 3: 151-154.

Zhang, L. 2015. Exploring N and P Reductions in Bioreactors. MS Thesis.

University of Minnesota; St. Paul, MN.

Zhao, Y., B. Liu, W. Zhang, C. Hu, and S. An. 2009. Effects of plant and influent C:N:P: ratio on microbial diversity in pilot-scale constructed wetlands. Ecological Engineering. 36: 441-449.

APPENDICES

Appendix A

Probes

Hach Nitratax Plus: 15 sec readings, response time = 1 - 12 wipes, default is 3 wipes, chosen method is 2X the default (6 wipes = 1.5 minutes), error = 3% of MW + 0.5, lower detection 0.1 mg L^{-1} and upper 100 mg L^{-1} NO_3-N, 2 mm measuring path. The nitrate probe was calibrated 1x/wk with DI water and a 50 mg L^{-1} NO3-N standard. Drift was checked daily using DI water - if the reading was > 0.2 mg L^{-1} NO_3-N, the probe was recalibrated, even if it had been less than a week since the last calibration.

Hach DR890 Colorimeter for Reactive Phosphorus (aka Orthophosphate): PhosVer 3 Absorbic Acid Method, range 0 to 2.50 mg L^{-1} PO_4^{-3} (standard deviation = ± 0.05 mg/L PO_4^{-3}, estimated detection limit = 0.05 mg/L PO_4^{-3}). The colorimeter was calibrated 1x/wk with DI water and a 1 mg L^{-1} PO_4^{-3} standard.

YSI 6 Series Multi-parameter Water Quality Sonde: ROX Optical DO (barometer accuracy for DO: ± 3 mm Hg within ± 15 C of the calibration temperature, range: 0 to 500% or 0 to 50 mg L^{-1}, resolution: 0.1% or 0.01 mg L^{-1}, accuracy (for the range of 0 to 200%): ± 1% of reading or 1% air saturation, whichever is greater), pH/ORP (range: 0 to 14 units, resolution: 0.01 unit, accuracy: ± 0.2 unit), temperature/conductivity (conductivity - range: 0 to 100 mS cm^{-1}, resolution: 0.001 to 0.1 mS cm^{-1} (range dependent), accuracy: ± 0.5% of reading plus 0.001 mS cm^{-1}; temperature - range: -5 to 50 ^oC, resolution: 0.01 ^oC, accuracy: ± 0.15 ^oC)

Sonde conductivity, pH, and DO were calibrated daily. DO was calibrated to barometric atmospheric pressure and pH calibrated to 4, 7, and 10 pH standards at initial installation then to a 7 pH standard daily. Conductivity was calibrated to a 1413 µS cm^{-1} standard. ORP was calibrated every 2 weeks using a Zobell

Solution containing potassium chloride and potassium ferrocyanide (231 mV at 25 C).

Bromide Reader: Thermo Scientific Orion Star A324 pH/ISE Meter (accuracy = ± 0.2 mV or ± 0.05% of reading, whichever is greater)
Bromide Probe: Thermo Scientific IonPlus Bromide Electrode
UMNRAL (Br^-): ion chromatography; low standard (1.0 to 100 ppm) error = ± 3% (0.97 to 1.03 ppm) over 16 analytical runs.
Pace (Br^-): Detection level = 0.80 mg L^{-1}, blank sample = non-detect

Appendix B

Detailed Model Equations

Continued after Figure 58.

Replace M with $\dot{M}\,dt$ and $\dot{R}$ with $\kappa_d C_{out} K_c T_d Q$

$$dM = \dot{M}_{in}\,dt - \dot{M}_{out}\,dt - \kappa_d C_{out} K_c T_d Q dt \tag{62}$$

Substitute $\dot{M}$ with CQ

$$dM = QC_{in}dt - QC_{out}dt - \kappa_d C_{out} K_c T_d Q dt \tag{63}$$

Then replace the QC terms with those that incorporate short-circuiting (f_s) from one tank to the next.

$$QC_{in} = Qf_s C_{in} + Q(1 - f_s)C'_{in} \tag{64}$$

Where f_s can refer to either f_{s1} (plug) or f_{s2} (CSTR), C refers to the previous reactor (whether plug reactor or any of the CSTRs), and C' refers to the 2nd previous reactor (for CSTR 1 this is C_p, for CSTR 2 this is C_0). For simplification, f_{s1} is set at 0 (no short-circuiting).

Substituting with the short-circuiting terms into the dM equation we get

$$dM = (Qf_sC_{in} + Q(1 - f_s)\,C'_{in})dt - QC_{out}dt - \kappa_d C_{out}K_cT_dQdt \tag{65}$$

By integrating over a time increment of Δt, we obtain

$$\begin{aligned}\int_t^{t+\Delta t} (Qf_sC_{in} + Q(1 - f_s)C'_{in})\,dt - \int_t^{t+\Delta t} QC_{out}dt \\ - \int_t^{t+\Delta t} \kappa_d C_{out}K_cT_dQdt = \int_{M(t)}^{M(t+\Delta t)} dM = M_{s2} - M_{s1} \\ = C_{out,2} * V_{cc} - C_{out,1} * V_{cc}\end{aligned} \tag{66}$$

Divide both sides by Q, split the C terms, and pull out K_cT_d and κ_d terms.

$$\begin{aligned}\int_t^{t+\Delta t} f_sC_{in}dt + \int_t^{t+\Delta t} (1 - f_s)C'_{in}dt - \int_t^{t+\Delta t} C_{out}dt - \kappa_d K_cT_d \int_t^{t+\Delta t} C_{out}\,dt \\ = K_cT_d(C_{out,2} - C_{out,1})\end{aligned} \tag{67}$$

By using average concentrations and removal rates over a time step (1 = previous time step, 2 = current time step), the integration terms are equal to the height of a rectangle multiplied by the width of Δt.

$$\begin{aligned}\left(\frac{C_{in,2} + C_{in,1}}{2}\right) f_s\Delta t + \left(\frac{C'_{in,2} + C'_{in,1}}{2}\right)(1 - f_s)\Delta t - \left(\frac{C_{out,2} + C_{out,1}}{2}\right)\Delta t \\ - \kappa_d K_cT_d \left(\frac{C_{out,2} + C_{out,1}}{2}\right)\Delta t = K_cT_d(C_{out,2} - C_{out,1})\end{aligned} \tag{68}$$

Pull the $-\left(\frac{C_{out,2}+C_{out,1}}{2}\right)$ term out of left side to get $-\left(\frac{C_{out,2}+C_{out,1}}{2}\right)(1 + \kappa_d)$.

$$\left(\frac{C_{in,2}+C_{in,1}}{2}\right)f_s\Delta t\ +\left(\frac{C'_{in,2}+C'_{in,1}}{2}\right)(1-f_s)\Delta t \\ -\left(\frac{C_{out,2}+C_{out,1}}{2}\right)(1+\kappa_d K_c T_d)\Delta t = K_c T_d\left(C_{out,2}-\ C_{out,1}\right) \tag{69}$$

On the left side, keep $\left(\frac{C_{in,2}+C_{in,1}}{2}\right)f_s\Delta t+\left(\frac{C'_{in,2}+C'_{in,1}}{2}\right)(1-f_s)\Delta t$ and move to the right (now negative). Factor out $-\left(\frac{C_{out,2}+C_{out,1}}{2}\right)(1+\kappa_d K_c T_d)$ to get $-\left(\frac{C_{out,2}}{2}+\frac{\kappa_d}{Q}\right)$ and $-\left(\frac{C_{out,1}}{2}+\kappa_d K_c T_d\right)$. Move $-\left(\frac{C_{out,1}}{2}+\kappa_d K_c T_d\right)$ to the right side (now positive). On the right side, factor out $K_c T_d\left(C_{out,2}-\ C_{out,1}\right)$ to get $K_c T_d\left(C_{out,2}\right)-K_c T_d(C_{out,1})$. Move $K_c T_d(C_{out,2})$ to the left (now negative). Lastly, switch all the signs.

$$K_c T_d\ C_{out,2}+\left(\frac{C_{out,2}}{2}+\kappa_d\ K_c T_d\right)\ \Delta\mathrm{t} \\ =\left(\frac{C_{in,2}+C_{in,1}}{2}\right)f_s\Delta t\ +\left(\frac{C'_{in,2}+C'_{in,1}}{2}\right)(1-f_s)\Delta t \\ +K_c T_d\ C_{out,1}-\left(\frac{C_{out,1}}{2}+\kappa_d\ K_c T_d\right)\ \Delta t \tag{70}$$

Move all the denominators under Δt and factor out $C_{out,2}$ from the left side.

$$\left(K_c T_d\ +\ (1\ +\kappa_d K_c T_d)\frac{\Delta\mathrm{t}}{2}\right)C_{out,2} \\ =\left(C_{in,2}+C_{in,1}\right)\frac{f_s\Delta t}{2}\ +\left(C'_{in,2}+C'_{in,1}\right)\frac{(1-f_s)\Delta t}{2} \\ +K_c T_d\ C_{out,1}-\left(C_{out,1}\ +\kappa_d K_c T_d\right)\frac{\Delta t}{2} \tag{71}$$

Combine the $C_{out,1}$terms on the right side.

$$\left(K_cT_d\ +\ (1\ +\kappa_dK_cT_d\ )\frac{\Delta t}{2}\right)C_{out,2}$$
$$= \left(C_{in,2} + C_{in,1}\ \right)\frac{f_s\Delta t}{2}\ + \left(C'_{in,2} + C'_{in,1}\right)\frac{(1-f_s)\Delta t}{2}$$
$$+\left(K_cT_d\ -(1\ +\kappa_d\ K_cT_d)\ \frac{\Delta t}{2}\ \right)C_{out,1} \tag{72}$$

Divide both sides by $\left(K_cT_d\ +\ (1\ +\kappa_dK_cT_d\ )\frac{\Delta t}{2}\right)$

$$C_{out,2} = \frac{\left(C_{in,2} + C_{in,1}\ \right)\frac{f_s\Delta t}{2}}{\left(K_cT_d\ +\ (1\ +\kappa_d\ K_cT_d)\frac{\Delta t}{2}\right)} + \frac{\left(C'_{in,2} + C'_{in,1}\right)\frac{(1-f_s)\Delta t}{2}}{\left(K_cT_d\ +\ (1\ +\kappa_d\ K_cT_d)\frac{\Delta t}{2}\right)}$$
$$+\frac{\left(K_cT_d\ -(1\ +\kappa_dK_cT_d\ )\ \frac{\Delta t}{2}\ \right)C_{out,1}}{\left(K_cT_d\ +\ (1\ +\kappa_d\ K_cT_d)\frac{\Delta t}{2}\right)} \tag{73}$$

Now, the concentration out of each CSTR (mg L^{-1}) for any given time step is

$$C_{out,2} = W_0\left(C_{in,2} + C_{in,1}\right) + W_1\left(C'_{in,2} + C'_{in,1}\right) + W_2\left(C_{out,1}\right) \tag{74}$$

Where

$$W_0 = \frac{f_s\left(\frac{\Delta t}{2}\right)}{\left(K_cT_d\ +\ (1\ +\kappa_dK_cT_d)\frac{\Delta t}{2}\right)} \tag{75}$$

$$W_1 = \frac{(1-f_s)\left(\frac{\Delta t}{2}\right)}{\left(K_cT_d\ +\ (1\ +\kappa_dK_cT_d)\frac{\Delta t}{2}\right)} \tag{76}$$

$$W_2 = \frac{\left(K_c T_d \ - (1 \ + \kappa_d K_c T_d) \ \frac{\Delta t}{2} \right)}{\left(K_c T_d \ + \ (1 \ + \kappa_d K_c T_d) \frac{\Delta t}{2}\right)} \tag{77}$$

W terms are dimensionless.

For the first CTSR, $f_s = 1$ (no short-circuiting from the plug) so the W terms are now

$$W_0 = \frac{\left(\frac{\Delta t}{2}\right)}{\left(K_c T_d \ + \ (1 \ + \kappa_d K_c T_d) \frac{\Delta t}{2}\right)} \tag{78}$$

$$W_1 = 0 \tag{79}$$

$$W_2 = \frac{\left(K_c T_d \ - (1 \ + \kappa_d K_c T_d) \ \frac{\Delta t}{2} \right)}{\left(K_c T_d \ + \ (1 \ + \kappa_d K_c T_d) \frac{\Delta t}{2}\right)} \tag{80}$$

In order to accurately capture the plug, it is important not to average the concentration at the beginning and end of the pulse. In order to capture the plug over these time increments, this requires replacing $\frac{\Delta t}{2}$ with Δt in the numerator of the W_0 and W_1 terms.

$$W_0 = \frac{\Delta t}{\left(K_c T_d \ + \ (1 \ + \kappa_d K_c T_d) \frac{\Delta t}{2}\right)} \tag{81}$$

$$W_1 = 0 \tag{82}$$

$$W_2 = \frac{\left(K_c T_d - (1 + \kappa_d K_c T_d)\frac{\Delta t}{2}\right)}{\left(K_c T_d + (1 + \kappa_d K_c T_d)\frac{\Delta t}{2}\right)} \tag{83}$$

Since we are not averaging over the first time step after t_{dp} (the beginning of the pulse input into the 1st CSTR), the C_{in} terms can be split. Since $W_1 = 0$, the C' terms can be removed.

$$C_{out,2} = W_0 C_{in,2} + W_1 C_{in,1} + W_2\left(C_{out,1}\right) \tag{84}$$

For the first CTSR, we need to take the concentration at the end of the time step before the pulse input ($C_{in,1}$), which is the first time step after t_{dp}. The previous time step of the plug reactor ($C_{in,2}$) can be neglected by creating a $W_0' = 0$ term when using the time step Δt.

Now

$$C_{out,2} = W_0 C_{in,2} + W_0{}' C_{in,1} + W_2\left(C_{out,1}\right) \tag{85}$$

And

$$W_0{}' = 0 \tag{86}$$

$$W_0 = \frac{\Delta t}{\left(K_c T_d \ + \ (1 \ + \kappa_d K_c T_d) \frac{\Delta t}{2}\right)} \tag{87}$$

$$W_1 = \ 0 \tag{88}$$

$$W_2 = \frac{\left(K_c T_d \ - (1 \ + \kappa_d K_c T_d) \ \frac{\Delta t}{2}\right)}{\left(K_c T_d \ + \ (1 \ + \kappa_d K_c T_d) \frac{\Delta t}{2}\right)} \tag{89}$$

It is important to also not average the concentration at the end of the pulse input. For this we need to use Δt as the time step and take the concentration at the beginning of the time step after the pulse input. This is accomplished by switching the W_0 and W_0' values.

Now

$$W_0{}' = \frac{\Delta t}{\left(K_c T_d \ + \ (1 \ + \kappa_d K_c T_d) \frac{\Delta t}{2}\right)} \tag{90}$$

$$W_0 = 0 \tag{91}$$

$$W_1 = \ 0 \tag{92}$$

$$W_2 = \frac{\left(K_c T_d \ - (1 \ + \kappa_d K_c T_d) \ \frac{\Delta t}{2}\right)}{\left(K_c T_d \ + \ (1 \ + \kappa_d K_c T_d) \frac{\Delta t}{2}\right)} \tag{93}$$

For the remaining time steps, in the middle of the pulse and beyond one time step after the pulse, $W_0' = W_0$ (when the time parameter in the numerator is $\frac{\Delta t}{2}$).

$$W_0{}' = \frac{\frac{\Delta t}{2}}{\left(K_c T_d \ + \ (1 \ + \kappa_d K_c T_d) \frac{\Delta t}{2}\right)} \tag{94}$$

$$W_0 = \frac{\frac{\Delta t}{2}}{\left(K_c T_d \ + \ (1 \ + \kappa_d K_c T_d) \frac{\Delta t}{2}\right)} \tag{95}$$

$$W_1 = \ 0 \tag{96}$$

$$W_2 = \frac{\left(K_c T_d \ - (1 \ + \kappa_d K_c T_d) \ \frac{\Delta t}{2}\right)}{\left(K_c T_d \ + \ (1 \ + \kappa_d K_c T_d) \frac{\Delta t}{2}\right)} \tag{97}$$

For the second CSTR, C' now refers back to the plug reactor. An additional term, W_1', is used to account for the jump in concentration from the plug reactor for the first time step after t_{dp} and for the first time step after the pulse input comes through.

$$C_{out,2} = W_0 C_{in,2} + W_0{}' C_{in,1} + W_1 C'_{in,2} + W_1{}' C'_{in,1} + W_2\left(C_{out,1}\right) \quad (98)$$

And

$$W' = 0 \quad (99)$$

$$W_0 = \frac{f_s(\Delta t)}{\left(K_c T_d + (1 + \kappa_d K_c T_d)\frac{\Delta t}{2}\right)} \quad (100)$$

$$W'_1 = 0 \quad (101)$$

$$W_1 = \frac{(1 - f_s)(\Delta t)}{\left(K_c T_d + (1 + \kappa_d K_c T_d)\frac{\Delta t}{2}\right)} \quad (102)$$

$$W_2 = \frac{\left(K_c T_d - (1 + \kappa_d K_c T_d)\frac{\Delta t}{2}\right)}{\left(K_c T_d + (1 + \kappa_d K_c T_d)\frac{\Delta t}{2}\right)} \quad (103)$$

For the time step after t_{dp}, the W terms (regular form and prime form) are switched to account for only the beginning of that time step for the plug reactor.

$$W' = \frac{f_s(\Delta t)}{\left(K_c T_d \ + \ (1 \ + \kappa_d K_c T_d)\frac{\Delta t}{2}\right)} \tag{104}$$

$$W_0 = 0 \tag{105}$$

$$W'_1 = \frac{(1 - f_s)(\Delta t)}{\left(K_c T_d \ + \ (1 \ + \kappa_d K_c T_d)\frac{\Delta t}{2}\right)} \tag{106}$$

$$W_1 = \ 0 \tag{107}$$

$$W_2 = \frac{\left(K_c T_d \ - (1 \ + \kappa_d K_c T_d)\ \frac{\Delta t}{2}\ \right)}{\left(K_c T_d \ + \ (1 \ + \kappa_d K_c T_d)\frac{\Delta t}{2}\right)} \tag{108}$$

The remaining time steps follow the original form of the equation (Eq. 75, 76, and 77) with $W_0' = W_0$ and $W'_1 = W_1$.

$$W'_0 = \frac{f_s\left(\frac{\Delta t}{2}\right)}{\left(K_c T_d \ + \ (1 \ + \kappa_d K_c T_d)\frac{\Delta t}{2}\right)} \tag{109}$$

$$W_0 = \frac{f_s\left(\frac{\Delta t}{2}\right)}{\left(K_c T_d \ + \ (1 \ + \kappa_d K_c T_d)\frac{\Delta t}{2}\right)} \tag{110}$$

$$W'_1 = \frac{(1 - f_s)\left(\frac{\Delta t}{2}\right)}{\left(K_c T_d \ + \ (1 \ + \kappa_d K_c T_d)\frac{\Delta t}{2}\right)} \tag{111}$$

$$W_1 = \frac{(1 - f_s)\left(\frac{\Delta t}{2}\right)}{\left(K_c T_d \ + \ (1 \ + \kappa_d K_c T_d)\frac{\Delta t}{2}\right)} \tag{112}$$

$$W_2 = \frac{\left(K_c T_d \ - (1 \ + \kappa_d K_c T_d)\ \frac{\Delta t}{2}\ \right)}{\left(K_c T_d \ + \ (1 \ + \kappa_d K_c T_d)\frac{\Delta t}{2}\right)} \tag{113}$$

Appendix C

Biochar Characterization

Property	Unit	Biochar	IBI	EBC
pH_{CaCl2}*		6.6		≤10
C_{total}	%	87.6		>50
C_{org}	%	87.6	≥10	
C_{inorg}	%	<0.1		
C_{fixed}	%	83.5		
N_{total}	%	0.44		
C_{org}:N	ratio	199		
H	%	2.85		
O	%	7.5		
H:C_{org}	ratio	0.39	<0.7	<0.7
O:C	ratio	0.064		<0.4
Ash_{550}	%	1.9		
Ash_{815}	%	1.6		
EC*	μS/cm	116		
SA	m^2/g	0.6264		
Ca	mg/kg	1400		
Fe	mg/kg	1700		
K	mg/kg	5000		
Mg	mg/kg	360		
B	mg/kg	5		
Cd	mg/kg	<0.2	1.4-39	<1.5
Cr	mg/kg	2	64-1200	<90
Cu	mg/kg	11	63-1500	<100
Hg	mg/kg	<0.07	1-17	<1
Mn	mg/kg	27		
As	mg/kg	<0.8	12-100	<13
Na	mg/kg	65		
Ni	mg/kg	1	47-600	<50
P	mg/kg	480		
Pb	mg/kg	3	70-500	<150
S	mg/kg	110		
Si	mg/kg	270		
Zn	mg/kg	5	200-7000	<400
PAHs	mg/kg	162	6-300	<12

all measurements are taken from dry basis unless otherwise noted
*measured using samples as received

IBI: International Biochar Initiative. Maximum threshold range is determined by the soil tolerance level of application.
EBC: European Biochar Certificate
SA: specific surface area (BET)
EC: electrical conductivity
PAHs: sum of EPA's 16 listed PAHs
(Source: Hackshaw, N. (2018) Linking functional microbial community dynamics to nitrate removal in mesoscale denitrifying wood chip bioreactors. Master's Thesis. The University of Minnesota, Minneapolis, Minnesota.)